Siliciclastic Depositional Systems in the Cretaceous Book Cliffs Utah

Applications to the Subsurface

Book Cliffs Geological Field Trip

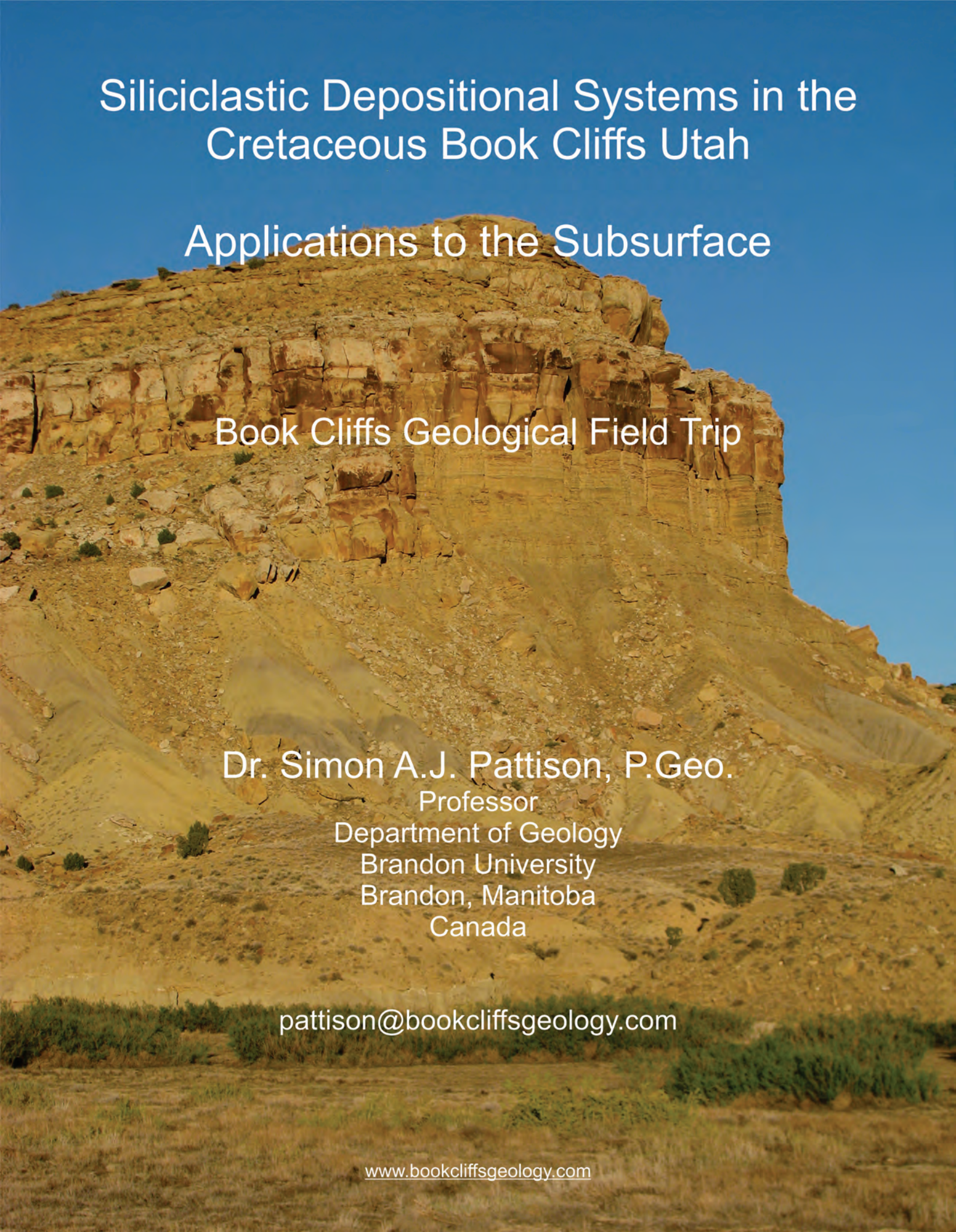

Dr. Simon A.J. Pattison, P.Geo.
Professor
Department of Geology
Brandon University
Brandon, Manitoba
Canada

pattison@bookcliffsgeology.com

www.bookcliffsgeology.com

Siliciclastic Depositional Systems in the Cretaceous Book Cliffs Utah:

Applications to the Subsurface

Book Cliffs
Geological Field Trip

Dr. Simon A.J. Pattison, P.Geo.
Professor
Department of Geology
Brandon University

pattison@bookcliffsgeology.com

Cover Photo:
Desert Member to Lower Castlegate Sandstone stratigraphic interval along the southeastern face of Crescent Canyon. Thick cliff-forming sandstones are Desert Member shallow marine deposits. These are capped by channel sandstones and coastal plain deposits of the Lower Castlegate Sandstone. Distal Grassy Member parasequences are expressed as colour bands near the base of the cliff section.

Citation Format:
Pattison, S.A.J., 2019, Siliciclastic depositional systems in the Cretaceous Book Cliffs Utah: Applications to the subsurface. Book Cliffs Geological Field Trip Guidebook, 164 p.

TABLE OF CONTENTS

List of Figures and Tables

BACKGROUND INFORMATION

Welcome to the Book Cliffs. This seminar comprises an intensive field course covering reservoir characterization of spectacularly-exposed fluvial (braided and meandering), coastal plain, shoreface/deltaic, and shelf deposits in the Book Cliffs of east-central Utah and western Colorado. These rocks are direct analogues to many clastic reservoirs worldwide, including those targeted by most oil and gas companies in North America.

The Book Cliffs form approximately 300 km of continuous exposure of the Upper Cretaceous (Campanian) Star Point Formation, Blackhawk Formation and Castlegate Sandstone, comprising a regressive set of fluvial/tide and wave-dominated shoreface/deltaic deposits some 500 meters thick. Most major oil companies have been actively involved in research and training in this area over the last thirty years as a direct analogue to subsurface hydrocarbon-bearing reservoirs. The mesa-topography and dissection of the Book Cliffs escarpment allows full 3D analysis of time-equivalent surfaces from offshore shelf deposits, through shoreface parasequences, onshore into the correlative coastal plain, thus providing an ideal proving ground to test and teach sequence stratigraphic concepts at the outcrop-scale and to determine the validity of applying such techniques to both exploration plays and field development in the subsurface.

This seminar has been specifically designed for geologists and engineers from a variety of disciplines and requires only a minimal background knowledge of sedimentological and sequence stratigraphic principles. The seminar will comprise field stops supplemented by field exercises. As such it aims to provide focused training which incorporates the use of the latest geological concepts and technologies.

Logistics

The outcrops we are visiting occur in the high-plains desert of the Colorado Plateau (Utah-Colorado). The weather is generally excellent and provides some of the best conditions for fieldwork. Early morning temperatures of around 10° C are common with afternoon temperatures approaching 25-30° C. Rain showers and/or snow flurries are unlikely, but participants should be prepared in case we encounter inclement weather. Keep in mind that while in Utah we will be at elevations of 1300-2000 meters and storms can occur at any time.

The outcrops which we will visit can only be accessed by driving on reasonably well maintained dirt and gravel roads and travel will therefore be 4-wheel drive vehicles for safety reasons. At the outcrops themselves we will undertake several hikes over moderate terrain which will require strong walking boots with good ankle support (not running shoes or safety boots). Because of the outcrops which we intend to visit, and the rather large distances involved following the cliff-line exposures, I have scheduled rather full days. In general we will take breakfast early and then will depart to the field. Packed lunches, drinks and snacks will be provided. If you have any special dietary requirements, please let me know in advance.

Safety

Safety is of utmost importance on this trip. Most accidents which have occurred to other field parties in this area have either involved climbing precipitous slopes in remote areas, or through speeding on dirt roads. We do not intend to be in either of these situations at any time during the field seminar. As we will be travelling extensively on dirt roads in Utah, drivers should exercise caution at all times. The maximum speed on dirt roads should never exceed 30 mph. Many of the corners have positive camber, causing the vehicle to slide towards the outside

of the bend. As we will be travelling in convoy, drivers should maintain an appropriate distance from the vehicle in front to avoid flying gravel, and to reduce the amount of dust entering your vehicle. In the unlikely event we encounter rain or snow in Utah, those tracks which traverse the Mancos Shale become very slippery and traction will be greatly reduced – be aware. For drivers and passengers there is also a real need to be aware of traffic when exiting the vehicles as some of our stops will be adjacent to the roadside

Another safety hazard in Utah comes from dehydration and sunburn. Because of the high altitude and westerly air flow, humidity rarely exceeds 20 %. This fact in combination with physical exertion, provides optimum conditions for dehydration. I strongly recommend that you equip yourselves daily with adequate supplies of water, fruit juices and minerals. In order to reduce the risk of sunburn and eye-strain, I recommend you bring a hat and polarizing sunglasses to combat the intense light and high degree of reflectivity off the white rocks. If you are susceptible to sunburn, bring appropriate protective lotion.

If you have any particular medical condition, please let me know in advance so that if you should be taken ill on the trip, I am aware of it. If any medical emergencies do arise, a clinic attended by a physicians' assistant is available in Green River, and fully staffed hospitals are located in Price Utah and Grand Junction Colorado. I will have several first aid kits for emergencies in the field.

Hotel Information

Comfort Inn
1975 East Main Street
Green River, UT 84525
Phone: (435) 564-3300
Fax: (435) 564-3299

INTRODUCTION

The Book Cliffs of eastern Utah and western Colorado (Figs. 0-1 and 0-2) are an excellent outcrop analog for many fluvial, deltaic and shoreface-to-shelf hydrocarbon reservoirs worldwide. Similarities include the depositional environments, sedimentary processes and facies, stacking patterns (vertical and lateral), 3D sedimentary architecture, and sequence stratigraphy. The Book Cliffs region in east-central Utah has been the site for petroleum industry-based research and training for many decades. For example, many AAPG-sponsored ancient clastics field seminars have a Book Cliffs component. The continuous outcrop exposure (100's of km's), numerous side canyons (3D control), desert environment (minimal vegetation), and near-horizontal structural orientation combine to make the Book Cliffs a world-class field laboratory for studying clastic sedimentology and sequence stratigraphy. It is truly one of the few areas in the world where you can walk and/or drive-out time equivalent depositional units all the way from their proximal fluvial/coastal plain environments through the shallow marine shoreface/deltaic environments and out onto the shelf. This field trip is designed as a practical and applied field seminar which is targeted to exploration geologists, production/development geologists, reservoir geologists, geophysicists, petrophysicists, reservoir engineers, production engineers and managers.

The field guidebook covers the following themes: (a) sedimentology and 3D architecture of fluvial, coastal plain, deltaic, and shoreface-to-shelf depositional systems, (b) stacking patterns in high vs. low accommodation settings, (c) distribution of reservoir and non-reservoir facies in a predictive sequence stratigraphic framework, (d) relative sea level, shoreline position and stratigraphic architecture, and (e) applications of outcrop analog data to the subsurface. The latter includes facies identification (core and well logs), stacking patterns (well logs), correlation (interwell spacing), modelling (exploration- to reservoir-scale), and reservoir geology-engineering (drilling, completion, perforation and development strategies). Field trip stops are organized as follows (Figs. 0-1 and 0-2):

Introduction to Fluvio-Deltaic, Coastal Plain and Shoreface-Shelf Deposits
Stop 1: Distal Book Cliffs, Thompson Overview
Stop 2: High Net:Gross Braided Fluvial Deposits, Castlegate Sandstone, Type Section
Stop 3: Low to Moderate N:G Meandering Fluvial and Coastal Plain Deposits, Blackhawk Fm.
Stop 4: River-Dominated Deltas, Distributary Mouth Bars, Gentile Wash

Shoreface-to-Shelf: Stacking, Correlation, Sea Level, and Sequence Stratigraphy
Stop 5: Wave-Dominated Shoreface/Deltaics, High to Low Accomm. Setting, PRC/Woodside
Stop 6: Strike Continuity of Wave-Dominated Shoreface/Deltaic, Beckwith Plateau
Stop 7: Shoreface-to-Shelf Transition, Green River Embayment/Gunnison Valley
Stop 8: Parasequences/Bedsets Compartmentalization, Grassy Member, Tusher Canyon

Incised Valleys or Channels?: Correlation and Sequence Stratigraphy
Stop 9: Channels Cutting Foreshore-Shoreface Deposits, Grassy Member, Tusher Canyon
Stop 10: Shallow Marine Deposits Cut by Channels, Desert Member, Tusher Canyon
Stop 11: Multistory vs. Single-Story Channels, Desert-Castlegate, The Basin

Channels, Coastal Plain & Shoreface-Deltaic Deposits: Architecture and Prediction
Stop 12: Desert-Castlegate Facies and Stratal Architectures, Crescent Canyon-Horse Heaven
Stop 13: Low Accommodation Space Setting, Desert-Castlegate, West of Blaze Canyon
Stop 14: High Resolution Sequence Stratigraphy, Desert-Castlegate, Blaze Canyon

Terrestrial to Marine Facies Belts: Reservoir-to-Exploration Scale
Stop 15: Reservoir-Scale Architecture Channel-Shoreface Reservoir Units, Thompson Canyon
Stop 16: Near-Field Exploration-Scale Terrestrial-Shoreface-Shelf Transition, Sagers Canyon

Book Cliffs Geology

The Cretaceous was a naturally occurring "greenhouse period" in Earth's history when the dinosaurs reigned supreme and the Western Interior of North America, from Arctic Canada to the Gulf of Mexico was flooded with sea water. Global sea level was up to 250 m higher than present day. The Cretaceous Western Interior Seaway (CWIS) dissected the North American continent into two parts: a mountainous western half and a lower-lying eastern half. The western half was tectonically active with only a narrow coastal plain separating the Sevier thrust front from the CWIS. Small- to moderate-sized, eastward-flowing rivers transported a significant volume of sediments into the CWIS, depositing a thick succession of sands, silts and clays.

Following deposition and lithification, these sedimentary rocks were slowly uplifted to form the magnificent scenery in the Western Interior of Canada and the United States. One of the most spectacular regions is the Canyonlands-area of east-central Utah which is home to two national parks and one of the longest continuous cliff-lines in the world, the 300-km-long Book Cliffs (Figs. 0-1 and 0-2). These famous rocks arguably represent the best exposed deltaic rocks in the world and have been used to develop, test and refine sedimentological and stratigraphic ideas and models over the years, including the principles and concepts of sequence stratigraphy (Van Wagoner et al. 1990; Posamentier and Allen 1999).

Study Area

The Book Cliffs extend from Helper, Utah to east of Grand Junction, Colorado (Fig. 0-1). These cliffs consist of Campanian (Upper Cretaceous) siliciclastic rocks that were sourced from the Sevier highlands to the west and deposited as a series of north-south trending depositional belts towards the east (Figs. 0-3 and 0-4). Each rock package consists of fluvial and coastal-plain deposits in the west, and time-equivalent shoreface-to-shelf deposits in the east (Fig. 0-5). The research data base used for this field guide consists of measured outcrop sections, well log suites, paleocurrent measurements, sandstone and mudstone samples for petrographic analysis, and near continuous photo-panoramas across all four sectors of the Book Cliffs (i.e. northwestern, central, southern, eastern). Five types of outcrop sections are included in the data base: (i) regional sections that were used to establish parasequence-scale thickness and sand content trends for the Blackhawk Formation and Castlegate Sandstone, (ii) detailed sedimentological, ichnological and stratigraphic measured sections across the Desert Member to Castlegate Sandstone interval in the Tusher Canyon to Sagers Canyon region, (iii) measured sections that covered the sedimentology and sequence stratigraphy of the entire Kenilworth Member, (iv) high-resolution sections that focused on the sedimentology and sedimentary architecture of a variety of stratigraphic intervals in the Price River Canyon to Sagers Wash area, and (v) high-resolution outcrop sections through the Hatch Mesa succession. Well log data was integrated with the outcrop data in order to extend the correlation of key surfaces and rock packages across a wide swath of eastern Utah and western Colorado (Fig. 0-6).

Regional Setting and Structure

The Campanian strata of east-central Utah was uplifted a few thousand meters during the Tertiary and forms part of the Colorado Plateau. Two structural features, the San Rafael Swell in east-central Utah and Uncompaghre Uplift in western Colorado, are directly linked to the generation of the 300-km-long Book Cliffs escarpment (Fig. 0-3). The northwestern, central and southern sectors of the Book Cliffs have eroded back from the San Rafael Swell, while the southern and eastern sectors have “peeled-back” from the Uncompaghre Uplift (Fig. 0-3). The widespread vertical uplift of the Colorado Plateau has lead to the near-horizontal preservation of stratigraphic rock packages across a wide area of east-central Utah and western Colorado. The net effect is that the Book Cliffs strata is relatively undeformed and has a gentle structural dip of 1° to 5° north.

Paleogeography

During the Campanian the CWIS covered the eastern half of Utah. Clastic sediments were supplied from the rising Sevier orogenic belt to the west (Fig. 0-4). At its maximum, the CWIS extended from the Arctic Ocean to the Gulf of Mexico. Offshore was generally in an

eastward-direction, however perturbations of the shoreline, such as the Utah Bight, produced southeasterly- and northeasterly-directed offshore trends (Fig. 0-4).

Paleoshoreline trends were mostly oriented north-to-south (McGookey et al. 1972). However, the orientation of the shoreline varied considerably through time: W-E oriented Panther Tongue Member shorelines (Newman and Chan 1991; Hwang and Heller 2002); NNW-SSE Kenilworth Member shorelines (Taylor and Lovell 1991, 1995; Pattison 1994a, 1994b, 1995; Hampson 2000); N-S or NNE-SSW oriented Grassy shorelines (O'Byrne and Flint 1993, 1995, 1996); NE-SW oriented Desert and Castlegate shorelines (van de Graaff 1972; Fouch et al. 1983; Chan and Pfaff 1991; Van Wagoner 1991, 1995; Miall 1993, 1994; Roberts and Kirschbaum 1995; Miall and Arush 2001). This reveals a counter-clockwise (Panther Tongue Member to Kenilworth Member) to clockwise (Kenilworth Member to Castlegate Sandstone) rotation of the paleoshoreline trends through time.

Stratigraphy

The bulk of the Campanian strata in the Book Cliffs of Utah consists of the Star Point Formation, the Blackhawk Formation and the Castlegate Sandstone, forming part of the Mesaverde Group (Young 1955). The Blackhawk Formation is subdivided into six members: Spring Canyon, Aberdeen, Kenilworth, Sunnyside, Grassy, and Desert (Fig. 0-5). These units grade from sandstone-dominated intervals in the west to the mudstone-dominated Mancos Shale in the east (Young 1955; Balsley 1980). Figure 0-5 shows a parasequence-scale correlation for the main stratigraphic units in the Book Cliffs, that is true to scale (i.e. vertical, lateral) and sand content, thus providing a "scaled" stratigraphic cross section that links the shoreface-to-shelf environments in both time and space.

Subsurface Data

There are an abundance of wells that penetrate the Campanian strata in east-central Utah and western Colorado (Figs. 0-6 to 0-12). The most densely drilled areas of east-central Utah are the coal bed methane fields in the Price region, Uinta Basin oil and gas fields in northeastern Utah, Greater Cisco Area gas fields (east of Thompson), and the Utah-Colorado border area gas fields. Many of the targets are deeper than the Cretaceous Mesaverde Group and therefore the well logs cover the Castlegate Sandstone-to-Blackhawk Formation-to-Star Point Formation stratigraphic interval. Six well log suites are included in this guidebook (Figs. 0-7 to 0-12). These well logs can be used to directly correlate the outcrop expression of our field trip stops with the subsurface expression of nearby time equivalent units. More importantly, these well log suites can be used as an "analog-bridge" between the Book Cliffs outcrops and similar clastic reservoirs, worldwide. A summary of each well log suite is given below.

PRICKLY PEAR U ST 13-16 well (Fig. 0-7). Located at SWSW-16-12S-15E. API Well Number 43-007-30933. Nine Mile Canyon Field. Gamma ray, SP, and resistivity logs from 8110 to 9150 feet. The top of the Castlegate Sandstone is 8206 ft. This well has the following stratigraphic-reservoir units:

Channel Sandstones	8206-8440	Castlegate Sandstone
Channel Sandstones and Coastal Plain	8440-8760	Blackhawk Formation
Shoreface/Deltaic Sandstones	8760-9150	Blackhawk Formation

PETERS POINT U FED 36-2 well (Fig. 0-8). Located at NWNW-36-12S-16E. API Well Number 43-007-30761. Peter's Point Field. Gamma ray, SP, and resistivity logs from 8100 to 9240 feet. The top of the Castlegate Sandstone is 8220 ft. This well has the following stratigraphic-reservoir units:

Channel Sandstones	8220-8420	Castlegate Sandstone

Channel Sandstones and Coastal Plain (CP)	8420-8672	Blackhawk Formation
Shoreface/Deltaic Sandstones	8672-9184	Blackhawk Formation
Shelf Mudstones	9184-9240	Mancos Shale

UTE TRIBAL 32-2A well (Fig. 0-9). Located at NWNW-32-14S-20E. API Well Number 43-047-33333. Flat Rock Field. Gamma ray, SP, and resistivity logs from 6200 to 6750 feet. The top of the Castlegate Sandstone is 6323 ft. From top to base this well has the following stratigraphic-reservoir units:

Channel Sandstones and Coastal Plain (CP)	6323-6399	Castlegate Sandstone
Shoreface/Deltaic Sandstones	6399-6411	Castlegate Sandstone
Channel Sandstones and Coastal Plain (CP)	6411-6440	Desert Member
Shoreface/Deltaic Sandstones	6440-6510	Desert Member
Shoreface/Deltaic Sandstones-Heterolithics	6510-6611	Desert Member
Shelf Mudstones	6611-6639	Mancos Shale
Shoreface/Deltaic Heterolithics	6639-6750	Grassy Member

MOON CANYON 1 well (Fig. 0-10). Located at NWSW-32-16S-21E. API Well Number 43-019-31398. Undesignated Field Grand County. Gamma ray, SP, and resistivity logs from 5910 to 6490 feet. The top of the Castlegate Sandstone is 5986 ft. This well has the following stratigraphic-reservoir units:

Channel Sandstones	5986-6042	Castlegate Sandstone
Shoreface/Deltaic Sandstones	6042-6052	Castlegate Sandstone
Channel Sandstones and Coastal Plain (CP)	6052-6070	Desert Member
Shoreface/Deltaic Sandstones-Heterolithics	6070-6245	Desert Member
Shelf Mudstones	6245-6296	Mancos Shale
Shoreface/Deltaic Heterolithics & Shelf Mudstones	6296-6490	Grassy Mb./Mancos Shale

EPR BLAZE CANYON 1 well (Fig. 0-11). Located at NESW-7-21S-20E. API Well Number 43-019-31228. Wildcat Grand County. Gamma ray and resistivity logs from 10 to 364 feet. The top of the Castlegate Sandstone is 0 feet (i.e. well spudded on top of the Castlegate Sandstone). From top to base this well has the following stratigraphic-reservoir units:

Channel Sandstones and Coastal Plain (CP)	0-54	Castlegate Sandstone
Shoreface/Deltaic Sandstones	54-85	Castlegate Sandstone
Channel Sandstones and Coastal Plain (CP)	85-116	Desert Member
Shoreface/Deltaic Sandstones-Heterolithics	116-250	Desert Member
Shelf Mudstones	250-362	Mancos Shale
Shoreface/Deltaic Heterolithics	364-366	Grassy Member

EPR SEGO CANYON 2 well (Fig. 0-12). Located at NW-27-20S-20E. API Well Number 43-019-31232. Wildcat Grand County. Gamma ray and resistivity logs from 500 to 1090 feet. The top of the Castlegate Sandstone is 599 ft. From top to base this well has the following stratigraphic-reservoir units:

Channel Sandstones and Coastal Plain (CP)	599-653	Castlegate Sandstone
Shoreface/Deltaic Sandstones	653-671	Castlegate Sandstone
Channel Sandstones and Coastal Plain (CP)	671-710	Desert Member
Shoreface/Deltaic Sandstones-Heterolithics	710-930	Desert Member
Shelf Mudstones	930-987	Mancos Shale
Shoreface/Deltaic Heterolithics	987-1000	Grassy Member
Shelf Mudstones	1000-1090	Mancos Shale

Facies

Thirteen shallow marine, ten channel, and six non-channelized coastal plain facies are noted in the Blackhawk Formation to Lower Castlegate Sandstone stratigraphic interval, including the time equivalent Mancos Shale mudstone belt to the east (Figs. 0-13 to 0-15; Table 0-1).

1 - Shallow Marine Facies

1A - Planar Laminated Sandstone
1B - Trough Cross Bedded Sandstone
1C - Swaley Cross Stratified Sandstone
1D - Hummocky Cross Stratified Sandstone
1E - Wave-Rippled Sandstone
1F - Sandy Siltstone
    1F-i - Moderate-to-High BI Sandy Siltstone
    1F-ii - Low BI Sandy Siltstone
1G - Silty Mudstone
    1G-i - Moderate-to-High BI Silty Mudstone
    1G-ii - Low BI Silty Mudstone
1H - Dark Grey Mudstone
1I - Classical Turbidite
1J - Wave-Modified Turbidite
1K - Hyperpycnite
1L - Coarse-Grained Lag Deposit
1M - Oolitic Ironstone

2 - Channel Facies

2A - Cross Bedded Sandstone
2B - Convolute Bedded Sandstone
2C - Planar Laminated Sandstone
2D - Current Rippled Sandstone
2E - Gently-Dipping Interbedded Sandstone and Mudstone (IHS)
2F - Carbonaceous-Rich Sandstone
2G - Carbonaceous-Rich Siltstone
2H - Carbonaceous-Rich Mudstone
2I - Mudstone-Clast Pebble Breccia
2J - Fossiliferous, Fe-Cemented Sandy Breccia (“Coquina”)

3 - Non-Channelized Coastal Plain Facies

3A - Current Rippled Sandstone
3B - Carbonaceous-Rich Sandstone
3C - Carbonaceous-Rich Siltstone
3D - Carbonaceous-Rich Mudstone
3E - Carbonaceous Shale
3F - Coal

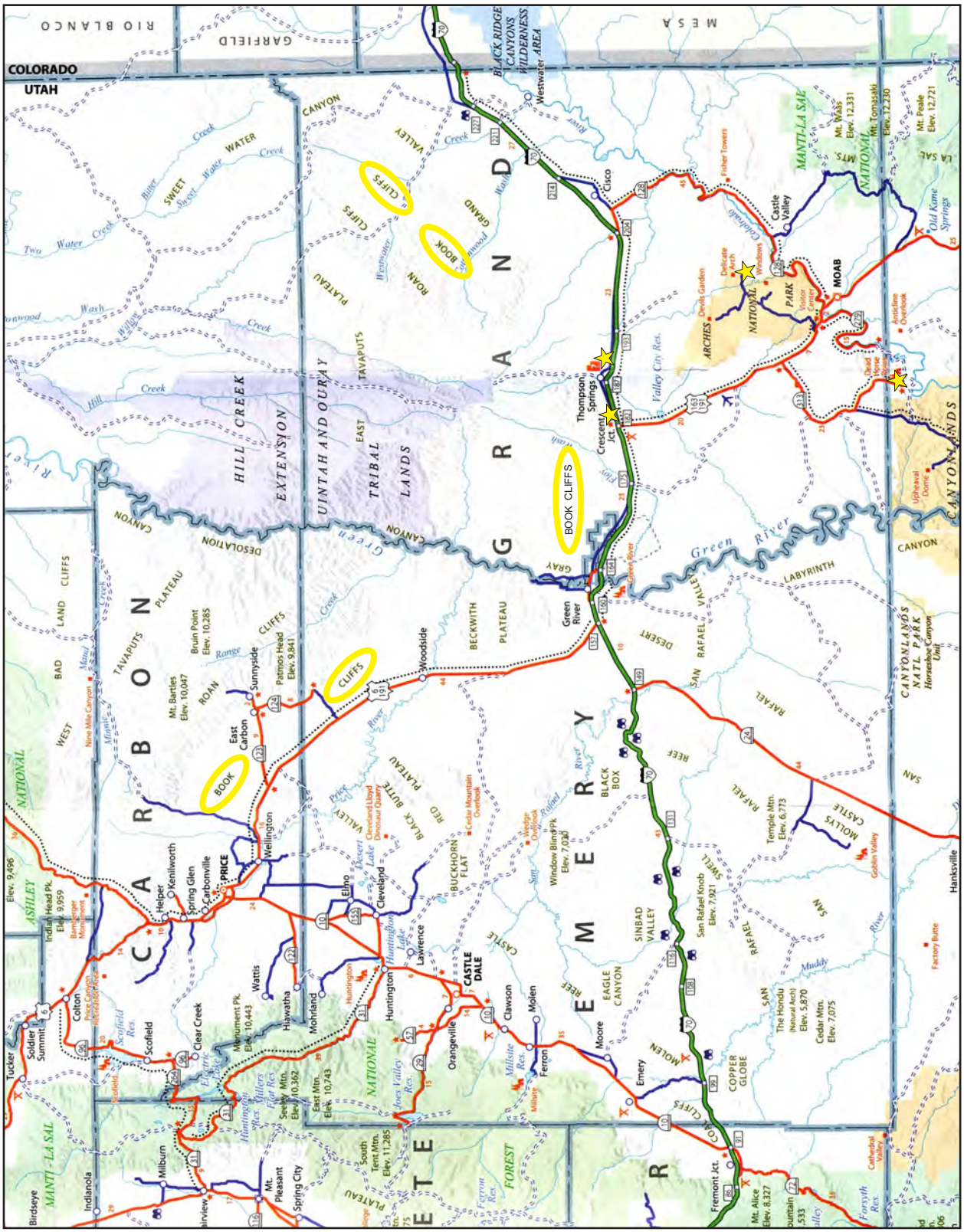

Figure 0-1. Road map of east-central Utah covering the field trip area.

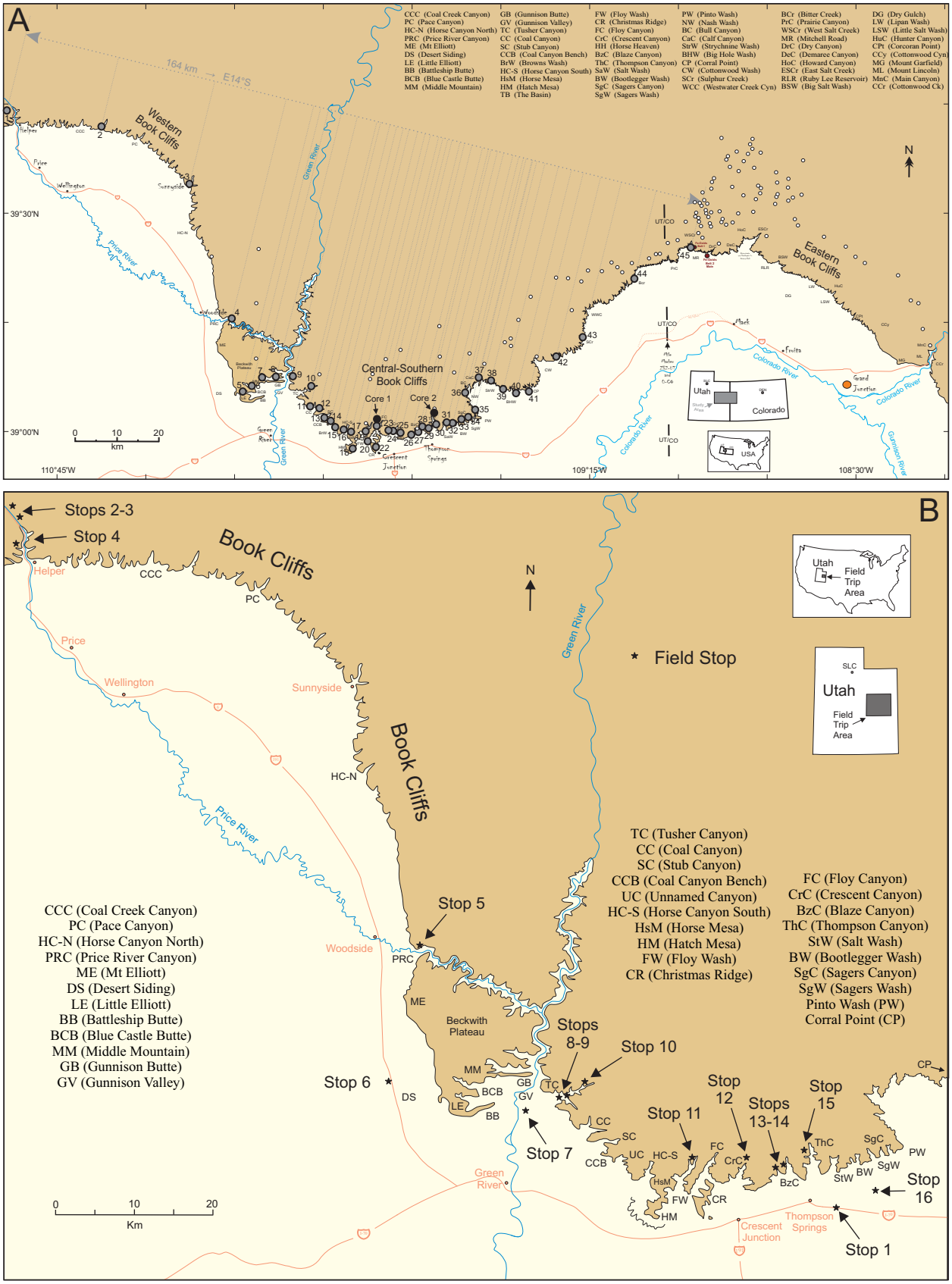

Figure 0-2. (A) Location map showing the entire Book Cliffs regions, from Helper Utah to Grand Junction Colorado. Book Cliffs are informally subdivided into three regions: western, central-southern, and eastern. Desert-Castlegate measured sections (grey circles, numbered 1 to 45), well logs (white circles), and Shell cores (black circles) are shown. Distances between adjacent Desert-Castlegate measured sections are projected orthogonal to the N14°E paleoshoreline trend, with these distances used for spacing on the high resolution correlation panel. Down-depositional-dip distance between "end-member" sections 1 (Castle Gate, UT) and 45 (West Salt Creek, CO) is 164 km. Key canyons, creeks, mesas, washes, buttes, and other landmarks are abbreviated. See legend at top for full names. Latitude and longitude is marked in 15 minute increments. (B) Map showing field stop localities.

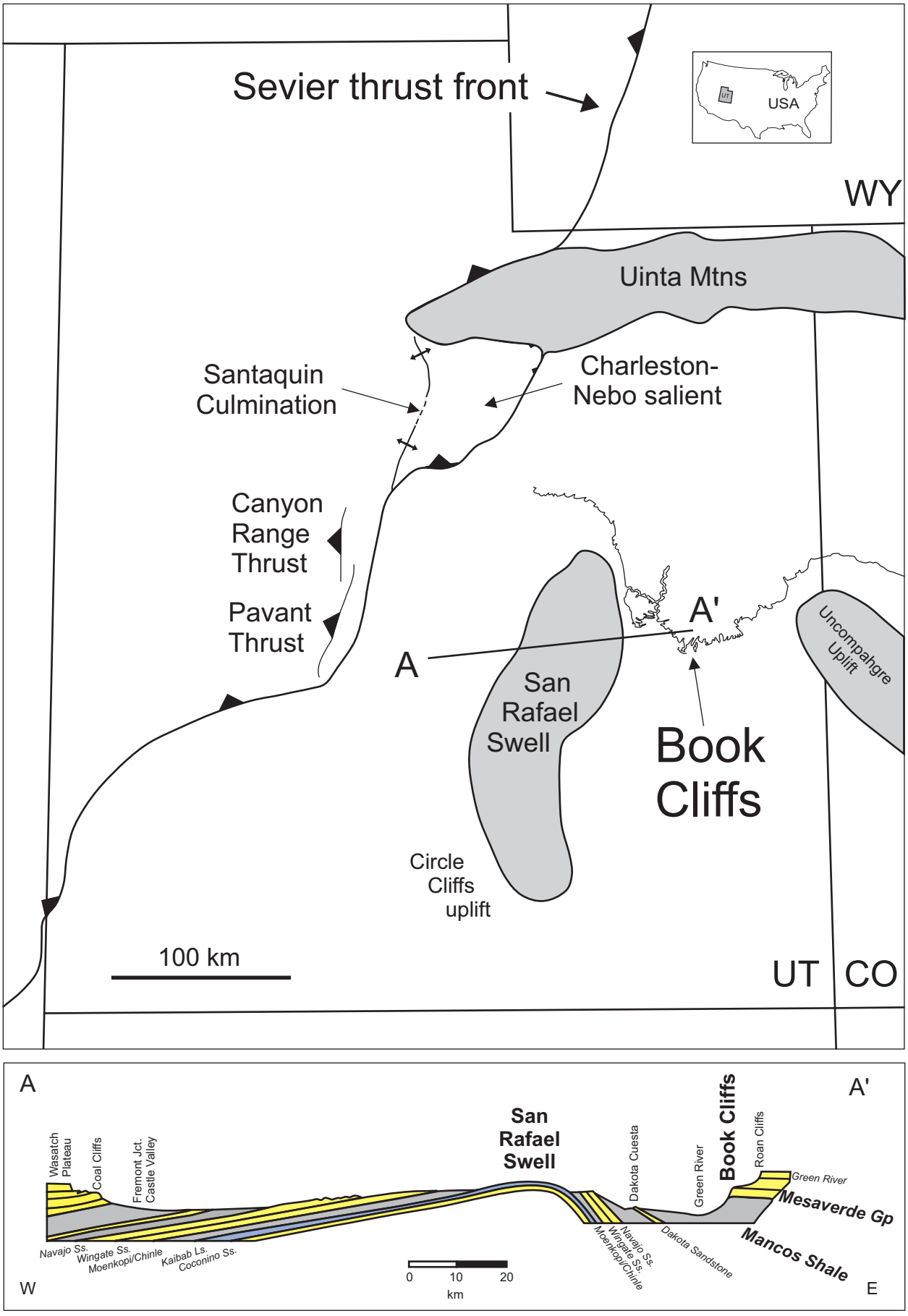

Figure 0-3. Map of key structural features in Utah (modified from Horton et al. 2004) and cross section across the San Rafael Swell (modified from Chronic 1990). Location of Utah on the USA inset map. UT (Utah), CO (Colorado), WY (Wyoming).

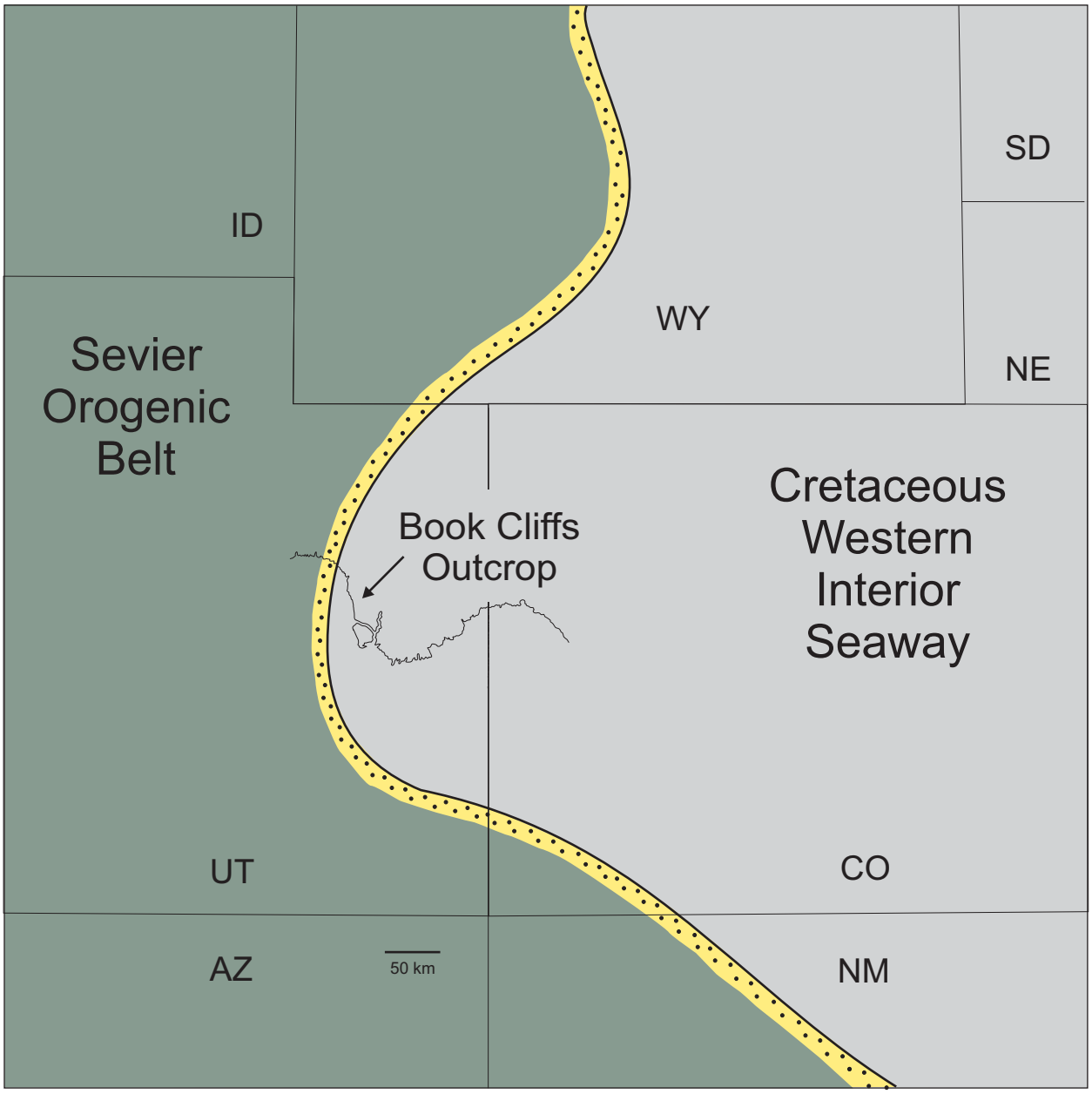

Figure 0-4. Paleogeography of the Cretaceous Western Interior Seaway (modified from McGookey et al. 1972). Outline of the Book Cliffs outcrop belt is superimposed onto the paleogeography. Terrestrial environments (green), shallow marine facies belts (yellow), and shelf environment (grey).

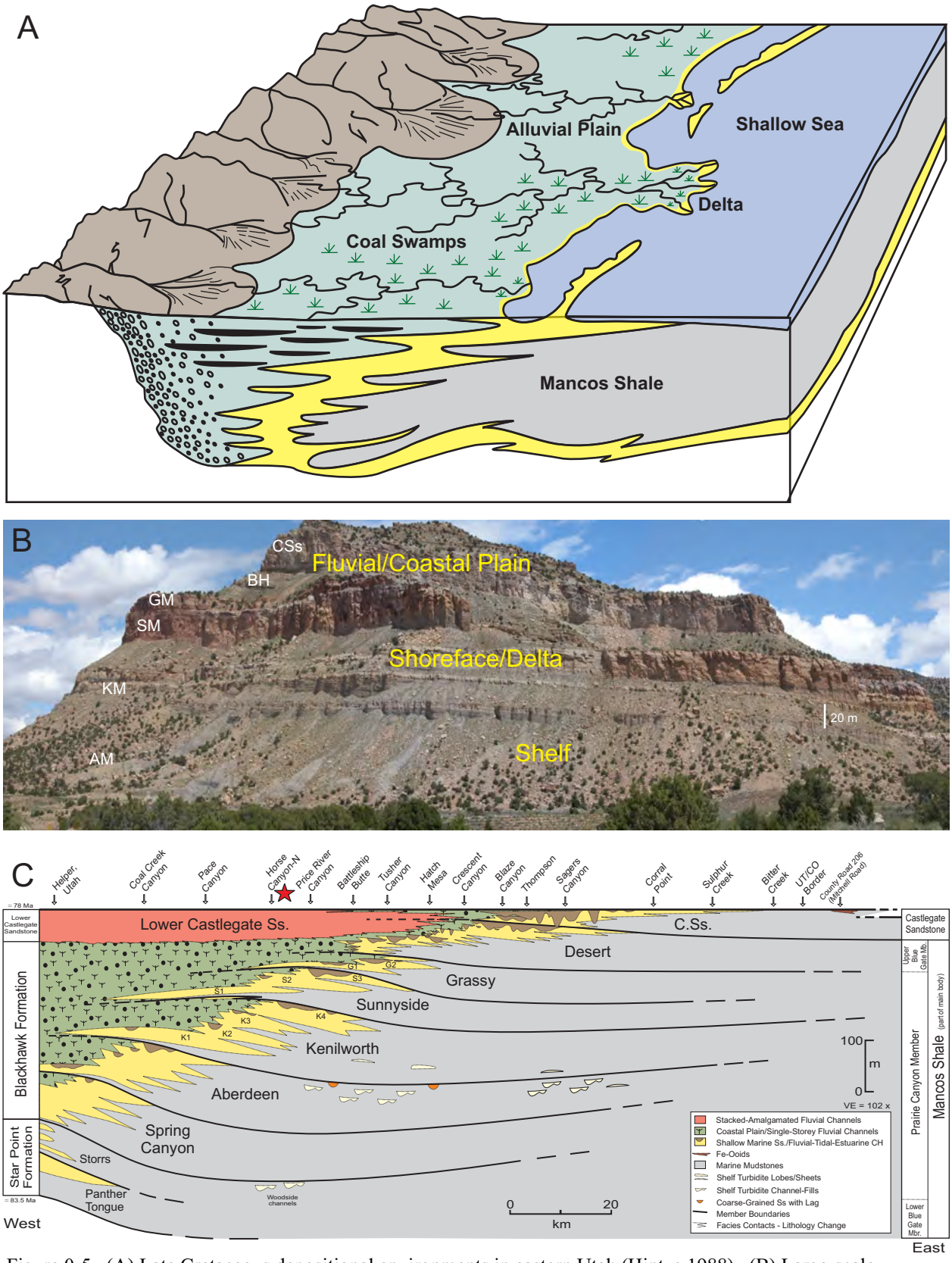

Figure 0-5. (A) Late Cretaceous depositional environments in eastern Utah (Hintze 1988). (B) Large-scale progradational stacking of shelf, shoreface-deltaic, and fluvial-coastal plain deposits, Horse Canyon-North. CSs (Lower Castlegate Sandstone), BH (Blackhawk Formation), GM (Grassy Member), SM (Sunnyside Member), KM (Kenilworth Member), AM (Aberdeen Member). (C) Scaled stratigraphic dip-oriented cross section of the Book Cliffs region, Helper Utah to western Colorado (modified from Young 1955; Cole et al., 1997; Pattison et al., 2007; Pattison 2010). Member boundaries have been extended westward into the undifferentiated Blackhawk Formation coastal plain, and eastward into the Mancos Shale. The Blackhawk Formation and Lower Castlegate Sandstone interfinger both laterally and vertically. This is a facies contact, not an unconformity. Key localities are shown along the top. Horse Canyon-North (red star). Approximate ages for the top of the Lower Castlegate Sandstone (≈ 78 Ma) and base Star Point Formation (≈ 83.5 Ma) is shown to the left (*as per* Fouch et al., 1983). CH (channels), K1-K4 (Kenilworth Member parasequences 1 to 4), S1-S3 (Sunnyside Member parasequences 1 to 3), G1-G2 (Grassy Member parasequences 1 and 2).

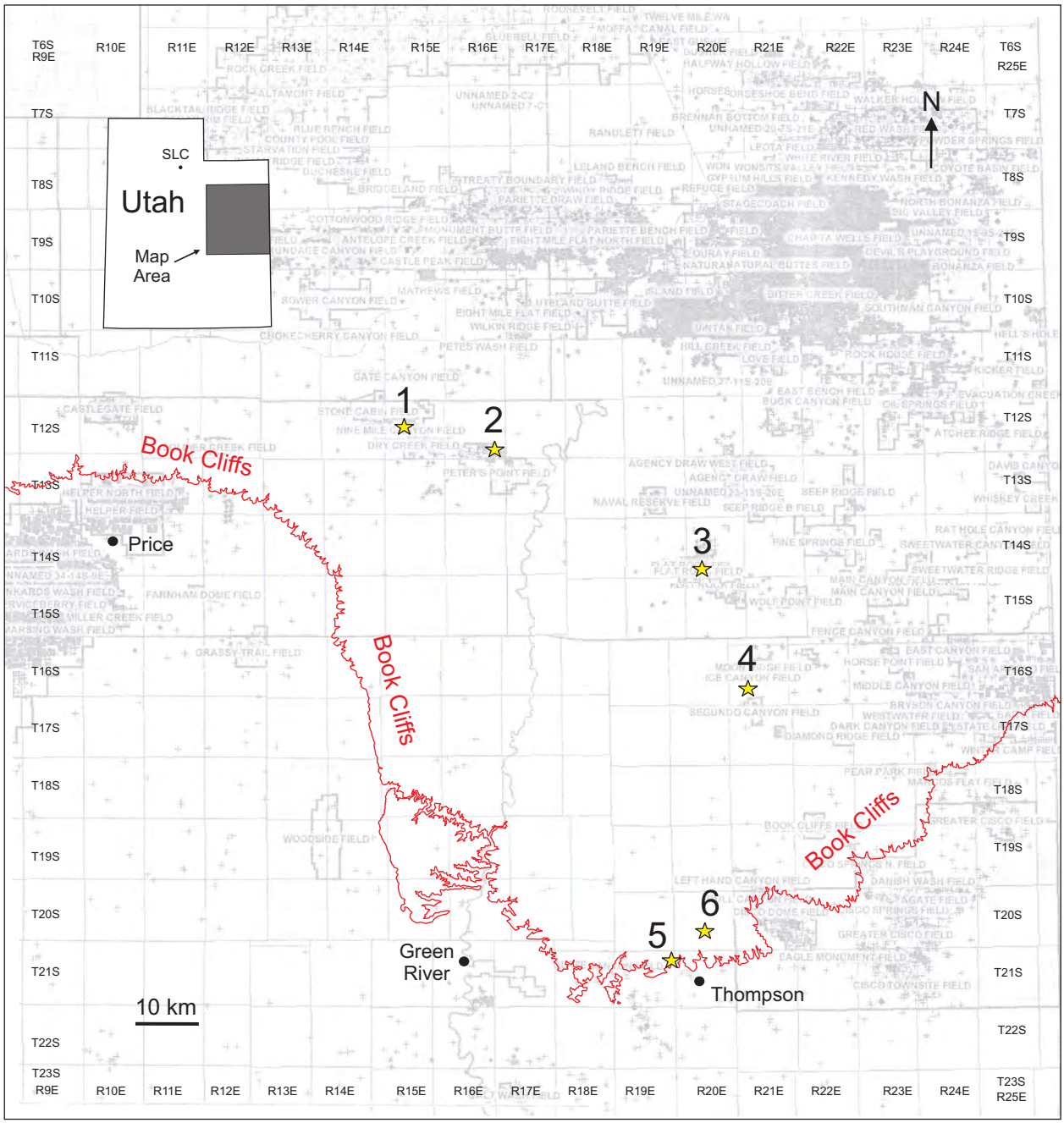

Figure 0-6. Location of six well log suites (yellow stars) included in this guidebook. Outline of the Book Cliffs outcrop belt, location of main oil and gas fields, and Twp-Range grid are shown. Wells are numbered as follows:

(1) PRICKLY PEAR U ST 13-16. Located at SWSW-16-12S-15E. API Well Number 43-007-30933. Nine Mile Canyon Field.

(2) PETERS POINT U FED 36-2. Located at NWNW-36-12S-16E. API Well Number 43-007-30761. Peter's Point Field.

(3) UTE TRIBAL 32-2A. Located at NWNW-32-14S-20E. API Well Number 43-047-33333. Flat Rock Field.

(4) MOON CANYON 1. Located at NWSW-32-16S-21E. API Well Number 43-019-31398. Undesignated Field Grand County.

(5) EPR BLAZE CANYON 1. Located at NESW-7-21S-20E. API Well Number 43-019-31228. Wildcat Grand County.

(6) EPR SEGO CANYON 2. Located at NW-27-20S-20E. API Well Number 43-019-31232. Wildcat Grand County.

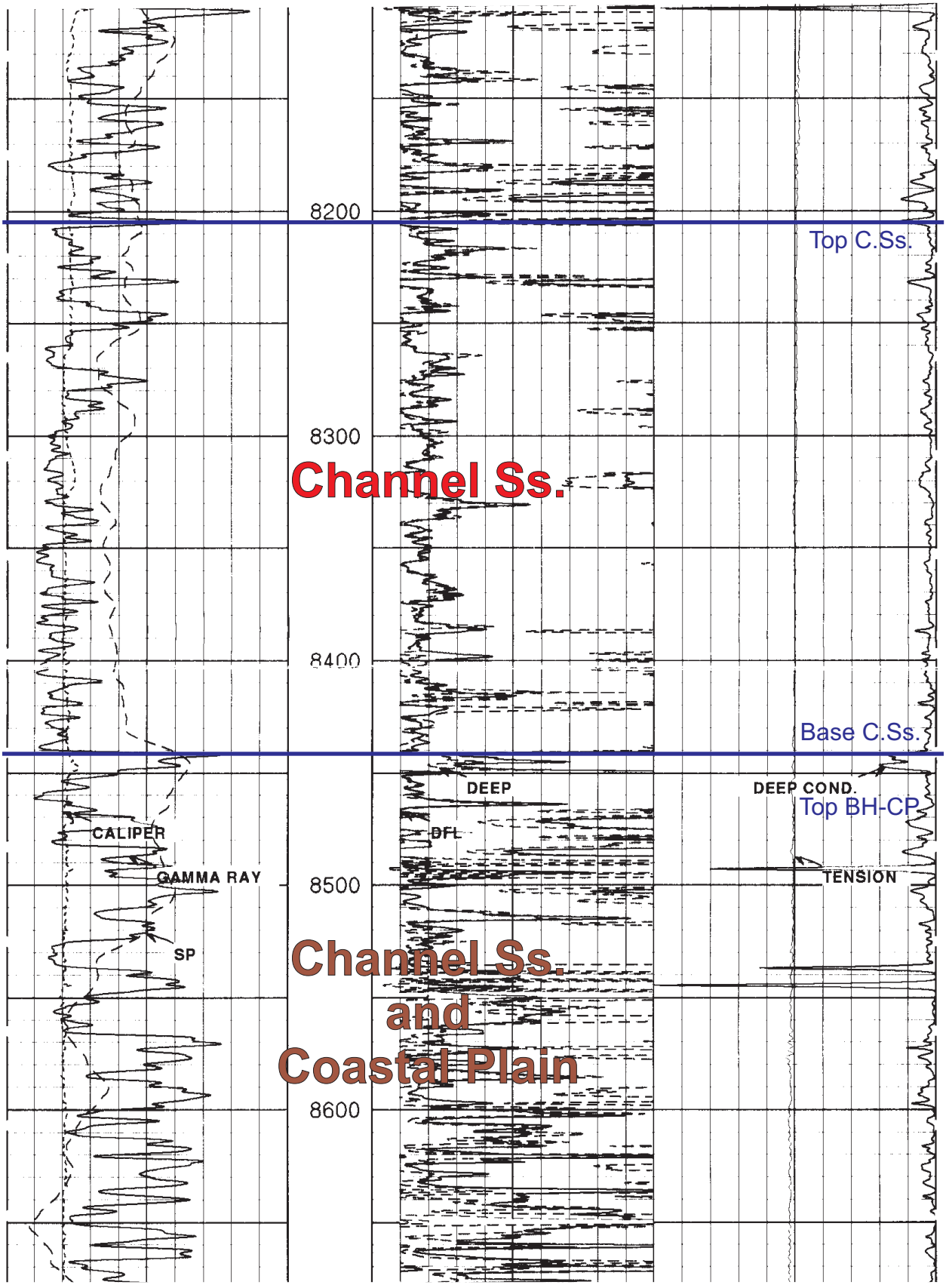

Figure 0-7. PRICKLY PEAR U ST 13-16 (1 of 2). Located at SWSW-16-12S-15E. API Well Number 43-007-30933. Nine Mile Canyon Field. C.Ss. (Castlegate Sandstone), BH (Blackhawk Formation), DM (Desert Member), GM (Grassy Member), MS (Mancos Shale), CP (Coastal Plain), S-D (shoreface/deltaic), Ss. (Sandstone), H (Heterolithics), Mst. (Mudstone).

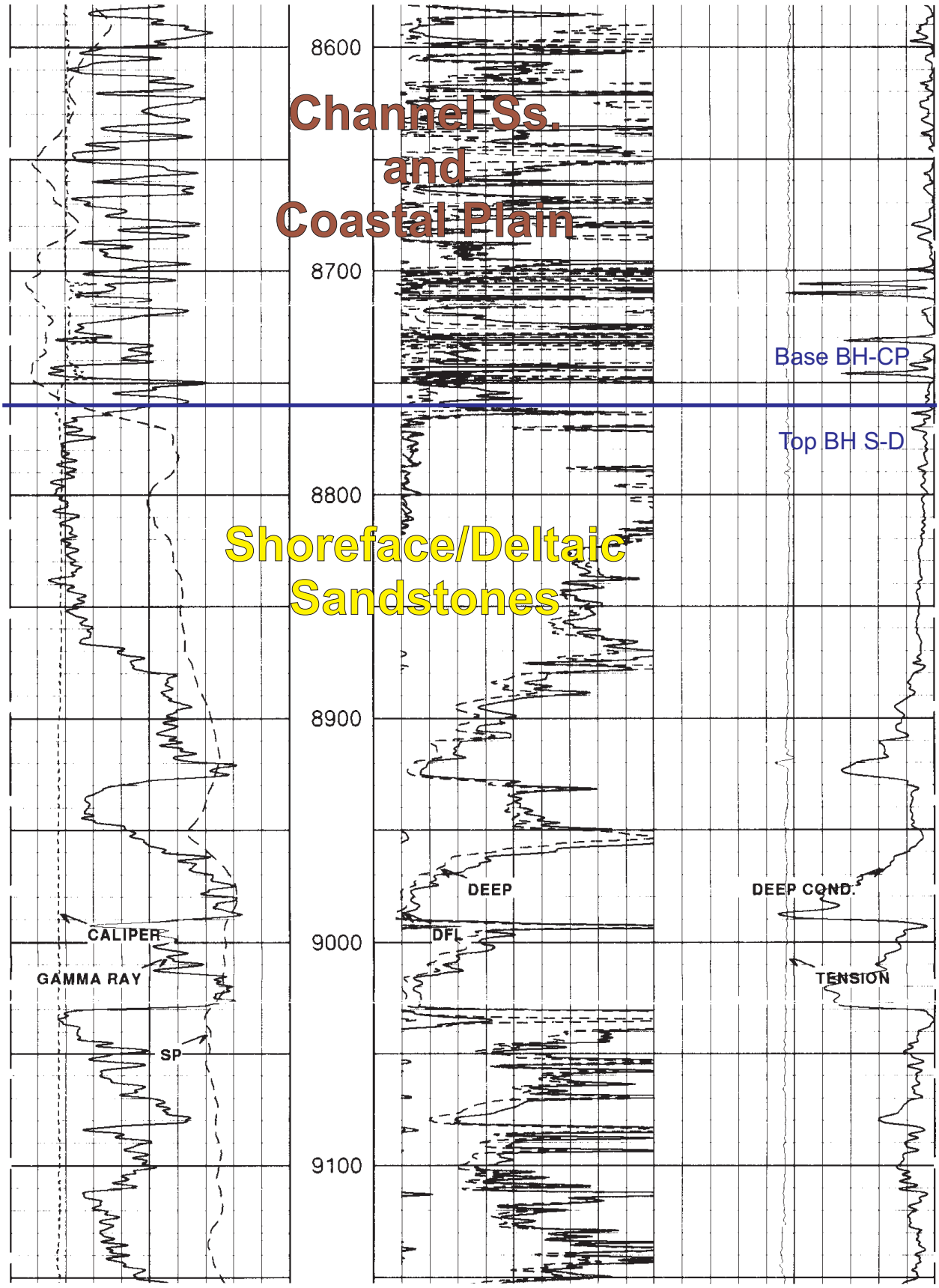

Figure 0-7 (con't). PRICKLY PEAR U ST 13-16 (2 of 2). Located at SWSW-16-12S-15E. API Well Number 43-007-30933. Nine Mile Canyon Field.

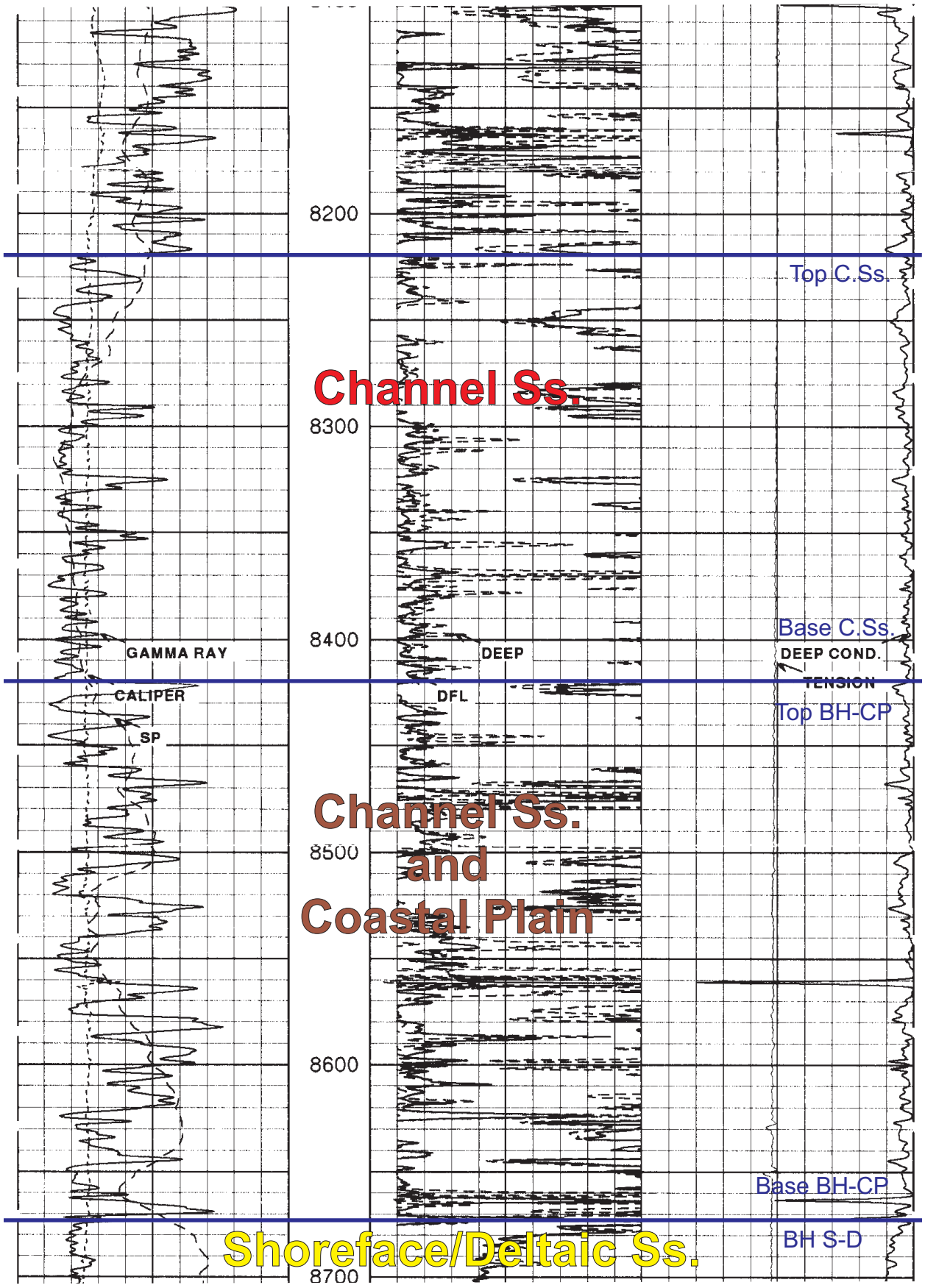

Figure 0-8. PETERS POINT U FED 36-2 (1 of 2). Located at NWNW-36-12S-16E. API Well Number 43-007-30761. Peter's Point Field.

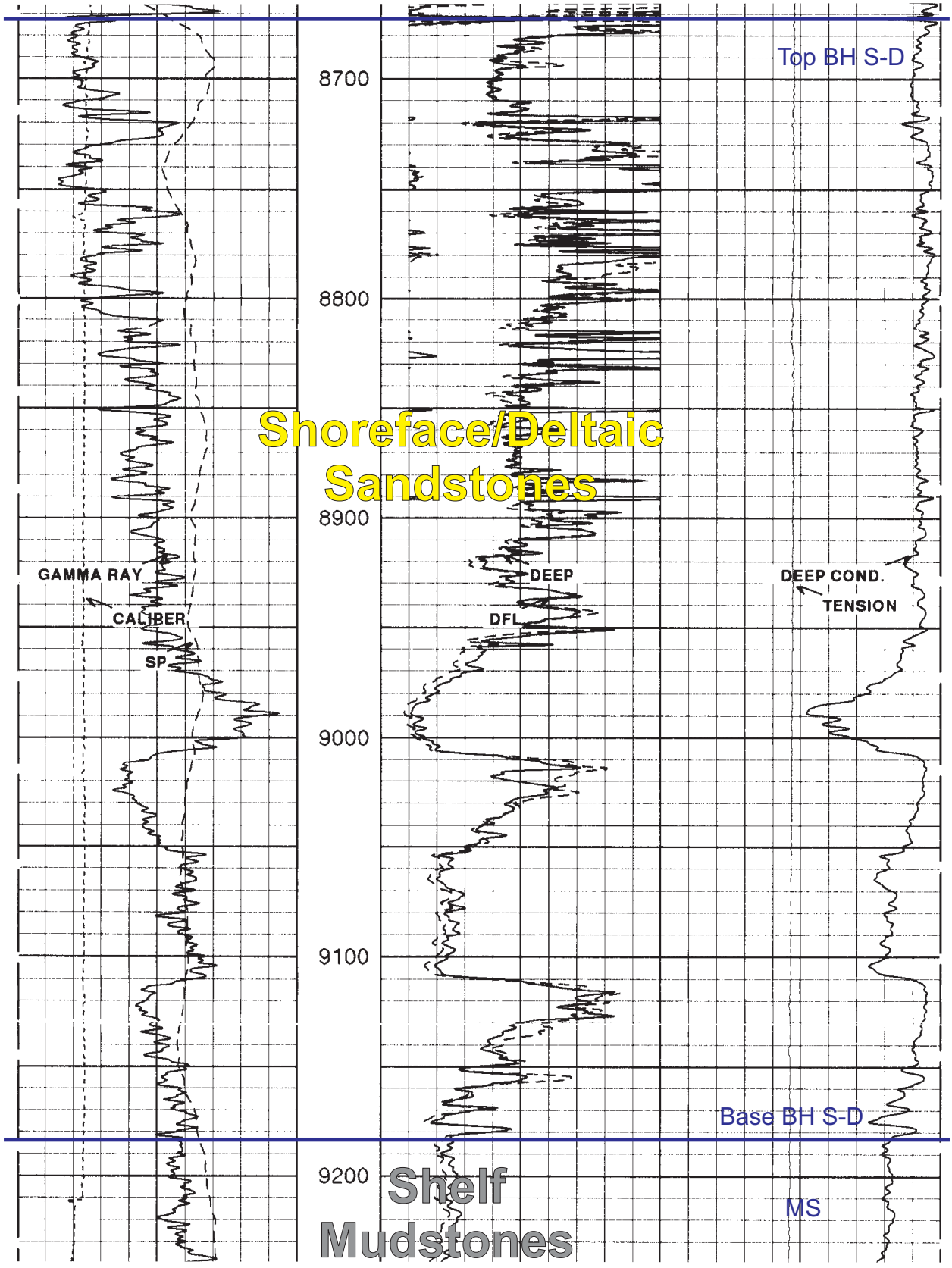

Figure 0-8 (con't). PETERS POINT U FED 36-2 (2 of 2). Located at NWNW-36-12S-16E. API Well Number 43-007-30761. Peter's Point Field.

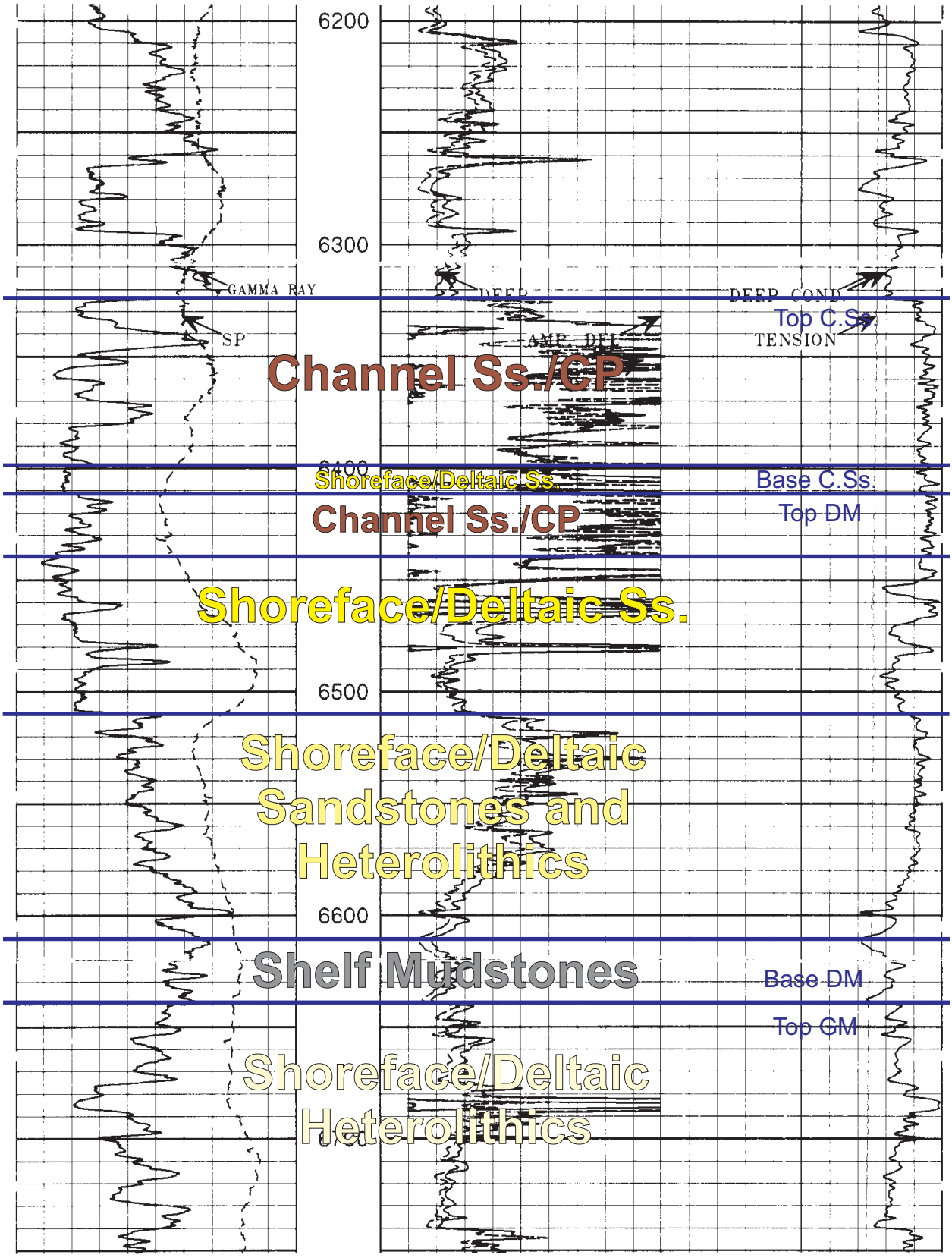

Figure 0-9. UTE TRIBAL 32-2A. Located at NWNW-32-14S-20E. API Well Number 43-047-33333. Flat Rock Field.

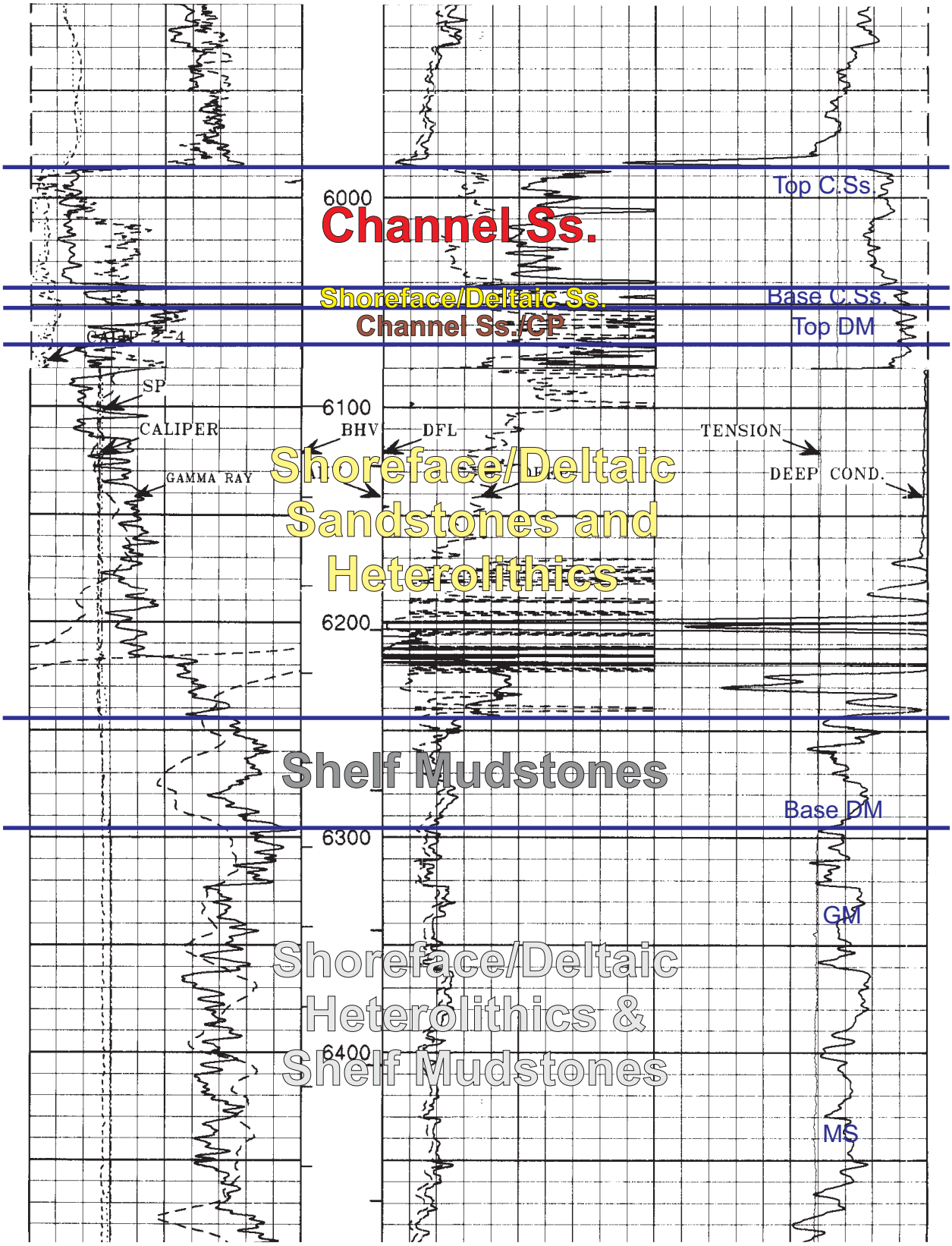

Figure 0-10. MOON CANYON 1. Located at NWSW-32-16S-21E. API Well Number 43-019-31398. Undesignated Field Grand County.

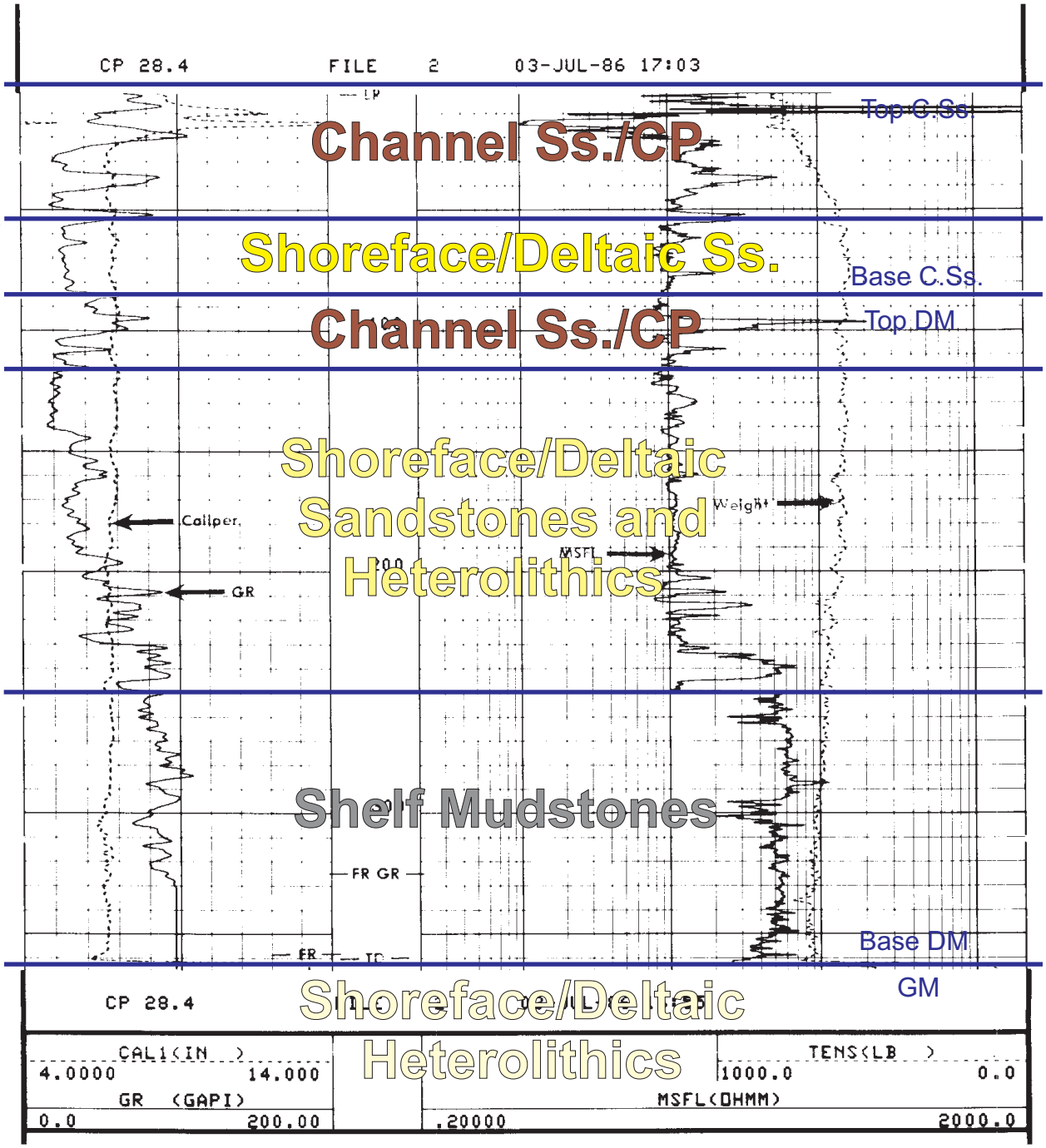

Figure 0-11. EPR BLAZE CANYON 1. Located at NESW-7-21S-20E. API Well Number 43-019-31228. Wildcat Grand County.

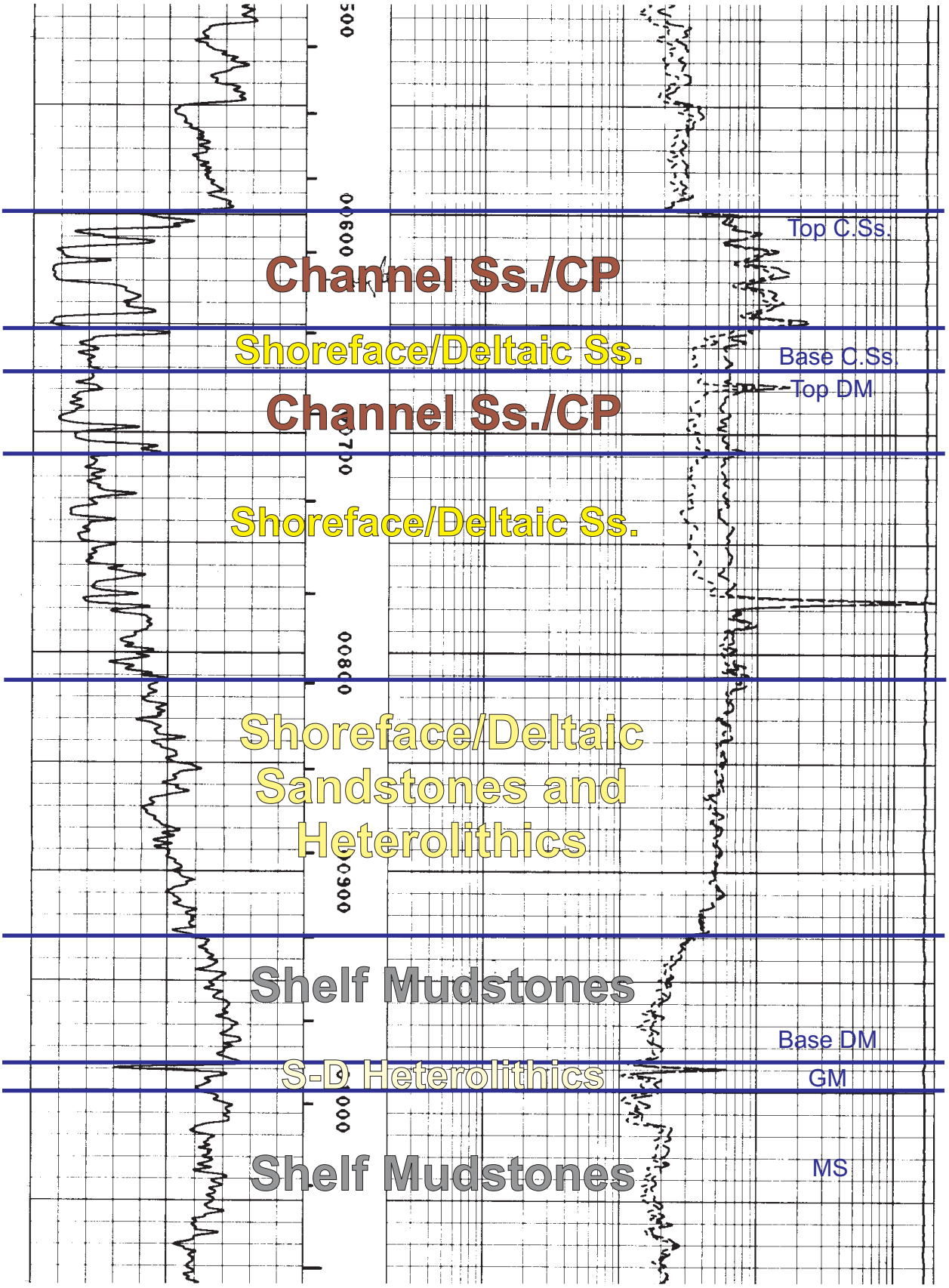

Figure 0-12. EPR SEGO CANYON 2. Located at NW-27-20S-20E. API Well Number 43-019-31232. Wildcat Grand County.

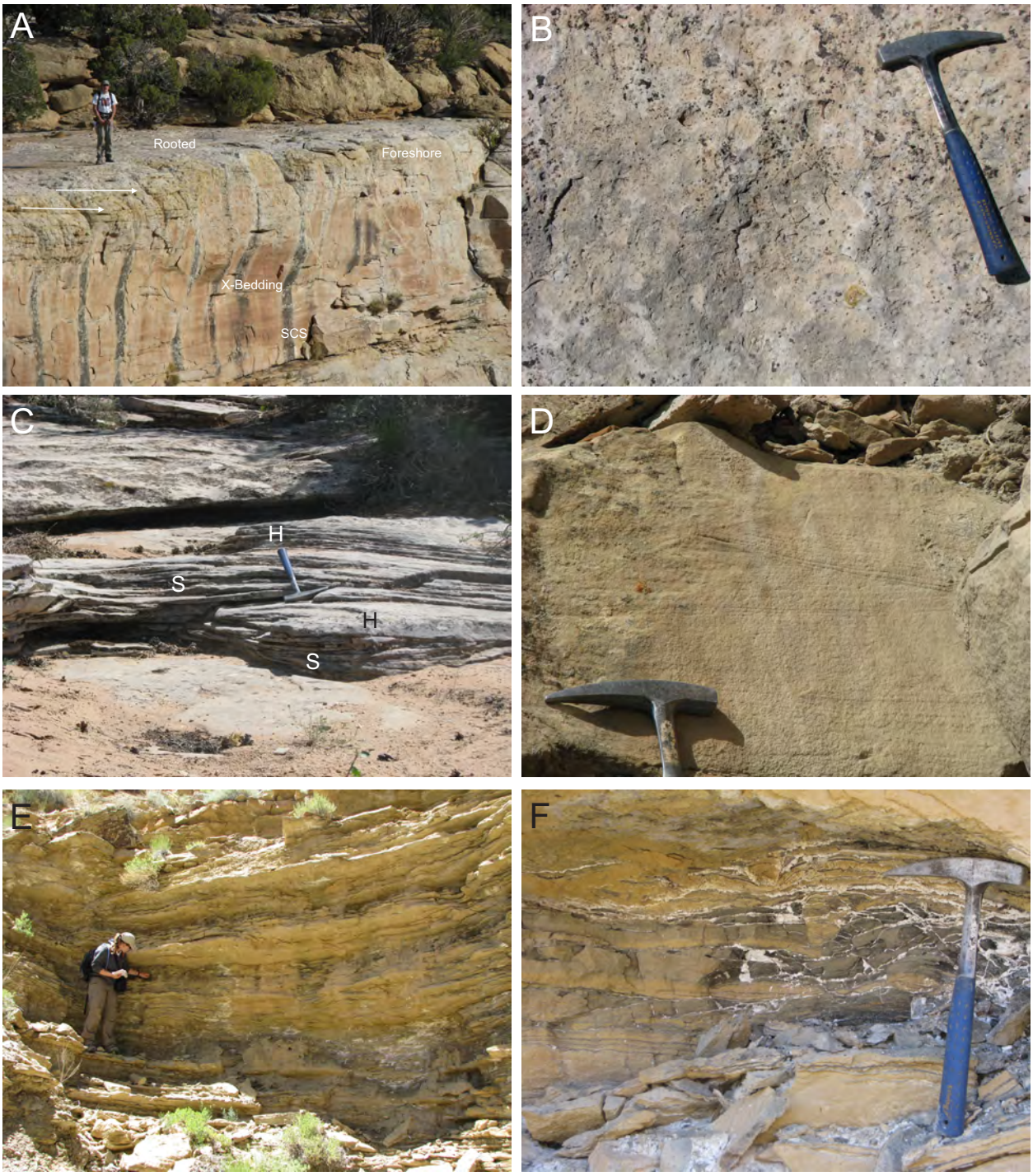

Figure 0-13. Shallow marine facies. (A) Flat-topped, rooted foreshore sandstones overlying upper shoreface facies in the upper part of parasequence D10, Horse Heaven NW Bowl. Gently dipping planar laminated sandstones (Facies 1A), trough cross bedded sandstones (Facies 1B), and swaley cross stratified (SCS) sandstones (Facies 1C). Arrows highlight the offshore-directed dip of the planar laminations. Geologist Mark Kirschbaum for scale. (B) Rooted top of the foreshore (beach) sandstones (Facies 1A), top of parasequence D10, Horse Heaven, SW Bowl. (C) Hummocky cross stratified (HCS) sandstones (Facies 1D), parasequence D10A, Thompson Canyon. Bedform has meter-scale wavelength, with well defined hummocks (H) and swales (S). Rock hammer for scale. (D) HCS sandstones (Facies 1D), basal part of parasequence D11A, West of Blaze Canyon. (E) Thinly bedded HCS and wave-rippled sandstones (Facies 1D and 1E), within bioturbated sandy siltstones (Facies 1F-i) and bioturbated silty mudstones (1G-i). These lower shoreface to inner shelf deposits are in Desert Member parasequence D5, Left Fork-The Basin. Geologist Jenna Phillips for scale. (F) Low BI silty mudstone (Facies 1G-ii) and thinly bedded wave-rippled sandstones (Facies 1E), parasequence D4, Horse Canyon.

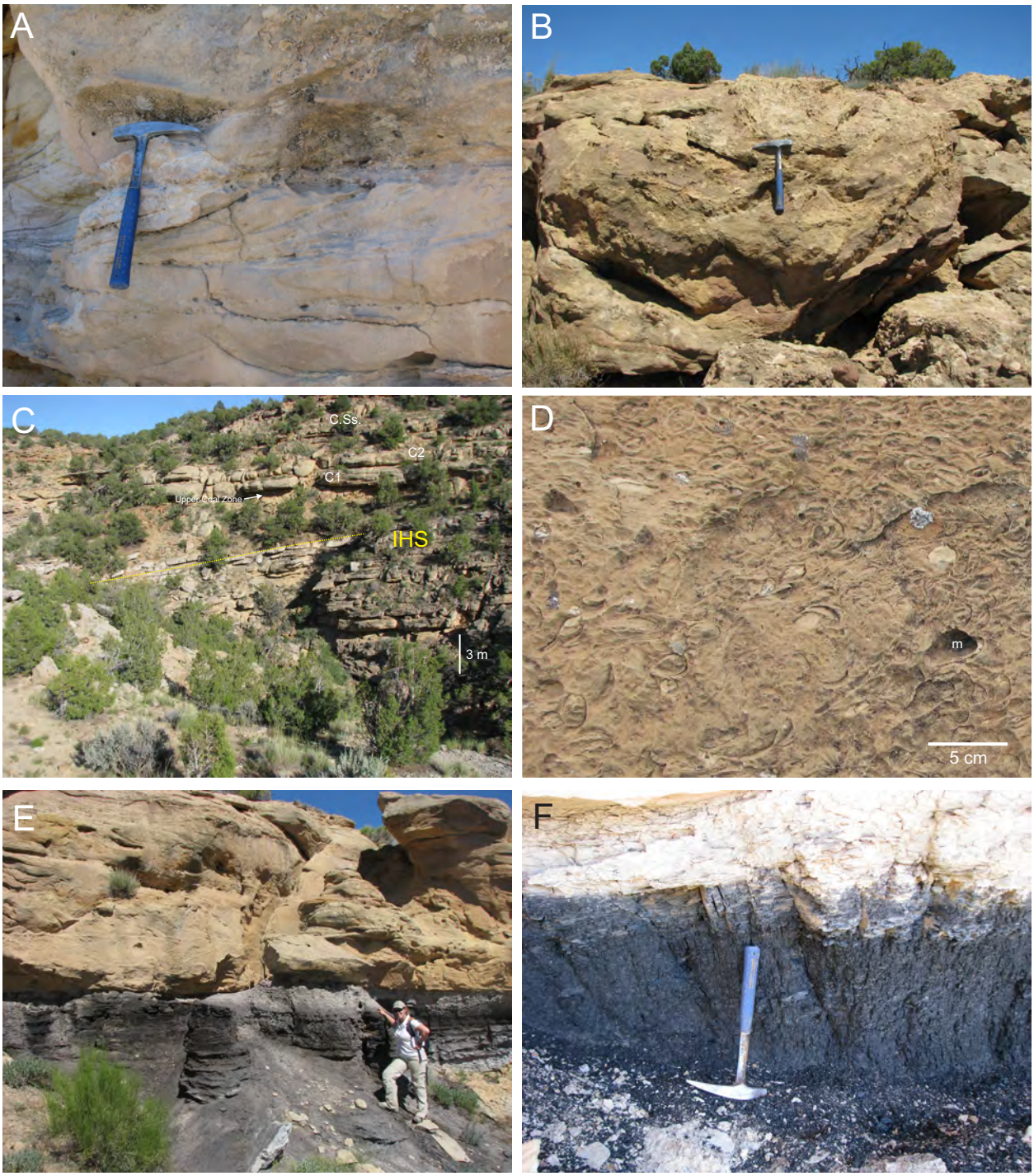

Figure 0-14. Channel and coastal plain facies. (A) Trough cross bedded fU-mL sandstone (Facies 2A), Lower Castlegate Sandstone, The Basin. (B) Convolute bedded fU-mL sandstone (Facies 2B), Lower Castlegate Sandstone, The Basin. (C) Large-scale inclined heterolithic strata (IHS) in parasequence D11, Thompson Canyon (Facies 2E). (D) Fossiliferous/Fe-cemented sandy breccia ("Coquina"; Facies 2J), Lower Castlegate Sandstone, Salt Wash Canyon. Mold (m). (E) Thick bed of carbonaceous-rich shale and mudstone (Facies 3E and 3D), The Basin. Sharply overlain by channel sandstones. Geologist for scale. (F) Coal (Facies 3F), Christmas Ridge.

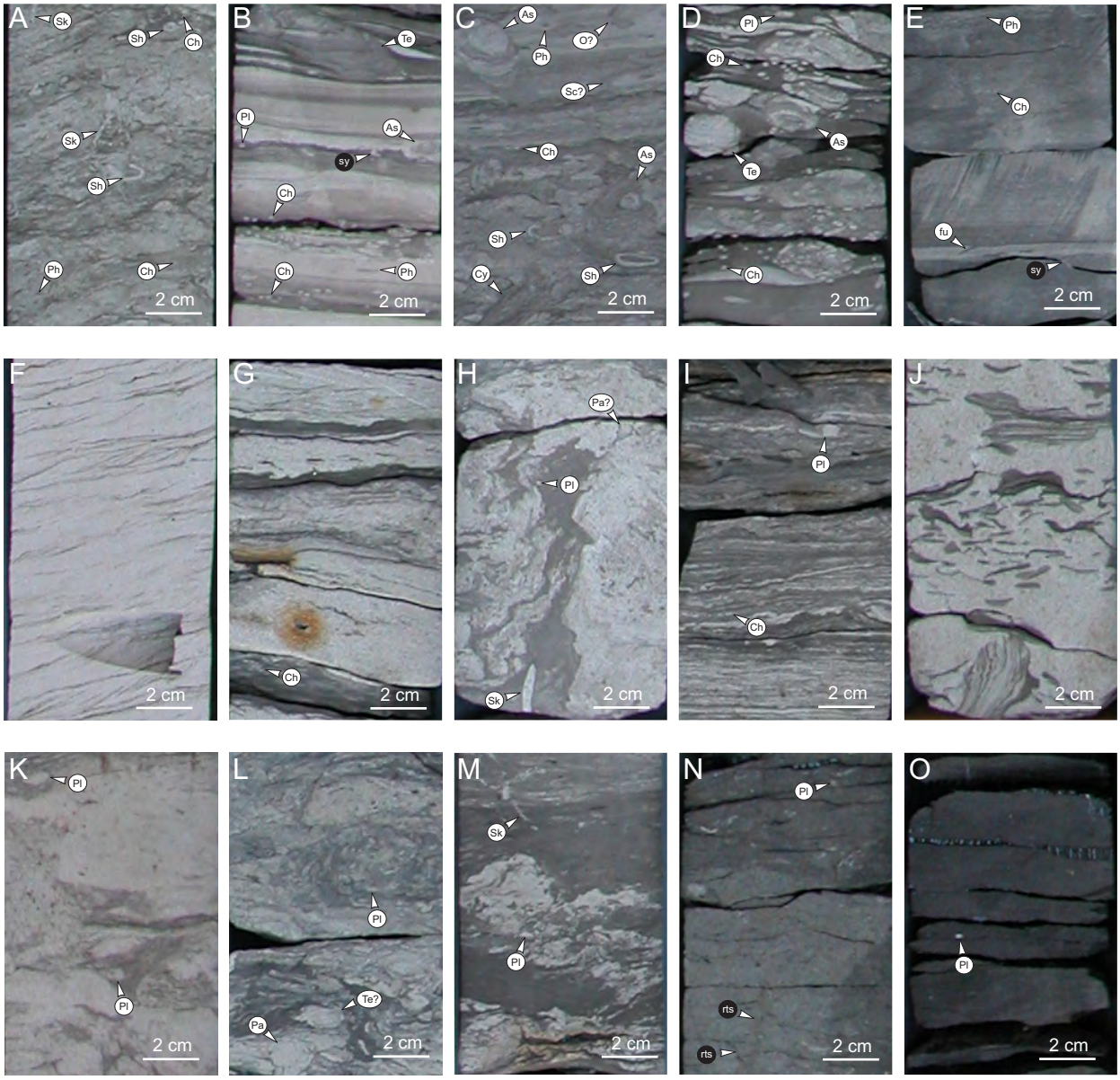

Figure 0-15. Core photographs of shallow marine facies (A-E), channel facies (F-J), and non-channelized coastal plain facies (K-O). All core photographs from the Desert Member-to-Lower Castlegate Sandstone interval. Shell cores from Floy Canyon (FC) and Thompson Canyon (TC). White circles with black latters: *Asterosoma* (As), *Chondrites* (Ch), *Cylindrichnus* (Cy), Fugichnia/Escape Trace (fu), *Ophiomorpha* (O), *Palaeophycus* (Pa), *Phycosiphon* (Ph), *Planolites* (Pl), *Scolicia* (Sc), *Schaubcylindrichnus* (Sh), *Skolithos* (Sk), *Teichichnus* (Te). Black circles with white letters: synaeresis cracks (sy), roots (rts). (A) Facies 1F-I. Thoroughly-bioturbated (BI = 5) sandy siltstone. Parasequence D9. TC, Depth = 401 ft. (B) Facies 1F-ii. Mildly-to-non-bioturbated (BI = 0-2) sandy siltstone, interbedded with wave rippled very fine-grained sandstone (Facies 2E). Parasequence D9. TC, Depth = 438.5 ft. (C) Facies 1G-I. Moderately-to-thoroughly bioturbated (BI = 4-5) silty mudstone. Parasequence D5. FC, Depth = 369 ft. (D) Facies 1G-ii. Mildly-bioturbated (BI = 2-3) silty mudstone. Base of parasequence D10. TC, Depth = 399 ft. (E) Facies 1H. Dark grey mudstone. Very thin-beds of normally-graded siltstone. Low degree of bioturbation (BI = 1-2). Parasequence D4. FC, Depth = 399.5 ft. (F) Channel Facies 2D. Current rippled fL sandstone. Inclined heterolithic strata. Abundant carbonaceous matter. TC, Depth = 219.5 ft. (G) Channel Facies 2E. Gently dipping sandstone and mudstone. Inclined heterolithic strata with coal clasts. FC, Depth = 156 ft. (H) Channel Facies 2F. Carbonaceous-rich sandstone. Convolute bedded. FC, Depth = 151 ft. (I) Channel Facies 2G. Carbonaceous-rich siltstone. Rhythmically pin-striped laminated. Fining-upward succession. FC, Depth = 78.5 ft. (J) Channel Facies 2I. Mudstone-clast pebble breccia. FC, Depth = 91.5 ft. (K) Coastal plain Facies 3B. Non-channelized, carbonaceous-rich sandstone. FC, Depth = 116 ft. (L) Coastal plain Facies 3C. Non-channelized, carbonaceous-rich siltstone. Bioturbated. FC, Depth = 150 ft. (M) Coastal plain Facies 3C. Non-channelized, carbonaceous-rich siltstone. Large angular coal clast. TC, Depth = 258 ft. (N) Coastal plain Facies 3D. Non-channelized, carbonaceous-rich mudstone. Roots and coal clasts. FC, Depth = 167.5 ft. (O) Coastal plain Facies 3E. Non-channelized, carbonaceous shale. Large coal clast. FC, Depth = 232 ft.

Shallow Marine Facies:

Depositional Environment	Facies Name	Description
Foreshore	1A - Planar Laminated Sandstone	Consists of well sorted, planar laminated, fL-mL sandstone. Numerous *Macaronichnus* locally, with a BI (Bioturbation Index) of 0-3. Offshore-directed low angle dips (2-5°) on the laminations. Flat, densely rooted top, with individual root traces up to 30 cm long. Most are 2-10 cm long and 1-2 mm wide. Bleached white sandstone at top, which are common in the Book Cliffs and referred to as a "white cap" (Young 1955). Overlain by fine-grained coastal plain and/or coal facies (3D, 3E, 3F), and underlain by cross bedded and/or SCS sandstones facies (1B, 1C).
Upper shoreface; fair weather deposition.	1B - Trough Cross Bedded Sandstone	Predominantly well sorted, trough cross bedded, fL-mU sandstone. Scattered *Macaronichnus*, and *Ophiomorpha*, with a BI = 0-2. Within each parasequence, the trough cross bedded sandstones are laterally continuous along depositional strike and are confined within a narrow facies belt (≈ 1 km) along depositional dip. Interbedded with SCS sandstones (Facies 1C). Typically overlain by planar laminated sandstones (1A) and underlain by HCS sandstones (1D). Cross beds reveal a mean paleoshoreline orientation of 215° (i.e. N35°E-S35°W). Vector magnitude = 56.5 (n=299).
Upper shoreface; storm deposition.	1C - Swaley Cross Stratified (SCS) Sandstone	Well to very well sorted, swaley cross stratified (SCS), vfU-fU sandstone. Uncommon and sporadically distributed *Ophiomorpha*. *Skolithos*, and *Schaubcylindrichnus*. Low BI varying from 0-2. Similar to the trough cross bedded facies, the SCS sandstones are laterally continuous along depositional strike (i.e. within a parasequence), but are confined within a narrow facies belt (≤ 1 km) along depositional dip. Meter-scale swale lengths are common, with a maximum of 5 m. Swale amplitudes are mostly 15-70 cm. Interbedded with trough cross bedded sandstones (Facies 1B) and HCS sandstones (1D).
Lower shoreface to inner shelf; storm deposition.	1D - Hummocky Cross Stratified (HCS) Sandstone	Hummocky cross stratified (HCS), well to very well sorted, vfL-fU sandstone. Diverse trace fossil suite dominated by *Macaronichnus*, *Phycosiphon*, *Ophiomorpha*, and *Cylindrichnus*, with lesser *Teichichnus*, *Rosselia*, *Skolithos*, *Asterosoma*, *Palaeophycus*, *Chondrites*, *Scolicia*, *Conichnus*, *Planolites*, and *Rhizocorallium*. BI = 0-4. Greater degree of bioturbation in the upper parts of most HCS beds. Laterally continuous along depositional strike. Wider facies belt compared to the trough cross bedded and SCS sandstones. Some HCS beds can be correlated for > 5 km down-depositional-dip. Beds become thinner and finer grained basinwards. Also show a progressive decrease in hummock wavelength and amplitude basinwards. HCS sandstone package wedges-out offshore, transitioning into siltstones and mudstones (Facies 1F, 1G, 1H). HCS beds have meter-scale wavelength and decimeter-scale amplitude. Wavelengths and amplitudes show a progressive decrease upwards. Many beds are capped by wave-rippled to combined flow-rippled sandstones. Fining-upward successions are common. Some pin-striped carbonaceous-rich laminae in upper parts of beds. The majority of HCS beds are sharp-based and erosive. Rare gutter-casts. Interbedded with SCS sandstones (Facies 1C), wave-rippled sandstones (1E), sandy siltstone (1F), and silty mudstone (1G). Sub-angular to sub-rounded, elongated mudstone clasts (fine sand to pebble size) are observed in the basal parts of a few HCS beds. Mudstone clasts comprise 5-15 % of these beds, and are concentrated in discrete layers, or scattered throughout. Tightly cemented (Fe-, Ca-, and/or Si-rich), concretionary-like HCS beds cap the tops of some parasequences.

Lower shoreface to inner shelf; mixed fair weather and storm deposition.	1E - Wave-Rippled Sandstone	Well to very well sorted, wave rippled, vfL-fL sandstone. Some coarse silt. Rare combined flow ripples and normally graded bedding. Diverse trace fossil suite includes *Asterosoma*, *Phycosiphon*, *Planolites*, *Teichichnus*, *Chondrites*, *Skolithos*, *Ophiomorpha*, *Cylindrichnus*, *Helminthopsis*, and *Schaubcylindrichnus*, with a BI varying between 0 and 4. Laterally continuous sandstone beds become progressively thinner and finer grained basinwards. Collectively the wave-rippled sandstone beds form a sheet-like geometry that wedges/thins both landwards and basinwards. Wave-rippled sandstones occur both as discrete beds and at the top of many HCS sandstone beds (Facies 1D). The latter is a gradational facies contact. Almost all beds are 2-10 cm thick and are sharp-based. Interlaminated mudstone occur infrequently. Wave-rippled sandstones are interbedded with sandy siltstone (1F), silty mudstone (1G), and dark grey mudstone (1H).
Lower shoreface to mid-shelf; no freshwater influence.	1F-i - Moderate-to-High BI Sandy Siltstone	Mostly coarse-grained siltstone with varying amounts of vfL-vfU sand and mudstone. Trace amounts of fU-mU sand. Moderately to moderately well sorted. Some wave ripples, combined flow ripples, and normally graded beds. Beds are 2-60 cm thick. Trace fossils include *Asterosoma*, *Chondrites*, *Phycosiphon*, *Ophiomorpha*, *Teichichnus*, *Planolites*, and *Cylindrichnus*, with associated *Schaubcylindrichnus*, *Skolithos*, and *Thalassinoides*. Scattered *Helminthopsis*, *Scolicia*, *Rosselia*, *Arenicolites*, and *Zoophycos*, as well as fugichnia. Moderate-to-high degree of bioturbation (BI = 3-6) generates a facies with thoroughly mixed silt, sand and clay. Facies package has a sheet-like geometry that wedges-out both landwards and basinwards. Laterally continuous along depositional strike. This facies dominates the medial parts of most parasequences and is basinwards of the main HCS sandstones facies belt. Interbedded with low BI sandy siltstone (Facies 1F-ii), silty mudstone (1G), wave-rippled sandstone (1E), and HCS sandstone (1D). More abundant than the low BI sandy siltstone facies (1F-ii). Rare carbonaceous-rich laminae. Scattered phyto-detritus (finely disseminated plant debris). Sparse SA to SR, medium sand- to pebble-sized, mudstone and coal clasts. No synaeresis cracks.
Lower shoreface to mid-shelf; commonly freshwater influenced.	1F-ii - Low BI Sandy Siltstone	Coarse-grained siltstone with varying amounts of vfL-vfU sand and mudstone. Moderately to moderately well sorted. Discretely bedded-laminated, with abundant pin-striped mudstone, siltstone and vfL-vfU sandstone laminae. Silt, sand and clay form discrete laminae and/or beds. Numerous wave ripples. Some combined flow ripples and normally graded beds. Low to very low bioturbation intensity(BI = 0-2), with some *Chondrites*, *Planolites*, *Phycosiphon*, and *Asterosoma*, and lesser *Teichichnus*, *Ophiomorpha*, *Cylindrichnus*, *Skolithos*, *Thalassinoides*, *Schaubcylindrichnus*, *Scolicia*, *Helminthopsis*, and *Zoophycos*. Rare fugichnia. Facies occurs sporadically, and is not as volumetrically abundant as Facies 1F-i. Overall sheet-like geometry. Mostly interbedded with moderate-high BI sandy siltstone (Facies 1F-i), bit also Facies 1D, 1E, and 1G. Abundant synaeresis cracks. Siltstone and sandstone beds are 1-4 cm thick and are sharp-based. Bed tops are sharp-to-gradational, with the latter due to minor bioturbation, coupled with a fining-upward grain size trend. A few carbonaceous-rich laminae.
Lower shoreface to outer-shelf; sporadically freshwater influenced.	1G-i - Moderate-to-High BI Silty Mudstone	Moderately-to-highly bioturbated (BI = 3-6) silty mudstone has a near equal mixture of clay and fine-grained silt, with some vfL-vfU sand and medium-to-coarse-grained silt thoroughly mixed into the background mudstone. This facies is moderately to moderately well sorted. Wave ripples, combined flow ripples, and normally graded beds are rarely observed. Trace fossil suite is characterized by *Phycosiphon*, *Chondrites*, *Teichichnus*, *Planolites*, *Asterosoma*, *Schaubcylindrichnus*, *Cylindrichnus*, and *Scolicia*, with subordinate *Thalassinoides*, *Rhizocorallium*, *Ophiomorpha*, *Conichnus*, and *Palaeophycus*. Isolated fugichnia. Forms a laterally continuous, sheet-like geometry that occurs in distal portions of each parasequence. It grades up-depositional-dip into moderate-to-high BI sandy siltstone (Facies 1F-i) and down-depositional-dip into dark grey mudstone (1H). Facies belt 1G is correlatable for many kilometers within each

		parasequence, both along depositional-strike and -dip. Interbedded with low BI silty mudstone (Facies 1G-ii), sandy siltstone (1F), wave rippled sandstone (1E), and dark grey mudstone (1H). Rare and disseminated silt-to-sand-sized phyto-detrital fragments (i.e. plant material) and sub-angular, elongated, sand-to-granule-sized coal clasts. Isolated synaeresis cracks.
Lower shoreface to outer-shelf; freshwater influenced.	1G-ii - Low BI Silty Mudstone	Dominantly mudstone with lesser amounts of coarse siltstone and vfL-vfU sandstone that are concentrated as discrete laminae and thin beds (1-3 cm thick). Pin-striped laminae of mudstone, siltstone and sandstone are common. Minor mixing of very fine-grained sand and silt into the mudstone. Rare fU-mL sand laminae. Even rarer dispersed or intermixed fU-mL sand. Moderately to moderately well sorted. Abundant wave ripples. Lesser combined flow ripples and normally graded beds. Trace fossils predominantly comprise *Chondrites*, with minor *Planolites*, *Teichichnus*, *Phycosiphon*, *Asterosoma*, and *Schaubcylindrichnus*. Sparse fugichnia. Low intensity of bioturbation (BI = 0-2). Facies 1G-ii sometimes occurs as patches-lenses within thicker packages of moderate-to-high BI silty mudstone (Facies 1G-i), comprising approximately 20% of Facies 1G. This facies belt is laterally continuous along depositional-strike and -dip, within distal portions of each parasequence. Interbedded with moderate-high BI silty mudstone (Facies 1G-i), wave rippled sandstone (1E), and low BI sandy siltstone (1F-ii). Sharp contacts are observed between the interbeds. Plentiful synaeresis cracks. Isolated carbonaceous-rich laminae (i.e. finely disseminated phyto-detritus).
Inner-shelf to outer-shelf; rarely freshwater influenced.	1H - Dark Grey Mudstone	Dark grey to grey mudstone with some coarse silt and vfL sand. Moderately well to well sorted. Coarse silt and very fine-grained sand are concentrated in laminae or rarely dispersed throughout the background mudstone. Rare wave ripples and normally graded beds. Predominantly laminated, locally very thinly bedded (1.0-1.5 cm thick). Trace fossils dominated by *Chondrites*, with uncommon *Phycosiphon*, *Asterosoma*, *Planolites*, and *Schaubcylindrichnus*. Rare escape traces. Bioturbation index varies widely (BI=0-6). Laterally continuous, sheet-like geometry in distal portions of each parasequence. Transitions up-depositional-dip into silty mudstone (Facies 1G). Fe-rich carbonate-cemented concretions are concentrated along distal flooding surfaces. Uncommon synaeresis cracks.
Inner-to-outer shelf.	1I - Classical Turbidite	Planar laminated sandstones are regularly overlain by ripple laminated sandstones. Most sandstone beds are planar laminated to current rippled, with some showing a massive division at the base. Other beds are current rippled only. The sandstones are well sorted, very fine- to fine-grained, and sharp-based with numerous sole marks, such as flute, groove, prod, and bounce marks. Finely comminuted plant material is locally abundant. Rare *Palaeophycus* and *Schaubcylindrichnus* trace fossils are observed at the base of some sandstones beds. Otherwise, the sandstones have a very low bioturbation index (BI = 0-2).
Inner-to-mid shelf; distal delta front-to-prodelta.	1J - Wave-Modified Turbidite	Many sandstone beds have planar laminated fine-grained sandstones at the base, with or without gentle undulations, up to combined flow rippled very fine- to fine-grained sandstones at the top. Some have long wavelength (up to 2 m) and low amplitude (1-10 cm) gently curving planar laminations, with or without low angle truncation surfaces. Ripple laminated sandstone beds are sharp-based, well sorted, consist of very fine-grained sands and are 1 to 50 cm thick. Weakly- to strongly-asymmetrical, combined flow ripple laminated sandstones are dominant, with subordinate amounts of current and wave ripples. Thick packages of climbing ripples are locally abundant. Convolute bedding, sand volcanoes, flame structures, load casts, and pinch-and-swell geometries characterize some sandstones. Finely comminuted plant matter is common throughout. Flattened and elongate coal fragments, 1-10 mm thick and 1-5 cm long, are concentrated along

		some horizons, as well as *Inoceramus* and *Baculites* fossil fragments. Trace fossils are rare and where found, are confined to the uppermost bedding plane, such as *Gyrochorte*, *Scolicia*, and chevron-like tracks-trails. BI = 0-2.
Distal delta front-to-prodelta; Inner-to-mid shelf.	1K - Hyperpycnite	Repetitive sets of planar and ripple laminated sandstones stack to form beds that are up to 60 cm thick. Contacts between the planar and ripple laminated divisions are gradational or diffuse. Up to twelve divisions occur in a single bed. Some beds begin with a ripple laminated division at the base, where others have planar laminations at the base. Weakly- to strongly-asymmetrical combined flow ripples are dominant, with lesser amounts of current ripples. Climbing ripple sets with a small angle of climb are common. Most of these planar laminated sandstone divisions have gently curving laminations with or without small scale truncation surfaces. Organic-rich laminations consisting of finely comminuted plant material are common. Rare moderately-bioturbated patches with *Teichichnus*, *Paleophycus*, *Thalassinoides* and *Ophiomorpha* trace fossils are noted. Bioturbation levels are low (BI=0-1).
Transgressive lag deposit; capping a parasequence or an isolated body encased in the offshore mudstone belt (i.e. sediment bypass surface).	1L - Coarse-Grained Lag Deposit	Coarse-grained lag deposits are patchily distributed, 0.5 to 3.5 m thick, and overlie erosional scours. They typically have a limited areal extent: a few meters to a few tens of meters wide and long. Most coarse-grained lag deposits have sharp and erosive basal contacts, with truncation surfaces, sigmoidal bedding, pinch-and-swell geometry, and both convex-up and concave-up bedding planes. Coarse-grained lag deposits consist of a mixture of fine-to-very coarse sandstone with granules, pebbles, mudstone clasts, bone fragments, shell debris and fish teeth. Sandstones have a salt and pepper texture and are moderately to poorly sorted. Angular to subangular mudstone clasts or chips are common (0.1 to 2.3 cm diameter). Wood fragments, coal fragments and finely comminuted plant matter occur in trace amounts. Recognizable fossil fragments include *Baculites* and *Inoceramus*. The coarse-grained lag deposits are mildly to moderately bioturbated. Trace fossils include *Paleophycus*, *Ophiomorpha*, *Thalassinoides* and *Skolithos*. Low angle cross bedding, trough cross bedding, gently curving planar laminations and current ripple laminations are the main sedimentary structures. Combined-flow and wave ripple-laminated sandstones are rare. Convolute bedding and normally graded beds are also observed. Coarse-grained deposits are rare in the Blackhawk Formation to Lower Castlegate Sandstone interval. Where found, these coarse-grained deposits are generally associated with a transgressive surfaces of erosion. Two of the best examples are transgressive lag deposits which cap the Kenilworth Member (Taylor and Lovell, 1991, 1995; Ainsworth and Pattison, 1994; Pattison, 1995) and Panther Tongue Member (Newman and Chan, 1991; Hwang and Heller, 2002).
Sediment starved shallow marine; linked to transgression.	1M - Oolitic Ironstone	Medium to coarse-grained oolitic ironstones occur at a few localities in the Campanian Book Cliffs. Chan (1992) described an oolitic ironstone body at Floy Wash which is completely encased in Mancos Shale mudstones. This body caps low lying mounds or hills in the Mancos mudstone belt and is up to 2 m thick. This deposit is iron-rich, tightly cemented and becomes coarser-grained upwards. Individual beds are 2 to 7 cm thick, and are planar- or ripple-laminated. The oolitic sandstone beds are interbedded with iron-rich siltstones. Pattison (2005a,b,c) correlates the Floy Wash oolitic ironstone to the top of the Aberdeen Member. Another example of an oolitic ironstone occurs in the distal portion of the Lower Castlegate Sandstone in western Colorado, along County Road 206 (i.e. old Mitchell Road; Van Wagoner 1995). Detailed petrographic descriptions are provided by Taylor et al. (2002). The Lower Castlegate Sandstone oolitic ironstone body is interpreted to have accumulated a few kilometers basinward of the terminal Castlegate shoreline (i.e. parasequence C6), which was a mud-dominated shallow marine succession heralding the onset of the Buck Tongue transgression (Pattison *in review-a,-b,-c,-d,-e*).

Channel Facies:

Depositional Environment	Facies Name	Description
Fluvial channel; tidal-fluvial channel.	2A - Cross Bedded Sandstone	Moderately to moderately well sorted, fL-cU sandstone. Interlaminated with carbonaceous-rich mudstone in places. Dominantly trough cross bedding, with lesser planar tabular cross bedding. Some herringbone cross bedding, double mud drapes, rhythmically laminated cross bedding (i.e. tidal bundles), and *Teredolites*-bored wood fragments. Bioturbation index is low (BI = 0-1). Cross bedded sandstones are typically confined within channel-fills. Lens- to sigmoidal-shaped, bar-form geometry. Single and multi-storey/amalgamated channel-fill packages are observed. Bar-forms are a variety of sizes (i.e. width 8-300 m; thickness 2-15 m), and exhibit both lateral and downstream accretion. In general, bar-form size decreases landwards. The widest and thickest bar-forms are usually within 2 to 5 km of the penecontemporaneous shoreline. Beds are 10-70 cm thick. Sharp-based. Base of facies erosively overlies shallow marine sandstones in some localities. Cross beds reveal a mean transport direction of 127° (i.e. E37°S). Vector magnitude = 63.8 (n=5,966). Abundant angular-to-sub-rounded, sand-to-pebble sized coal clasts concentrated in layers or scattered throughout. These comprise up to 25 % of Facies 2A in places. Sub-angular to sub-rounded mudstone clasts occasionally observed along with the coal clasts. The mudstone clasts are also sand-to-pebble sized, and for the most part, consist of carbonaceous-rich mudstone and shale (Facies 3D and 3E). Numerous finely disseminated plant fragments resembling coffee grounds (i.e. medium silt to coarse sand sized). Mainly occur as discrete laminae within the cross bedded sandstones, but also scattered throughout the facies. Rare bone fragments (dinosaur?). Cross bedded sandstones are interbedded with many different facies, but predominantly with convolute bedded sandstone (Facies 2B). Prolific and most common type of channel-fill facies.
	2B - Convolute Bedded Sandstone	Convolute bedded, fL-cU sandstone is moderately to moderately well sorted. This is an abundant facies within channel-fills, occurring in both single and multi-storey/amalgamated channel successions. Gently to tightly folded. Vertical dips occur in places. Scarce *Palaeophycus*, and *Psilonichnus* (BI = 0-1). Beds are 15-80 cm thick. Abundant angular-to-sub-rounded, sand-to-pebble sized coal and mudstone clasts. Laminations of carbonaceous matter are common. Some elongated wood fragments. Mostly interbedded with cross bedded sandstone (Facies 2A). Uppermost Castlegate Sandstone is commonly convolute bedded and tightly cemented. Fe-rich carbonate cements impart a distinct brown-red colour in these uppermost beds.
	2C - Planar Laminated Sandstone	Horizontal-to-gently dipping, moderately well sorted, planar laminated fL-mU sandstone. Rare *Palaeophycus*. Extremely low bioturbation index (BI = 0-1). Comprises minor amounts of bar-form, sigmoidal geometries in single- and multi-storey channel-fills. Beds are 10-30 cm thick. Sharp base and top. Moderate amounts of silt-to-fine sand sized, finely-disseminated plant material concentrated in laminae or thin beds (1-2 cm thick). Uncommon sand-to-granule sized, angular-to-sub-angular, elongated, coal and mudstone clasts. Rare wood fragments. Interbedded with cross bedded (Facies 2A) and convolute bedded (2B) sandstones. Scarce channel-fill facies.
	2D - Current Rippled	Current rippled vfU-mL sandstone. Isolated beds with intermixed mU-cL sand. Moderately well to well sorted. Interlaminated with carbonaceous-rich mudstone. Rhythmically laminated in places. Rare climbing ripples, with a

	Sandstone	shallow angle of climb. Sporadically distributed *Macanopsis*, and unidentified traces (BI = 0-1). Moderately abundant channel-fill facies, mostly within thinner and narrower single storey channel-fill deposits. Locally observed in large-scale IVF-IHS deposits at the top of the Desert Member and Castlegate Sandstone. Abundant laminae of finely comminuted (i.e. silt-to-fine sand size) plant material. Numerous sub-angular-to-sub-rounded, sand-to-granule sized coal clasts. Mudstone clasts are sparse. Beds are 5-60 cm thick. Localized and uncommon roots. Interbedded with Facies 2E, 2F and 2G. Sharp contacts between the facies.
	2F - Carbonaceous-Rich Sandstone	Moderately sorted, carbonaceous-rich fL-cU sandstone. Interbedded-interlaminated carbonaceous-rich mudstone, up to 20% of the facies. Variety of sedimentary structures: massive, current ripples, planar laminations, convolute bedding, and normal grading. Rhythmically laminated in places, with patterned alternations of carbonaceous-rich and sandstone-rich laminations. Isolated *Palaeophycus*, unidentified traces, *Planolites*, *Chondrites*, and *Skolithos*, with a BI of 0-3. This facies comprises minor-to-moderate amounts of sigmoidal bar-form geometries in both single-storey and multi-storey channel-fill complexes. Occurs at different levels throughout a channel-fill: basal lag deposits, mid-channel-fill, and uppermost terminal bar-form-fill. Numerous angular-to-sub-rounded sand-to-pebble-sized coal fragments and silt-to-sand-sized phyto-detritals. The latter are scattered throughout the facies or are concentrated as discrete laminae. Total carbonaceous matter is 15-25%. Sporadic sub-angular-to-sub-rounded, sand-to-granule sized carbonaceous-rich mudstone clasts. Some 5-10 cm thick basal lag deposits consisting of mL-cU sand, coal and mudstone clasts, with an upward decrease in grain size. Rare synaeresis cracks. Interbedded with a variety of channel-fill facies, such as cross bedded sandstones (Facies 2A), convolute bedded sandstones (2B), and mudstone-clasts pebble breccia (2I).
	2G - Carbonaceous-Rich Siltstone	Carbonaceous-rich fine-to-coarse siltstone, with interlaminated carbonaceous-rich mudstone and very fine-grained sandstone. Moderately sorted. Laminae are massive, normally graded or weakly current rippled. Predominantly rhythmically laminated. Subequal mudstone and siltstone beds, with lesser amounts of sandstone. Pin-striped laminations (1-3 mm thick) are common. Vertical trends of thickening and thinning laminae are commonly recorded. Some starved current ripples. Scattered unidentified traces, *Chondrites*, and *Planolites* (BI = 0-3). Generally confined to the upper and finer-grained portions of lateral accretion sets within channel-fill successions. Abundant silt-to-fine sand sized phyto-detritals. Rare angular-to-sub-angular, sand-to-granule sized, elongate coal fragments. Some Fe-rich cemented thin beds and cm-scale diameter nodules. Local synaeresis cracks. Interbedded with carbonaceous-rich sandstone (Facies 2F) and carbonaceous-rich mudstone (2H).
Estuarine-tidal channel.	2E - Gently-Dipping Interbedded Sandstone and Mudstone (IHS)	Heterolithic facies with interbedded, gently-dipping sandstone and mudstone. Relatively equal mixtures of each lithology. Overall, this facies is moderately well sorted. Sandstone beds are mainly fL-mU sand, with minor cL-cU sand. Sandstone beds are dominantly current rippled or massive, with lesser amounts of trough cross bedding, normal grading, planar laminations, convolute bedding and wave ripples. Rare double mud drapes and rhythmically laminated cross bedding (i.e. tidal bundles) in places, along with *Teredolites*-bored wood fragments. Mudstone beds have similar proportions of clay and silt, with some intermixed coarse-grained silt and very fine-grained sand. Mudstones are dark grey to black reflecting their carbonaceous-rich character. Dominantly inclined heterolithic strata (IHS) with all beds/laminae dipping at low angles, between 2-8°. Beds are sharp-based and 1-10 cm thick. Decimeter-to-meter-scale sets of beds or packages have consistent dips and dip directions. These are abruptly overlain by sets with different dip directions, varying 20-80° between adjacent sets. Rhythmically laminated sandstone and carbonaceous-rich mudstones.

		Upward, progressive-patterned thinning and thickening of laminations, resembling tidal rhythmites. Uncommon *Chondrites* and *Schaubcylindrichnus*, with a BI = 0-2. Carbonaceous-rich laminae and angular-to-sub-rounded, sand-sized coal clasts occur throughout. Isolated root traces, especially near the top of the IHS channel-fill successions. This facies is commonly observed in channel-fill successions characterized by large-scale lateral accretion sets. The uppermost Desert Member (i.e. D11 parasequence) has IHS accretion sets that are 200-350 meters wide and 15-20 m thick throughout the Horse Heaven to Thompson Canyon region. Similarly large-scale IHS accretion sets are observed in the uppermost Lower Castlegate Sandstone from Blaze Canyon to Pinto Wash, and in the mid-Desert Member interval (i.e. D6 parasequence) at Hatch Mesa. This facies is confined to large-scale, channel-fill successions within 10 km of the penecontemporaneous shoreline. The best examples are in the upper parts of the Desert Member and Lower Castlegate Sandstone, where deep and broad channels incise into the penecontemporaneous foreshore-shoreface sandstones.
Fluvial channel; tidal-fluvial channel; estuarine-tidal channel.	2H - Carbonaceous-Rich Mudstone	Dark grey to black mudstone, with lesser amounts of silt and very fine sand. Moderately well sorted. Massive. Sparse normal grading. Rare *Chondrites*, and *Schaubcylindrichnus*. Very low bioturbation index (0-2). Predominantly observed in the uppermost parts of channel-fill successions. Not an abundant facies. Pervasive clay- and silt-sized phyto-detritus. Fining-upward successions are dominant. Gradational lower contact with carbonaceous-rich siltstone (Facies 2G) or carbonaceous-rich sandstone (2F). Uncommon and sporadically distributed root traces, a few cm long. Channel abandonment.
	2I - Mudstone-Clast Pebble Breccia	Massive, matrix-supported, pebble breccia with > 30 %, > 2 mm angular-to-sub-angular carbonaceous-rich mudstone clasts. Mudstone clasts are carbonaceous-rich mudstone (Facies 2H) and siltstone (2G), and mostly pebble-sized, with fewer granule- and cobble-sized clasts. Matrix is moderately sorted fL-cU sandstone. Overall the entire facies is poorly sorted. Uncommon *Planolites*, *Chondrites*, and *Schaubcylindrichnus*, with a BI = 0-2. Facies occurs mostly as a basal lag deposits for single- and multi-storey channel-fills, and at contacts between adjacent channel-fills successions within the multi-storey bodies. Sparse facies. Beds are 5-30 cm thick, with sharp and erosive lower contacts, and gradational upper contacts. Some fining-upward successions, grading upwards into carbonaceous-rich sandstone (Facies 2F), cross bedded sandstone (2A), and/or convolute bedded sandstone (2B). Angular-to-sub-angular, elongated, sand-to-pebble sized coal clasts, finely disseminated plant material, and wood fragments are dispersed throughout this facies.
Tidal-fluvial channel; estuarine-tidal channel; wash-over fan; flood tidal delta.	2J - Fossiliferous, Fe-Cemented Sandy Breccia (“Coquina”)	Poorly to moderately sorted, matrix-supported, sandy breccia. Whole and broken, sand-to-pebble-sized bivalve and gastropod shell fragments comprise 15-40 % of this facies. Cream-to-light brown-coloured, sand to pebble-sized, sub-angular-to-rounded, mudstone and siltstone clasts are common. These clasts have little carbonaceous matter. Matrix is moderately well sorted vfU-mL sandstone. Some current ripples and trough cross beds. Mostly massive. Lateral accretion sets are common, commonly downlapping onto a flat/non-erosive base. Localized incision is observed. Rare *Skolithos* (BI = 0-1). Facies 2J is sparse. Only occurs at a few localities in the uppermost and distal parts of the Castlegate Sandstone in Salt Wash Canyon.

Coastal Plain Facies (non-channelized):

Depositional Environment	Facies Name	Description
Crevasse splay; wash-over fan; flood tidal delta.	3A - Current Rippled Sandstone	Moderately well to well sorted, current rippled vfL-fL sandstone. Beds are 2-10 cm thick, generally with a sharp lower contact and gradational upper contact. Some fining-upward grain size trends. Rare *Skolithos* and unburrowed to weakly bioturbated (BI = 0-1). Non-channelized, sheet-like geometry tapers in all directions. Beds only extend for a few tens of meters. Moderately rare facies. Some mudstone and coal clasts, sand-to-granule-sized and sub-angular-to-sub-rounded. Rare wood fragments. Finely disseminated carbonaceous matter dispersed throughout the facies. Isolated roots. Fe-rich cements occurs in patches. Generally this facies is tightly cemented. Interbedded with carbonaceous-rich siltstone (Facies 3C) and mudstone (3D).
Floodplain; overbank; lagoonal; paleosol.	3B - Carbonaceous-Rich Sandstone	Moderately to poorly sorted, carbonaceous-rich vfL-mU sandstone, with lesser amounts (i.e. 5-20%) of carbonaceous-rich silt and clay laminae. Beds are 1-20 cm thick. Rare normal grading and convolute bedding. Fe-rich nodules-concretions are common, some densely fractured, others with shrinkage cracks. Abundant finely comminuted plant matter. Numerous sand-to-pebble-sized, angular-to-sub-angular coal clasts. Some mudstone clasts. Sulfur-stained in places. Small-scale root traces, a few mm's to a few cm's long, are concentrated along specific horizons. A number of unidentified traces with minor *Planolites*. Wide variation in bioturbation intensity (BI = 1-5). Facies has a sheet- or patch-like geometry. Discontinuous. Transitions into carbonaceous-rich siltstone (Facies 3C) and mudstone (3D), with diffuse bed boundaries, both vertically and laterally. Rare synaeresis cracks.
	3C - Carbonaceous-Rich Siltstone	Dark grey carbonaceous-rich siltstone with intermixed silt, sand and clay. Predominantly medium-to-coarse grained silt. Sand is vfL-mU, scattered throughout, locally concentrated as laminae and/or thin beds, and constitutes 5-30 % of the facies volume. Convolute bedded in places. Nodules-concretions are common. Numerous unidentified traces and *Planolites*, with subordinate *Chondrites*, *Skolithos*, *Palaeophycus*, and *Teichichnus* (BI = 2-5). Abundant finely disseminated plant material. Lesser amounts of sand-to-granule-sized, sub-angular-to-sub-rounded coal and mudstone clasts. Some rhizoliths. Overall mottled-stirred, swirled and/or concretionary texture. Tightly cemented layers with white to red-brown nodular-concretionary beds. Fe-rich cemented with siderite, ferroan-dolomite, and ankerite. Fractures are common. Sheet-like geometry with variable thickness. Interbedded with carbonaceous-rich mudstone (Facies 3D) and shale (3E). Gradational lateral and vertical facies contacts. Cut by channel-fill facies.
	3D - Carbonaceous-Rich Mudstone	Mostly dark grey-black, carbonaceous-rich mudstone. Also light grey and light green in scattered localities. Inter-mixed to inter-laminated vfL-fU sand and coarse silt rarely comprises > 10% of the facies volume. Moderately well sorted and massive. Traces dominated by *Planolites*, unidentified traces, and scarce *Chondrites*, with BI ranging from 2-5. Sheet- or patch-like geometries, dissected by channel-fill deposits. Abundant phyto-detritus and sand-sized coal fragments. A few root traces that are mm-width and up to 4 cm long. Mottled texture. Fe-rich in places. Interbedded with carbonaceous-rich siltstone (Facies 3C), sandstone (3B), and shale (3E). Lateral continuity is often difficult to determine in outcrop due to vegetation and scree cover.

Margins of coastal mire; floodplain; overbank.	3E - Carbonaceous Shale	Massive dark black mudstone with trace amounts of vfL-vfU sand and coarse silt. No discernible vertical grain size trend. Localized and uncommon *Planolites* and unidentified traces (BI = 0-2). Sheet-to-patch-like geometry. Disseminated phyto-detritals and sub-angular-to-sub-rounded, sand-to-pebble-sized coal clasts. Roots are common. Predominantly interbedded with coal (Facies 3F) and carbonaceous-rich mudstone (3D). Gradational vertical contacts with coal beds. Scattered pyrite (very finely- to medium-crystalline) and rare free sulphur (i.e. yellow (patches).
Coastal mire.	3F - Coal	Dark black, shiny/reflective, cleated, sub-bituminous-to-bituminous coal. Sulphur-rich patches throughout. Rare finely-disseminated, finely crystalline pyrite. Abundant roots. No trace fossils. Interbedded with carbonaceous-rich shale (Facies 3E). Coal beds are 5-35 cm thick. Individual coal seams split and merge. Many coals are laterally continuous for hundreds of meters or more. Greatest lateral extent for are those that correlate with marine flooding surfaces (i.e. parasequence boundaries). For example, the coal zone demarcating the top of the D11 parasequence (i.e. top Desert Member) is correlatable for up to 8 km along depositional-dip (i.e. west-to-east).

Table 0-1. Comprehensive summary of all facies within the Lower Castlegate Sandstone to Blackhawk Formation to Mancos Shale stratigraphic interval. Thirteen shallow marine facies, ten channel facies, and six non-channelized coastal plain facies are recognized. These are grouped by depositional environment (i.e. left column).

FIELD DAY 1

INTRODUCTION, FLUVIAL, COASTAL PLAIN, AND DELTAIC/SHOREFACE DEPOSITS

Stop 1: Distal Book Cliffs, Thompson Overview

Stop 2: High Net:Gross Braided Fluvial Deposits, Castlegate Sandstone, Type Section

Stop 3: Low to Moderate Net:Gross Meandering Fluvial and Coastal Plain Deposits, Blackhawk Formation

Stop 4A: River-Dominated Deltas, Distributary Mouth Bars, Panther Tongue Member, Gentile Wash

Stop 4B: Wave-Dominated Shoreface/Deltaics, High Accommodation Setting, Storrs-to-Spring Canyon Members, Gentile Wash

STOP 1: DISTAL BOOK CLIFFS, THOMPSON OVERVIEW

The Book Cliffs are situated on the northern rim of the Colorado Plateau and have been eroded back from the San Rafael Swell in east-central Utah and the Uncompahgre Uplift in eastern Utah and western Colorado. This provides a gentle structural dip of 1-5° N throughout most of this region. The rocks are basically flat lying and are relatively undeformed. Small normal faults are observed in places. The Campanian strata consists of the Star Point Formation, Blackhawk Formation and Castlegate Sandstone, forming part of the Mesaverde Group (Fig. 1-1; Young 1955). The Blackhawk Formation is subdivided into six members: Spring Canyon, Aberdeen, Kenilworth, Sunnyside, Grassy and Desert (Young 1955). These sedimentary rocks are Late Cretaceous in age (Campanian), and grade from sandstone-dominated intervals in the west to the mudstone-dominated Mancos Shale in the east (Young 1955; Balsley 1980).

The Blackhawk Formation spans a 3.5 million year interval from approximately 82.5 Ma to 79 Ma (Fouch et al. 1983). The main facies belts are braided fluvial, meandering fluvial, coastal plain, river- and wave-dominated deltas, upper and lower shoreface, and offshore/inner shelf. During the Campanian, the Cretaceous Western Interior Seaway covered the eastern half of Utah and paleoshoreline trends were oriented approximately north to south (McGookey et al 1972). During Desert Member and Castlegate Sandstone deposition (i.e. cliff-forming sandstones in the Book Cliffs at Thompson), shoreline trends were oriented NE-SW with offshore towards the SE (Van de Graaff 1972; Miall 1993, 1994; Van Wagoner 1995). The Mancos Shale and the distal expression of the Blackhawk Formation and Castlegate Sandstone are exposed in the 250 m high Book Cliffs at Thompson (Fig. 1-2). The I-70 rest stop and the highway are directly on top of the Mancos Shale, which is over 1000 m thick in eastern Utah (Fig. 1-1). In eastern Utah and western Colorado, a 100 to 400 m thick section of the Mancos Shale has an anomalously high sandstone content along certain horizons (Kellogg 1977; Cole and Young 1991). These deposits were originally called the Mancos B interval and are now formally defined as the Prairie Canyon Member (Fig. 1-1; Cole et al. 1997). The Prairie Canyon Member is roughly time equivalent to the Star Point and Blackhawk formations further to the west (Cole et al. 1997; Hampson et al. 1999, 2001). Isolated shelf sandstone bodies are scattered throughout this region (Pattison 2005a, b, c; Pattison et al. 2007a; Pattison and Hoffman 2008).

Shallow marine and channel sandstones of the Castlegate Sandstone and Desert Member form the ridge-line top in the Thompson area (Fig. 1-2). Careful tracking along the Book Cliffs outcrop trend reveals an up-depositional-dip thickening (west) and a down-dip thinning (east) of these sandstones. The amalgamated Castlegate-to-Desert interval is approximately 110 m thick, with over 60 m of sandstone-dominated deposits. Distal thin-bedded sandstones and siltstones of the Grassy Member are exposed beneath the cliff-forming Castlegate-to-Desert interval.

Two other features are worth noting at this stop: (i) *white caps* and (ii) *coal burns*. The upper Desert Member is marked by white sandstones in places, called *white caps*. These white sandstones are effected by acidic waters sourced from the overlying coal-bearing coastal plain deposits that leach-out the iron-bearing minerals (Spieker 1931, 1949; Young 1955). The second feature worth noting are the reddish-brown sandstones that occur in the upper part of the Book Cliffs. These are called *coal burns*. The brick red sandstones are evidence of coal combustion, possibly triggered by lightning strikes. Both *white caps* and *coal burns* are indicators of overlying or interbedded coastal plain deposits and are useful proxies for a low-resolution or "first-pass" interpretation for the presence of overlying coastal plain deposits.

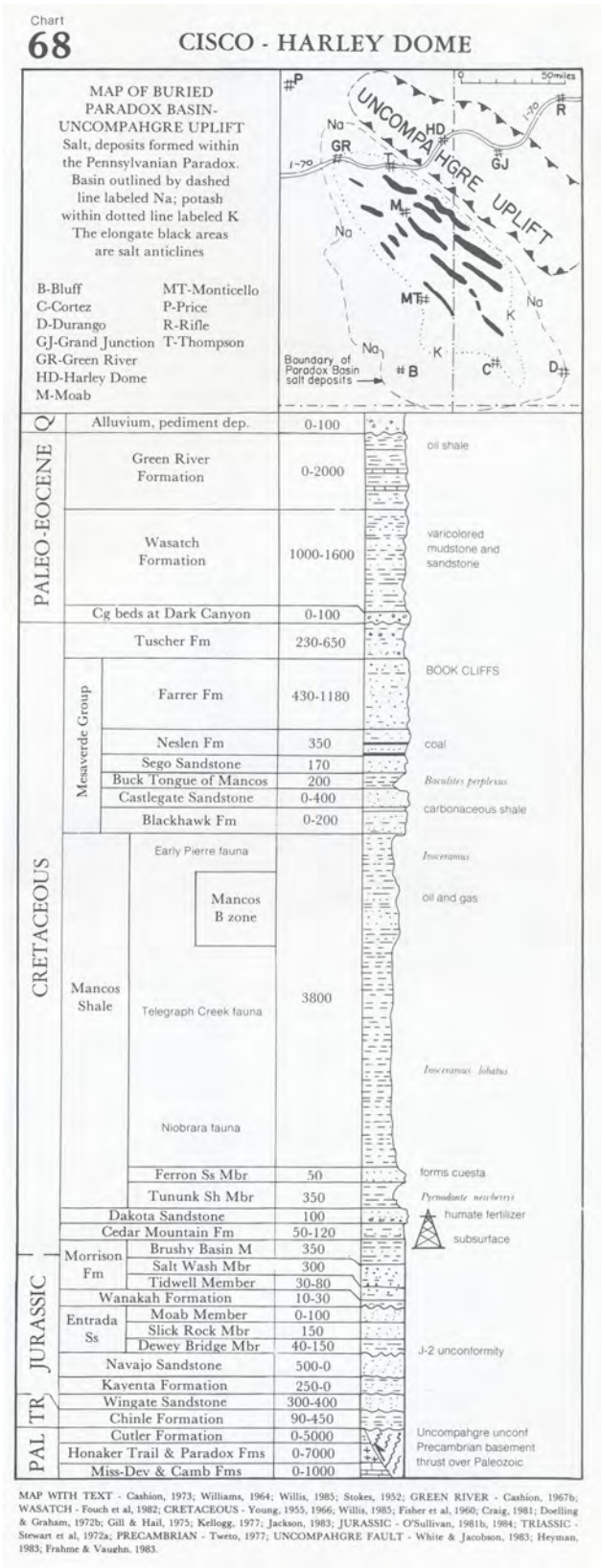

Figure 1-1. Geological columns with stratigraphic nomenclature (Hintze 1988). Chart 68: Cisco-Harley Dome, eastern Utah. This describes the stratigraphy in the vicinity of the Thompson rest stop, off I-70. Chart 44: Grand Junction area, western Colorado. This shows the detailed stratigraphy for the Colorado National Monument region.

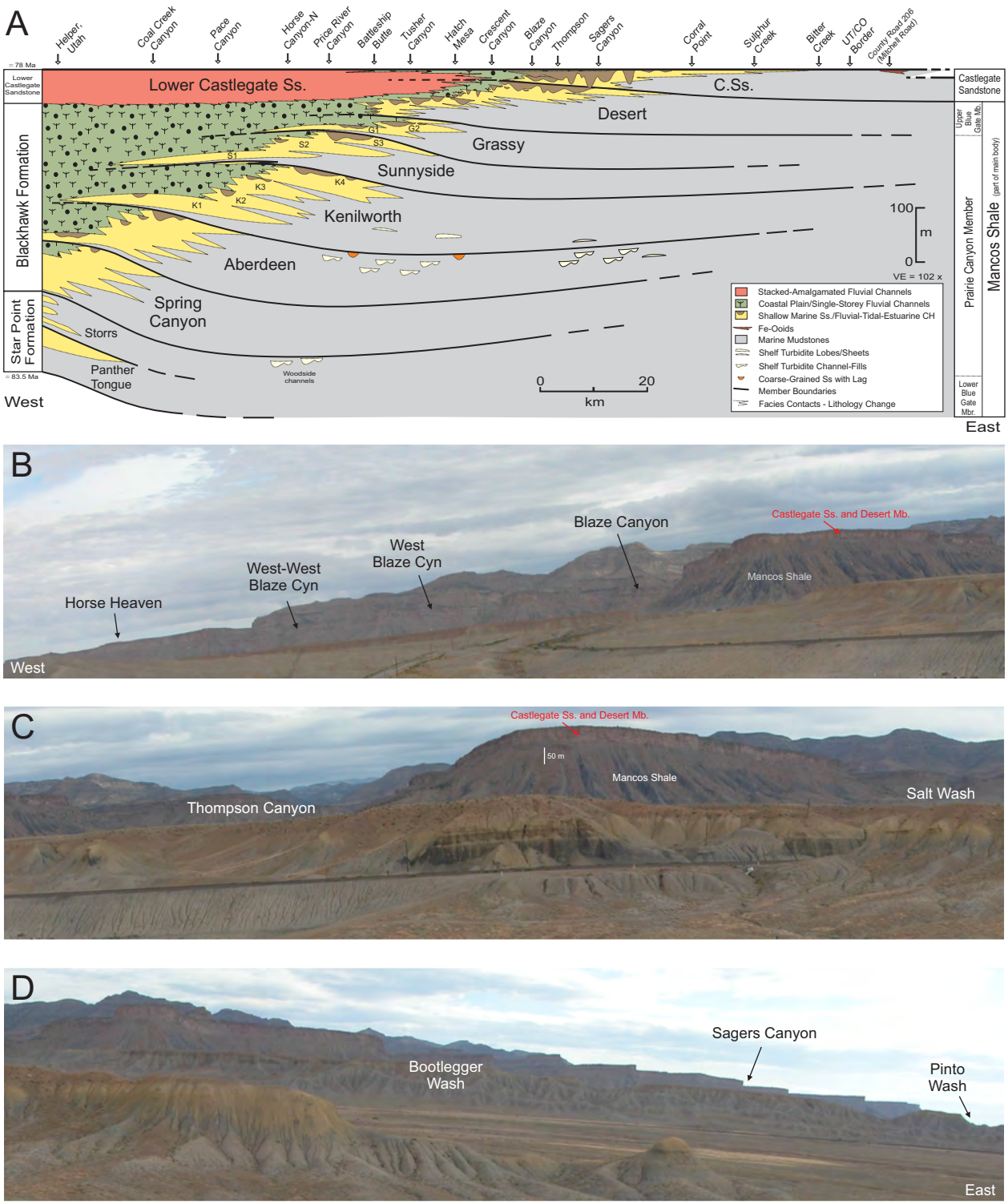

Figure 1-2 Thompson Rest Stop, north side I-70. (A) Scaled stratigraphic dip-oriented cross section of the Book Cliffs region, Helper Utah to Utah-Colorado border. Member boundaries have been extended both westward into the undifferentiated Blackhawk Formation coastal plain and Lower Castlegate Sandstone (C.Ss.), and eastward into the Mancos Shale using high resolution outcrop and subsurface correlations. Key field stop localities are shown along the top. (B-D) Continuous photo-panorama looking north towards the Book Cliffs. Field of view is approximately 13 km. The Castlegate Sandstone and Desert Member (Blackhawk Formation) combine to form the distinct cliff-line in the foreground. These sandstone-rich units are underlain by the distal Grassy Member (Blackhawk Formation), which rests on top of over 1000 m of Mancos Shale. Younger stratigraphic units overlying the Castlegate Sandstone are the Buck Tongue (Mancos Shale), Sego Sandstone, and Neslen Formation.

STOP 2: HIGH NET:GROSS BRAIDED FLUVIAL DEPOSITS, CASTLEGATE SANDSTONE, TYPE SECTION

The type section for the Castlegate Sandstone offers an excellent example of a stack of high net:gross (N:G) fluvial deposits and is located in the extreme northwestern corner of the Book Cliffs (Figs. 0-1 and 0-2). At this locality, the Lower Castlegate Sandstone rests sharply on top of the undifferentiated coastal plain deposits of the Blackhawk Formation. The sandstone-rich Lower Castlegate can be correlated for approximately 150 km down-depositional-dip into eastern Utah.

Sandstone-rich, braided fluvial channel deposits occur at this stop (Figs. 2-1 and 2-2). These rocks consist of moderately sorted, fine- to medium-grained, cross bedded and current rippled sandstones (Fig. 2-2). Convolute bedding, subangular to angular mudstone chips, wood fragments, coal clasts and finely-comminuted plant debris are common (Fig. 2-2). Laterally-discontinuous, organic-rich mudstone layers (a few cm's thick) comprising less than 5 % of the succession are interbedded with the sandstones. These mudstone layers rarely extend for more than a few meters. The sedimentary architecture is dominated by channel-bar forms with lateral and downstream accretion elements, most of which are lens-shaped (Fig. 2-2).

Similar types of high net:gross fluvial deposits have the potential to be excellent hydrocarbon reservoirs, with very good porosity and permeability. However, a seal is required. It is unlikely that the interbedded mudstone layers would be a barrier to fluid flow, but would likely cause a minor baffling effect. The Castlegate Sandstone is an outcrop analog for braided fluvial reservoirs worldwide, such as the Prudhoe Bay Oil Field in Alaska. Prudhoe Bay is the 16th largest oil field in the world, with over 13 billion barrels of recoverable oil reserves.

Adams and Bhattacharya (2005) have demonstrated that the Castlegate Sandstone consists of an amalgamated package of sandy channel-belt sheets, up to 80 m thick. Individual sheets are 4 to 7 m thick and contain less than 5 % mudstone. The average bar accretion thicknesses are 2 m, which corresponds to a water depth of 2 to 4 m. Adams and Bhattacharya (2005) argue for a similar fluvial style across the Blackhawk Formation and Castlegate Sandstone stratigraphic interval. They suggest that all of the Blackhawk and Castlegate rivers were braided, and that the differences in fluvial architecture (i.e. low net:gross in the Blackhawk vs. high net:gross in the Castlegate) is caused by tectonically-driven changes in accommodation space. Adams and Bhattacharya (2005) link the preservation of the thick overbank mudstones in the Blackhawk Formation to an increase in accommodation space.

The only definitive evidence for an unconformity at the base of the Lower Castlegate Sandstone is in the Wasatch Plateau, west of the Book Cliffs, where an angular unconformity has been recorded at a few localities (Spieker and Reeside, 1925; Horton et al., 2004). In proximal-to-medial Book Cliffs localities, the base of the Lower Castlegate Sandstone varies by ± 1-2 channel stories (Fig. 2-3). Therefore, in contrast to conventional sequence stratigraphic models (Van Wagoner et al. 1990; Van Wagoner 1991, 1995; Miall 1993), there is no single through-going unconformity separating all of the amalgamated channel sandstones of the Lower Castlegate Sandstone from the coal-bearing coastal plain deposits of the Blackhawk Formation. This is a facies contact, which interfingers both laterally and vertically. Two sequence stratigraphic modeling scenarios are considered: (1) conventional, classic, third-order SB, IVF, non-linked nearshore terrestrial and shallow marine facies belts, detached sand bodies are likely down-dip (Fig. 2-3A), and (2) alternative, no SB, no IVF, suite of discrete parasequence-scale shoreface-incised channels, temporally and spatially linked nearshore terrestrial and shallow marine facies belts, no detached sand bodies down-dip, attached only (Fig. 2-3B).

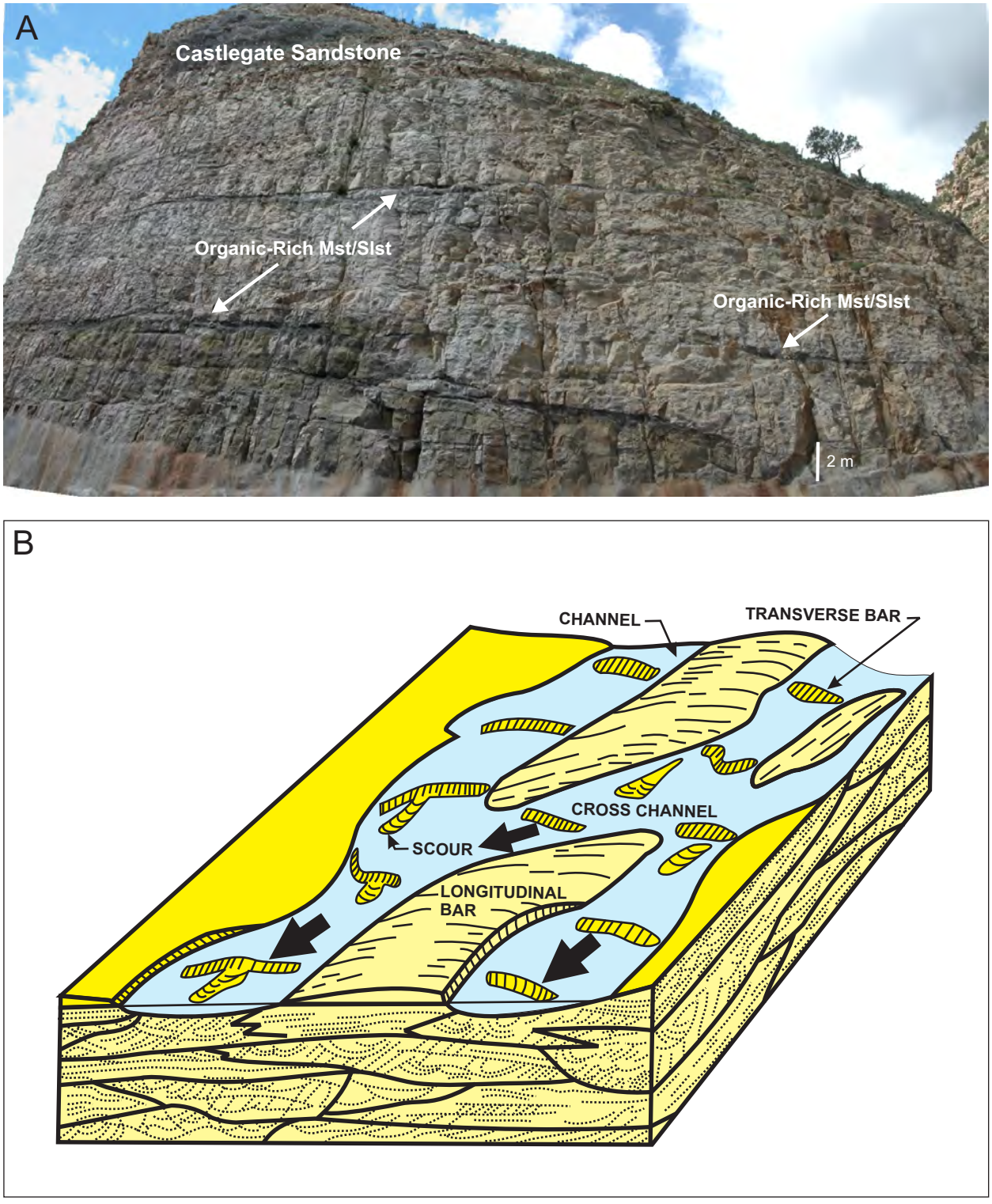

Figure 2-1. High net:gross fluvial deposits, Castlegate Sandstone, type section locality. (A) Panorama of the Highway 6 road cut (southwest side). Note the discontinuity of organic-rich mudstones and siltstones. According to locals, this outcrop site had a castle-like top prior to blasting, similar to that observed on the northeast side of the highway, and therefore was truly a "castle-gate". (B) Braided stream depositional model (Brown and Fisher 1980).

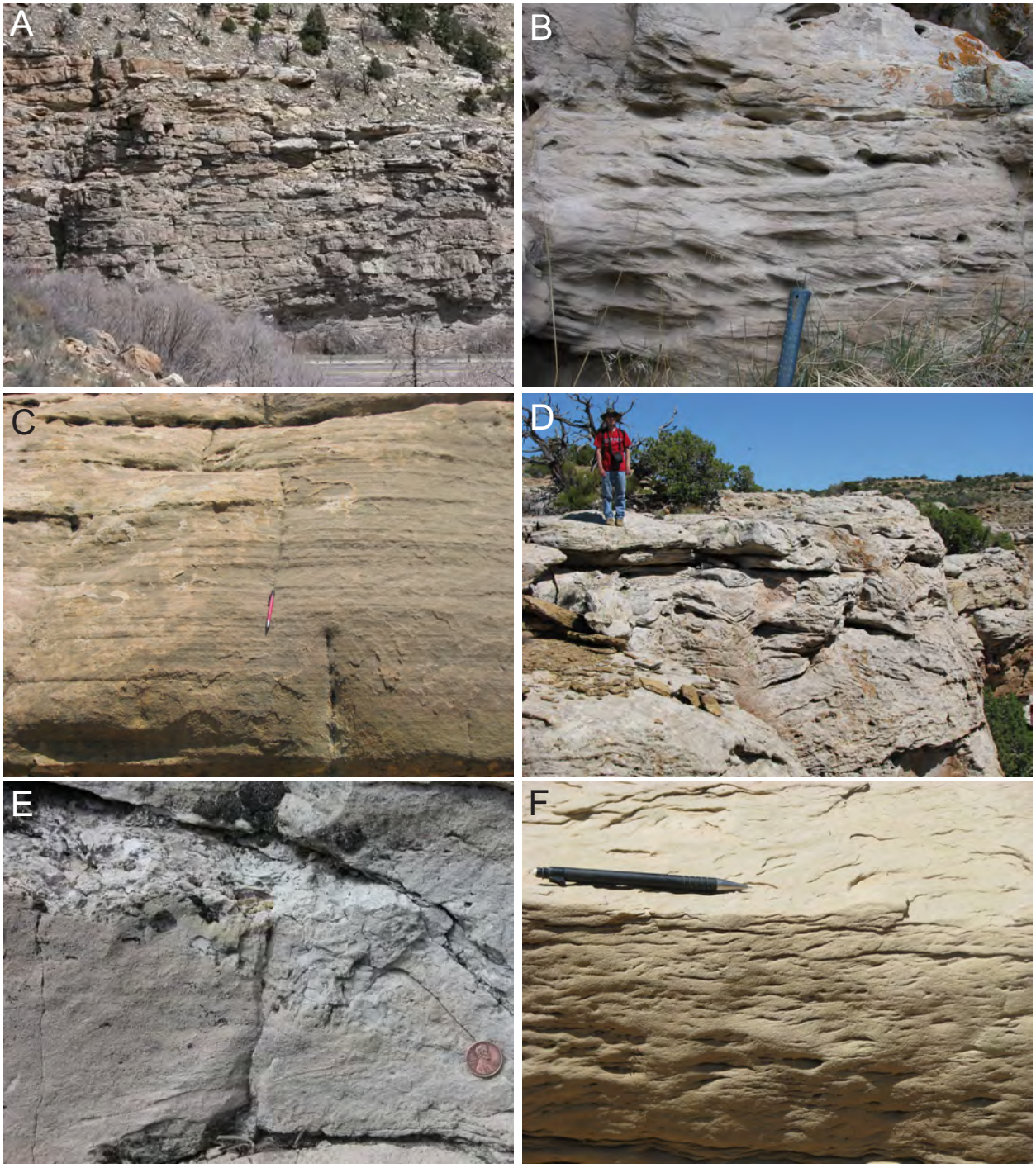

Figure 2-2. Sedimentary architecture and facies of braided river deposits, Book Cliffs, Utah. (A) Castlegate Sandstone type section, north side of Highway 6, approximately 7 km northwest of Helper, UT. Note the high net:gross ratio, lack of continuous mudstone layers, and meter-scale, lens-shaped, bar form geometries. (B) Cross bedded sandstones, Castlegate Sandstone type section. Rock hammer handle for scale. (C) Planar laminated fine-grained sandstones, Castlegate Sandstone, Horse Canyon-South. (D) Convolute bedded sandstones, Castlegate Sandstone, Crescent Canyon. (E) Abundant angular mudstone clasts at the top of a sandstone bed, USA penny coin for scale (1.9 cm diameter). Castlegate Sandstone, Highway 6. (F) Current rippled sandstones, Castlegate Sandstone, Christmas Ridge.

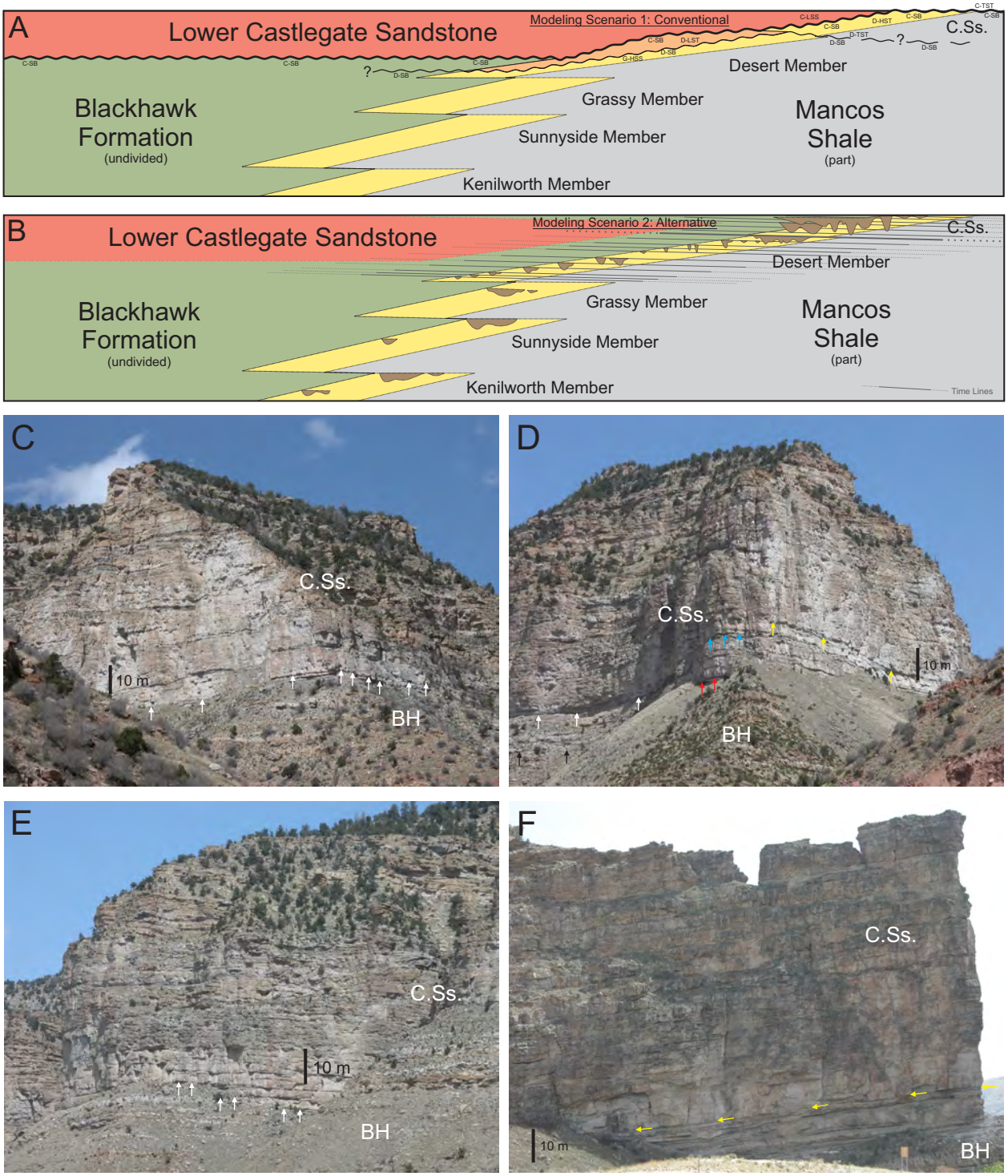

Figure 2-3. Contrasting sequence stratigraphic interpretations for the base of the Castlegate Sandstone. (A) Conventional sequence stratigraphic model of the Desert (D) Member to Lower Castlegate (C) Sandstone (C.Ss.) interval (Van Wagoner et al., 1990; Van Wagoner 1991, 1995). Third-order sequence boundaries (D-SB, C-SB) separate the terrestrial and shallow marine facies belts. HST (Highstand Systems Tract, LST (Lowstand Systems Tract), TST (Transgressive Systems Tract), G-HSS (Grassy Highstand Sequence Set), LSS (Lowstand Sequence Set). Modeling scenario 1: conventional, classic, third-order SB, IVF, non-linked nearshore terrestrial and shallow marine facies belts, detached sand bodies are likely down-dip. (B) Alternative sequence stratigraphic model (this study). Time lines connect the terrestrial and shallow marine facies belts (i.e. thick coal zones and flooding surfaces). *"Shoreface-incised"* channels are tidal-estuarine (light brown) and occur as discrete incisions in most Desert-Castlegate parasequences. Similar *"shoreface-incised"* channels exists in other members of the Blackhawk Formation. Modeling scenario 2: alternative, no SB, no IVF, suite of discrete parasequence-scale shoreface-incised channels, temporally and spatially linked nearshore terrestrial and shallow marine facies belts, no detached sand bodies down-dip, attached only. (C) Base of the Lower Castlegate Sandstone, type section locality, Castle Gate, Utah. White arrows point to the base of the stacked-amalgamated channel sandstones. Note that this surface is not at the same level within the field of view. Castlegate Sandstone (C.Ss.), Blackhawk Formation (BH). (D) Multiple possibilities for the base of the Lower Castlegate Sandstone (i.e. base of amalgamated channel sandstones), all five levels shown with different coloured arrows: black, white, red, yellow, and blue. (E) Three different levels for the base of the amalgamated-stacked channel sandstones. (F) Base of the Lower Castlegate Sandstone (yellow arrows), as identified by Miall and Arush (2001a, b). Type section. Castle turret on the east side of Highway 6.

STOP 3: LOW TO MODERATE NET:GROSS MEANDERING FLUVIAL AND COASTAL PLAIN DEPOSITS, BLACKHAWK FORMATION

This stop is located near the Castlegate Power Station off Highway 6 (Figs. 0-1 and 0-2) and serves as an introduction to the low-to-moderate net:gross fluvial and coastal plain deposits of the Blackhawk Formation. These non-marine deposits are time equivalent to the upper part of the Aberdeen Member and the Kenilworth Member. A shoreface sandstone occurs in the lowermost part (east) of the road cut and is part of the Aberdeen Member (Fig. 3-1). It is interesting to compare and contrast the sorting, grain size, organic content, sedimentary structures, and vertical facies succession of the Aberdeen shoreface deposits to the overlying fluvial sandstones and coastal plain deposits of the Blackhawk Formation.

Coastal plain facies are ubiquitous throughout the study area. Coal-bearing, mudstone-rich deposits are plentiful in the Blackhawk Formation. Coal clasts and roots are abundant. Sandstone facies are less common forming single story meandering fluvial deposits encased in fine-grained coastal plain (Figs. 3-1 and 3-2). Most fluvial sandstones are very fine- to fine-grained with moderate to poor sorting. Fining-upward successions are common. The dominant sedimentary structures are current ripples, climbing ripple sets and convolute bedding, with lesser amounts of trough cross bedding and planar laminations (Fig. 3-2). Abundant carbonaceous matter in the form of wood fragments, coal clasts, and plant remains are scattered throughout the channel facies (Fig. 3-2). Mudstone and siltstone chips or clasts with a variety of shapes (SA-A) and sizes are also observed. The degree of bioturbation is mostly low to moderate (BI = 0-3), with some *Planolites*, *Chondrites*, *Skolithos*, *Palaeophycus*, and *Teichichnus*. Specific trace fossil suites and bioturbation indices are compiled for all six coastal plain facies in Table 0-1.

The fluvial architecture at this stop consists of channel bar forms (point bars) with well defined lateral and downstream accretion surfaces and lens-shaped geometries (Figs. 3-1 and 3-2). Adams and Bhattacharya (2005) studied similar deposits in the Salina Canyon region, approximately 100 km south-southwest of Helper, and determined that the Blackhawk channels comprised isolated channel-belt sheet sandstones, 5 to 8 m thick, that are encased in thick floodplain mudstones. Average bar accretion thicknesses are 2 m which corresponds to water depths of 2 to 4 m. Adams and Bhattacharya (2005) suggests that there is no change in fluvial style across the Blackhawk Formation to Castlegate Sandstone stratigraphic interval, thus casting doubt on earlier interpretations which suggested that the Blackhawk channels were meandering. Adams and Bhattacharya (2005) argue that the Blackhawk channels were braided and had a similar sedimentology, sinuosity, and width:depth ratio as the Castlegate channels. The fluvial sandstones are interbedded with overbank/floodplain sandstones, siltstones, mudstones and coals (Fig. 3-2). One type of floodplain sandstone are the crevasse splay deposits (Fig. 3-1), which are defined as low energy ‘deltas’ that are perpendicular to the main channel and are formed during a levee break (Jackson 1997).

The main reservoir characteristics of the fluvial and coastal plain deposits of the Blackhawk Formation are as follows: (i) low-to-moderate net:gross, (ii) moderate porosity, (iii) low permeability, (iv) small reservoirs, (v) tortuous flow path, (vi) compartmentalization, (vii) low recovery factor, and (viii) limited pressure support. Crevasse splay sandstones may provide tortuous 3D pathways for fluid flow via connection with the isolated channel-belt sandstones.

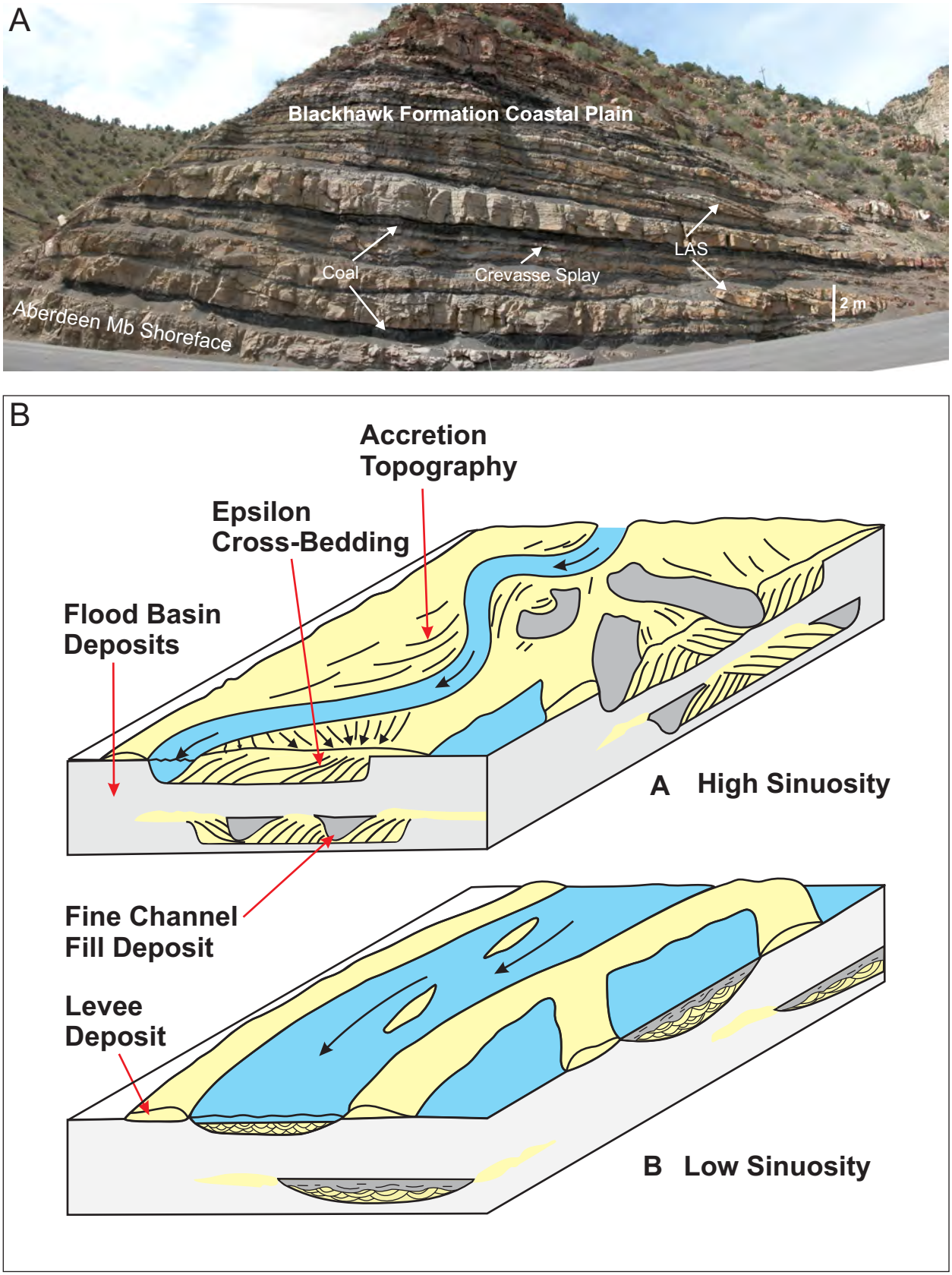

Figure 3-1. Low to moderate net:gross fluvial and coastal plain deposits, Blackhawk Formation, Castlegate power station locality. (A) Labelled panorama of the roadcut on the southwest side of Highway 6. (B) Depositional models of high versus low sinuousity river systems (Moody-Stuart 1966).

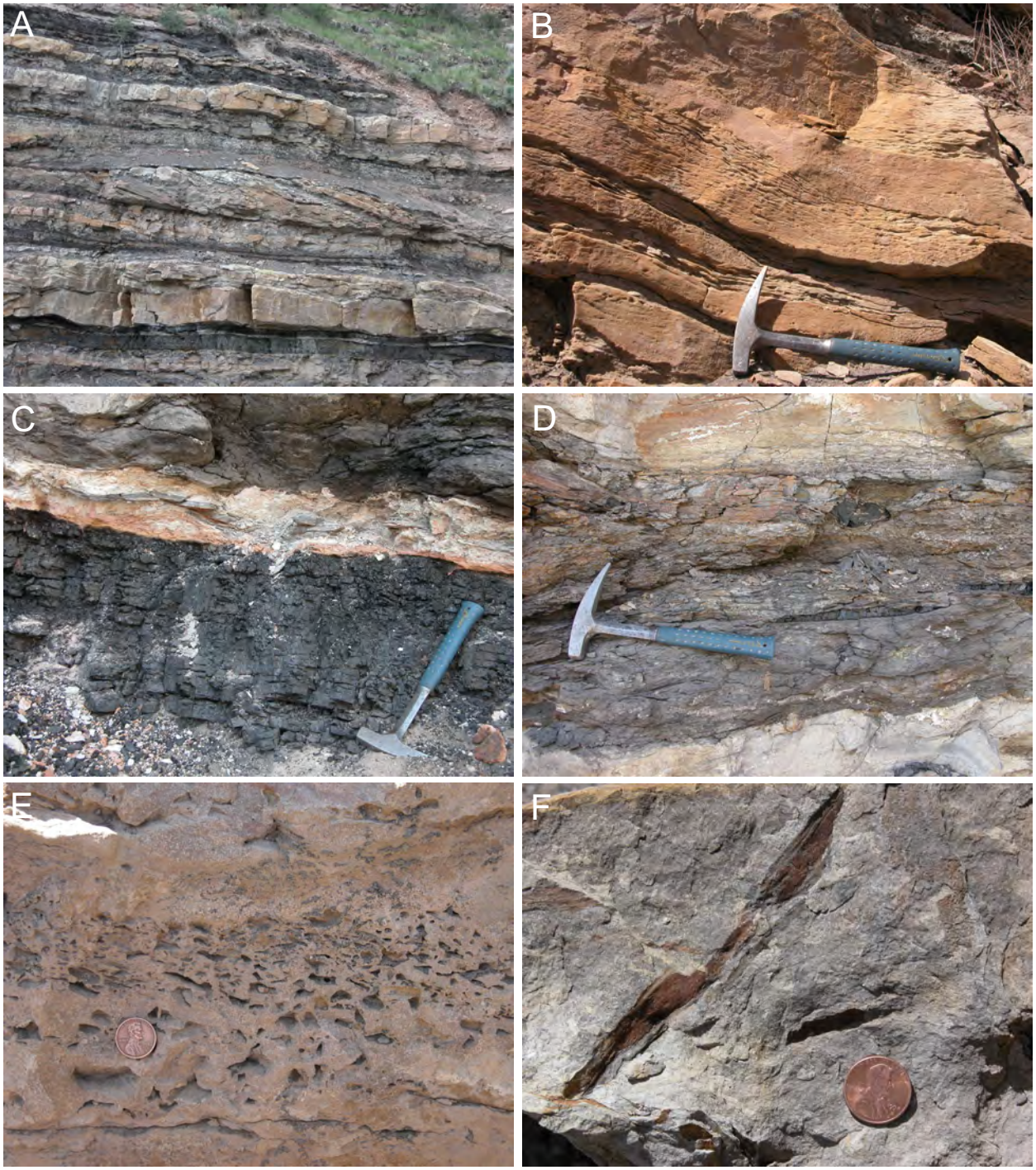

Figure 3-2. Sedimentary architecture and facies of meandering river deposits and fine-grained coastal plain facies, Book Cliffs, Utah. (A) (B) Current rippled sandstone beds along the lateral accretion surfaces shown in the center of Part A. (C) Coal bed. Blackhawk Formation, Highway 6 road cut northwest of Helper. (D) Dark grey mudstones with coal fragments and iron-staining, lower Blackhawk Formation, Castlegate Power Station. (E) Abundant angular mudstone clasts in ripple laminated fine-grained sandstone, Blackhawk Formation, Highway 6 roadcut northwest of Helper. Variety of clast shapes and sizes. USA penny coin for scale (1.9 cm diameter). (F) Wood fragments within dark grey mudstones, upper Blackhawk Formation, Horse Canyon-South.

STOP 4A: RIVER-DOMINATED DELTAS, DISTRIBUTARY MOUTH BARS, PANTHER TONGUE MEMBER, GENTILE WASH

Participants will be introduced to river-dominated deltaic deposits at this stop. The purpose is to closely examine the distributary mouth bar deposits of the Panther Tongue Member (Star Point Formation). Gentile Wash is located approximately 2 km north of Helper (Figs. 0-1 and 0-2). The emphasis of this stop is as follows: (i) sedimentology and architecture of distributary mouth bar deposits, (ii) key building blocks of river-dominated deltas, and (iii) 3D geometry and stacking patterns at a reservoir-scale.

There are a wide variety of deltas worldwide and these have been classified based on the relative influence of fluvial, wave and tidal processes. The best example of a modern river-dominated delta is the Mississippi Delta (Fig. 4-1). In river-dominated deltas, sediments are delivered to the delta front via distributary channels (Fig. 4-1). Field evidence suggests that the Panther Tongue channels were terminal distributary channels (subaqueous) located in the proximal portion of a mouth bar (Olariu et al. 2001, 2005: Olariu and Bhattacharya 2006). Channel facies are characterized by abundant cross bedding, convolute bedding, steep and overhanging margins, and large mudstone/siltstone clasts floating within the sandstones. High rates of sedimentation are indicated by the slumped, contorted and over-steepened (i.e. greater than the angle of repose) sandstone beds. It is likely that the channels were cut and filled very rapidly. A *Teredolites* ichnofacies (woodground) is indicative of a salt water or marine influence.

Distributary mouth bars are built at the terminus of the distributary channels where the flow becomes unconfined (Fig. 4-1). The distributary mouth bar facies at Gentile Wash includes interbedded mudstones, siltstones and very fine- to medium-grained sandstones (Fig. 4-2). These deposits consist of wave-modified Bouma-like T_{abc}, T_{bc} and T_c turbidite beds or shallow water turbidites (Fig. 4-2). The dominant sedimentary structures are current-, combined-flow- and wave-ripple laminations, planar laminations, hummocky cross stratification (HCS) and convolute bedding. Numerous sole marks (i.e. groove, flute, tool, prod) occur at the base of the sandstone beds indicating a southerly flow direction (Fig. 4-2). Regional studies have shown that the Panther Tongue shorelines were oriented west to east, with offshore directed towards the south (Newman and Chan 1991; Hwang and Heller 2002). Carbonaceous matter is locally abundant and consists of wood fragments, coal clasts and finely comminuted plant debris. The distributary mouth bar deposits are moderately- to thoroughly-bioturbated by *Ophiomorpha*, *Skolithos*, *Diplocraterion*, *Paleophycus*, *Terebellina*, *Teichichnus* and *Rosselia* traces (Fig. 4-2). Evidence for shallow water deposition includes the presence of wave- and combined-flow-ripple laminated sandstones, HCS sandstones, and a diverse and fully marine ichnofaunal suite.

The Panther Tongue distributary mouth bar deposits exhibit well defined coarsening- and thickening-upward successions (Fig. 4-2). Up to 5 successions are observed at any given locality. Mouth bars have lobate geometries with a diameter ranging from hundreds of meters to a few kilometers. Similar to other river-dominated successions, the Panther Tongue mouth bars have well defined clinoforms that dip 1-5° (Fig. 4-2). The Panther Tongue Member is capped by a transgressive lag deposit up to 30 cm thick (Newman and Chan 1991; Hwang and Heller 2002).

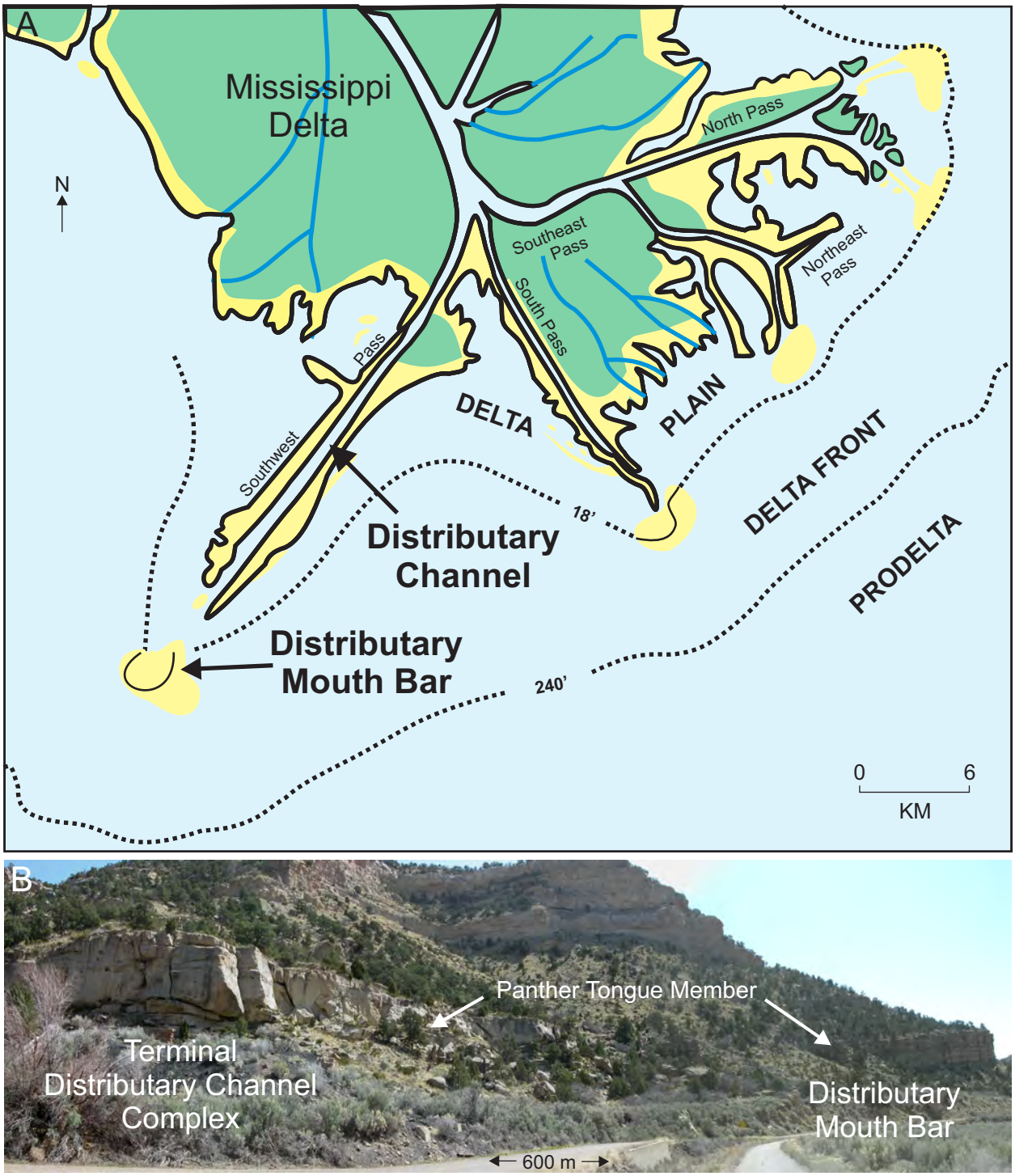

Figure 4-1. River-dominated deltaic deposits: distributary channels and mouth bars. (A) Morphological elements of the Mississippi Delta (modified from Gould 1970, Elliott 1986). (B) Terminal distributary channel passing down-depositional-dip into distributary mouth bar facies, Panther Tongue Member.

Figure 4-2. River-dominated deltaic deposits: distributary mouth bars, Panther Tongue Member, Gentile Wash. (A) Stacked distributary mouth bar deposits, north wall of Gentile Wash. Overall coarsening-upward succession. Transgressive surface of erosion (TSE). Person for scale (circle). (B) Stacked distributary mouth bar deposits, east side of Highway 6. (C to F) Distributary mouth bar facies: stacked Bouma-like T_{bc} and T_{c} turbidite beds (C), wave ripples capping a Bouma-like T_{bc} turbidite bed (D), *Ophiomorpha* (E), and sole marks (F).

STOP 4B: WAVE-DOMINATED SHOREFACE/DELTAICS, HIGH ACCOMMODATION SETTING, STORRS-TO-SPRING CANYON MEMBERS, GENTILE WASH

We will be examining the wave-dominated shoreface deposits in the Storrs Member (Star Point Formation) and Spring Canyon Member (Blackhawk Formation) at this locality (Figs. 0-1 and 0-2). The Spring Canyon Member rests stratigraphically above the Star Point Formation and outcrops further-up-canyon in Gentile Wash compared to the Panther Tongue Member. This stop is a classic outcrop locality that was prominently featured in the AAPG publication *Siliciclastic Sequence Stratigraphy in Well Logs, Cores and Outcrops, Methods in Exploration Series No. 7* (Van Wagoner et al., 1990), which integrated outcrop and nearby subsurface data (i.e. wireline logs and cores).

Despite having examined river-dominated deltaic deposits at the previous stop, most of the shallow marine deposits in the Book Cliffs are wave-dominated (i.e. deltas, shorefaces), in both high and low accommodation settings. The focus of this stop is on a high accommodation setting (Fig. 4-3). We will examine lower accommodation settings later in this trip. Participants will have an opportunity to compare and contrast wave-dominated shoreface/deltaic deposits with the river-dominated deltaic deposits that were observed earlier (Panther Tongue Member). We will examine the following key building blocks of a wave-dominated shoreface/deltaic system at this stop: (i) foreshore-upper shoreface sandstones, (ii) lower shoreface heterolithics (interbedded mudstones and sandstones), and (iii) offshore to inner shelf mudstones (Fig. 4-3; Table 0-1). These shallow marine deposits stack into coarsening-upward successions that pass from dark grey mudstones and silty mudstones near the base, through sandy siltstones with thin bedded wave-rippled sandstones, up to hummocky (HCS) and swaley cross stratified (SCS) sandstones, and finally to trough cross bedded and planar laminated sandstones (Table 1). A wide variety of trace fossils are observed throughout the stack of shallow marine facies including *Arenicolites*, *Asterosoma*, *Chondrites*, *Conichnus*, *Cylindrichnus*, *Helminthopsis*, *Macaronichnus*, *Ophiomorpha*, *Palaeophycus*, *Phycosiphon*, *Planolites*, *Rhizocorallium*, *Rosselia*, *Schaubcylindrichnus*, *Scolicia*, *Skolithos*, *Teichichnus*, *Thalassinoides* and *Zoophycos*. The bioturbation index is relatively low (BI = 0-2) in the sandstones, but consistently higher in the mudstones and siltstones (BI = 3-6). However, some mudstones and siltstones have a low BI (0-2), with associated synaeresis cracks. Details on the BI and specific trace fossil suites within each shallow marine facies is provided in Table 0-1.

As we hike up through Gentile Wash, participants will note a stack of coarsening-upward cycles or parasequences, with at least two parasequences in the Storrs Member and four or five parasequences in the Spring Canyon Member (Fig. 4-3). A parasequence is defined as "a relatively conformable succession of genetically related beds or bedsets bounded by marine flooding surfaces and their correlative surfaces" (Van Wagoner et al. 1990). In general these are characterized by a coarsening-upward (CU) vertical facies succession, with sandstone beds getting thicker upwards and the degree of bioturbation decreasing upwards. Parasequences pass from distal facies at the base to more proximal facies at the top. Parasequences are bounded above and below by marine flooding surfaces and are the fundamental building block in sequence stratigraphy. Note that all of the parasequences in the Storrs Member and Spring Canyon Member show a gradational vertical transition in facies. Gradationally-based shoreface successions are typical of normal regression (i.e. CU successions), which is the main shoreface stacking style in a high accommodation setting. In contrast, low accommodation settings are characterized by forced regressions which are manifested by sharp-based shoreface successions. We will see some examples of forced regressive shoreface successions later in the field trip.

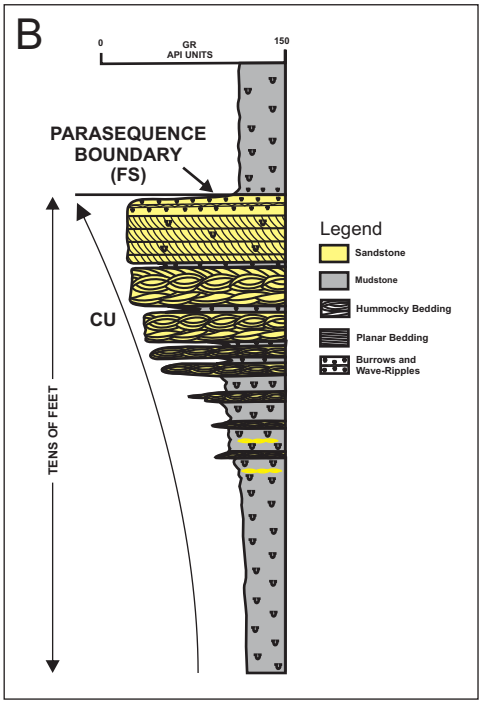

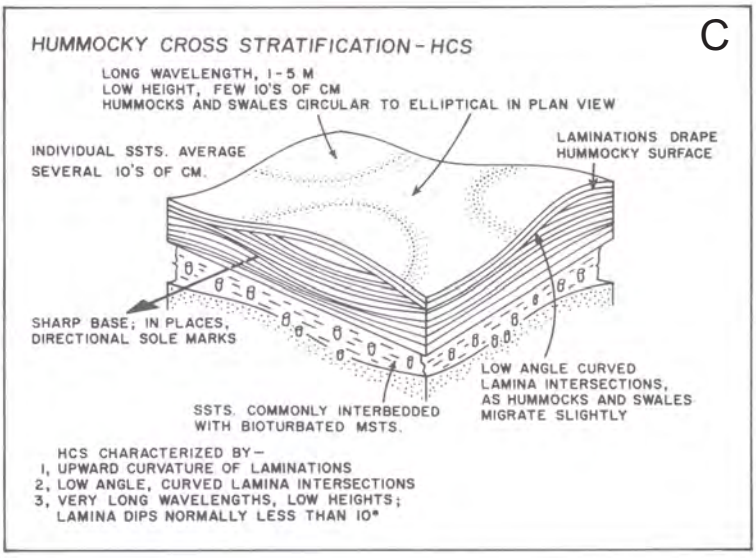

Figure 4-3. Wave-dominated shoreface deposits: high accommodation setting, Spring Canyon Member, Gentile Wash. (A) Storrs Member, Spring Canyon Member, and Aberdeen Member. Note the prominent white caps. (B) Parasequence (Van Wagoner et al. 1990). (C) Hummocky cross stratification (Walker 1982).

FIELD DAY 2

STACKING, CORRELATION, SEA LEVEL AND SEQUENCE STRATIGRAPHY

Stop 5: Wave-Dominated Shoreface/Deltaics, High to Low Accommodation Setting, Kenilworth Member, Price River Canyon/Woodside

Stop 6: Strike Continuity of Wave-Dominated Shoreface/Deltaic Deposits, Beckwith Plateau, Desert Siding, Mile Marker 291

Stop 7: Shoreface-to-Shelf Transition, Kenilworth Member, Green River Embayment/Gunnison Valley

Stop 8: Parasequence-to-Bedset Compartmentalization, Grassy Member, Tusher Canyon

STOP 5: WAVE-DOMINATED SHOREFACE/DELTAICS, HIGH TO LOW ACCOMMODATION SETTING, KENILWORTH MEMBER, PRICE RIVER CANYON/WOODSIDE

This stop focuses on the Kenilworth Member which is the third oldest member in the Blackhawk Formation (Figs. 5-1 to 5-6). The Kenilworth Member consists of a stack of wave-dominated shoreface/deltaic deposits at Price River Canyon, east of Woodside. This area is located along the north banks of the Price River, approximately 6 km east of Woodside (Figs. 0-1 and 0-2). The Book Cliffs are approximately 300 m high in the Price River Canyon to Woodside region. The Kenilworth is the lowermost series of cliff-forming sandstones at this locality (Fig. 5-3). The upper Kenilworth (KPS4) is marked by a 28-33 m thick package of upper shoreface sandstones. For the purpose of this field trip, the definitions of upper and lower shoreface are based on practical-applied reservoir geology concepts and are non-traditional (Fig. 5-1). Strictly speaking, the shoreface zone is defined as being above fair weather wave base and is variously subdivided in academia (Fig. 5-1). The depth to fair weather wave base varies depending on the wave energy of the coastline, and is usually 5-15 m water depth. Storm wave base is defined as the depth to which storm waves can "touch-the-bottom" and generally varies from 30-70 m water depth. During this field trip, the upper shoreface is defined as the zone of thick bedded shoreface sandstones, while the lower shoreface is defined as the zone of thin bedded heterolithics (Williams and Davies 2006). A reservoir geology-based definition of the upper shoreface encompasses most of the traditionally-defined shoreface zone, while the lower shoreface definition straddles the traditionally defined shoreface-to-offshore transitional zone (Fig. 5-1; Williams and Davies 2006). One of the reasons for these reservoir geological subdivisions is that hydrocarbon production is common from thick and thin bedded shallow marine deposits, with each having distinct flow behaviors (i.e. kv/kh; Williams and Davies 2006).

A stack of CU successions or shelf-to-shoreface cycles or parasequences comprise the Kenilworth Member (Figs. 5-3 and 5-5). As we hike up through the side canyon, participants will note an aggradational to progradational stack of at least four coarsening-upward cycles or parasequences in the Kenilworth, KPS1 to KPS4 (Figs. 5-3 and 5-5). Most parasequences are wave-dominated, with abundant wave-rippled, hummocky cross stratified (HCS), swaly cross stratified (SCS), trough cross bedded and planar laminated sandstones. The only exception is KPS2 which has Bouma-like T_{bc} and T_c beds, wave-modified turbidites, thick packages of climbing combined flow ripple-laminated sandstones, carbonaceous-rich mudstones, siltstones and sandstones, and non-bioturbated mudstones, siltstones and sandstones. These suggest a river influenced shoreface-to-shelf setting, probably a distal delta front to prodelta environment. Shallow water turbidity currents were triggered during storm events leading to interbedded classical turbidites, wave modified turbidites, hyperpycnites, and HCS sandstones in KPS2

KPS1 to KPS3 stack to form an aggradational to progradational parasequence set interpreted as part of a HST, while the strongly progradational KPS4 comprises the falling stage (FSST) and/or attached lowstand (LSTa) systems tract (Ainsworth and Pattison 1994; Pattison 1995) (Fig. 5-3). A fifth parasequence, KPS5, is located in the western Book Cliffs and constitutes the transgressive systems tract (TST). Both KPS3 and KPS4 are subdivided into smaller-scale cycles or bedsets (e.g. K4a-c; Fig. 5-6). The KPS4 bedsets show a retrogradational bedset stacking pattern, which likely heralded the onset of transgressive ravinement.

The top of KPS4 is marked by a transgressive lag deposit defining the transgressive surface of erosion (TSE). Two transgressive lag deposits occur in the uppermost part of the Kenilworth Member (Fig. 5-5). Both of these transgressive lags overlie the shoreface-incised

channel complex. These lags are 10 to 40 cm thick and consist of coarse- to very coarse-grained sand, shell fragments, shark's teeth, granules, pebbles and rare wood fragments. A 2 m thick, thoroughly bioturbated, transgressive sandstone package is sandwiched between these lags (Fig. 5-5). Thorough bioturbation could result from the slower rates of sedimentation during the turn-around in relative sea level. The entire transgressive package (i.e. lower lag deposit - bioturbated transgressive sandstone - upper lag deposit) is interpreted to represent an overall transgression that was punctuated by a stillstand. The stillstand would allow time for deposition of the shoreface sandstones and thorough bioturbation prior to renewed sea level rise.

This stop provides the first opportunity to observe a channel complex incising into the top of a wave-dominated shoreface/deltaic sandstone package (Fig. 5-5). The upper shoreface sandstones of KPS4 are cut by a 2 to 6 m thick channel complex (Fig. 5-5). The K4-CH is dominated by cross-bedded sandstones, with some herring-bone cross bedding (tidal channel?). Organic-rich laminae consisting of finely comminuted plant material ("coffee grounds") and organic-rich siltstones are abundant. Bioturbation is moderate and includes *Ophiomorpha*, *Thalassinoides* and *Skolithos*. Bar-form architectures with lens-shaped geometries and lateral-downstream accretion surfaces are dominant. Various sequence stratigraphic interpretations are possible for the K4-CH. Earlier interpretations invoked an incised valley-fill (IVF) resting on the Kenilworth sequence boundary (K-SB). The K-SB was interpreted as a third-order SB, with sediment bypass to Hatch Mesa (Taylor and Lovell 1991, 1995). A conventional IVF interpretation implies a drop in relative sea level and the presence of falling stage or lowstand sand bodies further down-depositional-dip (Taylor and Lovell 1995). A variation on this conventional interpretation is a channel "floored" by a high frequency SB (i.e. HFSB), with no detachment of shallow marine sand bodies. The HFSB interpretation has an attached falling stage and/or lowstand sand body (Fig. 5-3D; Ainsworth and Pattison 1994; Pattison 1995). This hybrid modeling scenario includes components of both the conventional and alternative models, such as HFSBs, parasequence-scale IVFs, temporally and spatially linked nearshore terrestrial and shallow marine facies belts, no detached sand bodies down-dip, attached only (Fig. 5-3D). An alternative sequence stratigraphic interpretation proposes that the K4-CH is a shoreface-incised channel (i.e. tidally influenced distributary channel) temporally and genetically related to the progradation of the K4 shoreface succession (Pattison, 2018, 2019a). This alternative model has temporal and spatial linkage between the nearshore terrestrial and laterally adjoining shallow marine facies belts. No SB exists (i.e. no third-order SB nor HFSB), hence no IVF. There is no evidence of sediment bypass, no detached lowstand deposit further down-depositional-dip, and K4-CH is interpreted as a tidally influenced distributary or tidal-estuarine channel-fill.

As discussed earlier, two sequence stratigraphic end-member modeling scenarios are considered throughout this field trip: (1) conventional, classic, third-order SB, IVF, non-linked nearshore terrestrial and shallow marine facies belts, detached sand bodies are likely down-dip (Fig. 2-3A), and (2) alternative, no SB, no IVF, suite of discrete parasequence-scale shoreface-incised channels, temporally and spatially linked nearshore terrestrial and shallow marine facies belts, no detached sand bodies down-dip, attached only (Fig. 2-3B). Each sequence stratigraphic interpretation carries a radically different prediction of sand body distribution and lateral extent. Selecting the correct correlation style for the shoreface-incised channels has implications for sand body continuity and connectivity between geographically isolated localities (i.e. subsurface wells), and also for the prediction of falling stage and lowstand sand bodies further basinwards. These correlation options will be examined in further detail when we study the Desert-Castlegate interval later in the field trip.

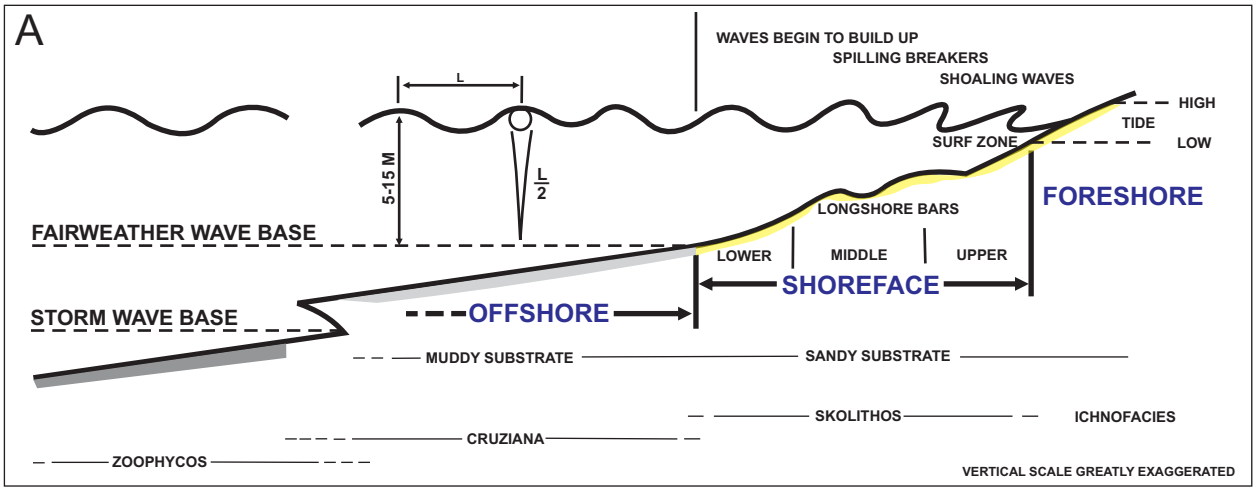

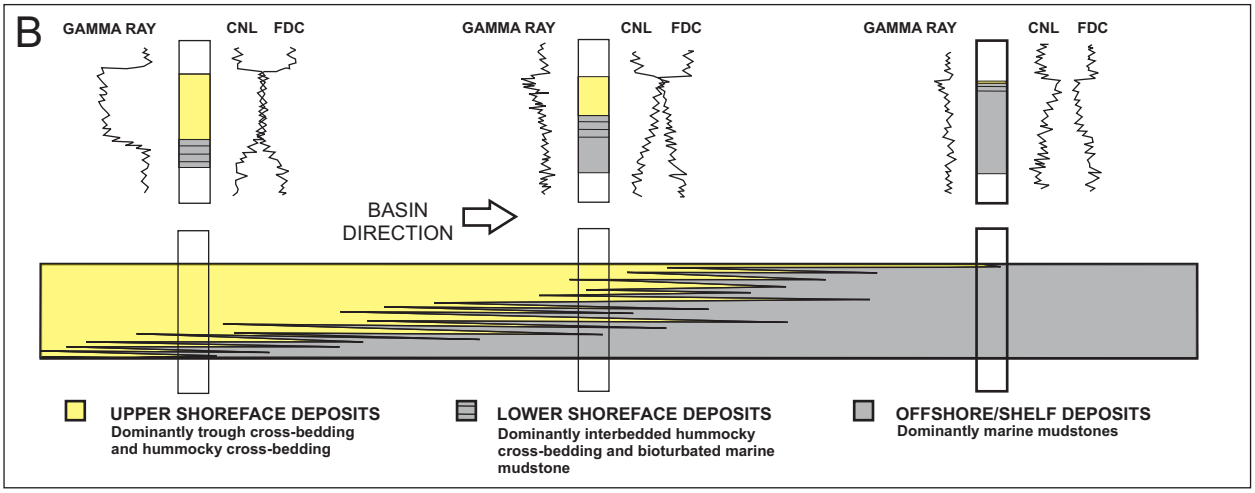

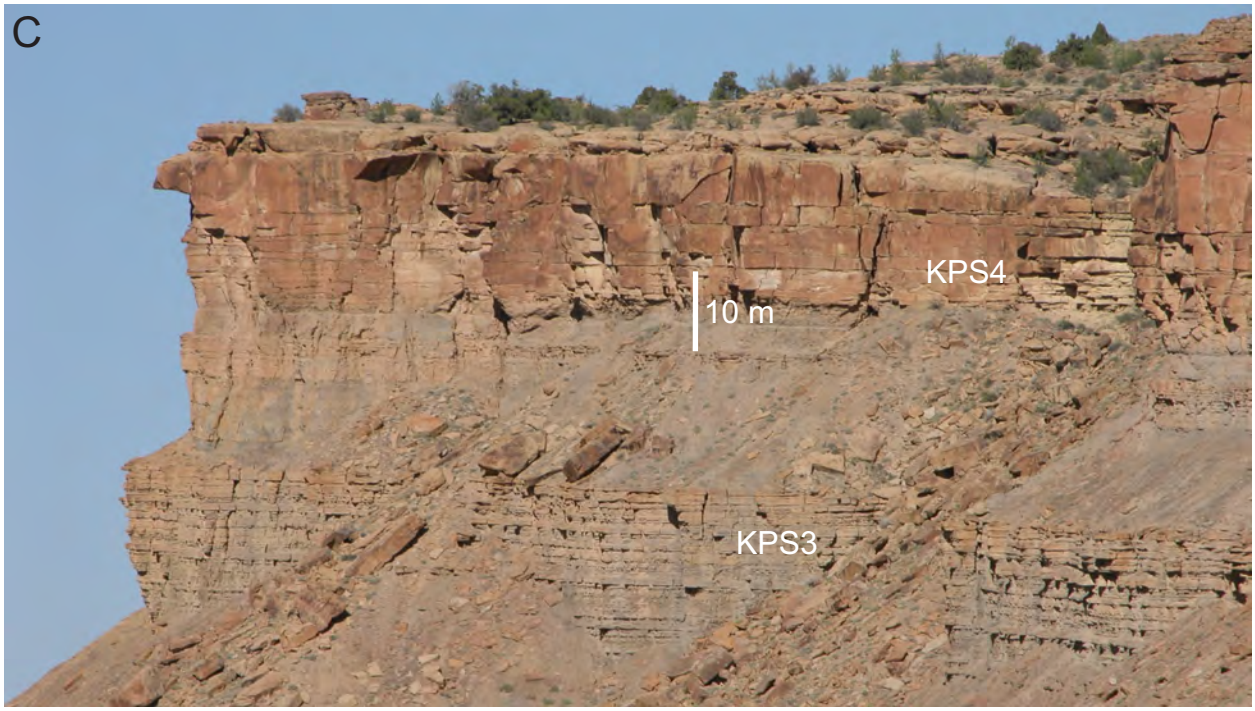

Figure 5-1. Wave-dominated shallow marine depositional systems. (A) Cross section across a shoreface-to-shelf environment (Walker 1985). (B) Cross section through a parasequence highlighting the transition from thick bedded upper shoreface sandstones into thin bedded lower shoreface heterolithics (modified from Williams and Davies 2006). (C) Progradational stack, Kenilworth Member parasequences KPS3 and KPS4, Woodside-Price River Canyon.

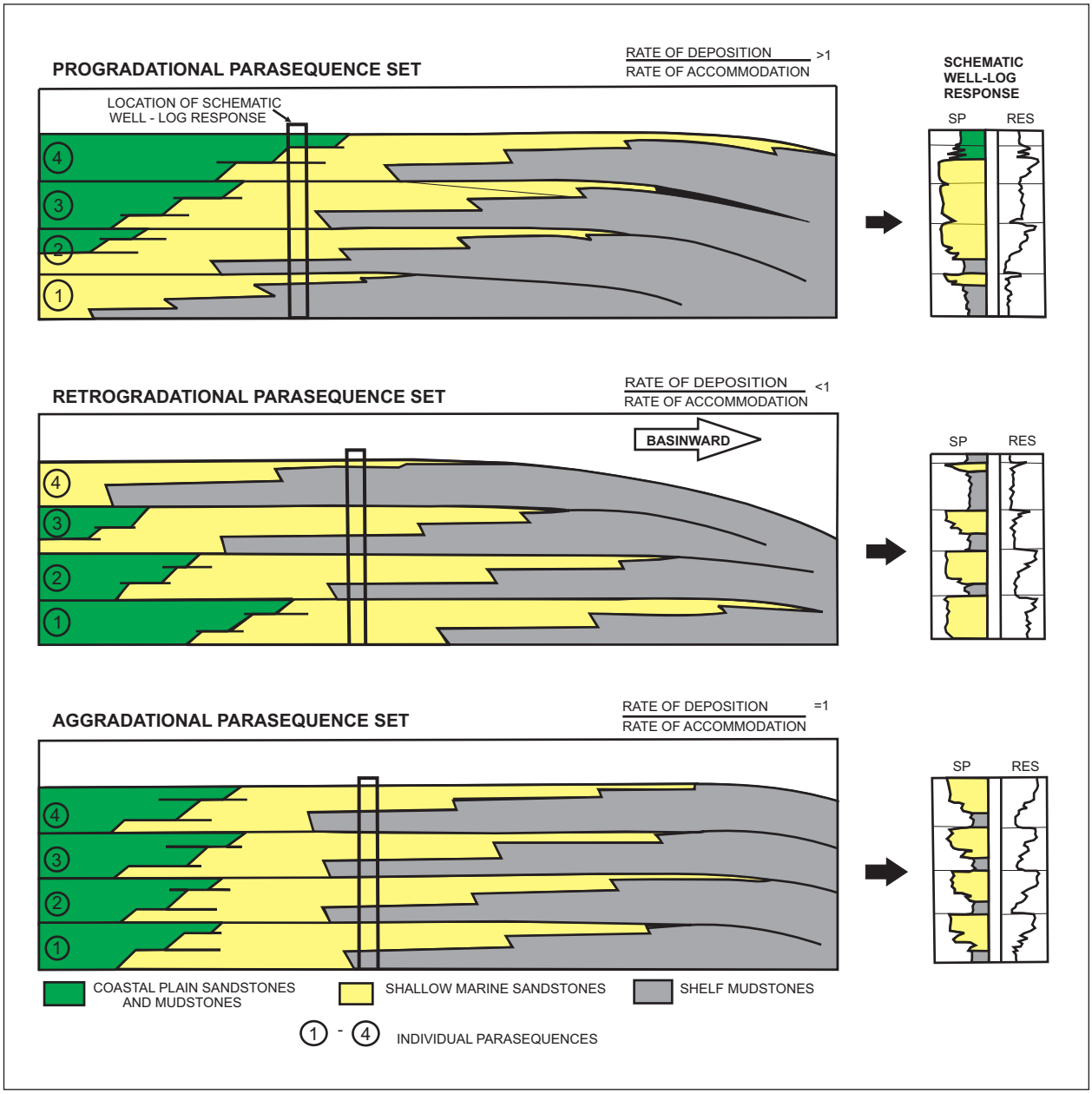

Figure 5-2. Parasequence stacking patterns. Progradational, retrogradational and aggradational parasequence sets (Van Wagoner et al. 1990).

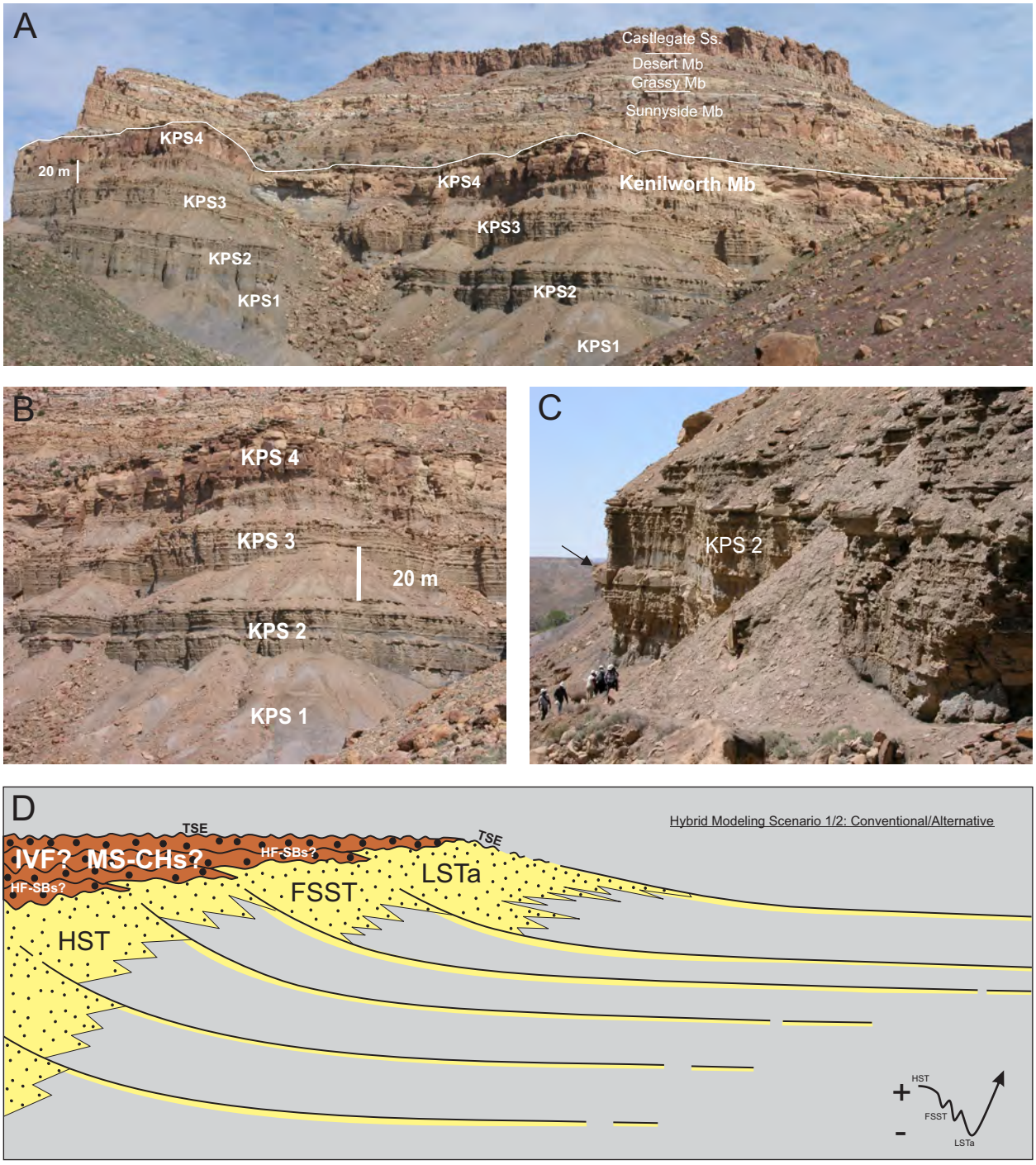

Figure 5-3. Wave-dominated shoreface/deltaic deposits: high to low accommodation setting, Kenilworth Member, Woodside/Price River Canyon. (A) North side of Price River at parking spot. Kenilworth parasequences (KPS1 to KPS4). (B) Kenilworth Member. (C) Edge of KPS2 outcrop (arrow) mimics a gamma ray profile. (D) Sequence stratigraphy of the Kenilworth Member. Depositional-dip-oriented schematic cross section. No vertical or lateral scale is implied. Hybrid modeling scenario 1/2: components of both the conventional and alternative models, HFSBs, parasequence-scale IVFs, temporally and spatially linked nearshore terrestrial and shallow marine facies belts, no detached sand bodies down-dip, attached only. Relative sea-level curve at bottom right showing possible genesis of highstand (HST), falling stage (FSST), and lowstand-attached (LSTa) systems tracts. This is one possible solution in a sequence stratigraphic solution set (*as per* Hampson 2016). Other combinations of autogenic and/or allogenic processes could have generated these stratal architectures. Fluvial-tidal channel sandstones (red), shoreface-deltaic sandstones (yellow), marine mudstones (gray). Parasequence flooding surfaces shown by bold smooth lines, facies changes indicated by zigzag lines, erosional surfaces are bold wiggle lines. TSE (transgressive surface of erosion), IVF (incised valley-fill), MS-CHs (amalgamated multi-storey channels), HF-SBs (high-frequency sequence boundaries).

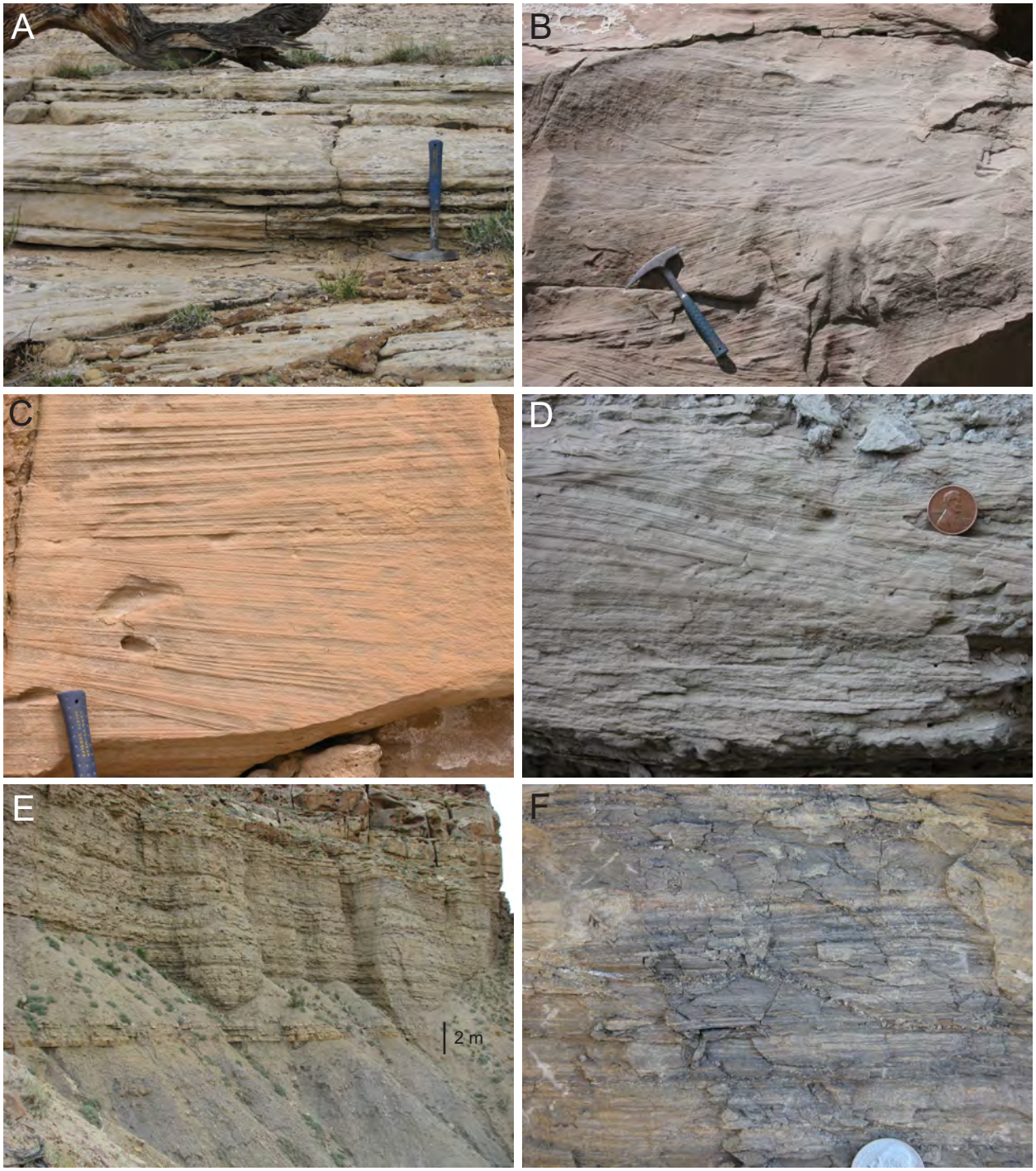

Figure 5-4. Wave-dominated shallow marine deposits: foreshore and upper shoreface sandstones (A-C), lower shoreface sandstones (D), and inner shelf heterolithics and mudstones (E-F). (A) Planar-laminated fine-grained foreshore sandstones (Facies 1A), Desert Member, Christmas Ridge. (B) Trough cross bedded fine- to medium-grained upper shoreface sandstones (Facies 1B), Spring Canyon Member, Gentile Wash. (C) Swaley cross-stratified fine-grained upper shoreface sandstones (Facies 1C), Kenilworth Member, Price River Canyon. (D) Hummocky cross stratified very fine-grained sandstones (Facies 1D) passing upwards into wave ripple laminated sandstones (Facies 1E), Storrs Member, Gentile Wash. (E) Thin bedded inner shelf sandstones and mudstones (Facies 1F and 1G), Desert Member, Christmas Ridge. (F) Thin bedded heterolithics (Facies 1G and 1H), upper Aberdeen Member, northwest of Willow Bend, Gunnison Valley. USA nickel coin for scale (2.1 cm diameter).

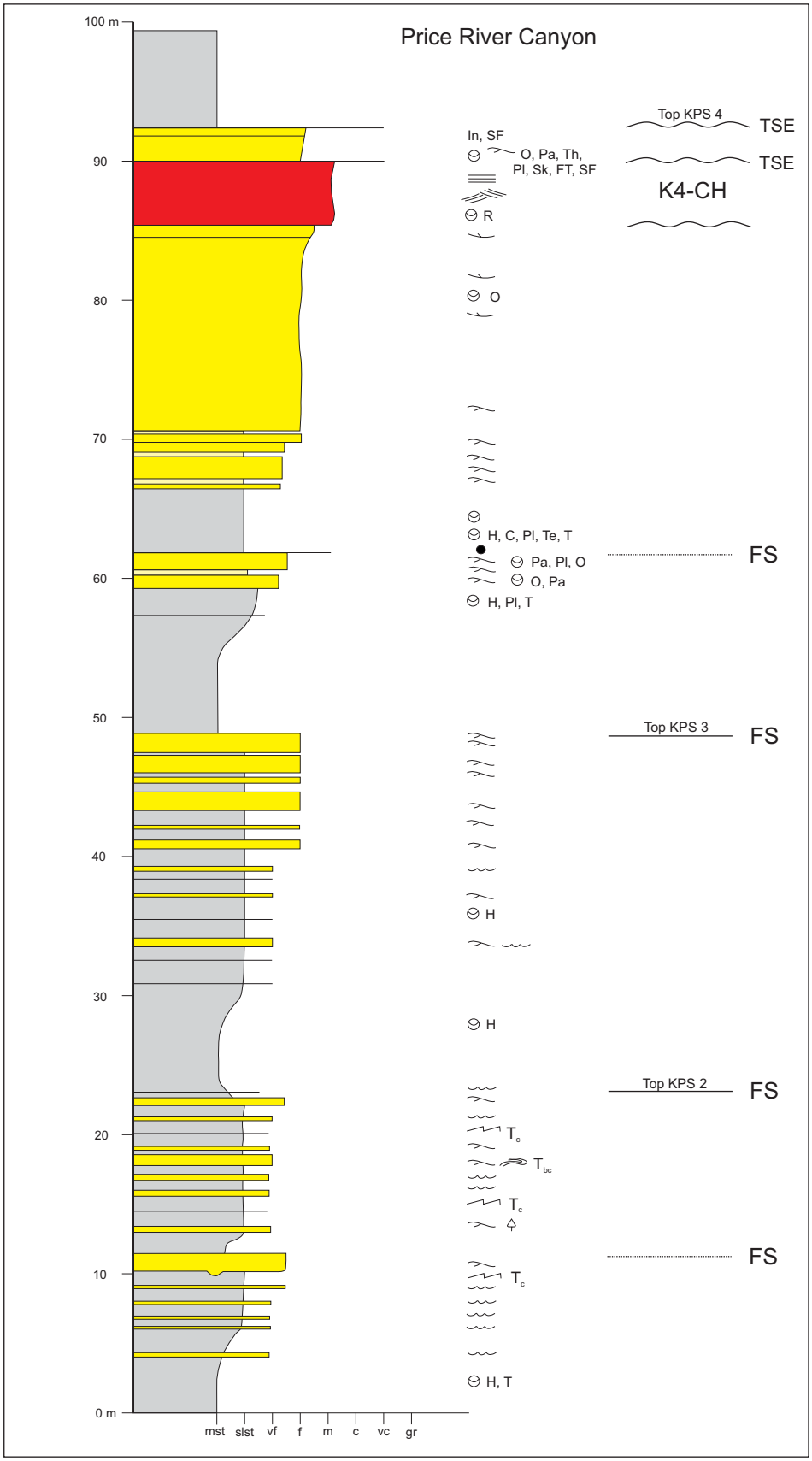

Figure 5-5. Measured section, Kenilworth Member, Price River Canyon (modified from Pattison 1994a, 1995). Shoreface sandstones (yellow), channel sandstones (red), marine mudstones (grey). Simplest explanation for the tidally-influenced channel-fill succession at the top of Kenilworth Member parasequence is a tidally-influenced distributary channel and/or tidal channel (Pattison 2019a), and not an incised valley-fill as per previous conventional sequence stratigraphic interpretations (i.e. Pattison 1995; Taylor and Lovell 1995). Flooding surface (FS), transgressive surface of erosion (TSE).

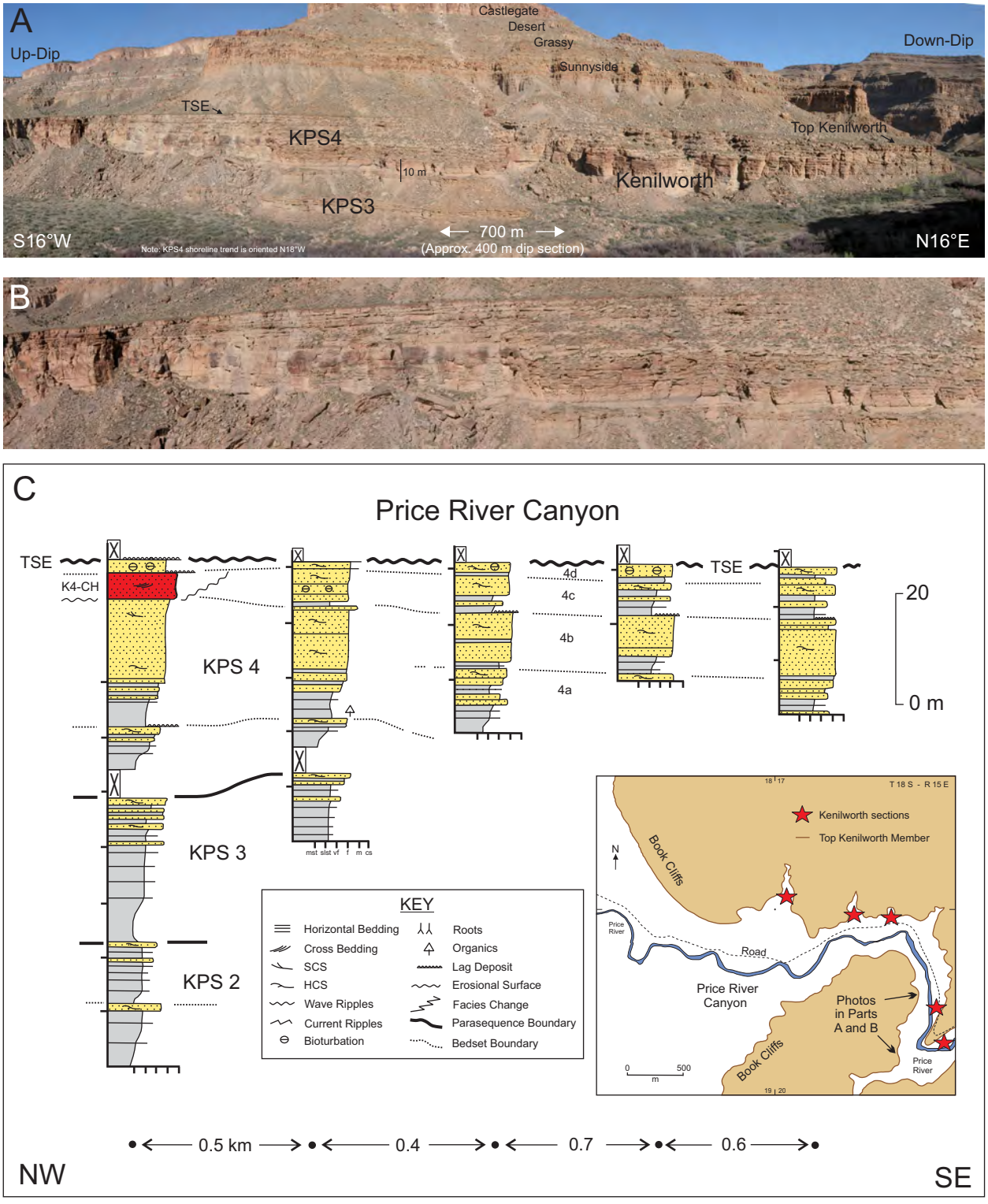

Figure 5-6. Down-dip compartmentalization of a shoreface parasequence, KPS4 bedsets, Kenilworth Member, Woodside/Price River Canyon meander bend. (A) Oblique-to-depositional-strike photo-panorama looking west. Up-dip to the left. (B) Top of KPS4 splitting into bedsets. Same position as previous photo: close-up of the left-side of Part A. (C) Depositional-dip-oriented cross section, Kenilworth Member, Price River Canyon (modified from Pattison 1995). Five closely-spaced measured sections with continuous cliff-forming outcrop between the sections. Datum is the top Kenilworth Member. Kenilworth parasequences (KPS2 to KPS4), bedsets (4a to 4d), transgressive surface of erosion (TSE), upper Kenilworth shoreface-incised channel (K4-CH). Inset map shows the location of the photos and sections.

STOP 6: STRIKE CONTINUITY OF WAVE-DOMINATED SHOREFACE/DELTAIC DEPOSITS, BECKWITH PLATEAU, DESERT SIDING, MILE MARKER 291

The Beckwith Plateau strike-section viewing stop at Mile Marker 291 provides an exceptional opportunity to examine the depositional-strike continuity of wave-dominated shoreface/deltaic deposits. Pull the vehicles safely off of Highway 6 (west side of road) just south of Mile Marker 291 and climb the small Mancos Shale hill to view the Book Cliffs (Figs. 0-1 and 0-2). This depositional strike section covers approximately 15 km from Mount Elliott in the north to Little Elliott Mesa in the south (Fig. 6-1). These along-strike dimensions are equivalent to the length of many large oil fields including the Brent Field - North Sea (14 km long) and the Agbada Field - Niger Delta (12 km long), among others. The Book Cliffs are at a near maximum height at Mt. Elliott (approximately 600 m high), and vary from 300 to 500 m at this stop. Three main cliff-forming sandstone packages or benches are observed, and from top to bottom include the following:

(i) Castlegate Sandstone and Desert Member,
(ii) Grassy Member and Sunnyside Member, and
(iii) Kenilworth Member (Fig. 6-1).

The distal deposits of the Aberdeen and Spring Canyon members are in the lower part of the cliff section. The Spring Canyon Member is marked by a prominent series of mudstone-rich benches near the base of the Book Cliffs which can be correlated from the area north of Woodside approximately 30 km southwards into the Battleship Butte-to-Blue Castle region (Fig. 6-1).

The Blackhawk Formation and Castlegate Sandstone define an overall progradational stacking pattern, which is also manifested or nested at a smaller-scale within each of the main cliff-forming sandstone packages. In all cases there is an upward increase in proximal facies. For example, the Castlegate Sandstone consists of high net:gross channel-fill deposits that form a sheet-like complex resting sharply on top of the Desert Member coastal plain deposits characterized by lower net:gross channel-fill complexes.

The middle cliff-forming package is dominated by the shoreface sandstones of the Grassy and Sunnyside members (Fig. 6-1). There are two prominent white caps in this middle cliff-forming sandstone package: GPS1 and SPS3. These layers can be traced for an additional 80+ km northwards using the subsurface well control north and east of the Book Cliffs outcrop belt.

The lower cliff-forming sandstone package is comprised of the Kenilworth Member. The uppermost Kenilworth includes the stacked shoreface sandstones of KPS4 which form a 28-33 m cliff-forming sandstone package. These are underlain by shallow marine sandstones and mudstones (i.e. heterolithic facies) of KPS3. Together, KPS4 and KPS3 form a 50-60 m thick cliff-forming sandstone package. Laterally discontinuous mudstone- to heterolithic-dominant benches of KPS2 and KPS1 occur directly below the KPS4/KPS3 cliff-forming sandstones. The discontinuity of the KPS2 and KPS1 benches is explained by the intersection of a 2D cliff face with the 3D gently lobate geometry of these lower shoreface deposits.

Most of the shoreface sandstones in the Kenilworth, Sunnyside, and Grassy members are wave-dominated successions. These are laterally continuous across the entire 15 km of depositionally-strike oriented outcrop, attesting to the vigorous storm and wave regime characteristic of the Campanian Seaway. Sediment input points (i.e. rivers-deltas) are scattered along the length of the shoreline trends, with the main feeders generally located every 10-20 km (Hampson and Howell 2005). Evidence from KPS2 indicates river-influenced shoreface-to-shelf deposits in the Price River Canyon and Gunnison Butte regions, a distance of approximately 15 km along strike (Pattison 2005a, b, c; Pattison and Hoffman 2008).

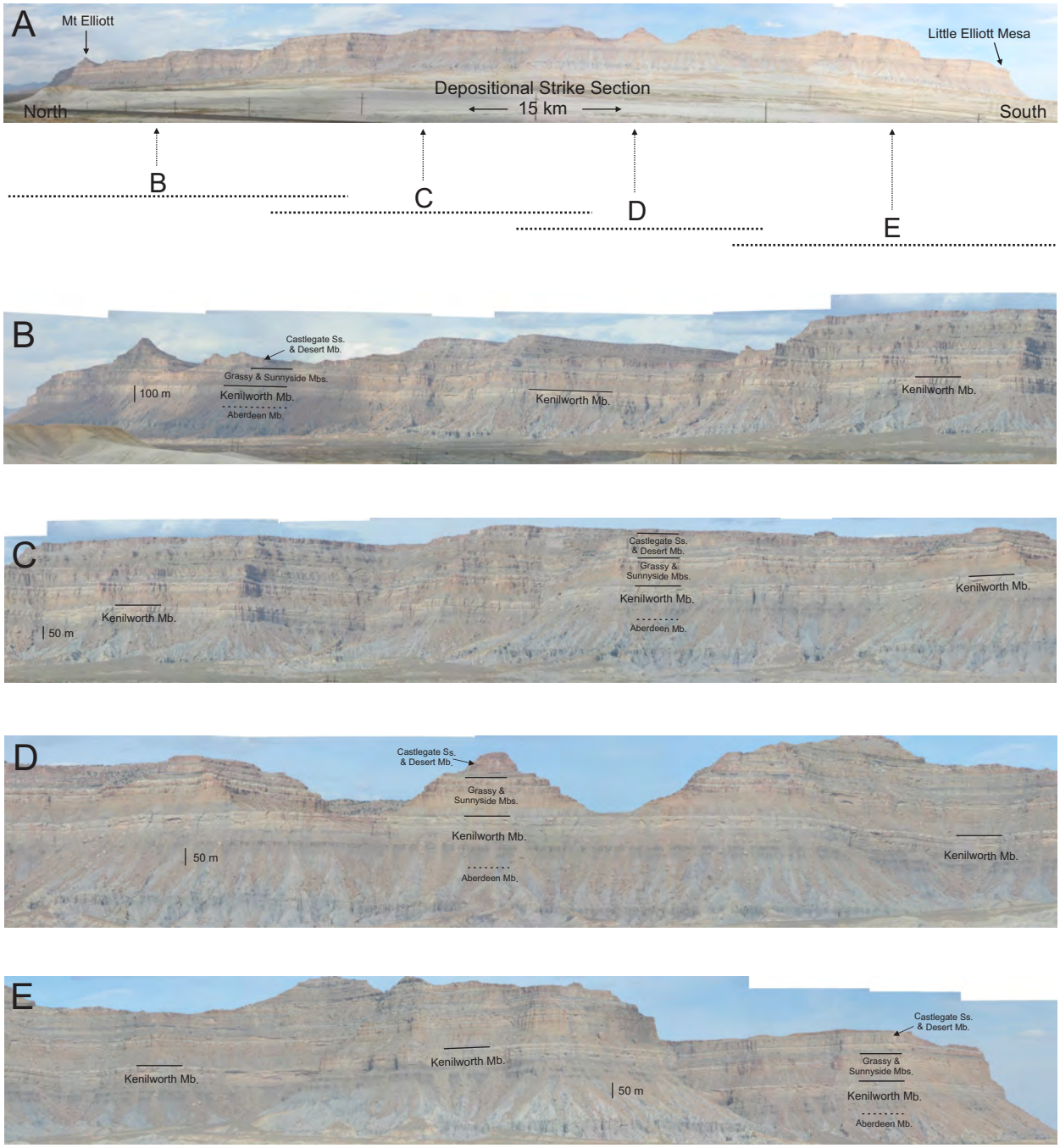

Figure 6-1. Strike continuity of wave-dominated shoreface/deltaic deposits, Blackhawk Formation, Beckwith Plateau, Desert Siding region. (A) Photo-panorama from Mount Elliott (north) to Little Elliott Mesa (south) covering approximately 15 km. (B to E) Four close-up panoramas with positions shown in (A).

STOP 7: SHOREFACE-TO-SHELF TRANSITION, KENILWORTH MEMBER, GREEN RIVER EMBAYMENT/GUNNISON VALLEY

The Gunnison Valley overview stop is a world class example of a depositional-dip transect that records the transition from wave-dominated shoreface-deltaic deposits to mudstone-dominated shelf deposits (Fig. 7-1). Drive approximately 6 km north of the city of Green River along the eastern banks of the Green River and park the vehicles at an overlook point (Figs. 0-1 and 0-2). This locality is approximately 60 km down-depositional-dip from the western-most Book Cliffs outcrop in the Helper region. Battleship Butte, Blue Castle Butte, Blue Castle, Middle Mountain, Gunnison Butte, Tusher Canyon and Hatch Mesa are the main physiographic features in this region. The lateral field of view along Battleship Butte (western edge of the visible outcrop to the bow of Battleship Butte) is approximately 5 km of depositional-dip-oriented section (Fig. 7-1). An additional 7 km of depositional-dip-oriented section is prominently displayed from Blue Castle Butte to the western edge of Tusher Canyon (Fig. 7-1). The Tusher Canyon to Hatch Mesa outcrop belt spans 20 km representing approximately 8 km of depositional-dip-oriented section (Fig. 7-1). Therefore the entire field of view at the Gunnison Valley stop encompasses a staggering *20 km of dip-oriented outcrop section*.

The Castlegate Sandstone forms a prominent ridge-line cap along much of the Book Cliffs in this region and is composed of high net:gross channel-fill deposits (Fig. 7-1). Most of the Blackhawk Formation is also well exposed in this dip-oriented section. The Desert Member is comprised of shoreface sandstones, channel sandstones and heterolithics, and fine-grained coastal plain deposits. The Desert Member frequently merges with the overlying Castlegate in a sandstone-on-sandstone contact (Fig. 7-1). The Grassy and Sunnyside members are comprised of a stack of shoreface-to-shelf parasequences showing a gradual basinward (eastward) thinning and fining. The bow of Battleship Butte is marked by the 30 m thick KPS4 sandstone body (. 7-1 and 7-2). This sandstone is underlain by lower shoreface heterolithics of KPS3 package on the extreme eastern edge of Battleship Butte, which in turn is underlain by two *ratty* cliff-forming mudstone packages which are KPS2 and KPS1. When tracing the Kenilworth basinwards, these cliff-forming units occur as three distinct benches (KPS4, KPS3, KPS2/1) near the base of the Book Cliffs in the Gunnison Butte region (Fig. 7-1). Eventually these mudstone-rich benches fade into the background marine mudstones. However the top of the Kenilworth can still be correlated into the Hatch Mesa region because of a prominent colour change in the mudstones which demarcates the Kenilworth-Sunnyside contact (Pattison 2005a, 2005b) (Figs. 7-1 and 7-2).

The Aberdeen Member is mostly composed of marine mudstones, however, sandstone- and heterolithic-rich subaqueous channel-fill deposits are observed in the Battleship Butte to Middle Mountain region, and are extremely well preserved at the base of the Book Cliffs in the Gunnison Butte to Tusher Canyon region (Pattison 2005c; Pattison et al. 2007) (Fig. 7-2). The contact between the Aberdeen-Kenilworth is marked by iron-rich siltstones and mudstones, with isolated pods of fossiliferous coarse-grained lag deposits and oolitic ironstones (Fig. 7-2). Excellent examples of the latter occur along the extreme eastern edge of Middle Mountain (Toad Stool outcrop section), between Tusher Canyon and Horse Canyon-South, and in the Hatch Mesa to Floy Wash region (Chan 1992; Pattison 2005c). The Spring Canyon Member is highlighted by the mudstone-dominated cliff sections at the base of the Book Cliffs at Battleship Butte and Blue Castle (Fig. 7-1). These layers can be continuously traced northwards and westwards into the proximal Spring Canyon Member deposits in the Helper-to-Price region.

The down-depositional-dip transition from shoreface-to-shelf environments is beautifully displayed in the wave-dominated Kenilworth Member along the 20 km of dip-oriented section. The following key points have been revealed from previous studies:

(i) All of the Kenilworth shoreface sandstone successions show a basinward facies change into offshore or inner shelf mudstones.
(ii) Hampson (2000) measured KPS4 clinoform dips of 0.5-0.9° in the upper shoreface, 0.1-0.7° in the proximal lower shoreface, 0.02-0.1° in the distal lower shoreface, and 0.01-0.03° in the offshore shelf/ramp in the Battleship Butte to Gunnison Butte region. These dips are significantly less than the clinoform dips in a river-dominated system (e.g. anther clinoforms dip 1-5°).
(iii) The upper shoreface sandstones pass into lower shoreface heterolithics over a distance of 1 to 2 kilometers down-depositional-dip.
(iv) The lower shoreface heterolithics pass into offshore mudstones over 1 to 3 kilometers down-dip.
(v) Parasequences split basinward into a series or thinner cycles or bedsets (e.g. 30 m thick KPS4 sandstone splits into at least 3 bedsets) (Fig. 7-3).
(vi) Parasequences exhibit a gradual basinward thinning.
(vii) The bedset stacking pattern is progradational to retrogradational in the uppermost Kenilworth parasequence, KPS4.
(viii) If the top Kenilworth was picked as the uppermost sandstone body, the top would drop stratigraphically towards the east (i.e. implications for mis-correlation).
(ix) KPS2 becomes thicker and sandier towards the east in the Gunnison Butte-Tusher Canyon and Hatch Mesa regions. These basinward sandying packages are interpreted as shoreface-detached prodelta turbidite complexes (Pattison 2005a, 2005b, 2005c; Pattison and Hoffman 2008).

A simple set of correlation rules and guidelines have been distilled for similar wave-dominated shoreface-to-shelf systems (Williams and Davies 2006; Pattison, Williams and Davies 2007a, 2007b, 2007c; Pattison 2010):

(i) parasequences show a gradual basinward thinning,
(ii) parasequences exhibit an abrupt decrease in sandstone content basinwards that is matched by an equally abrupt increase in mudstone,
(iii) inner shelf mudstone facies can be quartz-silt dominant and therefore have a similar compaction factor as the up-dip shoreface sandstones,
(iv) parasequences split basinward into thinner cycles or bedsets, and
(v) no steeply dipping clinoforms in a wave-dominated shoreface-shelf system.

The subsurface implications of applying the correct correlation scenario for a shallow marine shoreface/delta-to-shelf environment includes the following (Williams and Davies 2006; Pattison, Williams and Davies 2007a, 2007b, 2007c; Pattison 2010):

(a) avoid cycle or parasequence skips,
(b) develop a tight correlation framework and a robust static geological model,
(c) increase the likelihood of a history matched dynamic reservoir model,
(d) improve the prediction of fluid flow, and
(e) optimize development activities.

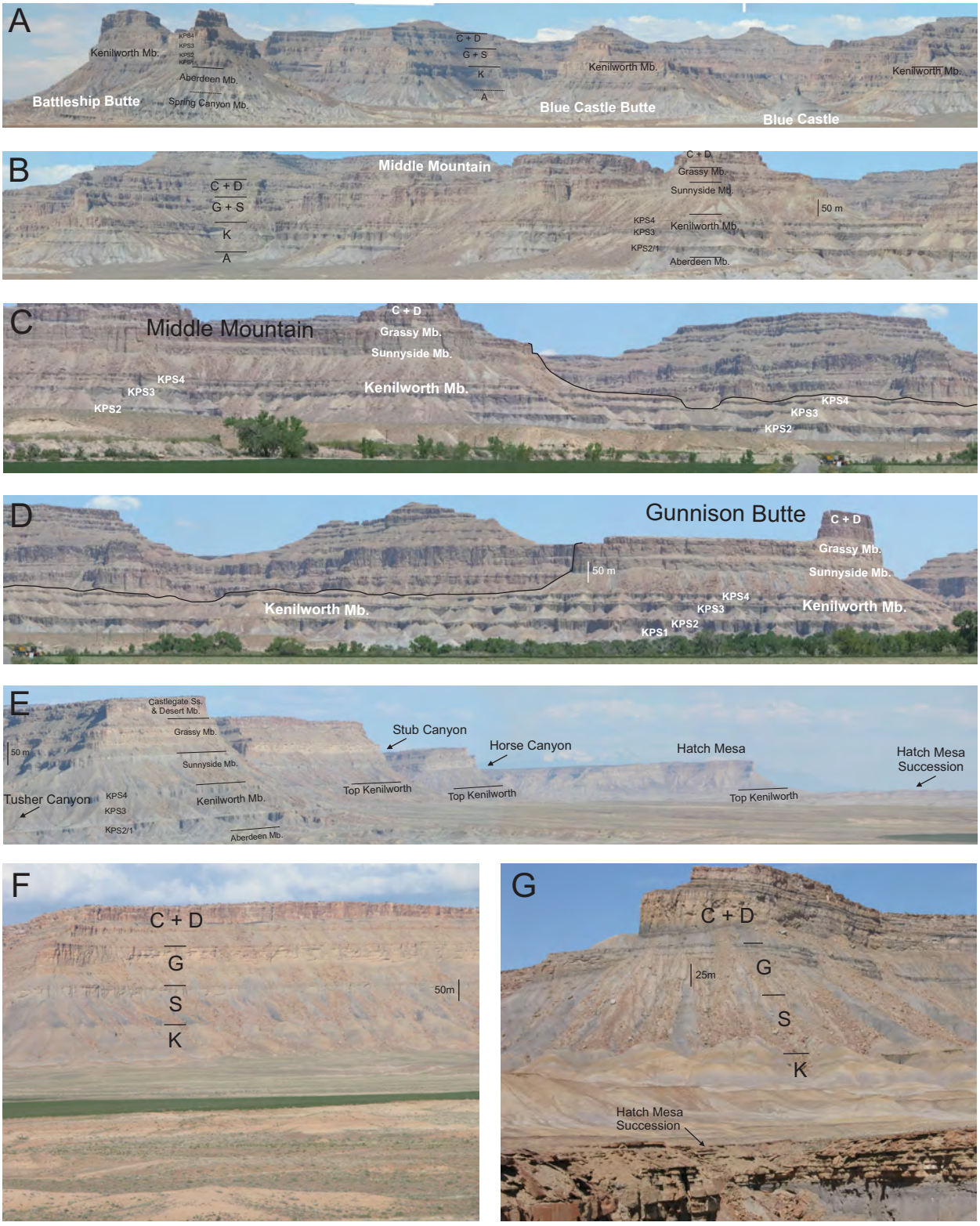

Figure 7-1. Shoreface-to-shelf transition: wave-dominated deltaic system, Kenilworth Member, Green River embayment depositional-dip section. Location abbreviations given earlier. (A) BB to BCB to BC to western MM photo-panorama. (B) Western MM photo-panorama. (C) Eastern MM photo-panorama. (D) Eastern MM to GB photo-panorama. (E) TC to SC to HC-S to HM photo-panorama. (F) Between Tusher Canyon and Coal Canyon. C (Castlegate), D (Desert), G (Grassy), S (Sunnyside), and K (Kenilworth). (G) Hatch Mesa and Hatch Mesa succession (time equivalent to KPS2).

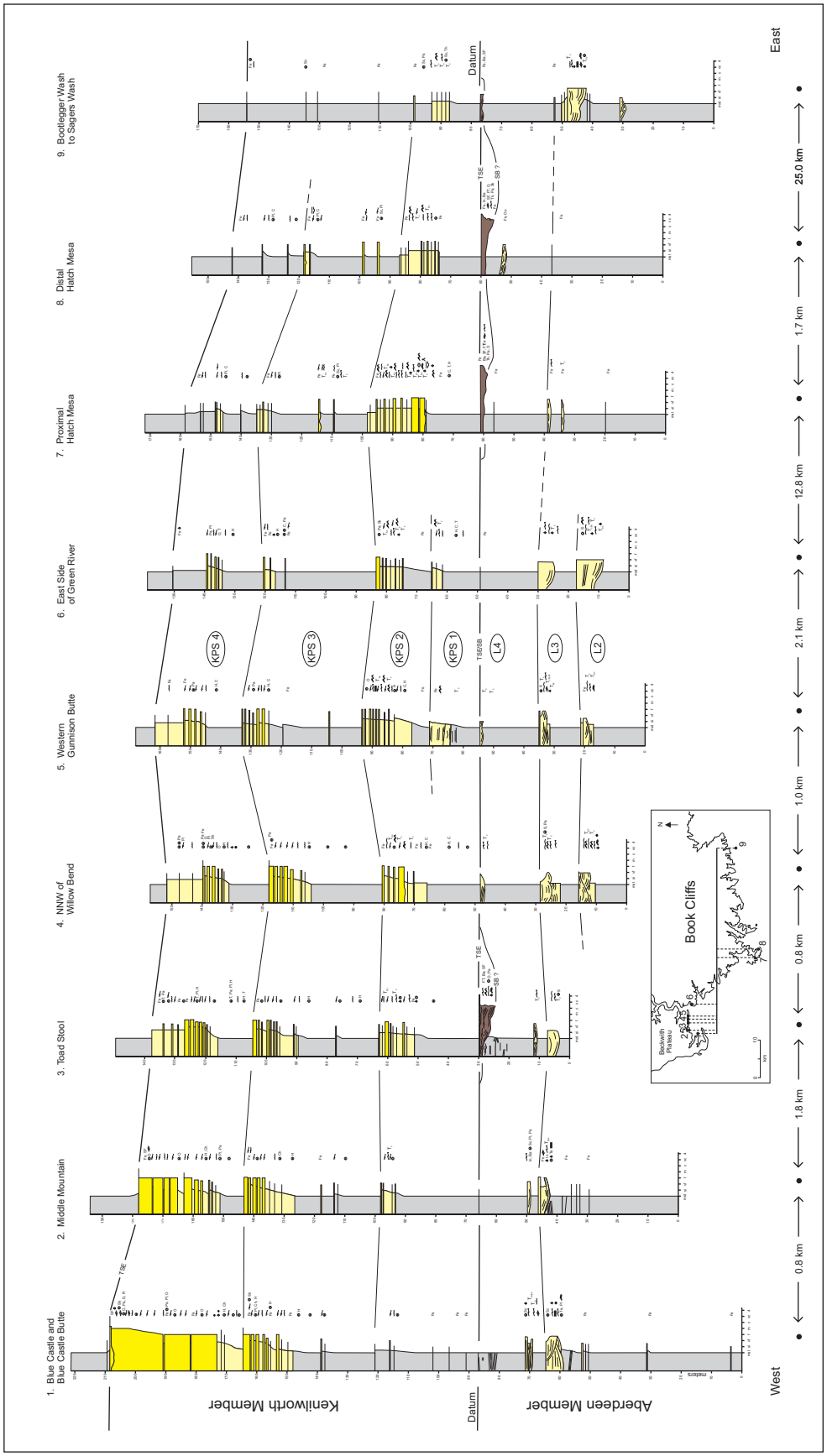

Figure 7-2. Dip-oriented cross section, Kenilworth Member to upper Aberdeen Member stratigraphic interval: BCB to BW (Pattison et al. 2007a). Datum is the top Aberdeen.

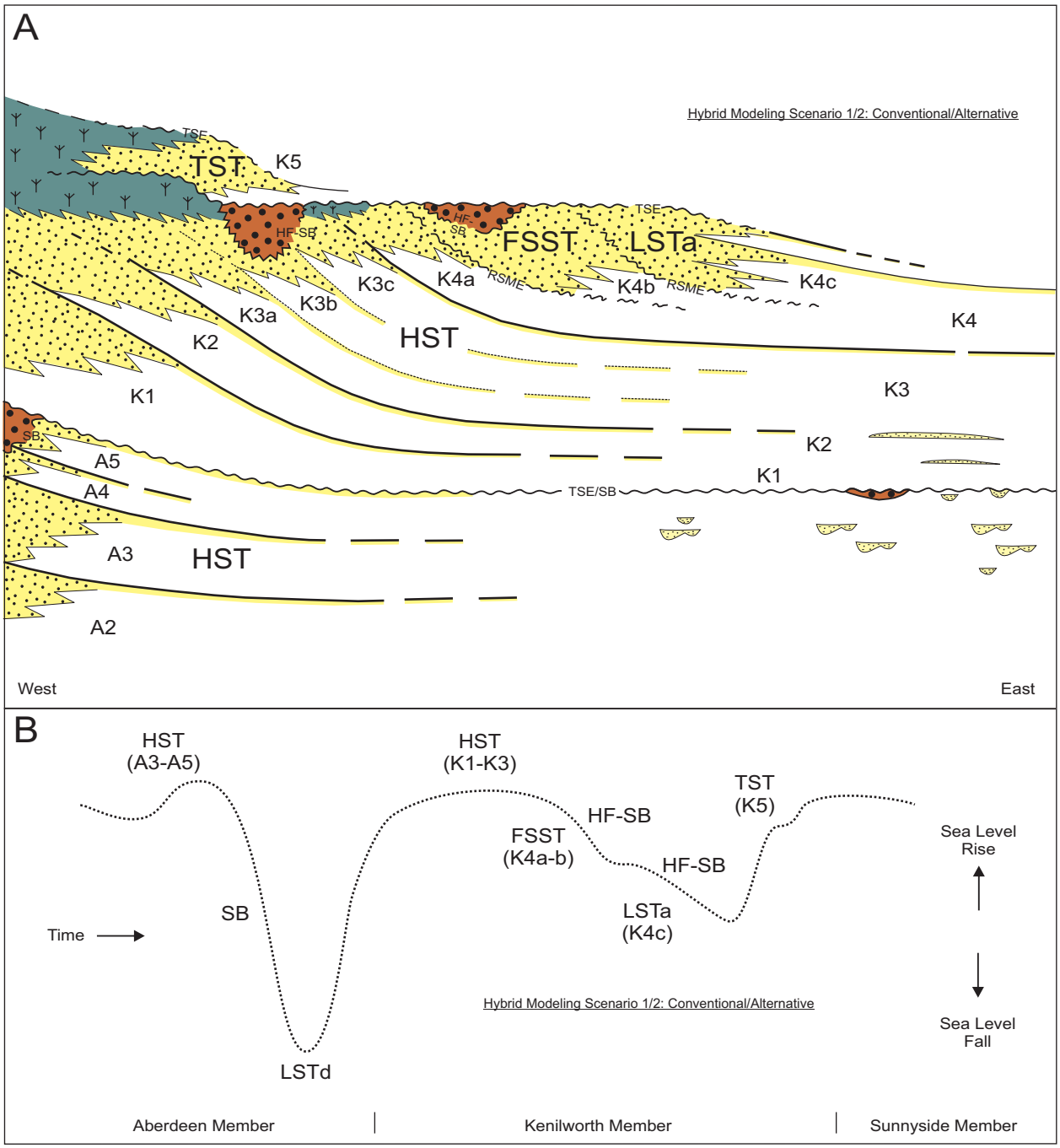

Figure 7-3. Modified conventional sequence stratigraphic interpretation for the Kenilworth Member (Pattison 1995). Hybrid modeling scenario 1/2: components of both the conventional and alternative models, HFSBs, parasequence-scale IVFs, temporally and spatially linked nearshore terrestrial and shallow marine facies belts, no detached sand bodies down-dip, attached only. The classic conventional interpretation shows detached lowstand sandstone bodies at Hatch Mesa (Taylor and Lovell 1991, 1995). Both the classic and modified conventional interpretations identify an incised valley-fill along the top of the progradational parasequence set, with lowstand deposits either attached (LSTa; Pattison 1995) or detached (LSTd; Taylor and Lovell 1991, 1995) from the highstand. (A) Modified conventional high resolution sequence stratigraphy of the Kenilworth and Aberdeen members in east-central Utah (modified from Pattison 1995; Pattison et al. 2007a). A2-A5 (Aberdeen parasequences), K1- K5 (Kenilworth parasequences), HST (highstand systems tract), FSST (falling stage systems tract), LSTa (attached lowstand systems tract), TST (transgressive systems tract), HF-SB (high frequency sequence boundary), RSME (regressive surface of marine erosion), TSE (transgressive surface of erosion). (B) Relative sea level curve (dotted line) for the upper Aberdeen Member to lower Sunnyside Member stratigraphic interval.

STOP 8: PARASEQUENCE-TO-BEDSET COMPARTMENTALIZATION, GRASSY MEMBER, TUSHER CANYON

This stop targets the Grassy Member, which is the second youngest member in the Blackhawk Formation, and specifically focuses on the second Grassy parasequence (GPS2). Continue driving east on the Tusher Canyon road and stop a few kilometers east of the previous locality (Figs. 0-1 and 0-2). We will make multiple road side stops in order to allow participants to study the shoreface/deltaic cyclicity at a variety of scales (Fig. 8-1). O'Byrne and Flint (1993, 1995, 1996) noted that the Grassy parasequences split into a series of reservoir compartments or bedsets. Bedsets are one level of hierarchy lower than a parasequence (Van Wagoner et al. 1990). GPS2 splits into at least three bedsets in the Tusher Canyon area, with the thickness of each bedset ranging from 5 to 12 m (Fig. 8-1). At other localities in the Green River area, O'Byrne and Flint (1993, 1995, 1996) identified up to nine bedsets in GPS2. A near Book Cliffs well log suite illustrates the subsurface recognition of Grassy bedsets and parasequences (Fig. 8-2). These are correlated to the nearby outcrop, which is less than 6 km away (Fig. 8-2).

It is important to recognize bedset cycles when establishing a correlation framework in a shoreface environment. Observations from the Book Cliffs provide some general rules to help in establishing the correct correlation framework: (i) parasequences gradually thin and fine in a basinward direction, (ii) parasequences split or subdivide into a stack of thinner coarsening-upward cycles or bedsets, however, the overall parasequence thickness does not increase but continues to gradually decrease in a basinward direction, (iii) parasequence flooding surfaces are of a greater magnitude than bedset flooding events and therefore should be easier to identify on well logs (i.e. greater contrast in petrophysical properties across the flooding surface: for example a higher contrast in API units on the gamma ray well logs), and (iv) bedset and parasequence flooding surfaces can act as baffles and/or barriers to fluid flow. Bedset flooding surfaces are often very difficult to identify in a landward direction because sandstone-on-sandstone contacts mask the location of the bedset flooding surface. Similar problems exist on a bigger scale when trying to identify parasequence flooding events in proximal regions. However, in the case of parasequence flooding events, these are often manifested as cemented horizons (i.e. can be identified on density well logs) and/or thoroughly bioturbated intervals (i.e. could be observed in core) in proximal sandstone-on-sandstone regions.

There are numerous recent studies on the intra-parasequence architecture-anatomy of solitary regressive wave-dominated shoreline transects (Hampson 2000; Hampson and Storms 2003; Storms and Hampson 2005; Somme et al. 2008; Charvin et al. 2010, 2011; Eide et al. 2014; Forzoni et al. 2015; Ainsworth et al. 2017). Initial oversimplified "sand-tank" interpretations for wave-dominated shorelines has been superseded via recognition of bounding surfaces and heterogeneities at the intra-parasequence scale, including nondepositional and erosional discontinuities (Hampson 2000; Charvin et al. 2010, 2011), and discontinuous mudstone beds (Eide et al. 2014). These record fluctuations in accommodation and sediment supply, driven both allogenically and autogenically during a single shoreline transit across the shelf (Ainsworth et al. 2017). Thus what previously appeared as one "sand-tank" wave-dominated parasequence is actually a complex assemblage of smaller depositional elements bounded by surfaces of erosion and non deposition, some draped by mudstones (Eide et al. 2014; Ainsworth et al. 2017). Bedset flooding surfaces could compartmentalize a hydrocarbon reservoir and therefore need to be properly identified and correlated in order to optimize development activities such as drilling (well trajectory), completion-perforation (compartments, fracing), and production strategies (sweep efficiency, water injection).

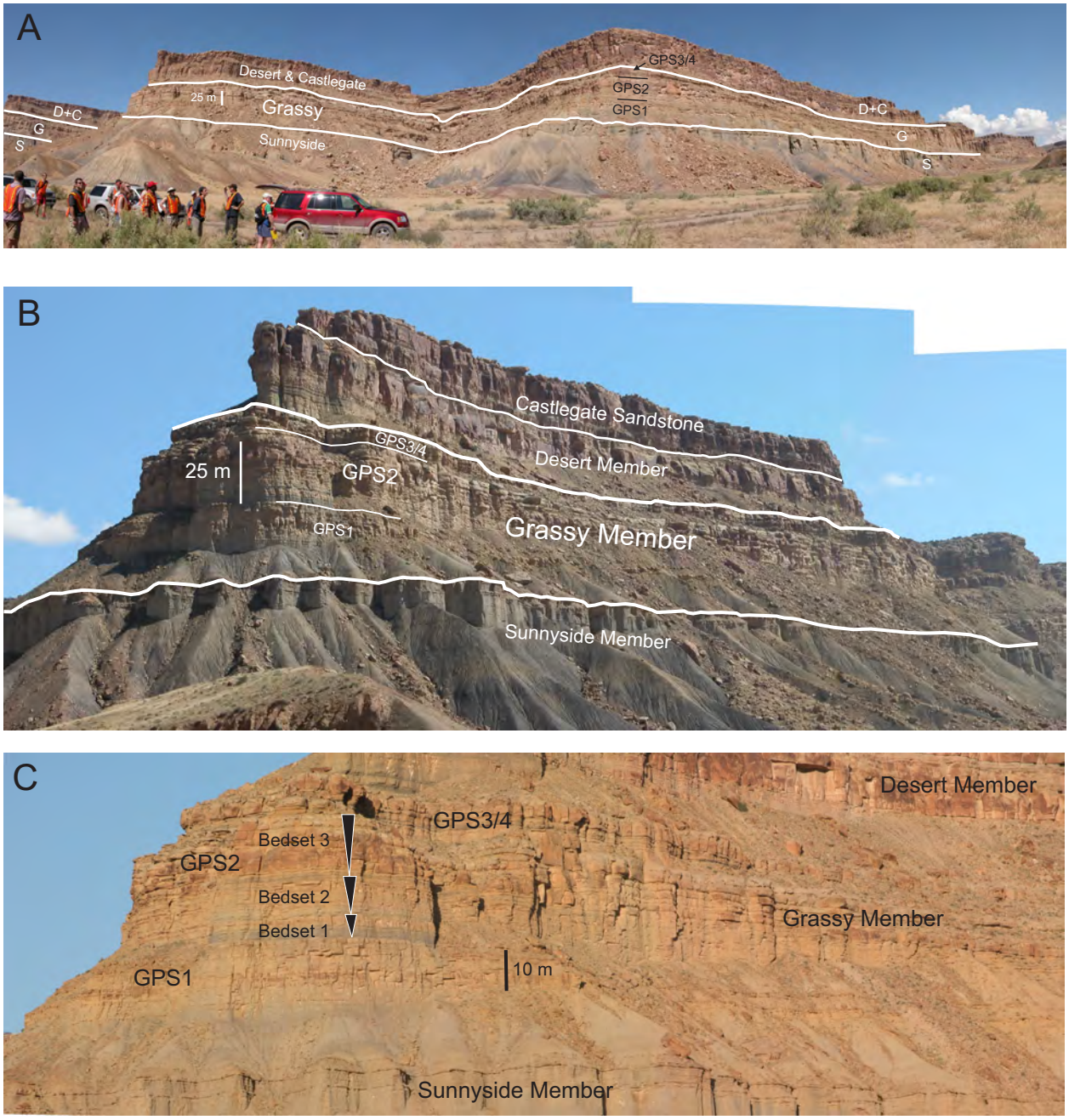

Figure 8-1. Parasequences and bedsets, Grassy Member (GPS2), Tusher Canyon. (A) Northern wall of Tusher Canyon. (B) Promitory on southern wall of Tusher Canyon. (C) Close-up of left side of previous photo showing three bedsets in GPS2.

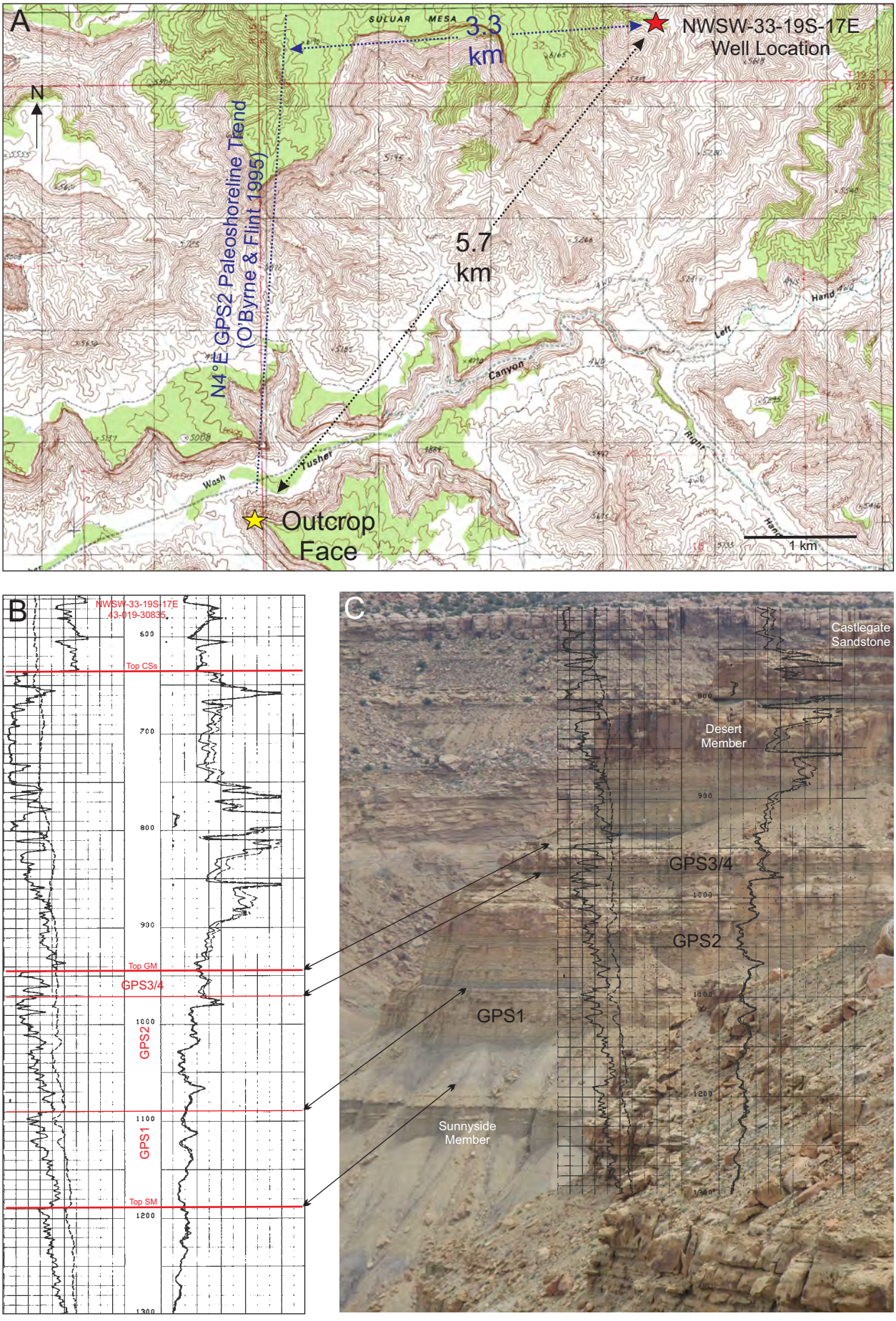

Figure 8-2. Parasequence- to bedset-scale correlation of the Grassy Member from Tusher Canyon to a near subsurface well log. (A) Topo map showing the Tusher Canyon outcrop and the well location, which are 5.7 km apart or 3.3 km along depositional dip (i.e. N4°E paleoshoreline trend from O'Byrne and Flint, 1995). (B) Gamma ray and resistivity well logs from NWSW-33-19S-17E. (C) Correlation of outcrop and well log, plotted at the same scale.

FIELD DAY 3

INCISED VALLEYS OR CHANNELS?
CORRELATION AND SEQUENCE STRATIGRAPHY

Stop 9: Channels Cutting Foreshore-Shoreface Deposits in a Low Accommodation Setting, Grassy Member, Tusher Canyon

Stop 10: Strongly Progradational Shallow Marine Deposits Cut By Channel-Fill Complexes, Desert Member, Tusher Canyon

Stop 11: Multistory vs. Single-Story Channels, Desert-Castlegate, The Basin

STOP 9: CHANNELS CUTTING FORESHORE-SHOREFACE DEPOSITS IN A LOW ACCOMMODATION SETTING, GRASSY MEMBER, TUSHER CANYON

The purpose of this stop is to examine the relationship between tidally influenced (tidal-estuarine?) shoreface-incised channel-fills and foreshore-shoreface sandstones, in a low accommodation setting (Fig. 9-1). Drive along the Tusher Canyon road and park your vehicle after entering Tusher Wash (Figs. 0-1 and 0-2). View the cliff face along the northern wall of Tusher Canyon, which is approximately 1 km to the north. Previous work by O'Byrne and Flint (1993, 1995, 1996) has led to the identification of four parasequences in the Grassy Member: GPS1 to GPS4. These parasequences are well exposed in the southern sector of the Book Cliffs, and are also recognized in the subsurface of eastern Utah. A prominent *white cap* demarcates the top of GPS2 (Fig. 9-2). In places, this *white cap* is erosively removed and replaced by a heterolithic- and mudstone-rich channel-fill complex. O'Byrne and Flint (1993, 1995, 1996) identified channel-fill complexes along the tops of GPS2 and GPS4 (Fig. 9-2). The GPS2 shoreface-incised channel complex is "gently" incised into the underlying foreshore-to-upper shoreface sandstones (Fig. 9-3). The GPS2 shoreface-incised channel is up to 12.3 m thick (O'Byrne and Flint 1995; Pattison et al. 2007a), and is completely contained within the upper part of the GPS2 parasequence which has a maximum thickness of 34.2 m in Coal Canyon (Young 1955; O'Byrne and Flint 1993, 1995, 1996; Pattison 2005a). O'Byrne and Flint (1993, 1995, 1996) assign a third-order sequence boundary (SB) to the base of the GPS2 channel complex, therefore, interpreting this complex as an incised valley-fill (IVF) (Figs. 9-2B, 9-3).

Criteria used to recognize IVFs include the down-cutting through one or more parasequences, a basinward shift of facies across the base of the valley, and an abrupt juxtaposition of channel facies on top of lower shoreface or inner shelf deposits (Fig. 9-2C; Dalrymple et al. 1992; Zaitlin et al. 1994). IVFs are characterized by tripartite facies zonations, with fluvial sandstones at the head of the valley and tidal-marine sandstones at the mouth (Fig. 9-1). A mudstone- or heterolithic-dominant central zone separates the sandstones at either end of the valley-fill (Fig. 9-1). It is possible that this gently incised GPS2-"IVF" is similar to the *"unincised valleys"* described by Posamentier (2001), which may form during falling stage and lowstand on a ramp-like margin (i.e. Type II sequence boundaries; Van Wagoner et al. 1990).

Detached lowstand sand bodies were interpreted for the "G2-IVF" including small-scale scours or pods, thought to be the dendritic edges of an IVF complex. Hummocky cross stratified (HCS) sandstone beds pass completely through the G2 pods, with dark brown iron-cemented HCS sandstones within the pods, grading laterally on either side into light-coloured non-iron-cemented HCS beds (Pattison, 2018). These pods do not have a basal erosional surface and are interpreted as early diagenetic iron-rich concretions, similar to parasequence-capping carbonate nodules found elsewhere in the Book Cliffs (Taylor et al. 1995, 2000, 2004; Taylor and Gawthorpe 2003). A larger scale detached IVF-lowstand shoreline complex was identified in the Bootlegger Wash to Sagers Wash region (O'Byrne and Flint 1993, 1995, 1996; Hampson et al. 1999). Subsequent work correlates these detached sand bodies to the Aberdeen Member rather than the G2 parasequence, and re-interprets them as prodeltaic turbidite channel-fill and lobe complexes, rather than lowstand IVF and shoreline deposits (Pattison 2005c; Pattison et al. 2007b; Buatois et al. 2019). An alternative interpretation is that the GPS2 channel complex is a shoreface-incised, parasequence-scale, tidally-influenced distributary and/or tidal-estuarine channel-fill. There is no evidence of a basinward shift of facies across a regionally mappable sequence boundary, no sediment bypass with concomitant development of detached falling stage and lowstand shoreface-deltaic sand bodies, and therefore no incised valley-fill deposits.

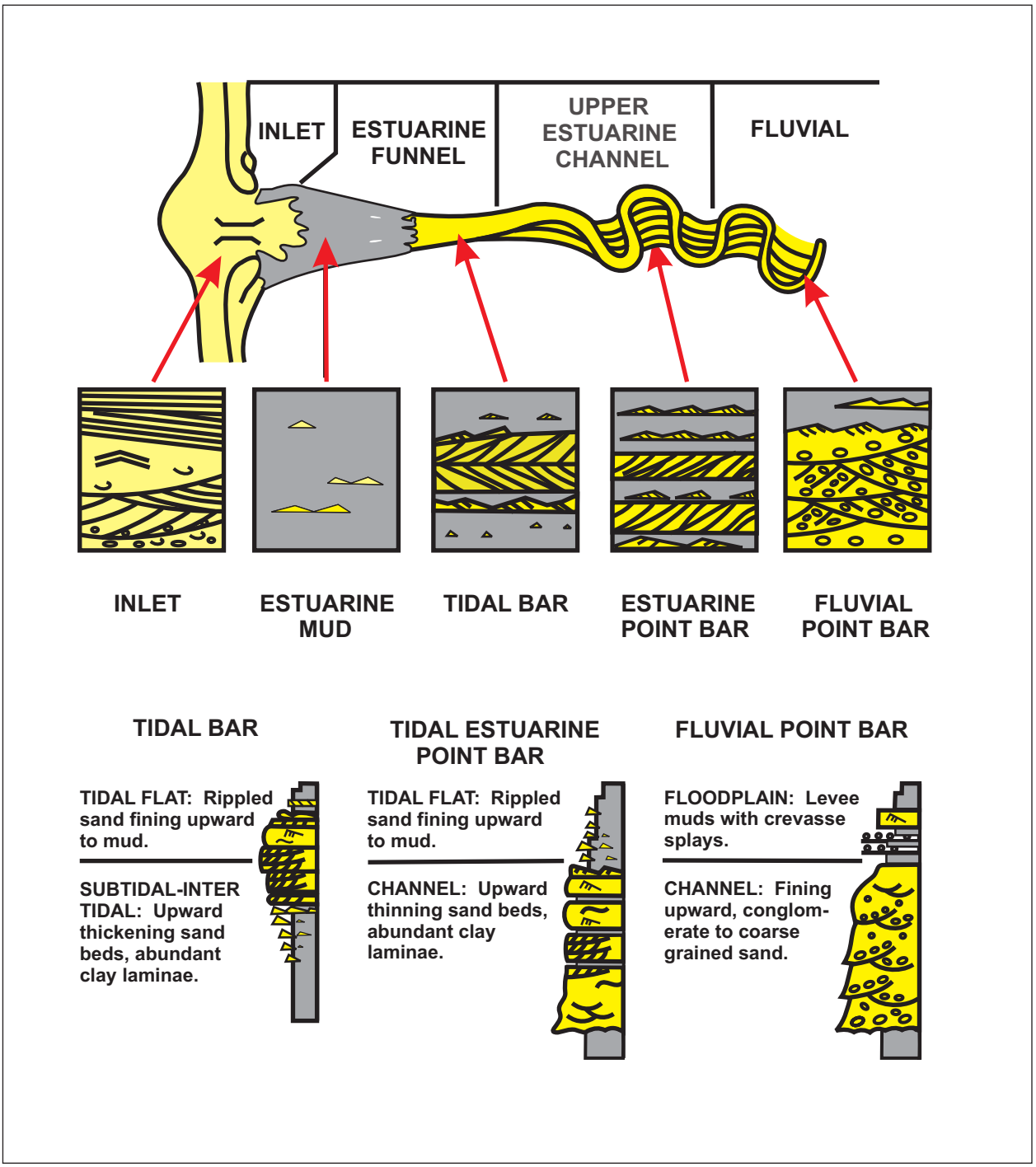

Figure 9-1. Tripartite facies model for estuarine/incised valley-fill systems, based on the Gironde-type macrotidal estuarine facies zones (Allen 1991). The tripartite zonation is defined by the occurrence of sandstone-mudstone-sandstone along the length of the estuary or valley. The marine sandstones at the mouth of the estuary/valley have significantly different sedimentological, biological and architectural characteristics (egs. grain size, sorting, sedimentary structures, trace fossils, degree of bioturbation, body fossils, stacking, sedimentary architecture) compared to the fluvial sandstones at the head of the estuary/valley. Tidally-influenced deposits occur under meso- to macro-tidal conditions. Funnel-shaped valleys amplify the tidal energy, leading to deposits shown above.

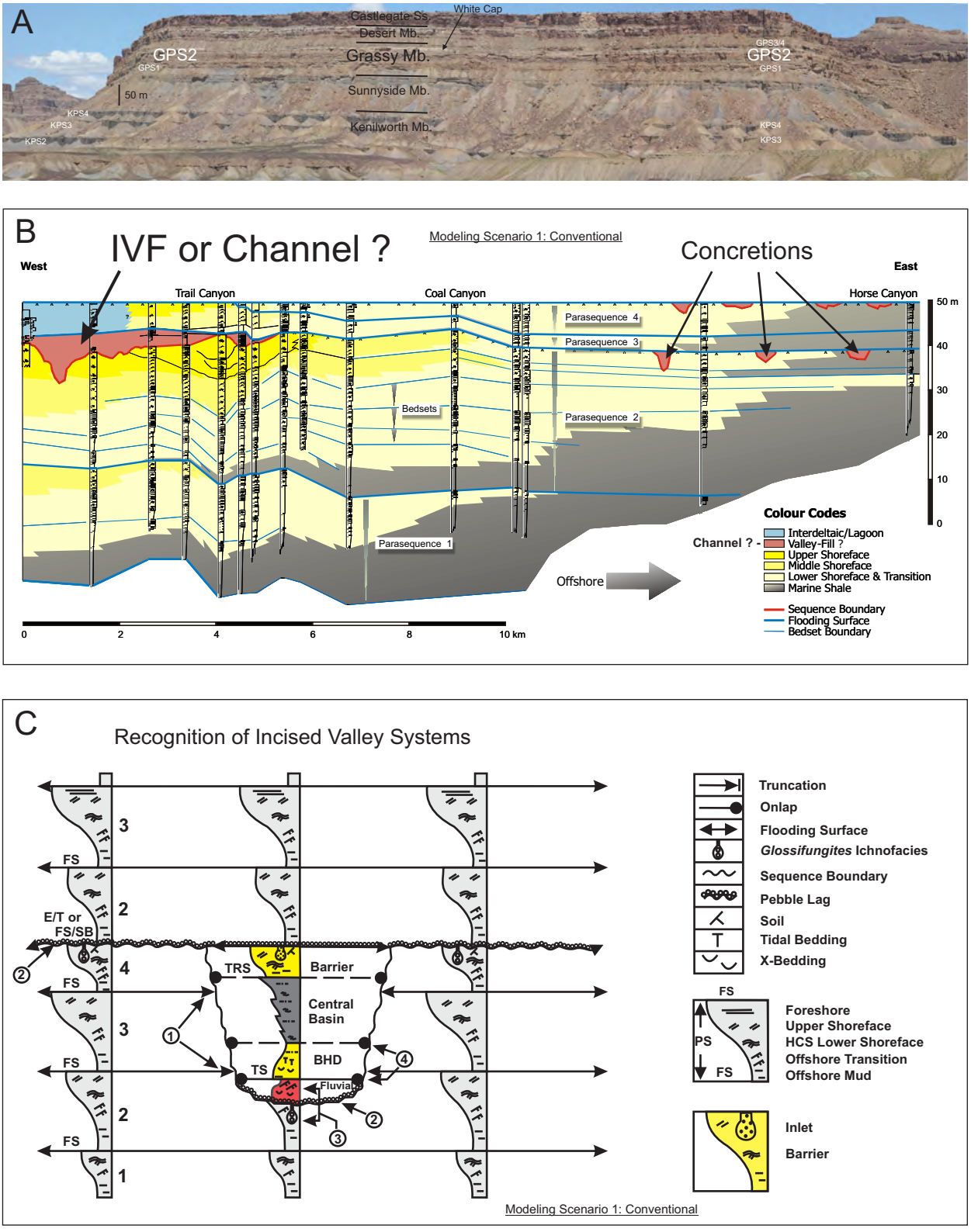

Figure 9-2. Wave-dominated low accommodation setting: channels and shoreface, Grassy Member, northwestern entrance to Tusher Canyon. (A) Photo-panorama along the north wall-entrance to Tusher Canyon. GPS2 (Grassy parasequence 2) has a white cap at the top which is cut by an incised valley-fill (IVF) complex. (B) Dip-oriented cross section, Grassy Member, Green River embayment region (modified after O'Byrne and Flint 1993, 1995, 1996; Williams and Davies 2006). Datum is the top of the Grassy Member. Modeling scenario 1: conventional, classic, third-order SB, IVF, non-linked nearshore terrestrial and shallow marine facies belts, detached sand bodies are likely down-dip.Note an IVF? or channel? cutting GPS2. Pod-like concretions shown in the eastern half of the cross section are tightly cemented with Fe-bearing minerals (Pattison et al. 2009), and are not related to an IVF as originally interpreted by O'Byrne and Flint (1993). (C) Criteria used to recognize an incised valley-fill system (Zaitlin et al. 1994), as per conventional sequence stratigraphic model.

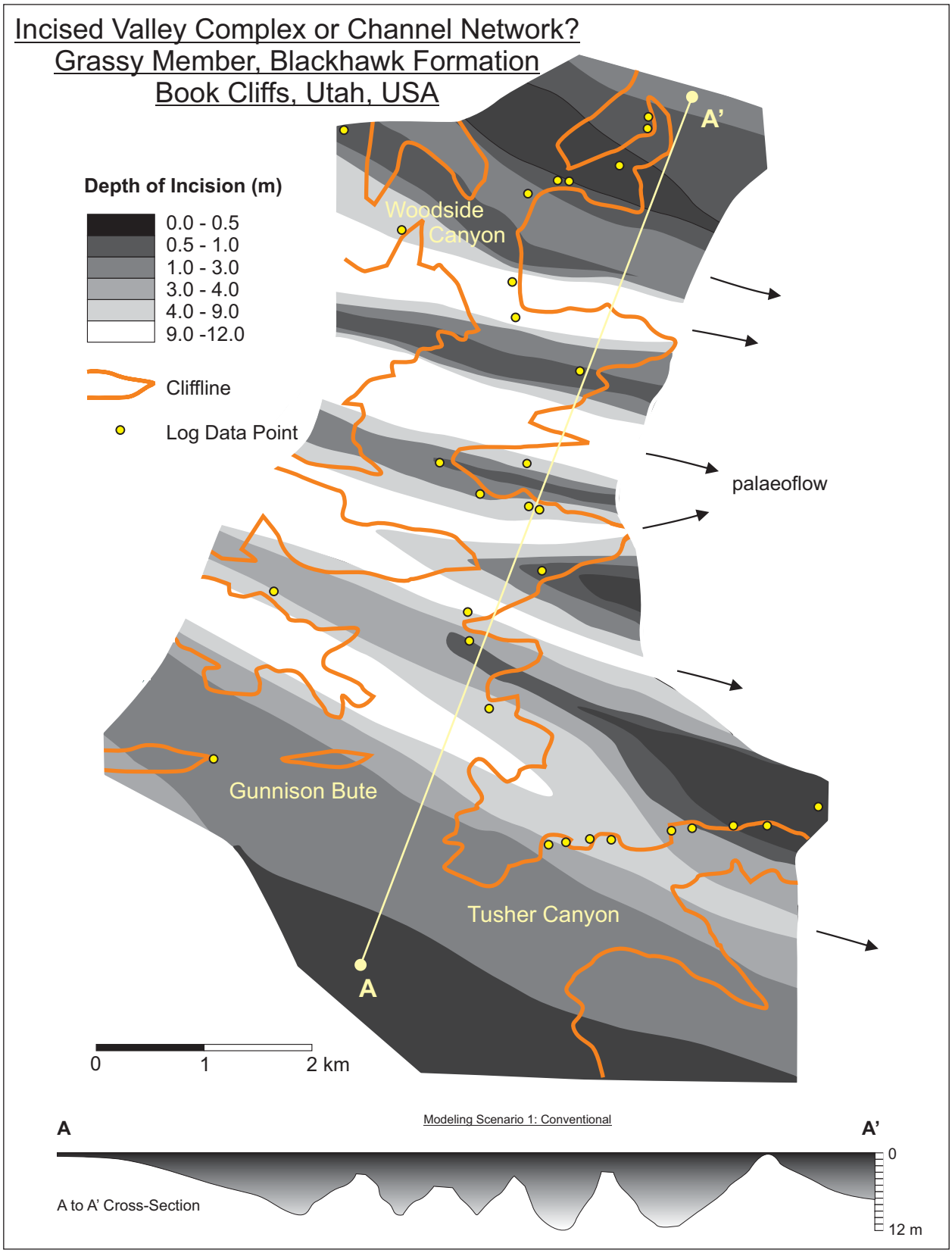

Figure 9-3. Depth of incision for the GPS2-IVF (O'Byrne, 1992). Modeling scenario 1: conventional, classic, third-order SB, IVF, non-linked nearshore terrestrial and shallow marine facies belts, detached sand bodies are likely down-dip (O'Byrne and Flint 1993, 1995, 1996). Is this a valley-fill or channel network? What field criteria can be used to distinguish between a valley and shoreface-incised channel? What are the implications for correlation, modelling and prediction of sand bodies? Deepest incisions on the map are white, while interfluves are black.

STOP 10: STRONGLY PROGRADATIONAL SHALLOW MARINE DEPOSITS CUT BY CHANNEL-FILL COMPLEXES, DESERT MEMBER, TUSHER CANYON

This stop concentrates on the Desert Member, which is the youngest member in the Blackhawk Formation. Drive into Tusher Canyon until the Desert Member is exposed at road level and park the vehicles where the road bends sharply to the north (Figs. 0-1 and 0-2). This stop is approximately 6 km down-depositional-dip from the head of Tusher Canyon. From base to top, the cliff-forming packages exposed at road level consist of wave-dominated shoreface sandstones of Desert Member parasequences D4 and D5, shoreface-incised channel-fill complexes, Desert Member fine-grained coastal plain deposits, and Lower Castlegate Sandstone sheet-like, amalgamated, high net:gross channel-fills (Figs. 10-1 to 10-6). Two basic sequence stratigraphic interpretations are considered for the channel-fill successions that cut Desert Member parasequence D5 and occasionally D4: (1) conventional-classic interpretation: IVF with a third-order SB at the base, IVF and no temporal, genetic or spatial linkage between the laterally adjoining nearshore terrestrial and shallow marine facies belts (Figs. 2-3A, 10-1), versus (2) an alternative interpretation: discrete, parasequence-scale, shoreface-incised channels with temporal, genetic and spatial linkage between the laterally adjoining nearshore terrestrial and shallow marine facies belts, but no SB, no IVF, and no significant basinward sediment bypass (Fig. 2-3B). All remaining field stops will concentrate on the Desert-Castlegate interval, allowing ample opportunity to critically appraise the utility of each sequence stratigraphic model.

The shallow marine facies combine to form five coarsening-upward cycles, Desert Member parasequences D1 to D5, that are 5 to 16 m thick (Figs. 10-2 and 10-3). The D1 to D3 parasequences are dominated by silty mudstones and sandy siltstones, with thin beds of hummocky cross stratified (HCS) and wave rippled very fine-grained sandstones near the top of each cycle. These are interpreted as mid-to-inner shelf deposits (Table 0-1). The D4 and D5 parasequences are dominated by HCS sandstones, with lesser amounts of sandy siltstones, and are interpreted as lower shoreface deposits (Table 0-1). All five Desert Member parasequences at Tusher Canyon show a normal regressive coarsening-upward pattern, with the exception of D5, which in places is characterized by a sharp and slightly erosive contact between the amalgamated HCS sandstones and underlying shelf mudstones with interbedded gutter casted HCS sandstones (Figs. 10-4 and 10-5). A regressive surface of marine erosion (RSME) marks this sharp mudstone-to-sandstone facies contact, which is consistent with forced regression (Fig. 10-4D). Elsewhere this contact is gradational and normally regressive in nature. Therefore the D5-RSME is linked to an individual ECS or bedset, rather than the entire D5 parasequence. Hampson (2000) described similar patterns (i.e. sharp and gradational bases) in the lower portions of Kenilworth Member parasequence K4 at Battleship Butte. Solitary shoreline tongue trajectories for D1 to D5 are very low to low angle ascending regressive, varying from +0.0004° to +0.171° (Pattison, 2018, 2019a, 2019b, 2019c, *in review-a, -b*).

Foreshore-shoreface sandstones in the D5 parasequence are cut by a shoreface-incised channel-fill complex (i.e. D5-CH) that is heterolithic-to-sandstone-rich in proximal regions (Figs. 10-2 to 10-5). The D5-CH occasionally cuts out the entire D5 parasequence (≈ 5-7 m), plus a significant portion of the underlying D4 parasequence. Both single- and multi-story channel-fill successions are observed, with the latter having a maximum thickness of 19.2 m (Fig. 10-2). The D5-CH facies at Tusher Canyon include (i) cross bedded sandstones, some with repetitive pairs (i.e. doublets) of carbonaceous-rich mudstone laminae, herringbone cross bedding and *Teredolites*-bored wood fragments, (ii) current rippled sandstones, (iii) inclined heterolithic strata, and (iv) carbonaceous-rich siltstones and mudstones (Table 0-1, Figs. 10-4

and 10-5). The D5-CH is capped by a thick coal zone in proximal regions, which is coincident with the D5 flooding surface (FS) further down-depositional-dip. This D5-FS/coal marker horizon is correlatable throughout the Tusher Canyon region, and is also traceable westwards into the coastal plain deposits at Gunnison Butte, Long Canyon and Middle Mountain, landwards of the D5 foreshore sandstone evolution point. There is no evidence to indicate that the erosional surface at the base of the D5-CH extends any higher stratigraphically up-section, beyond the D5 FS/coal marker horizon. Shoreface-incised channel-fills, such as D5-CH at Tusher Canyon, are interpreted as an IVF (Van Wagoner 1991, 1995) or as a tidally-influenced distributary channel-fill (Pattison, 2018, 2019a, 2019b, 2019c, *in review-a,-b*).

The D5 foreshore-shoreface sandstones and shoreface-incised channel-fill are consistently overlain by a 7-12 m thick package of coal-bearing coastal mudstones with single-story meandering fluvial sand bodies (Fig. 10-2). Coal beds are plentiful, as are carbonaceous-rich mudstones, siltstones and sandstones. Channel sandstones are mostly cross bedded and convolute bedded, with abundant carbonaceous matter and some rhythmically-laminated/bedded inclined heterolithic strata, herringbone cross bedding, double mud drapes and *Teredolites*-bored wood fragments (Table 0-1).

The coastal plain facies belt laterally adjoins the D5 shallow marine sandstones to the east and the amalgamated channel sandstones to the west. Facies transitions are both gradational and sharp between the neighboring facies belts, but always conformable. Vertical transitions define a progradational stacking at all localities, with the D5 foreshore-shoreface sandstones and shoreface-incised channel-fills consistently overlain by coastal plain deposits, which in turn are overlain by the amalgamated channel sandstones. The only exception to the progradational vertical stacking pattern is the uppermost part of the Lower Castlegate Sandstone which transitions from the amalgamated sheet-like fluvial sandstones back into the mudstone-dominated coastal plain deposits (Figs. 10-2 and 10-3E). These cap the upper 3-12 m of the Lower Castlegate Sandstone throughout the southern Book Cliffs, likely heralding the onset of the Buck Tongue transgression (Pattison, 2019c, *in review-a*).

The main cliff-forming Desert-Castlegate package at Tusher Canyon is comprised of a stack of amalgamated, sheet-like, braided fluvial sandstones with minor discontinuous carbonaceous-rich mudstones and thin coals, up to 30 m thick (Figs. 10-2, 10-3, 10-6). Dominant facies are cross bedded, convolute bedded and current rippled sandstones, all with abundant carbonaceous matter, including finely disseminated sand-sized phyto-detritals and sand-to-pebble-sized, angular-to-sub-angular coal clasts (Table 0-1). Net:gross ratios vary between 80-90 percent. Mean cross bed orientations indicate a dominant E36.5°S fluvial transport pathway (n = 4995; vector magnitude = 66.9; Pattison, 2019c). Rare landward-directed cross beds comprise only 4.1 percent of the readings (Pattison, 2019c). These braided fluvial channels are smaller compared to the shoreface-incised distributary channels (i.e. D5-CH) at Tusher Canyon, with a mean bankfull width of 21.8 m and a mean bankfull depth of 5.5 m. Mudstone-dominated coastal plain deposits bound the sheet-like sandstones above and below. The braided fluvial sandstones also grade into finer-grained coastal plain deposits to the east. Contrary to conventional sequence stratigraphic interpretations (e.g. Van Wagoner, 1991, 1995; Miall, 1993, 2014), there is no evidence of an unconformity nor sequence boundary at the base of the amalgamated fluvial sandstone package, nor a valley shape-container along depositional-strike or –dip (Pattison, 2018, 2019a, 2019b, 2019c, *in review-a,-b*). Although the facies contact between the coastal plain mudstones and the amalgamated fluvial sandstones is often sharp, these laterally adjoining facies belts have a conformable contact.

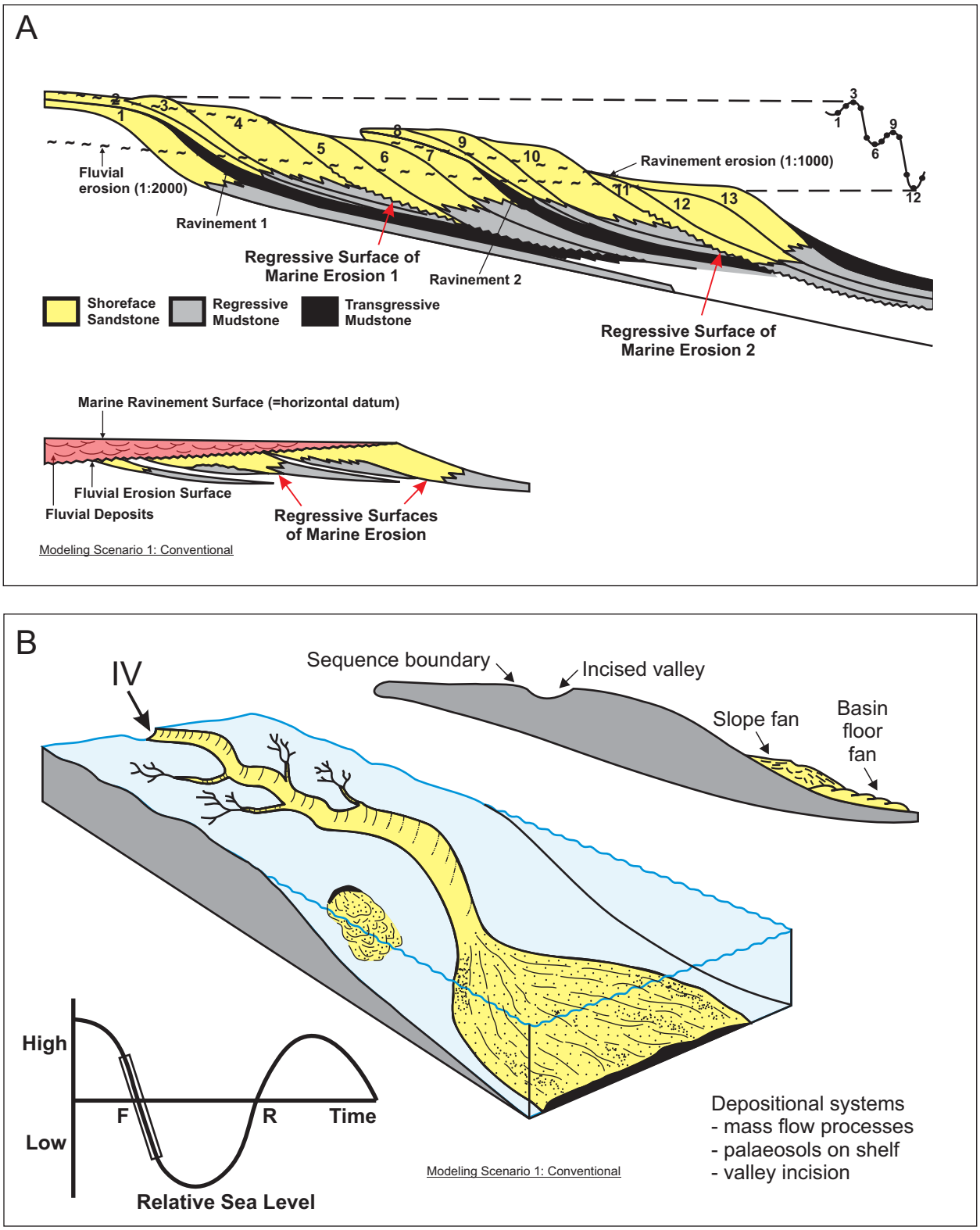

Figure 10-1. Stratal architectures typical of relative sea level (RSL) fall. Both diagrams depict sequence stratigraphic modeling scenario 1: conventional, classic, third-order SB, IVF, non-linked nearshore terrestrial and shallow marine facies belts, detached sand bodies are likely down-dip. (A) Falling stage systems tract and regressive surfaces of marine erosion (Plint and Nummedal 2000). Note that regressive surfaces of marine erosion (i.e. sharp-based shorefaces) are formed during maximum falls of sea level. (B) Falling stage systems tract with a shelf break (modified from Howell and Flint 1996). Note that RSL fall has sediment bypass, incised valley (IV) development, and a third-order sequence boundary, as per conventional sequence stratigraphic model (Van Wagoner et al. 1990).

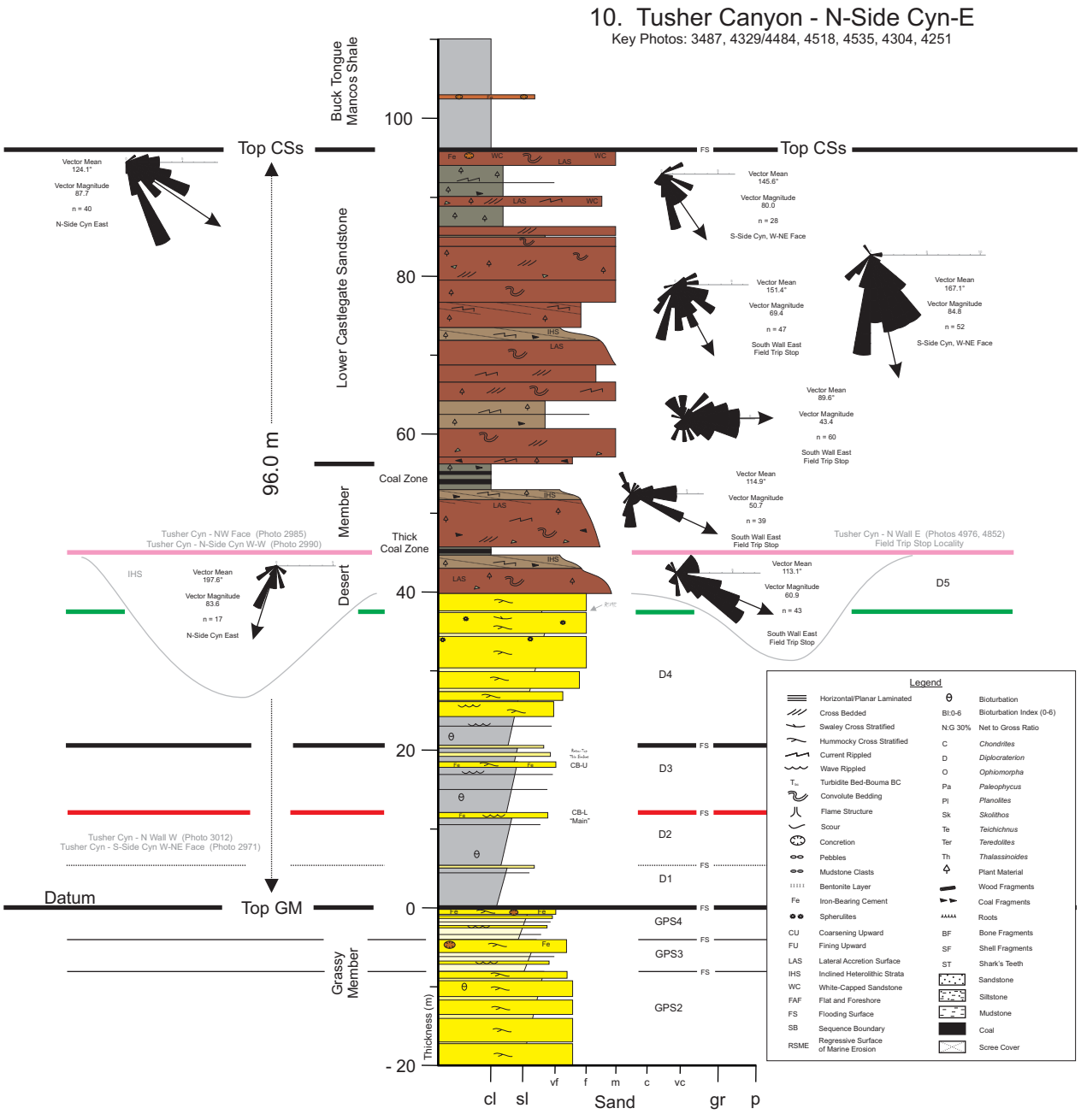

Figure 10-2. Measured outcrop section #10, Tusher Canyon, North Side Canyon East. Shoreface-incised channel along the D5 parasequence level. Cuts into the uppermost part of the underlying D4 parasequence. The maximum thickness of the D5-CH is 19.2 m. Regional correlation of the D5-CH extends away from the measured section locality (light grey lines).

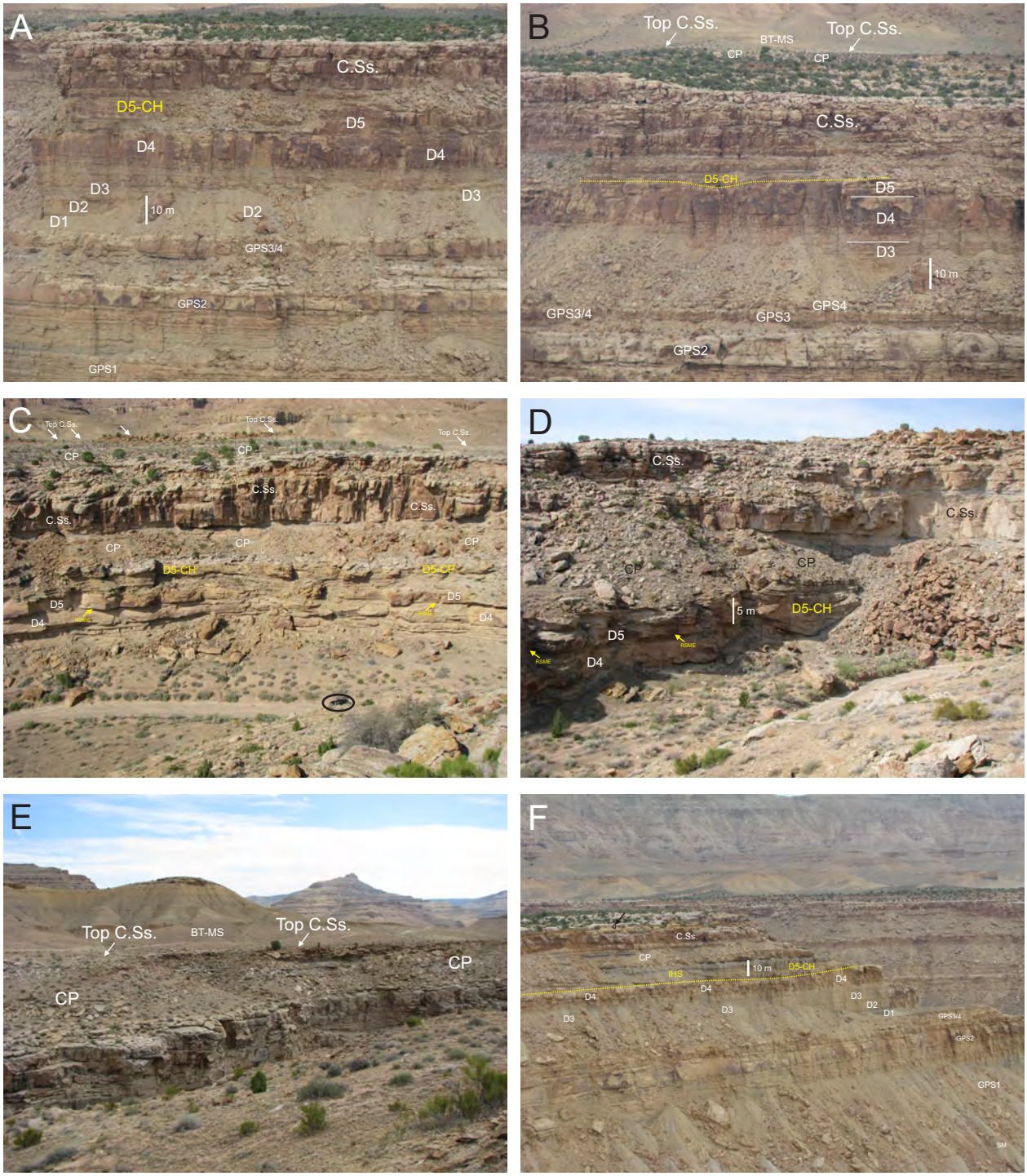

Figure 10-3. Stratal architectures of the Desert Member (DM) to Lower Castlegate Sandstone (C.Ss.) interval in Tusher Canyon. Desert parasequences D4 and D5. Coastal plain (CP). Note that the amalgamated cliff-forming fluvial sandstones of the C.Ss. are bracketed above and below by coal-bearing, mudstone-rich coastal plain (CP) deposits. The uppermost 10 m of the C.Ss. is characterized by single-storey fluvial channel sandstones encased in fine-grained coastal plain deposits. The contact with the overlying Buck Tongue of the Mancos Shale (BT-MS) is usually a mudstone-on-mudstone contact. (A) Heterolithic-filled shoreface-incised channel (D5-CH) cuts through the D5 shoreface sandstones, N Side Cyn West, Tusher Canyon. (B) Thinner mudstone-and-heterolithic-filled D5-CH, N Side Cyn Central, Tusher Canyon. A 7-12 m thick coal-bearing CP mudstone package caps the Lower C.Ss. throughout the Tusher Canyon region. (C) Well defined shoreface-incised channel (D5-CH) in parasequence D5, North Wall East, Tusher Canyon. Occasionally cuts the uppermost part of the underlying D4 parasequence. Sharp-base to the D5 shoreface sandstones is defined as a regressive surface of marine erosion (RSME). Carbonaceous-rich mudstone top to the C.Ss. (white arrows). Note the black SUV for scale (black oval) in lower right. (D) Shoreface-incised channel (D5-CH) cutting the D5 and D4 parasequences, Tusher Canyon, North Wall East. Channel "evolves" from the top D5 surface. Surface of origin for D5-CH is coincident with the D5 flat-topped foreshore (FAF) sandstones elsewhere. The sharp based D5 shoreface sandstones are marked by a RSME (yellow arrows). (E) Very low net:gross, coal-bearing CP mudstones with isolated single-storey channel sandstones, uppermost 8-13 m, Lower C.Ss., North Side Canyon-East, Tusher Canyon. Note the road just above the top of the C.Ss. (F) Heterolithic- to mudstone-rich shoreface-incised channel-fill (D5-CH) cutting the D5 parasequence, Coal Canyon, NW Bowl. Lateral accretion sets are 7-10 m thick with well-defined inclined heterolithic strata (IHS). Base of the channel-fill shown by a dashed yellow line. Thick CP deposits blanket the top of D5. Geologist for scale in upper left (black oval and arrow). Grassy Member parasequences (GPS1-GPS4), Sunnyside Member (SM).

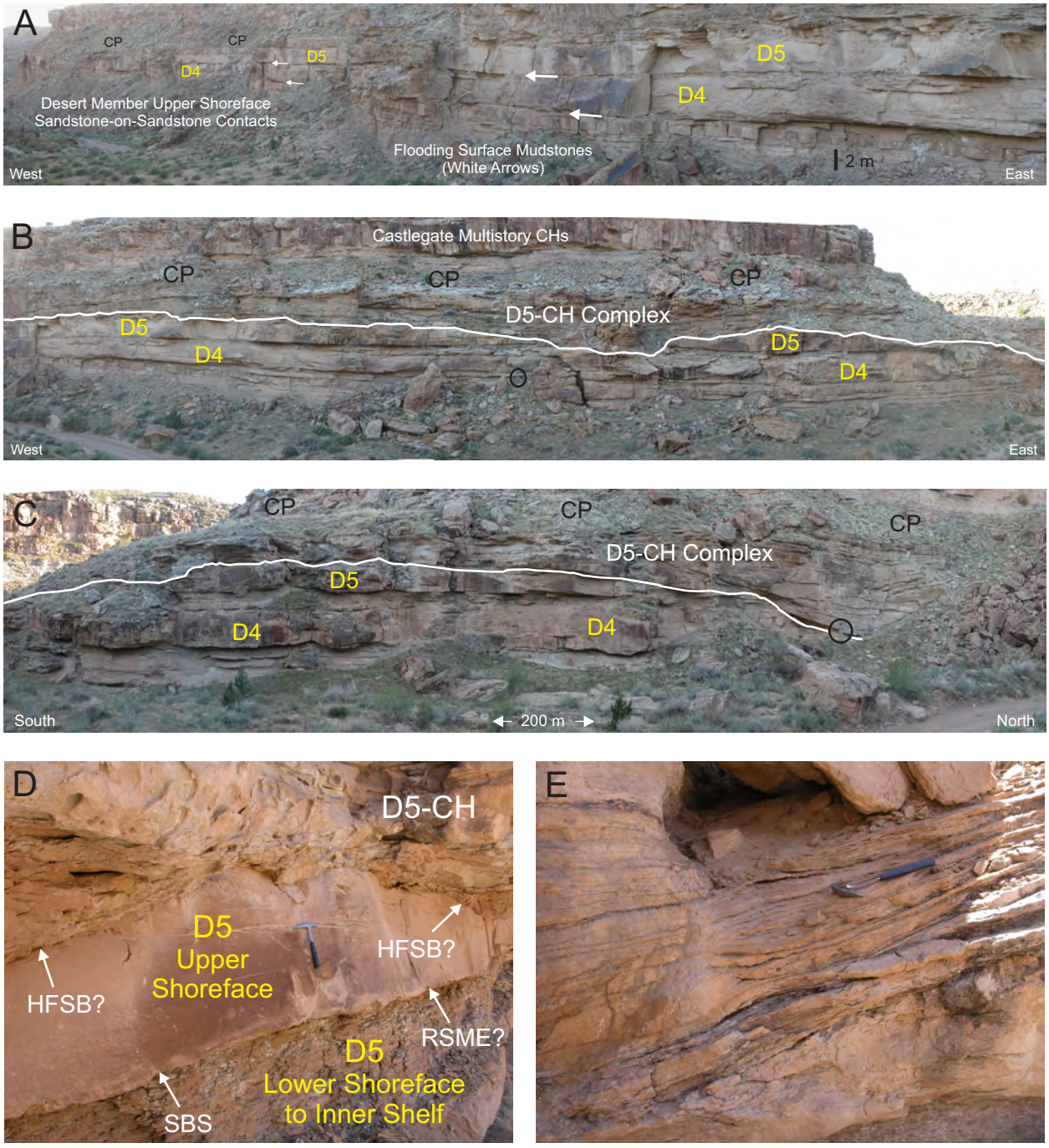

Figure 10-4. Channels (CH), coastal plain (CP), and shallow marine deposits, Desert Member, Tusher Canyon. Evidence for a strongly progradational system that was driven by high rates of sedimentation and/or low rates of accommodation include a channel complex (D5-CH) incised into Desert Member parasequence D5 and sharp-based shoreface sandstones. (A) Dip-oriented section. D4 and D5 shallow marine sandstones coalesce up-depositional-dip (left). (B) Desert Member shoreface sandstones cut by the D5-CH complex: dip-oriented section. Note the thick coal-bearing coastal plain (CP) mudstones that blanket the D5-CH. Person for scale (circle). (C) Desert Member shoreface sandstones and the D5-CH complex: strike-oriented section. Person for scale (circle). (D) D5-CH complex cutting upper shoreface sandstones. Possible high frequency sequence boundary (HFSB) marks the channel-shoreface contact. Upper shoreface rests abruptly on top of thin bedded lower shoreface/inner shelf heterolithic facies, thus defining a sharp-based shoreface (SBS) which is potentially a regressive surface of marine erosion (RSME). (E) Carbonaceous-matter-rich, tidally influenced distributary channel deposits. The carbonaceous-matter-rich layers are rhythmically interbedded with sandstones, and are interpreted as slack water deposits during highest and lowest tide. These laminae occur in sets or bundles, which define neap and spring cyclicity.

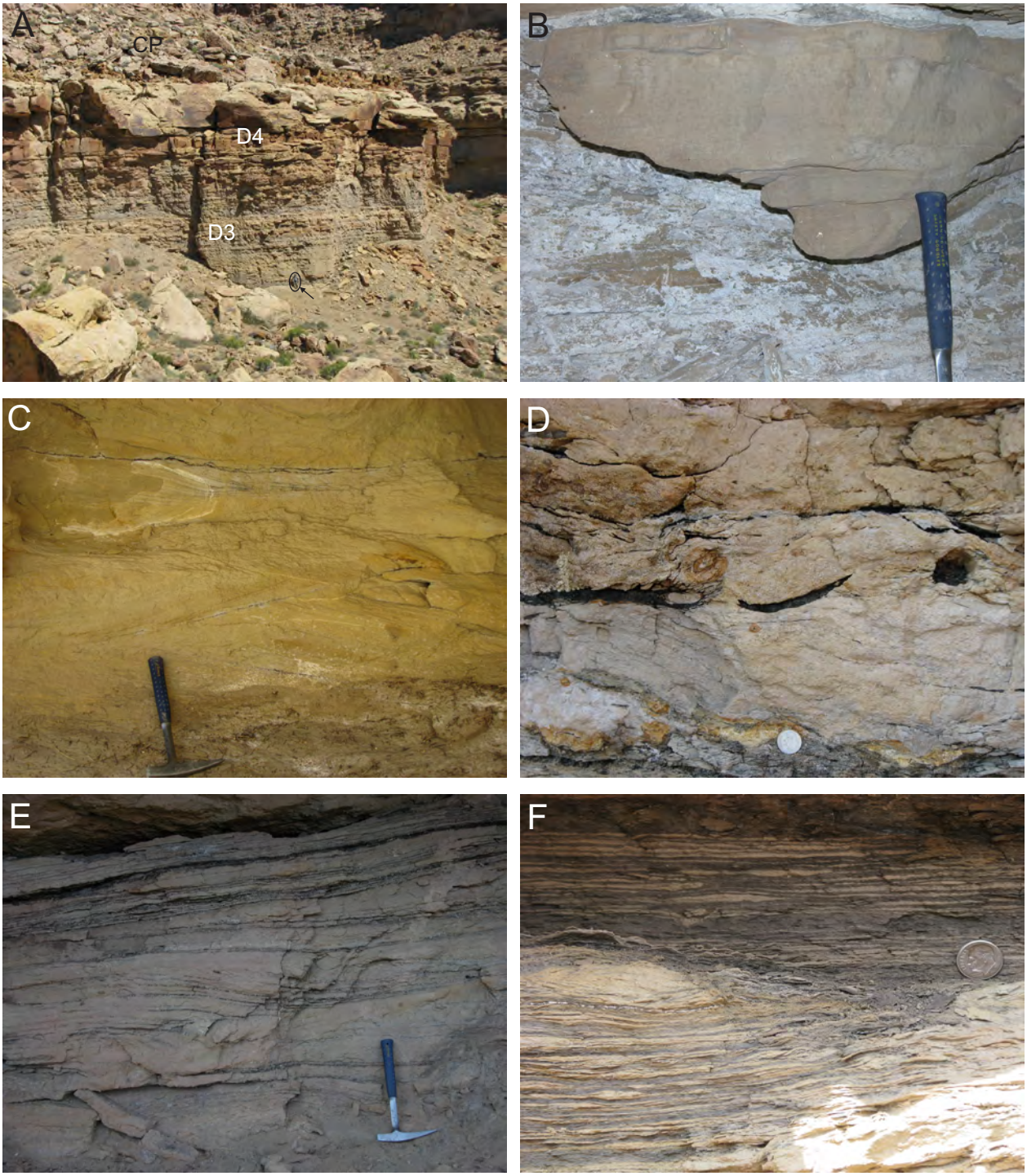

Figure 10-5. Desert Member (DM) facies, Tusher Canyon. (A) Coarsening-upward shallow marine cycles, D3 and D4 parasequences, North Side Cyn East, Tusher Canyon. Geologist for scale at base of cliff (oval and arrow). The Desert Member shoreface parasequences are blanketed by up to 15 m of coastal plain (CP) mudstones. (B) Gutter-casted thin bedded, hummocky cross stratified sandstones, basal part of D5 parasequence, North Side Cyn East, Tusher Canyon. (C) Cross bedded sandstone with carbonaceous-rich mudstone laminae, shoreface-incised channel (D5-CH), North Wall East, Tusher Canyon. (D) Cross bedded sandstone with abundant angular-to-sub-angular coal clasts, North Wall East, Tusher Canyon. USA dime coin for scale in lower middle (1.79 cm diameter). (E) Rhythmically-laminated and -bedded sandstones and carbonaceous-rich mudstones on lateral accretion surfaces, shoreface-incised D5-CH, North Wall East, Tusher Canyon. USA dime coin for scale. (F) Pin-stripe laminated current rippled sandstone and mudstone, coastal plain deposits blanketing the D5 parasequence, North Wall East, Tusher Canyon.

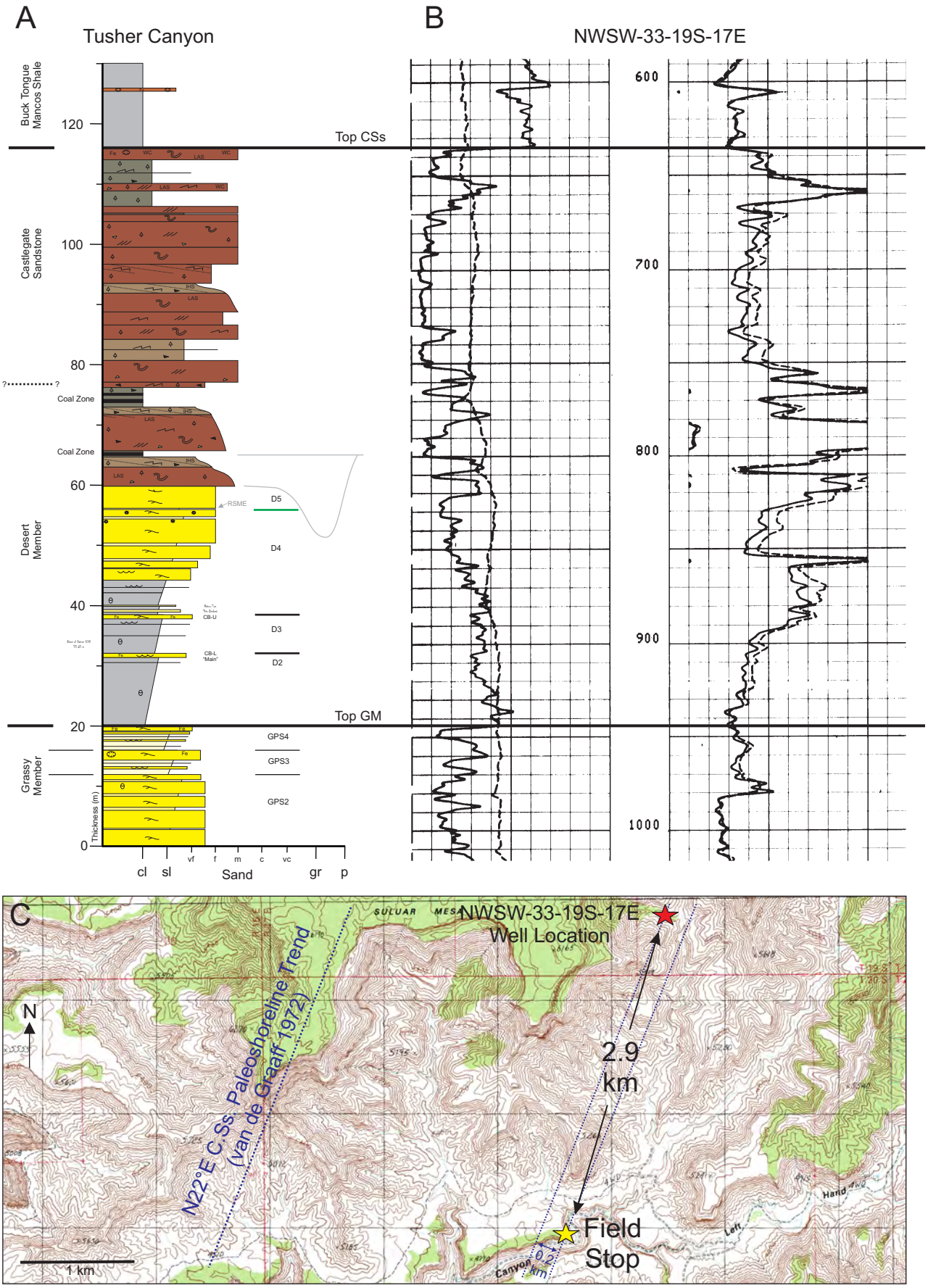

Figure 10-6. (A) Measured section from Tusher Canyon field stop area. (B) Gamma ray and resistivity well logs from a near subsurface well at NWSW-33-19S-17E (API 43-019-30835). Key surfaces are correlated between the outcrop section and the well logs. (C) Topographic map showing the 2.9 km distance between the outcrop section and the well location, although only 0.2 km of depositional dip distance separates these locations using the N22°E paleoshoreline trend for the Castlegate Sandstone (van de Graaff 1972).

STOP 11: MULTISTORY VS. SINGLE-STORY CHANNEL-FILLS, DESERT-CASTLEGATE, THE BASIN

We next have an opportunity to examine the sedimentology and stratal architectures in the nearshore terrestrial facies belt of the Desert Member to Lower Castlegate Sandstone stratigraphic interval. One aspect of this analysis is to compare and contrast the stacking patterns, size, depth of incision, and facies of single versus multistory channel-fill successions. Another aspect is to critically appraise the likelihood that the multistory channel-fill complexes are the nearshore terrestrial expression of an incised valley-fill (IVF). The single and multistory channel-fills represent two end-member stratal architectural patterns for fluvial sandstones in the study area. Although often considered to be in separate lithostratigraphic formations (i.e. Blackhawk-single story, Castlegate-multistory), some of the earliest Book Cliffs studies identified both single-story and multistory channel sandstones within the Lower Castlegate Sandstone (Spieker and Reeside 1925; Spieker 1931, 1949; Young 1955).

This stop is located approximately 20 km down-depositional-dip (east) of our previous stop in Tusher Canyon. We will concentrate our observations in a beautifully exposed, three-dimensional amphitheater and side canyon along the northwestern edge of Trough Spring Ridge, approximately 11 km north of I-70 (Figs. 0-1, 0-2, 11-1 to 11-8). This region is part of the northwestern extension of the Salt Valley Anticline, which is well exposed to the southeast in Arches National Park. The central core of the Salt Valley Anticline is characterized by a collapsed crest or axial graben called the Salt Valley Graben (Fig. 11-1; Walton 1956). This extends northwestwards across I-70 into the Trough Spring Ridge-to-Christmas Ridge region and is prominently exposed as we drive into The Basin. Note that the vegetated top of the Lower Castlegate Sandstone is exposed at road level in The Basin, compared to its cliff-top exposures along Horse Mesa (to the west) and Trough Spring Ridge (to the east). Up to 200 m of offset is observed in places. Time permitting, we will park our vehicles at the end of the road next to the Blaze A-1 well, which has produced oil at a depth of 9045 feet from the Jurassic Navajo Sandstone (Fig. 11-2). Or alternatively, we will view this well from the top of the white capped sandstone cliffs in the amphitheater. Southwest-to-northeast trending faults cut the northwestern nose of the Salt Valley Graben providing structural closure on the Navajo Sandstone (Walton 1956), hence the Jurassic oil production from this well locality.

From base to top, the main architectural elements in The Basin are as follows: (i) marine mudstones and inner shelf to lower shoreface heterolithics of Desert Member parasequences D1 to D5, (ii) thick bedded foreshore-shoreface sandstones of Desert parasequences D6 to D8, (iii) shoreface-incised channel-fill successions along the tops of D7 and D8, and (iv) interbedded coastal plain (i.e. organic-rich mudstones, coal, thin-bedded sandstones) and channel-fill (i.e. organic-rich cross bedded sandstones) deposits of the amalgamated uppermost Desert Member and Lower Castlegate Sandstone (Figs. 11-3 to 11-8). Note that the shallow marine section is easy to correlate along the cliff face, while the fluvial and coastal plain deposits are difficult to correlate, even at a relatively close spacing of a few hundred meters.

The stop beside the Blaze A-1 well affords an exceptional opportunity to study reservoir-scale changes in the sedimentary architecture and stacking of channel-fill, coastal plain and shallow marine depositional systems. Desert Member and Lower Castlegate Sandstone outcrops are wonderfully exposed and are highly visible in three-dimensions at this locality (Fig. 11-2). This is an excellent chance to examine the reservoir geology of channel-shallow marine depositional systems at a quarter-quarter-section or LSD spacing (Figs. 11-2 and 11-3). The near road outcrop in the Blaze A-1 well vicinity neatly fits into a quarter-section grid (½ mile x ½

mile), while the section-scale changes can be investigated by hiking through the various side canyons or carefully climbing nearby ridges (Figs. 11-2 and 11-3). A thick package of fluvial and coastal plain deposits (Desert Member and Lower Castlegate Sandstone) rests stratigraphically above the Desert Member shallow marine deposits in this region. The top of the Desert Member shallow marine section is a prominent white-cap-sandstone which comprises the floor of the amphitheater or bowl (Figs. 11-5 and 11-6).

Terrestrial facies stacking patterns in The Basin show significant changes over relatively short distances (i.e. 50-100 m). Note the presence of at least three multistory (MS-1 to MS-3; Figs. 11-4 to 11-6) channel complexes of variable thickness and lateral continuity, as well as numerous single-story channel-fills, including some with convolute bedded sandstones (Fig. 11-5). The excellent 3D outcrop control in this amphitheater allows one to determine the lateral continuity of each type of channel sandstone package, thus providing an excellent analogue for correlating similar types of reservoir units in the subsurface (i.e. spatial distribution, net:gross patterns, sand body continuity and connectivity). Most multistory sand bodies have relatively flat bases, with the exception of MS-2 which incises 4-5 meters into the underlying fine-grained coastal plain deposits and coals (Fig. 11-5C). Both allocyclic (i.e. base level fall) and/or autocyclic (i.e. flow convergence) processes are viable explanations for the origin of the multistory channel-fill complexes. An allocyclic control (i.e. incised valley) would be corroborated with evidence of forced regression in the time-equivalent shallow marine section including a basinward shift of facies, a progradational parasequence set stacking pattern, a descending shoreline trajectory, and a suite of sharp-based shorefaces with regressive surfaces of marine erosion. In contrast, an autocyclic origin would be favored if there was no apparent link between the non-marine facies stacking patterns and the shallow marine stacking patterns or sedimentary architecture. The answer lies within the observations and descriptions of the sedimentary rocks down-dip, in the Crescent Canyon-to-Sagers Canyon region. There will be ample opportunity to observe and describe the Desert Member to Lower Castlegate Sandstone stratigraphic interval as we progressively move down-dip (i.e. east) throughout the remainder of this field trip. This will allow participants to formulate, test and refine multiple working hypotheses, and to select the most viable interpretation.

Overall, the sheet-like geometry of the amalgamated channel sandstones tapers eastwards, eventually grading into a coal-bearing coastal plain mudstones with single-story channel sandstones, similar to what we observe in The Basin. Marking this transition is the break-up of the multistory sheet-like geometry into a multistory ribbon- or finger-like geometry, with 2 to 5 channel stories per package (Fig. 11-5). Excellent examples occur elsewhere throughout the Hatch Mesa to Horse Heaven region. Channel-fill successions in the multistory ribbons have similar dimensions compared to their neighboring multistory sheet-like bodies, with a mean bankfull width of 15.0 m and a mean bankfull depth of 2.3 m. Channels are incised into one another with small amounts of erosion, rarely cutting deeper than the uppermost part of the underlying story (Fig. 11-5). As such, most channel bases are horizontal-to-sub-horizontal (Figs. 11-4 to 11-6). Individual channel-fill successions commonly extend a few meters beyond the edge of the underlying channel story, generating a wing-like geometry or irregular margin for many ribbon-to-finger-like multistory channel complexes. Similar geometries have been described from multistory channel sand bodies in the Williams Fork Formation, Piceance Basin of Colorado (Pranter et al. 2007, 2009; Pranter and Sommer 2011; Chamberlin and Hajek 2015). Irregular and uneven margins are one field criterion used to indicate an avulsion origin rather than an incised valley origin for a multistory channel sand body (Chamberlin and Hajek 2015).

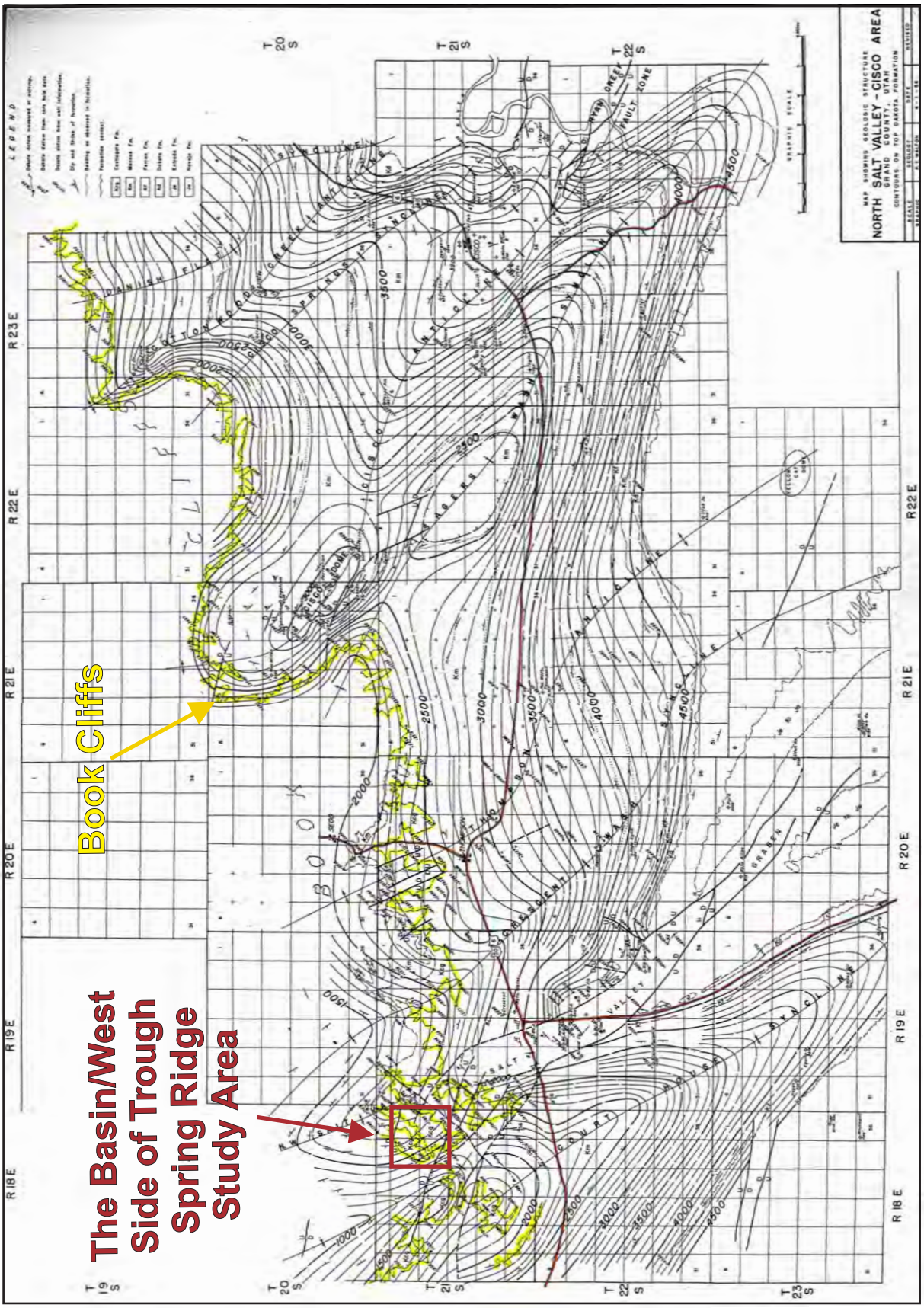

Figure 11-1. Structural geology of the North Salt Valley - Cisco area (Walton 1956). Structure contours (feet) on top Dakota Formation.

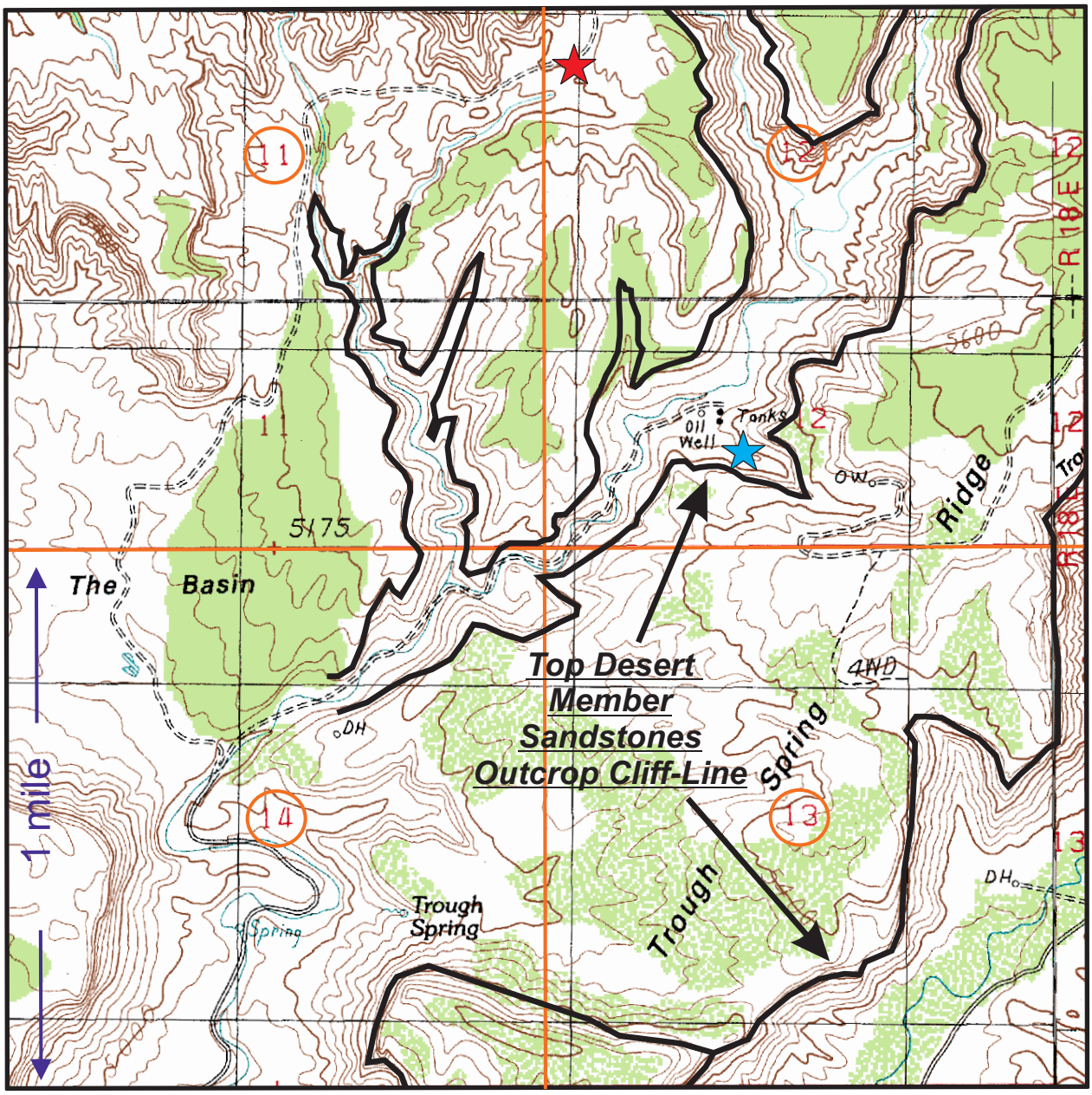

Figure 11-2. The Basin and Trough Spring Ridge. Topographic map of a four-section-area (Sections 11-14, T21S, R18E) in The Basin to west side of Trough Spring Ridge region. This 4 square mile area is highlighted by an excellent three-dimensional view of Castlegate Sandstone and Desert Member outcrop. The top of the Desert Member shallow marine sandstones are cliff-forming (thick black line). Blaze A-1 oil well (blue star), situated at NESW-12-21S-18E (API Well Number 43-019-30207). This well has produced oil from the Jurassic Navajo Sandstone, which is structurally trapped on the NW nose of the NW-SE trending Salt Valley Anticline (i.e. collapsed crest or axial graben). SW-NE trending faults provide the structural closure in this region (Walton 1956). The field stop vehicle parking location is at the north edge of The Basin and is marked by a red star.

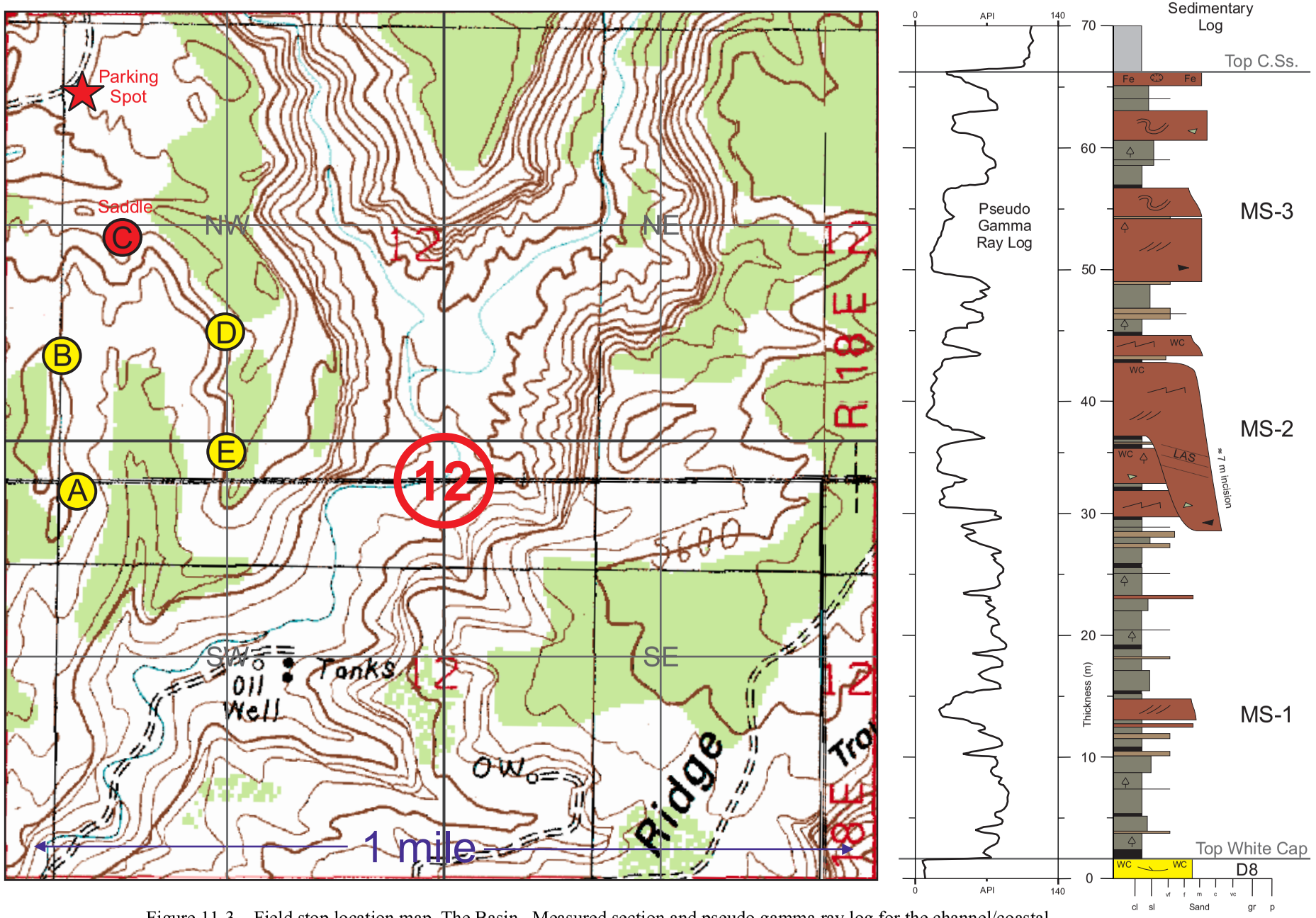

Figure 11-3. Field stop location map, The Basin. Measured section and pseudo gamma ray log for the channel/coastal plain succession. MS (Multistory channel complex), C.Ss. (Castlegate Sandstone), D8 (Desert Member parasequence).

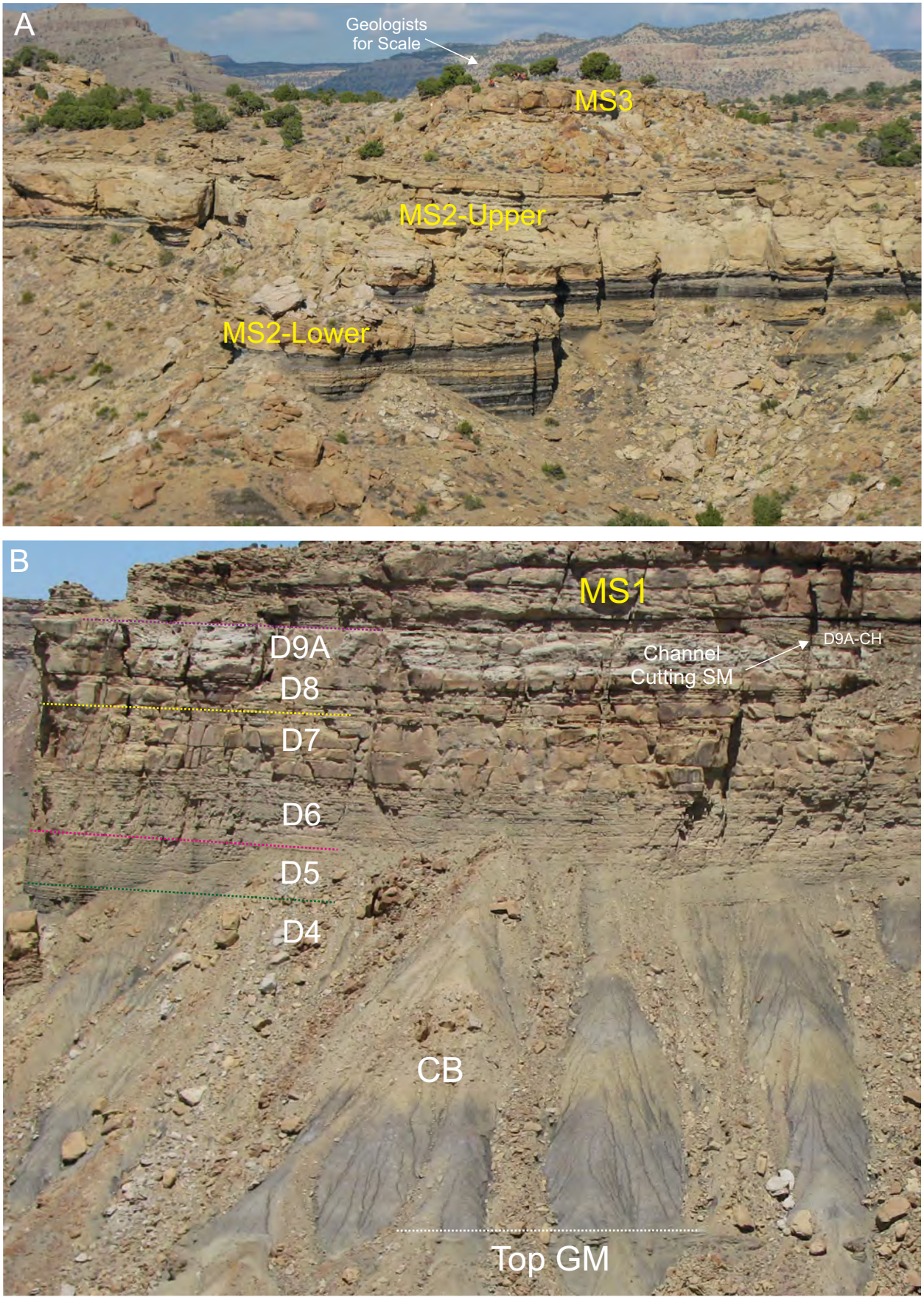

Figure 11-4. (A) Interbedded fine-grained coastal plain deposits and channel sandstones, Mid Basin, The Basin (photo 5030; photo location is plotted on Fig. 11-6A). Multistory (MS) channel deposits are recognized at two discrete levels: MS-2 and MS-3. Geologists for scale near top Castlegate Sandstone. Photo is coincident with section D at the field stop. (B) Progradational stack of facies and parasequences (D4 to D9A), capped by multi-storey channel complex MS-1, SE Face, Trough Spring Ridge (photo 1564; location of photo shown on Fig. 11-6A). Note that MS-1 incises into parasequence D9A and cuts out some of the white cap. GM (Grassy Member), CB (Colour Band), SM (Shallow Marine).

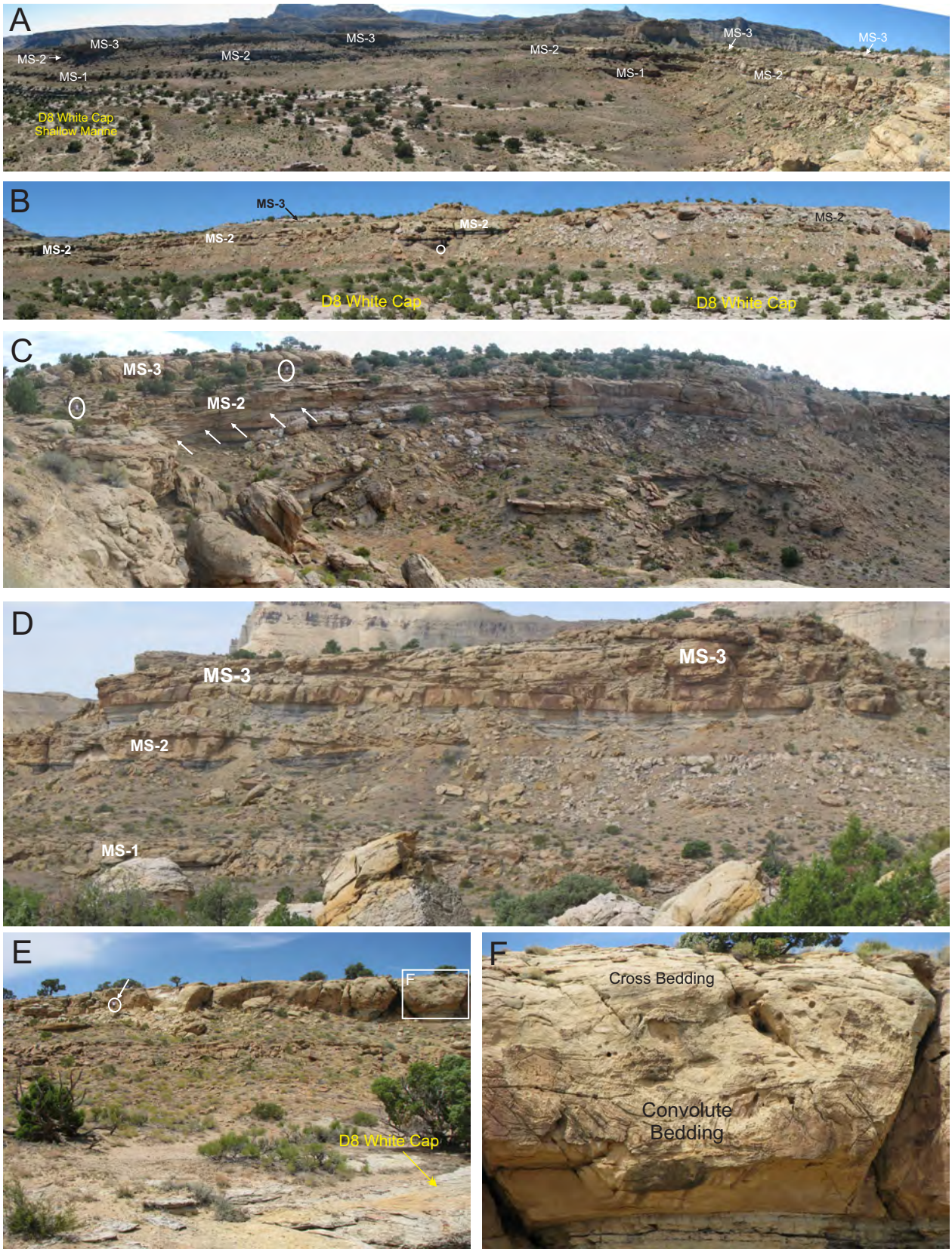

Figure 11-5. The Basin. Sedimentary architecture and correlation of coastal plain and channel packages. MS (multistory channel complex). (A) Panorama looks SW to NW. (B) Panorama looks N to E. Geologist for scale (circle). (C) Panorama in northern part of bowl, looking east. Heterolithic-rich channel-fill of MS-2 cuts deeply into underlying coal and fine-grained coastal plain facies (arrows). Geologists for scale (circles). (D) Well exposed MS-3 channel complex in SW part of bowl. Consists of at least 4 stacked channel-fills. MS-2 and MS-1 are labelled below. (E) Convolute bedded, single-story channel-fill deposits, Left Fork, The Basin. Geologist for scale (circle and arrow). Inset rectangle shows Part F photo location. (F) Convolute bedding is restricted to the lower half of the channel-fill.

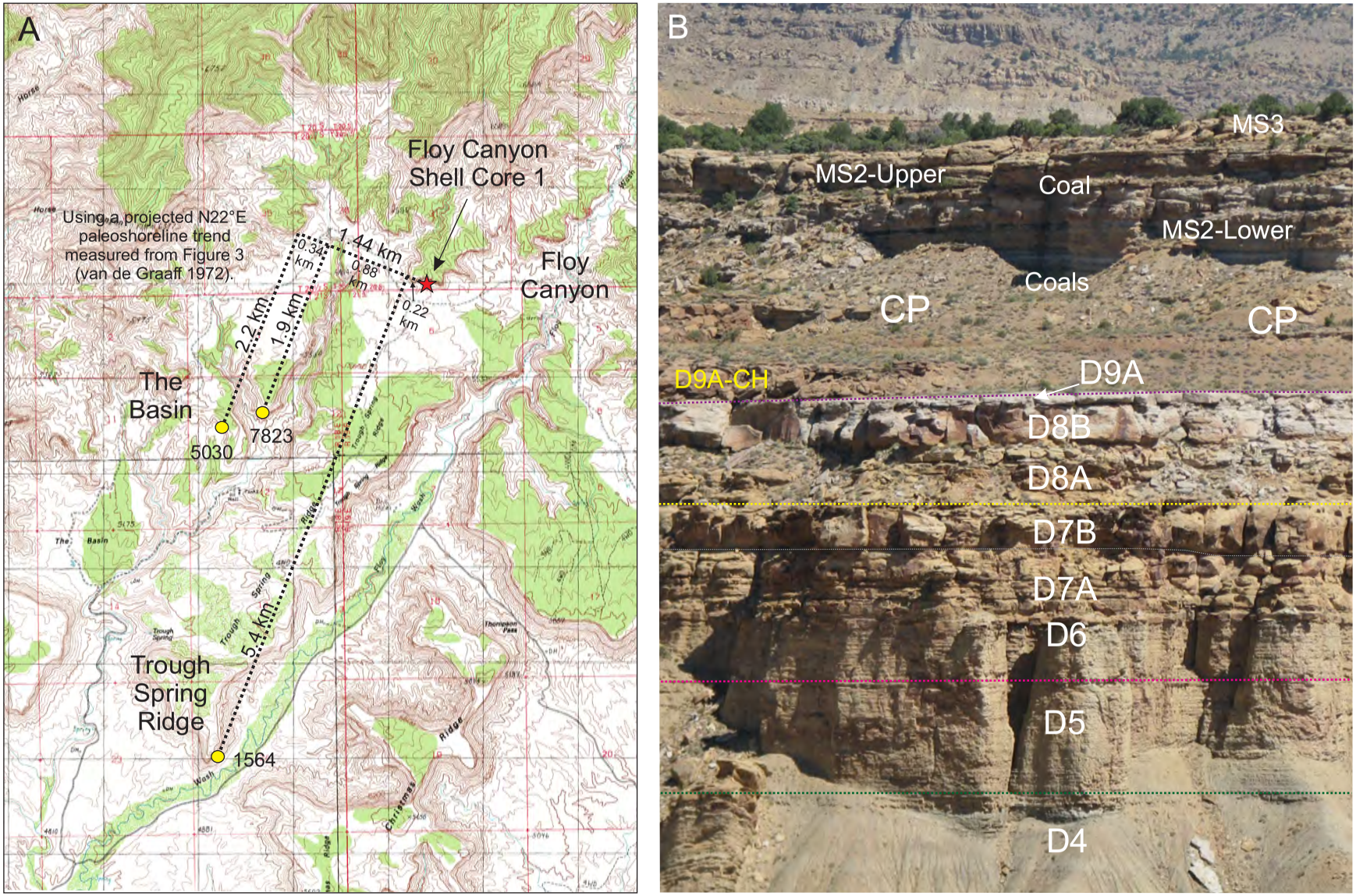

Figure 11-6. (A) Topographic map of the Trough Spring Ridge to Floy Canyon region. Locations of three photographs and Shell Core #1 are shown. Distances are plotted using a N22°E paleoshoreline trend as per van de Graaff (1972). Photo 5030 is coincident with the field stop in The Basin. (B) Progradational stack of parasequences D4 to D9A overlain by coastal plain and channel deposits. The tops of parasequences D8B and D9A form excellent correlation markers through this region. They are horizontal, laterally extensive and demaracated by prominent white caps. This photograph (7823) is of a ridge-line approximately 500 meters east of the field stop, Left Fork, The Basin. MS (Multistory Channel Complex), CP (Coastal Plain).

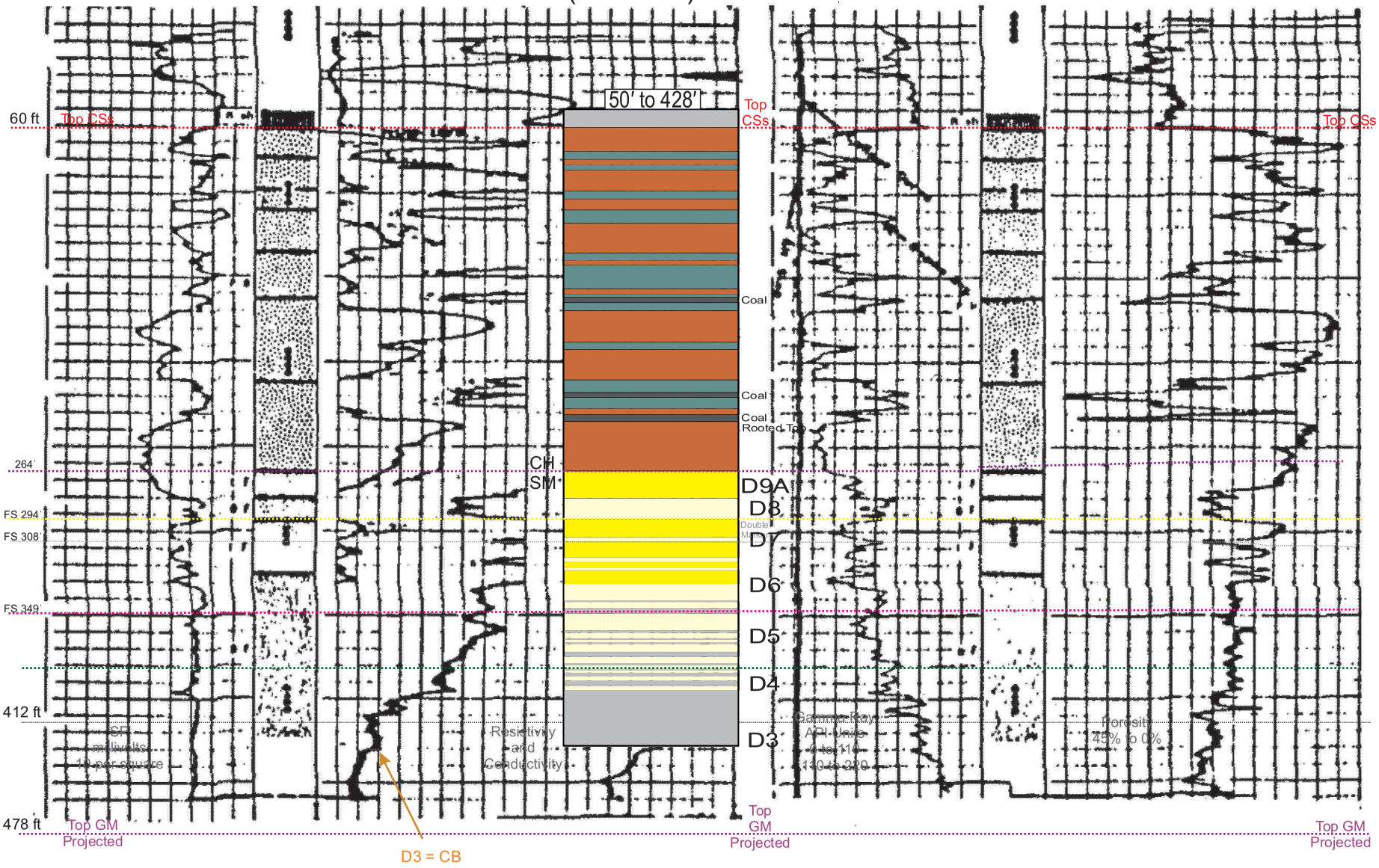

Figure 11-7. Shell Core Hole #1, Floy Canyon. Located at SESESW-31-20S-19E. Well logs are correlated to a basic core description: red (fluvial), green (coastal plain), black (coal), dark yellow (upper shoreface), light yellow (lower shoreface), grey (offshore shelf). Desert Member parasequences D3 to D9A are recognized. SM (shallow marine), CH (channel), CSs (Castlegate Sandstone), GM (Grassy Member), CB (Colour Band), FS (Flooding Surface).

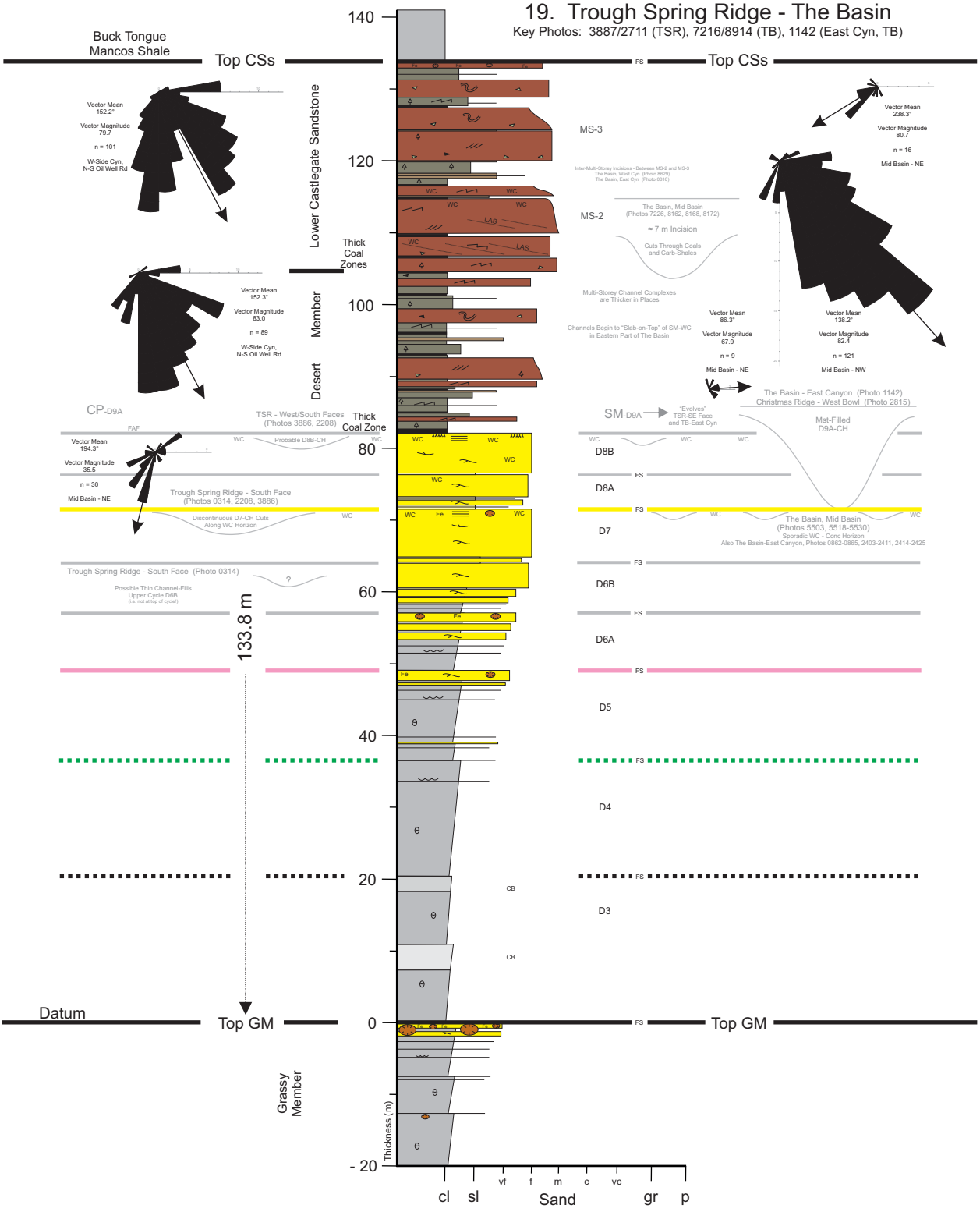

Figure 11-8. Measured outcrop section #19, Trough Spring Ridge-The Basin. Desert Member parasequences D3-D8 are recognized. MS (Multistory Channel), Grassy Member (GM), CSs (Castlegate Sandstone).

FIELD DAY 4

CHANNELS, COASTAL PLAIN & SHOREFACE: ARCHITECTURE & PREDICTION

Stop 12: Facies and Stratal Architectures of the Desert-Castlegate, Crescent Canyon to Horse Heaven

Stop 13: Low Accommodation Space Setting, Desert Member and Castlegate Sandstone, West of Blaze Canyon

Stop 14: High Resolution Sequence Stratigraphy, Desert Member and Castlegate Sandstone, Blaze Canyon

STOP 12: FACIES AND STRATAL ARCHITECTURES OF THE DESERT-CASTLEGATE, CRESCENT CANYON-HORSE HEAVEN

One of the best exposed channel-shoreface packages in the Book Cliffs region straddles the Desert Member to Castlegate Sandstone stratigraphic interval. Channel-dominated outcrops are concentrated in east-central Utah while shoreface-dominated outcrops are located further east. The transition from the channel- to shoreface-dominated intervals are beautifully exposed in three-dimensions in the numerous canyons and side-canyons in the southern sector of the Book Cliffs. Crescent Canyon is located approximately 6.5 km east of The Basin (Figs. 0-1 and 0-2), while Horse Heaven is the next locality east (Figs. 12-1 to 12-3). This is an extraordinary area that is characterized by some of the best three-dimensional outcrop in the entire Book Cliffs, with numerous side canyons, bowls and cliff-forming walls (Figs. 0-1, 0-2, 12-1 to 12-7). This region encompasses approximately 30 km^2, and is critically positioned at the transition from the nearshore terrestrial to shallow marine facies belts.

The shallow marine facies include planar laminated, cross bedded, swaley cross stratified (SCS), hummocky cross stratified (HCS), and wave rippled sandstones; bioturbated siltstones and mudstones; and non-bioturbated dark mudstones (Figs. 12-1 to 12-3; Table 0-1). White cap sandstones and iron-rich nodules/beds occur within the shallow marine deposits forming excellent marker beds. Most shallow marine facies stack to form gradationally-based coarsening-upward successions that progressively pass from mudstones and siltstones at the base, to wave-rippled, HCS, SCS, cross bedded and planar laminated sandstones at the top (Figs. 12-1 to 12-3). Some of these successions are sharp-based, characterized by a rapid vertical transition from mudstones and siltstones to thickly bedded sandstones (e.g. base of D9A; Fig. 12-1). Each succession is capped by a flooding surface at the top. The uppermost parasequence generally shows a gradational facies change into the overlying channel-fill and coastal plain facies (Figs. 12-1 and 12-2), although these are also cut by shoreface-incised channels (Fig. 12-3). Deep incisions into the lower shoreface or inner shelf heterolithics, characteristic of incised valley-fills, are not observed in the Crescent Canyon area. The nearshore terrestrial facies includes fine-grained coastal plain deposits, single-story channel-fill, and multistory channel-fill complexes (Figs. 12-1 to 12-7). Fine-grained coastal plain deposits include silty sandstone-to-sandy siltstone with iron-staining and organic matter; iron-rich siltstone to sandstone with plant debris and coal fragments; light grey-green organic-rich mudstone; carbonaceous-rich shale ("carb-shale"); and coal. Thick packages of coastal plain deposits occur throughout the Crescent Canyon region and these are often highly weathered and covered by vegetation and/or scree. Coastal plain facies have a wide range of grain size and sorting, and are often iron-stained, rich in organic matter (i.e. finely comminuted plant debris; wood, leaf and coal fragments; roots and rootlets), and have a sheet-like geometry. Coals are sub-bituminous-to-bituminous, have variable thickness (i.e. beds are generally 10 to 100 cm thick), and are locally to regionally extensive. Channel facies are dominated by cross-bedded, convolute-bedded, planar laminated and current ripple-laminated sandstones; sandstones with mud- and coal-fragments; and silty sandstone/sandy siltstone with iron-staining and organic matter.

The "big picture" stratigraphy is a stack of shallow marine facies (Desert Member) overlain by a stack of non-marine facies (upper Desert Member and Lower Castlegate Sandstone), thus defining an overall progradational or shallowing-upward vertical facies succession (Figs. 12-1 to 12-7). Desert Member parasequences D3 to D11 and Lower Castlegate Sandstone parasequences C1 and C2 are recognized in the Crescent Canyon to Horse Heaven region. Shoreface-incised channel complexes cut into D10, D11, C1 and C2, and are

heterolithic- and/or sandstone-rich fills. The uppermost Desert Member is marked by a thick, heterolithic-rich, channel-fill succession (D11-CH) with large-scale lateral accretion surfaces that occurs directly beneath a prominent coal (i.e. Upper or Road Level Coal; Figs. 12-1 to 12-7).

Desert Member parasequences D5 to D9 stack to form a progradational parasequence set (Figs. 12-1 to 12-3). In Crescent Canyon, parasequences D5 to D8 occur as gradationally-based coarsening-upward (CU) successions, while parasequence D9A occurs as a sharp-based CU succession with a regressive surface of marine erosion (RSME) at the base of the amalgamated sandstone beds (Fig. 12-1). To the east, parasequence D9 splits (i.e. along the contact marked by the white cap layer) into two cycles (D9A and D9B). Parasequence D10 consists of varying proportions of shallow marine and non/marginal-marine (channel sandstones, coastal plain) facies. Non/marginal-marine deposits are dominant to the west, while shallow marine sandstones are abundant towards the east, where package D10 splits into three sub-cycles or bedsets (D10A to D10C; Figs. 12-5 to 12-7). Parasequence D10 thickens from west-to-east across the area. Parasequence D11 is comprised of non/marginal-marine strata at Crescent Canyon, and is highlighted by the sporadic outcropping of channel-fill deposits with large-scale (i.e. hundreds of meters in length) sandstone- or heterolithic-rich lateral accretion surfaces (Fig. 12-4A). D11 is bounded above and below by coal-bearing, carbonaceous-rich zones. The Upper Coal zone is labelled Coal 2 or the *"Road Level Coal"*, while the Lower Coal zone is labelled Coal 1 or the *"Cattleguard Coal"* (Fig. 12-1). Correlation of the Upper and Lower Coal zones is easily achieved thus forming excellent marker horizons throughout the Crescent Canyon to Blaze Canyon region (Figs. 12-1 to 12-7). Multistory channel-fill complexes are spread throughout this region. Some are correlatable for a few hundred meters, while others are not. Most multistory channel-fill complexes are comprised of a stack of sandstone- and/or heterolithic-rich channel-fill successions, with a maximum of five channel stories per stack. Individual channel stories can incise up to 5 m into the underlying channel-fill successions. Some of these are characterized by large-scale lateral accretion surfaces (Fig. 12-4D).

The Lower Coal zone caps the cliff-forming shallow marine sandstones (i.e. top D10) and thins eastwards along the South Face of Horse Heaven (Figs. 12-5 to 12-7). This horizon is also marked by the sporadic outcropping of thin (meter-scale) heterolithic channel-fill deposits in the South Face-East of Horse Heaven to West of Blaze Canyon (Figs. 12-2, 12-3, 12-7D). Van Wagoner (1995) interprets this layer as a high frequency sequence boundary. The heterolithic channel-fill and coal might be indicative of tidal-estuarine conditions and marine flooding, respectively. A sandstone-rich channel-fill succession topped by a white cap sandstone rests stratigraphically above the Lower Coal zone and is defined as parasequence D11 (Figs. 12-6 and 12-7). Parasequence D11 first appears in the Horse Heaven region, along with the shoreface-incised channel-fill complex D11-CH (Fig. 12-6). The Upper Coal zone marks the top of D11, thus explaining the prominent white cap. The Upper Coal zone extends along the entire eastern edge of the cliff-forming South Face of Horse Heaven, and is an excellent marker bed for correlation (Figs. 12-5 to 12-7). It is overlain by the foreshore-shoreface sandstones of parasequences C1 and C2 in the eastern half of Horse Heaven, and these in turn are cut by a multistory channel-fill complexes, C2-CH and C3-CH. Similar to D11, all of these rock packages first appear or evolve in the eastern part of Horse Heaven (Figs. 12-3, 12-6, 12-7). Collectively, the first appearance of D11, D11-CH, C1, C2, C2-CH, and C3-CH in the eastern half of Horse leads to a significant thickening of the cliff-forming sandstones in the Desert-Castlegate interval (Figs. 12-5 to 12-7). The parasequence and shoreface-incised evolution points can be easily accessed and studied in three-dimensions in this exceptional outcrop region.

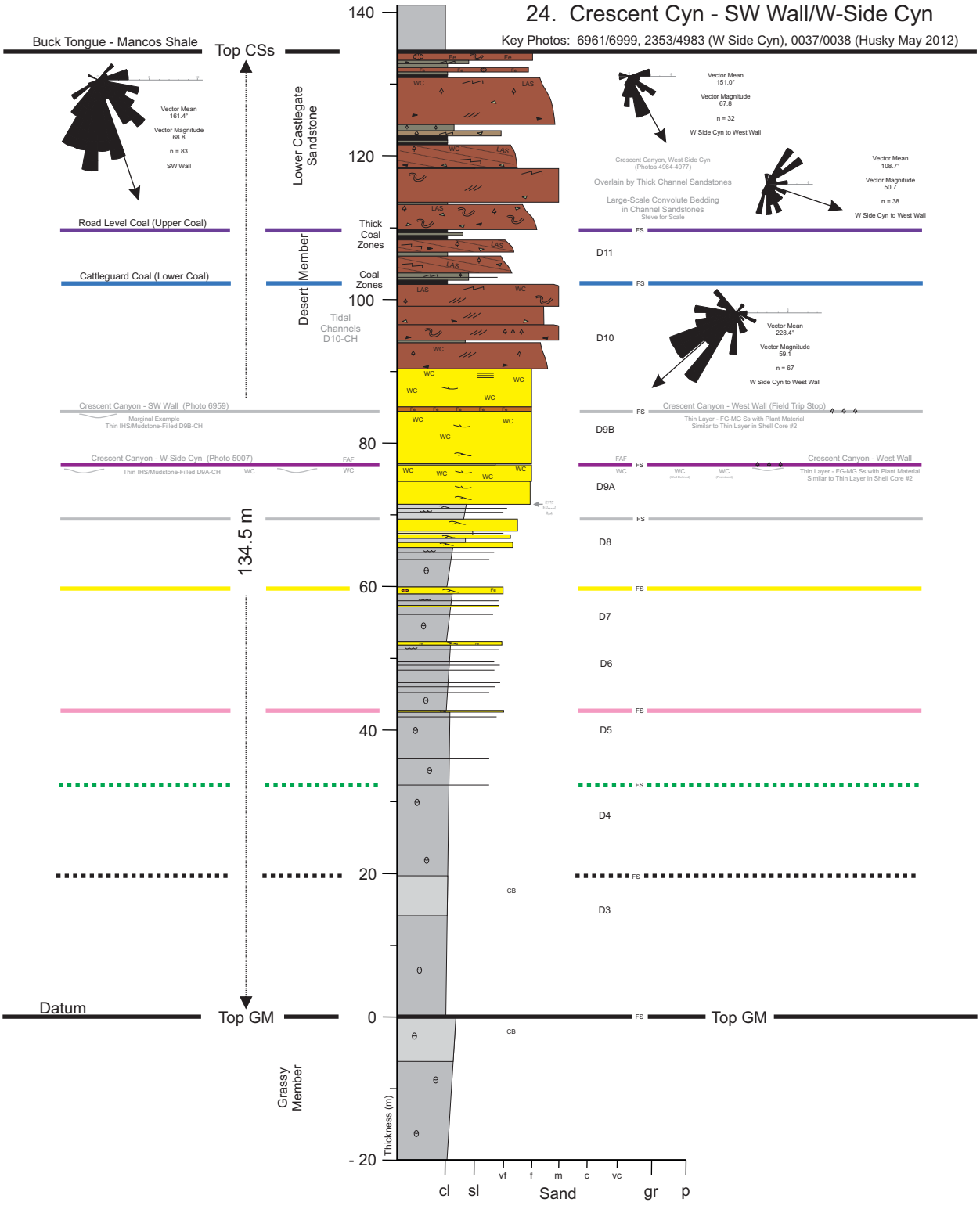

Figure 12-1. Measured outcrop section #24, Crescent Canyon, SW Wall/W-Side Cyn. Desert Member parasequences D3-D10 are recognized. Time equivalent coastal-plain deposits (parasequence D11) are bracketed by two prominent coal zones: Lower Coal (Cattleguard Coal) and Upper Coal (Road Level Coal). Legend nested in Figure 10-2. Grassy Member (GM), CSs (Castlegate Sandstone).

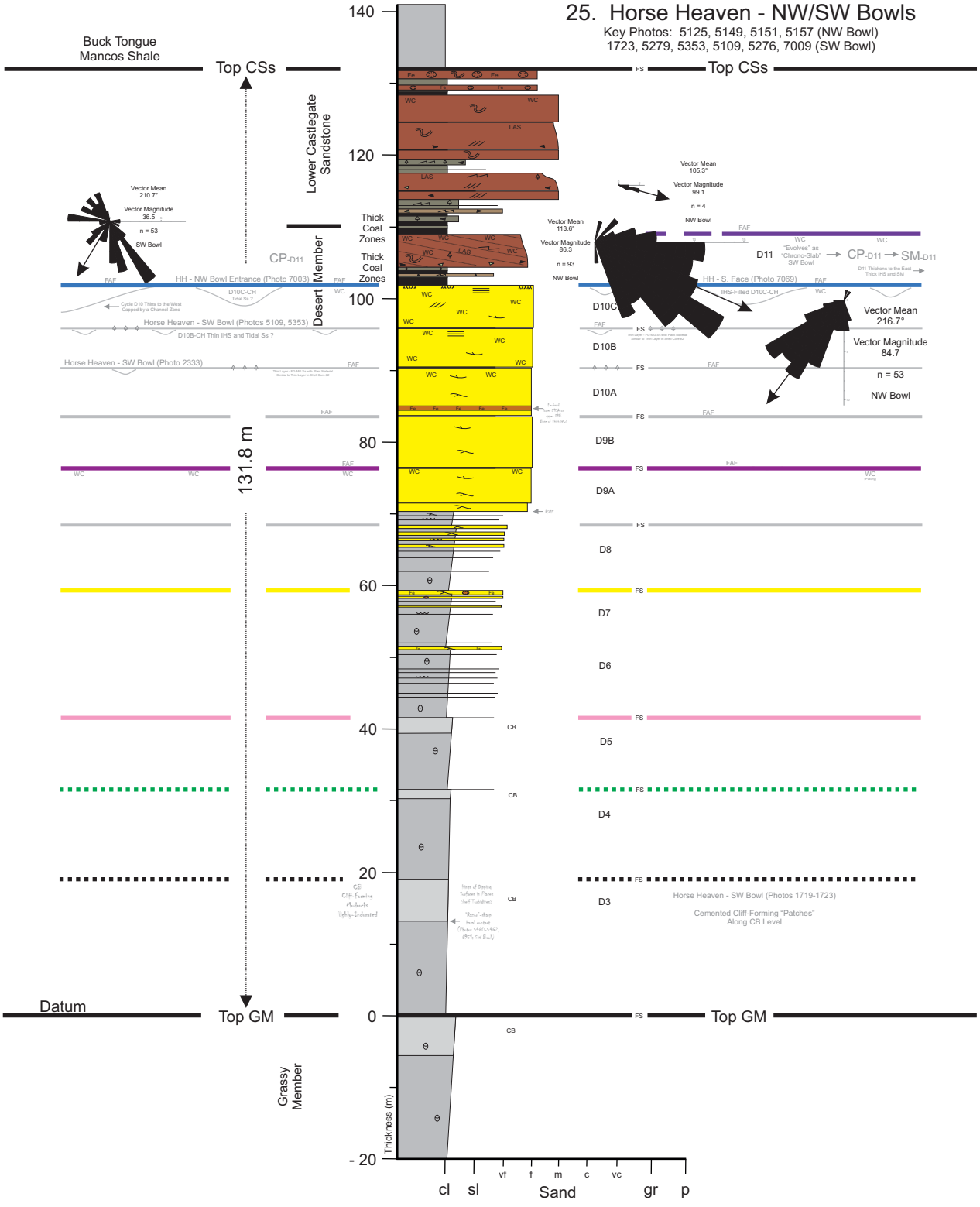

Figure 12-2. Measured outcrop section #25, Horse Heaven, NW-SW Bowls. Desert Member parasequences D3-D10 are recognized. Time equivalent coastal-plain deposits (parasequence D11) are bracketed by two prominent coal zones: Lower Coal (Cattleguard Coal) and Upper Coal (Road Level Coal). Legend nested in Figure 10-2. Grassy Member (GM), CSs (Castlegate Sandstone). Location shown on Figure 12-5.

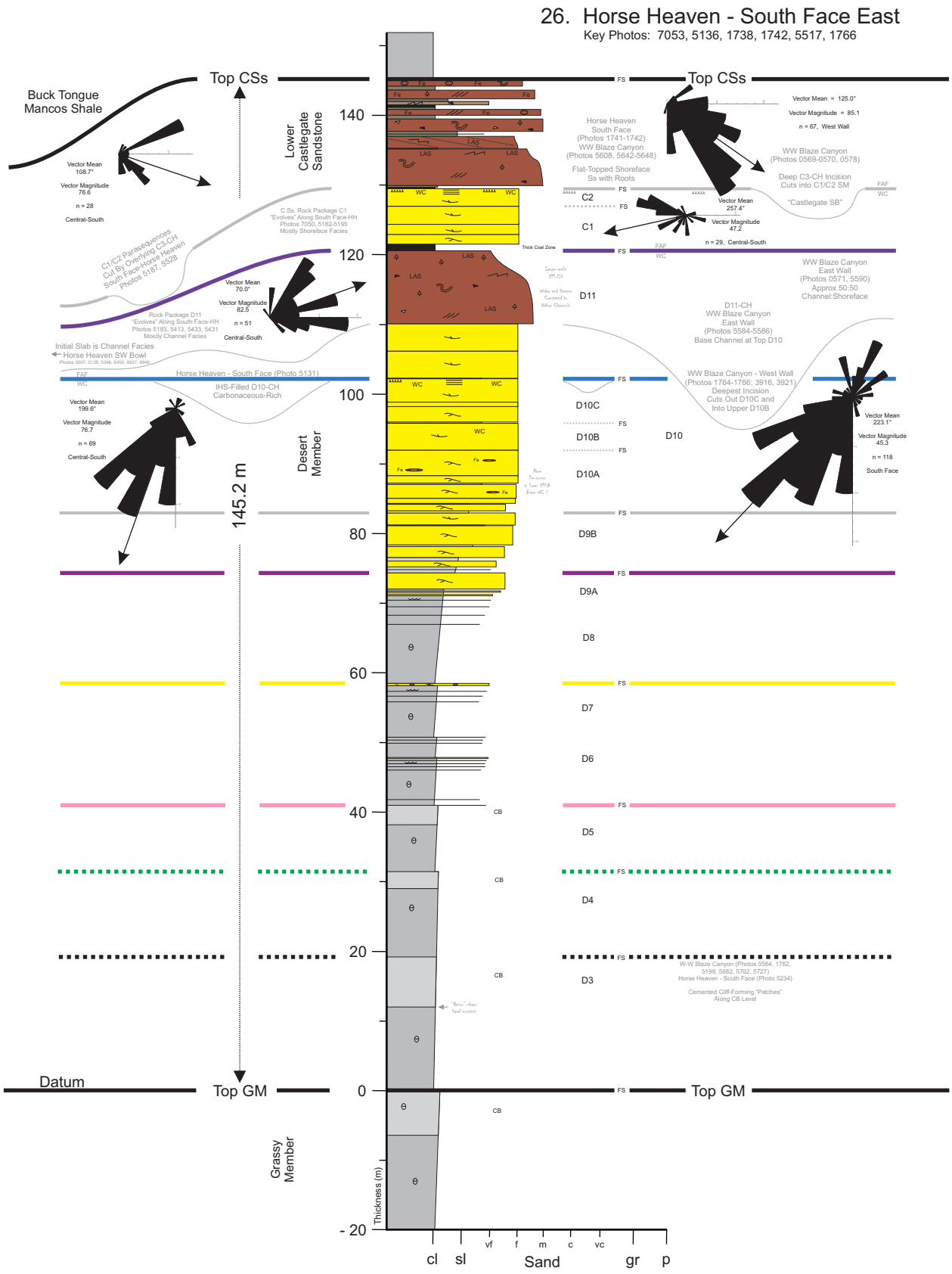

Figure 12-3. Measured outcrop section #26, Horse Heaven, South Face East. Desert Member parasequences D3-D11, and Lower Castlegate Sandstone parasequences C1-C2 are identified. Prominent shoreface-incised channels cut the D11 parasequence (i.e. D11-CH) and the C1-C2 parasequences (i.e. C2-CH). These channel-fills are sandstone- to heterolithic-rich, multistory, and relatively thick (i.e. up to 26.1 m thick). They are interpreted as tidally influenced distributaries and/or tidal-estuarine channels. Note the thinner, mudstone- to heterolithic-filled shoreface-incised channels cutting the top of D10. These are interpreted as terminal distributaries. Grassy Member (GM), CSs (Castlegate Sandstone). Location shown on Figure 12-5. Legend nested in Figure 10-2.

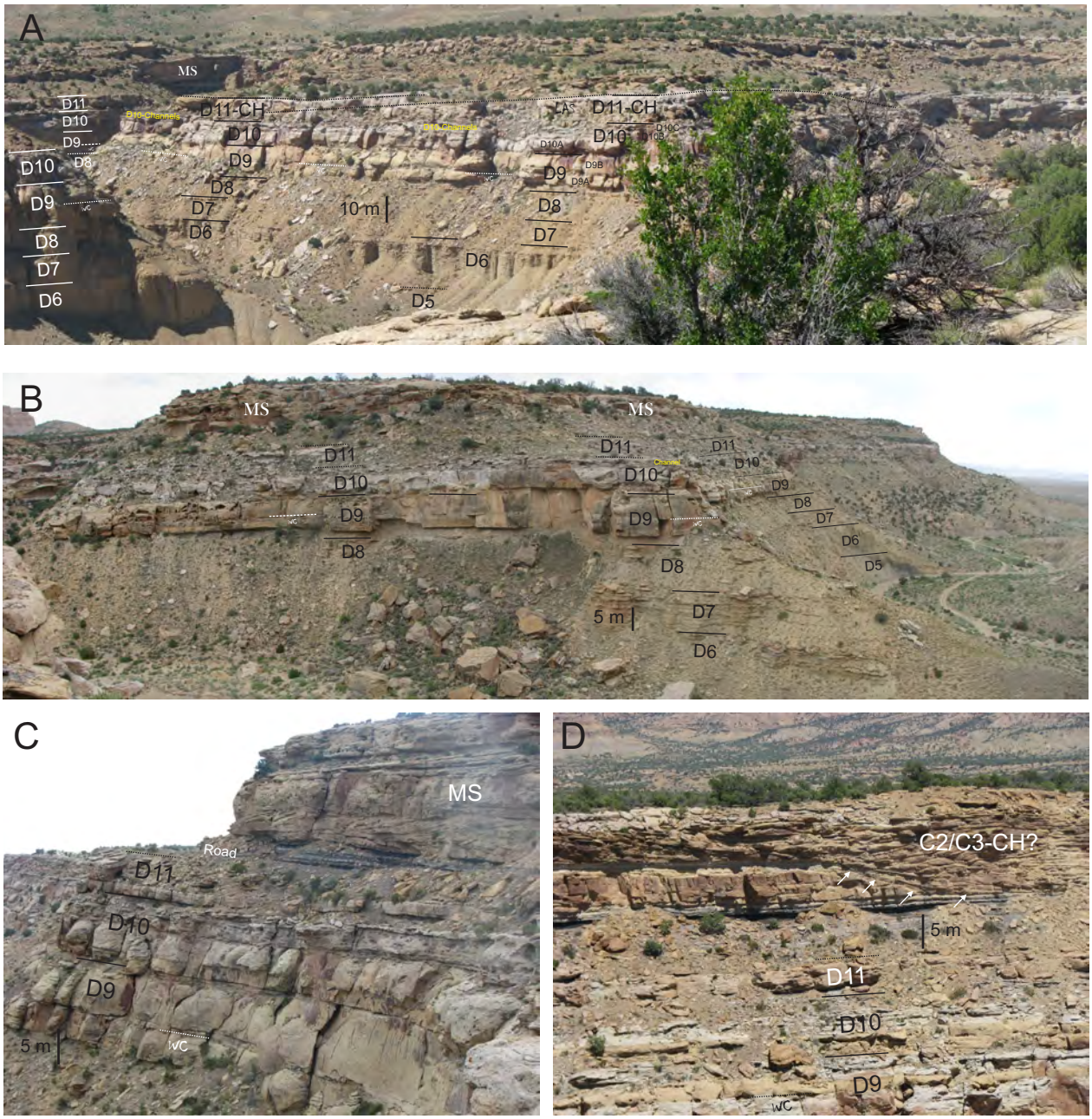

Figure 12-4. Crescent Canyon. (A) Photo-panorama showing the correlation of Desert Member parasequences D5 to D11, West-Side Canyon to West Wall, Crescent Canyon. Camera position along the Southeast Wall of Crescent Canyon, looking northwest. White-cap (WC) sandstone within parasequence D9 splits this cycle into two bedsets, D9A and D9B. The WC is a useful correlation marker. Large-scale lateral accretion surfaces (LAS) highlighted by dashed lines within the D11 shoreface-incised channel (D11-CH). MS (multistory channel complex). Crescent Canyon road in the upper right. (B) Photo-panorama, Southeast Wall, Crescent Canyon. Note the large-scale incision, lateral accretion surfaces, and 12-15 m thickness of the MS. (C) Lateral accretion in MS, West Wall, Crescent Canyon. Desert Member parasequences D9 to D11 are labelled. (D) Deep channel incision (white arrows), northeast face, East Bowl, Thompson Pass. This channel complex is large-scale, heterolithic-filled with IHS, and is likely the equivalent of the C2 and/or C3 shoreface-incised channel complex (i.e. C2-CH and/or C3-CH) observed at Blaze Canyon.

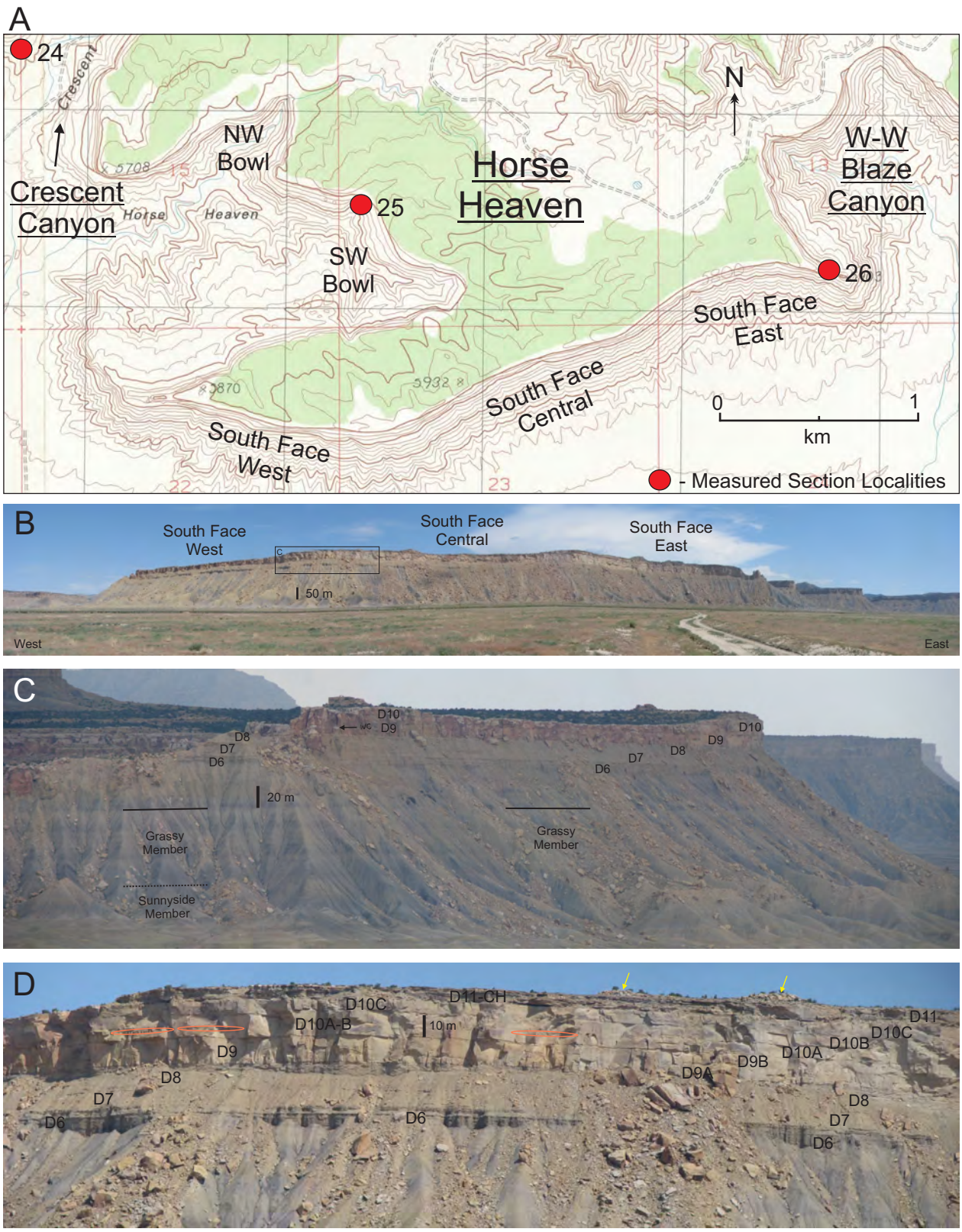

Figure 12-5. Horse Heaven. (A) Portion of the Crescent Junction USGS topographic map highlighting the location of Horse Heaven. Informal physiographic subdivisions include the Northwest Bowl, Southwest Bowl and the South Face (West, Central, East). Location of measured sections 24-26 is also shown. (B) Photo-panorama of the entire South Face of Horse Heaven. Three informal physiographic zones are recognized: South Face-West, South Face-Central, South Face-East. Inset box shows the position on Part D. Camera position is along the old highway, looking north. (C) South Face-West, Horse Heaven. Desert Member parasequences D5 to D10 are highlighted. Underlying Mancos Shale colour bands correspond to the Grassy Member and upper portion of the Sunnyside Member. Photo taken from the SE Bowl of Christmas Ridge, looking northeast. (D) Eastern edge of the South Face-West, Horse Heaven outcrop. Location shown in Part B. Shallow marine sandstone-rich rock packages (i.e. parasequences D9-D10) split into five smaller packages towards the east (i.e. bedsets D9A-D9B, D10A-D10B-D10C). Note the iron-rich nodule-bearing layer within bedset D10A (elongated ovals). Top of the channel-rich package (arrows at the cliff top) is equivalent to the white cap sandstone in the SW Bowl, which demarcates the top of parasequence D11, which is overlain by the Upper Coal Zone, hence the prominent white-cap.

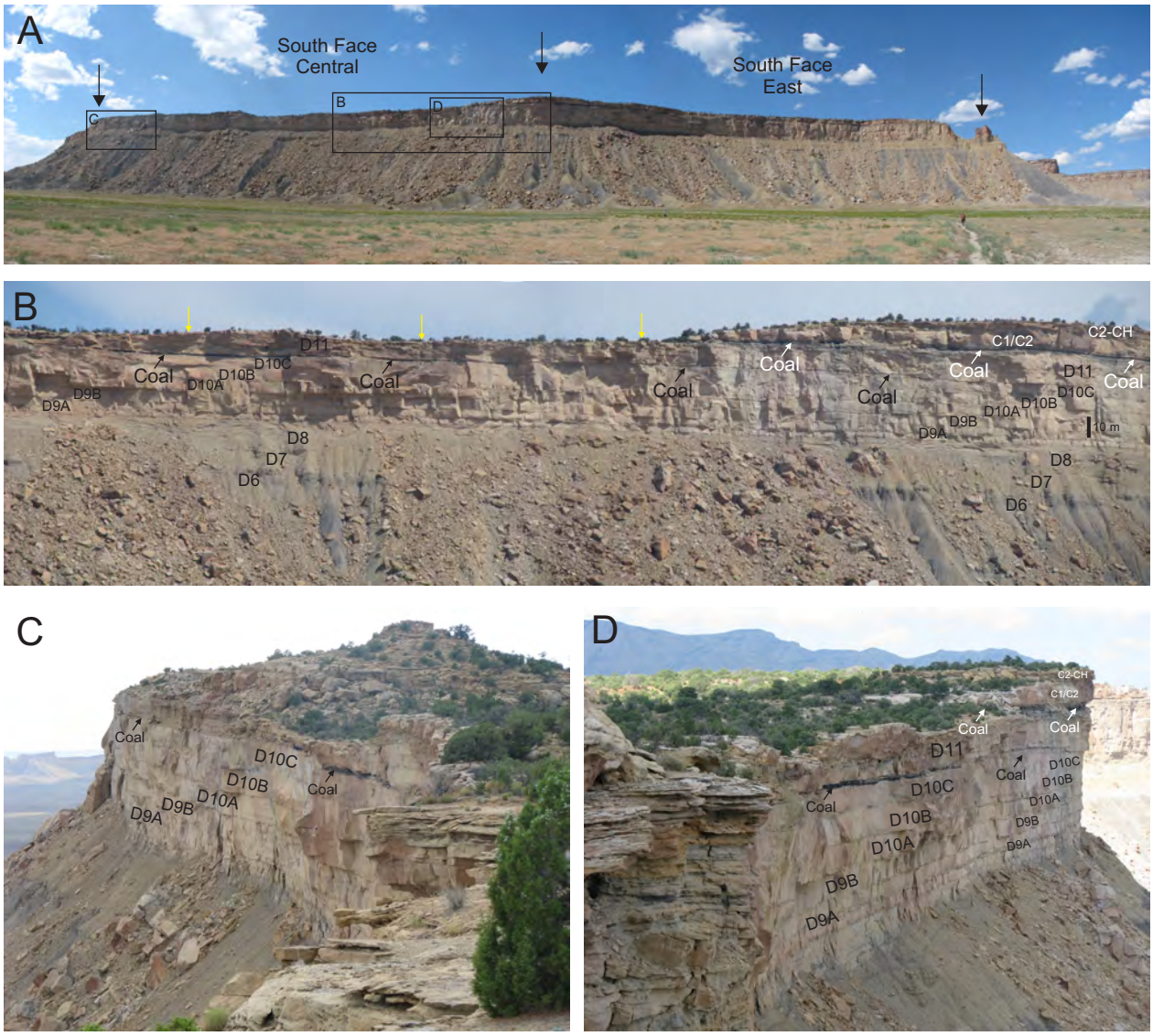

Figure 12-6. Horse Heaven, South Face-Central. (A) Photo-panorama of the South Face (Central and East), Horse Heaven. Camera position on the old highway looking north. South Face-Central ridge-line is 1.3 km long (between two black arrows), while the South Face-East ridge-line is approximately 1.2 km long (between two black arrows). Inset rectangles shows the position of Part B, C and D. (B) South Face-Central, Horse Heaven, photographed from the desert floor looking north. Desert Member parasequences D6 to D10 can be correlated beneath the lower coal bed (black arrows and labels). The lower coal caps parasequence D10. It thins to the east (right). Channel-fill sandstones and heterolithics equivalent to parasequence D11 are sandwiched between the lower and upper coals (white arrows and labels), with the top of D11 corresponding to the white cap channel sandstones observed throughout the SW Bowl of Horse Heaven. A sandstone-rich rock package consisting of Lower Castlegate Sandstone parasequences C1 and C2, and the shoreface-incised C2 channel (C2-CH) overlies the upper coal bed. This sandstone-rich package becomes permanently "fused/welded" onto the underlying D10 sandstone beds from this area, eastwards. (C) South Face-Central, Horse Heaven, western side. Camera position on top looking west. (D) South Face-Central, eastern side. Camera position on top looking east.

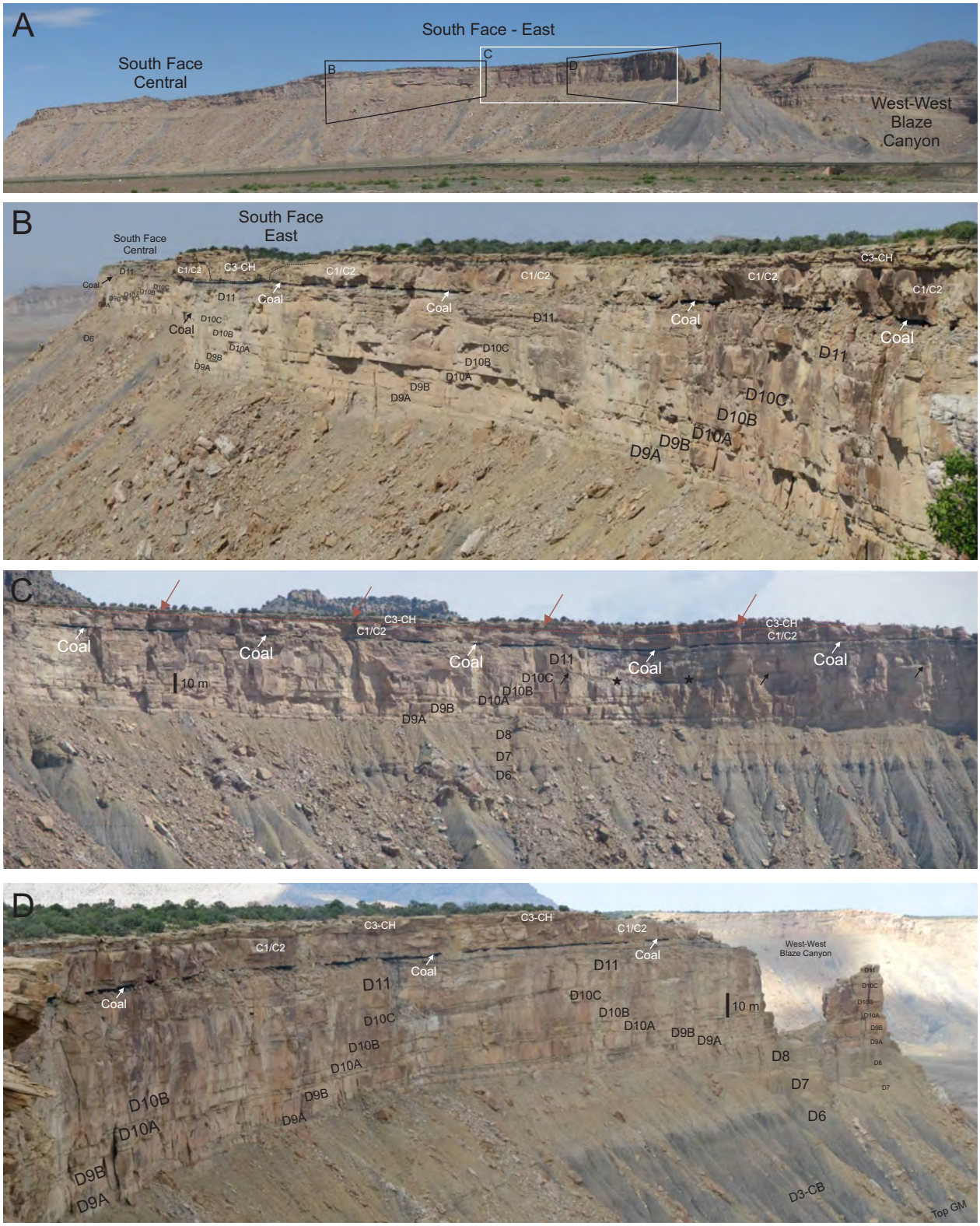

Figure 12-7. Horse Heaven, South Face-East. (A) Panorama of the South Face-Central to South Face-East region, Horse Heaven. West-West of Blaze Canyon is located immediately to the east. Inset rectangle shows the position of Part C, inset trapeziums show the location of Parts B and D. (B) South Face-East, Horse Heaven, western side. Location shown in Part A. D9A-D9B and D10A-D10B-D10C are labelled. Lower (black labels and arrows) and upper (white labels and arrows) coals bound parasequence D11. Amalgamated C1 and C2 parasequences are shown. These are either gradationally-conformably overlain by coastal-plain mudstones or sharply-conformably cut by the C3 shoreface-incised channel (i.e. C3-CH). The western edge of the South Face-Central outcrop is visible in the distance. (C) Photo-panorama from the South Face-East, Horse Heaven. Location shown in Part A. Upper coal bed (white arrows and labels) extends to the eastern edge of the South Face. The lower coal bed horizon is also identified (black arrows) on the eastern half of the panorama and is marked by a heterolithic channel-fill (black stars), the D10-CH. This horizon can be confidently correlated further east into West-West of Blaze Canyon, West of Blaze Canyon, and Blaze Canyon. An additional sandstone-rich layer occurs near the skyline and is "welded/fused" on top of the underlying sandstones (arrows and dashed line at base). This sandstone package is the C1-C2 parasequences, cut by C3-CH. (D) South Face-East, Horse Heaven, eastern side. Location shown in Part A. D9A, D9B and D10A have increased mudstone eastwards. CB (Colour Band), GM (Grassy Member).

STOP 13: LOW ACCOMMODATION SPACE SETTING, DESERT MEMBER AND CASTLEGATE SANDSTONE, WEST OF BLAZE CANYON

This region comprises two separate stops, each within an un-named canyon located west of Blaze Canyon and east of Horse Heaven (Figs. 0-1 and 0-2). The first stop will be an overview of the West-West of Blaze Canyon region, while the second stop will allow for examination of the strata at West of Blaze Canyon (Figs. 13-1 to 13-3). The purpose of these stops is to examine the distribution and 3D sedimentary architecture of non-marine and shallow marine facies, and to extend the correlation framework that was established in the Crescent Canyon to Horse Heaven region, eastwards.

West-West of Blaze Canyon is located directly around the corner (east) from the South Face-East of Horse Heaven. Correlations can be seamlessly extended from the South Face of Horse Heaven into West-West of Blaze Canyon, where Desert parasequences D7 to D11, Castlegate parasequences C1 and C2, and shoreface-incised channel-fills D10-CH, D11-CH, and C3-CH are clearly recognized (Figs. 13-1 to 13-3). Shoreface sandstones of D9 and D10 are extremely well developed at West-West of Blaze Canyon, forming the lowermost portion of the sandstone-rich cliff-forming succession (Fig. 13-2A). The amalgamated shallow marine sandstones near the base of D10 are occasionally sharp-based, defining a regressive surface of marine erosion. The top of D10 is variably truncated by the D11-CH complex, with up to 5 m of incision along the West Wall of West-West of Blaze Canyon. The D11-CH has some large-scale, heterolithic-rich, lateral accretion surfaces, especially along the north and east walls. D11 and the D11-CH are overlain by a thick Upper Coal zone, which in turn is overlain by Castlegate parasequences C1 and C2 and multistory channel-fill deposits of the C3-CH complex. In some areas the C1-C2 shoreface package is completely cut-out, leading to a channel-on-channel contact between the C3-CH and the underlying D11-CH. The Castlegate channel complexes are characterized by a mixture of sandstone-, heterolithic- and mudstone-rich channel-fill deposits. These in turn are overlain by at 8-12 m of coal-bearing coastal plain mudstones with single-story fluvial channels, which caps the uppermost part of the Lower Castlegate Sandstone.

West of Blaze Canyon has a similar suite of sequence stratigraphic rock packages and surfaces as those observed at the previous field stops (i.e. Crescent Canyon to West-West of Blaze Canyon). Shallow marine parasequences D7 to D11 and C1 to C2, and shoreface-incised channels D11-CH and C3-CH are easily identified and correlated (Fig. 13-2B, C). These combine to form two progradational parasequence sets: Desert parasequences D3-D11 and Lower Castlegate Sandstone parasequences C1-C2. The Upper Coal zone records the boundary between the two progradational parasequence sets, thus representing a regional flooding or landward shift of facies belts. The top of D10 is marked by thin heterolithic channel-fills (D10-CH) that are coincident with the thin channels observed along the South Face-Central to South Face-East of Horse Heaven (Fig. 12-7). D11 is comprised of foreshore-shoreface sandstones cut by the D11-CH shoreface-incised channel. The D11-CH complex is characterized by large-scale lateral accretion surfaces, with heterolithic-to-mudstone-rich channel-fill deposits. In places, the D11-CH cuts into D10C. D11 is overlain by the Upper Coal zone, which is spectacularly exposed in the cliff-forming northern and eastern walls of this canyon. This marks the top of the Desert Member. Castlegate parasequences C1 and C2 overlie the Upper Coal zone. These are variably truncated by the overlying multistory channel complex (C3-CH) which is comprised of sandstone and heterolithic, large-scale lateral accretion surfaces. In places, the C3-CH entirely cuts out the C1 and C2 sandstones (Figs. 13-2B, C). However it does not appear to cut through the Upper Coal zone as it conformably rests or “seats” on the top of this interval (Fig. 13-2).

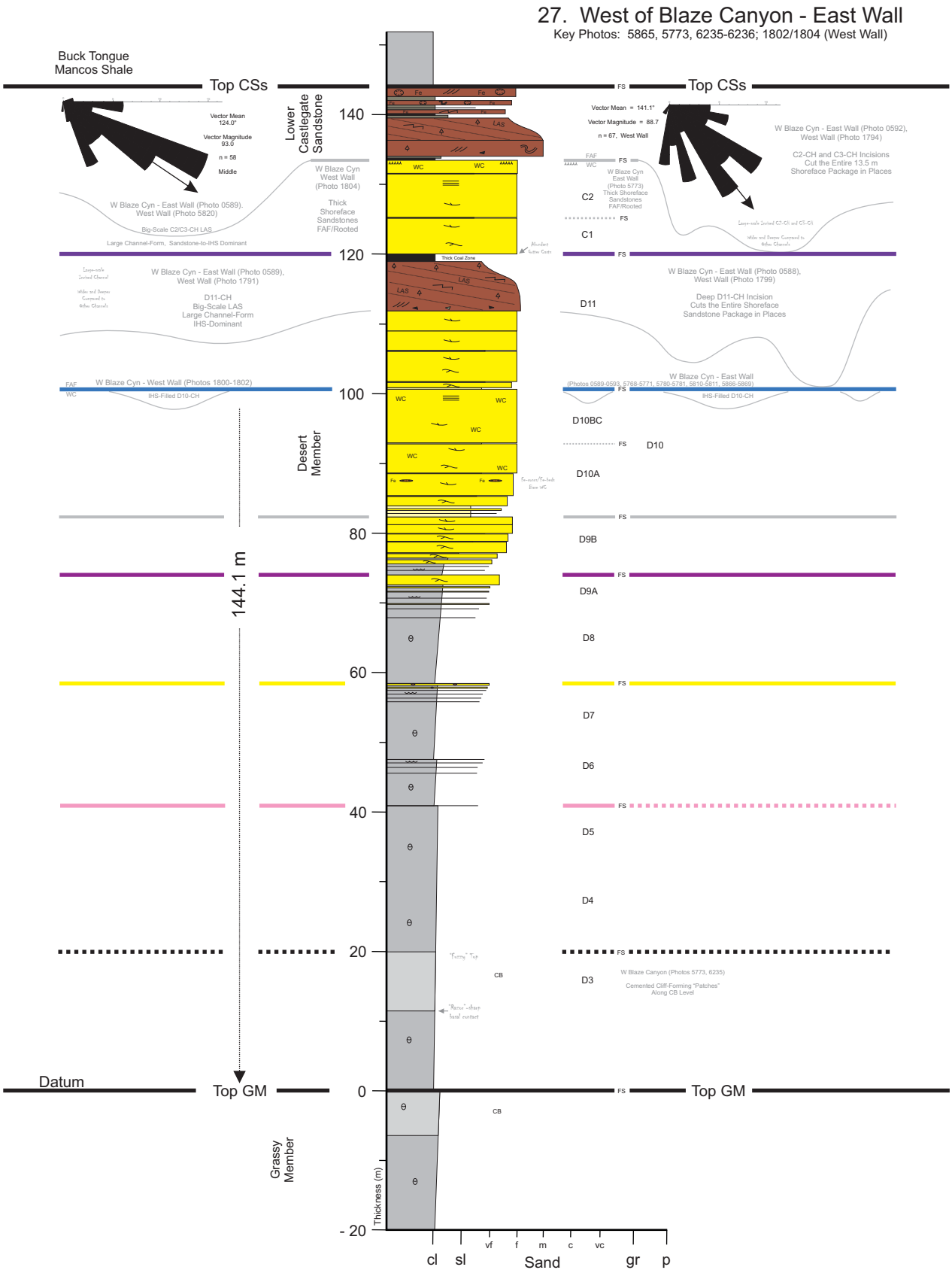

Figure 13-1. Measured outcrop section #27, West of Blaze Canyon, East Wall. Desert Member parasequences D3-D11, and Lower Castlegate Sandstone parasequences C1-C2. Two large-scale shoreface-incised channels: D11-CH and C3-CH. Both are heterolithic- to sandstone-rich, multistory, tidally influenced distributaries/tidal-estuarine channel fills. Thinner mudstone-filled terminal distributaries in the upper part of D10 (i.e. D10-CH). Grassy Member (GM), CSs (Castlegate Sandstone). Legend nested in Figure 10-2.

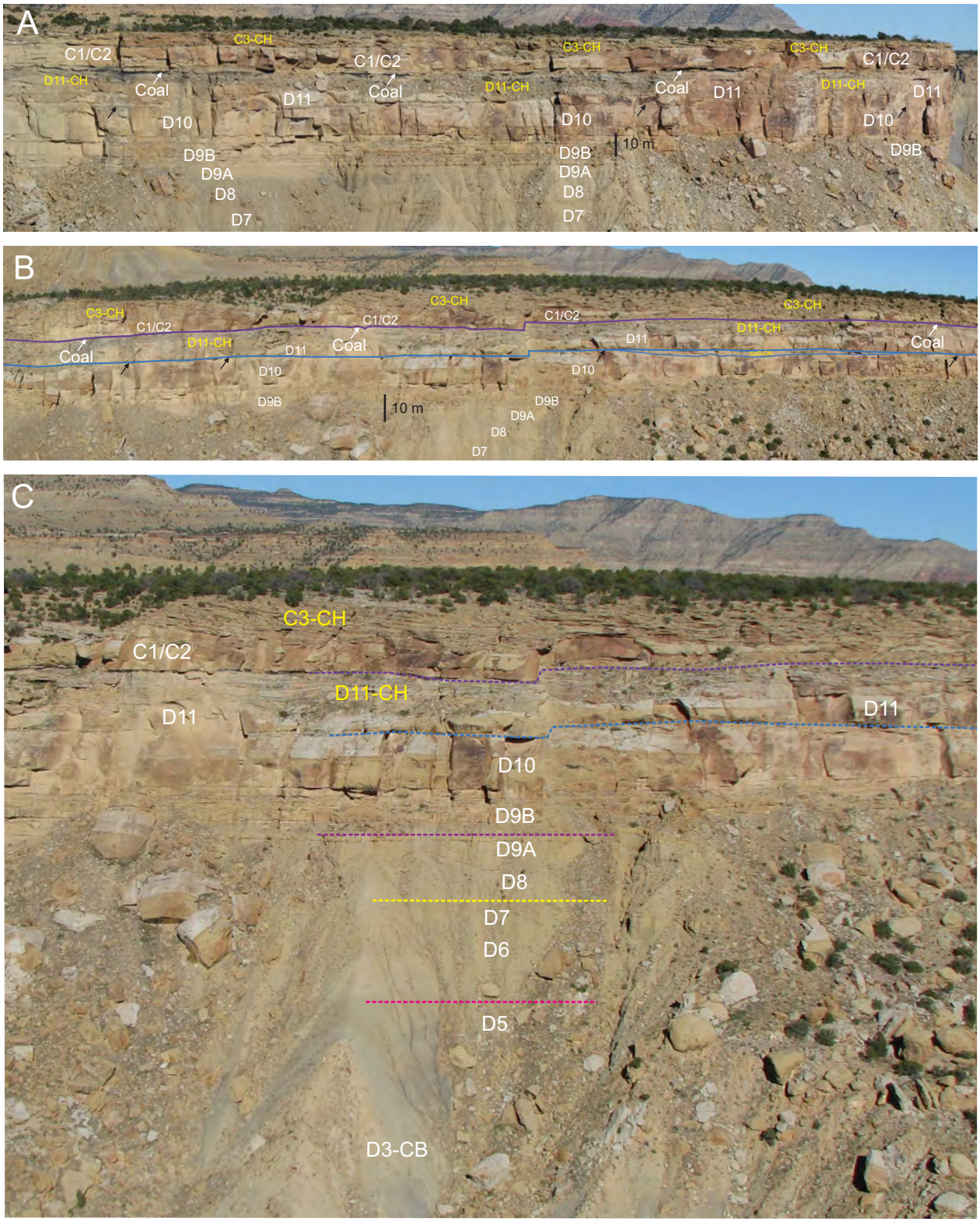

Figure 13-2. (A) West-West of Blaze Canyon, East Wall. Desert Member parasequences D7 to D11, and overlying Lower Castlegate Sandstone parasequences C1 and C2 are correlated. Two prominent shoreface-incised channels cut the shallow marine sandstones: D11-CH and C3-CH. The top of D10 (black arrows) is time equivalent to the lower coal zone at Horse Heaven, while the top of D11 is coincident with the upper coal zone (white arrows). The D11 shoreface-incised channel (i.e. D11-CH) has well-defined, large-scale lateral accretion surfaces that are mostly heterolithic-rich. (B) West of Blaze Canyon, East Wall. Similar rock packages as Part A. Note that the top D10 horizon (black arrows) has thin shoreface-incised channel-fill successions (i.e. D10-CH), and that the C3-CH entirely cuts out the C1 and C2 shoreface sandstones in places. Well defined heterolithic channel-fill deposits (i.e. D11-CH) incise into the upper part of D11. (C) Close-up view of the D3 to D11 parasequences, C1 and C2 parasequences, D11-CH, and C3-CH. East Wall, West of Blaze Canyon. Colour Band (CB).

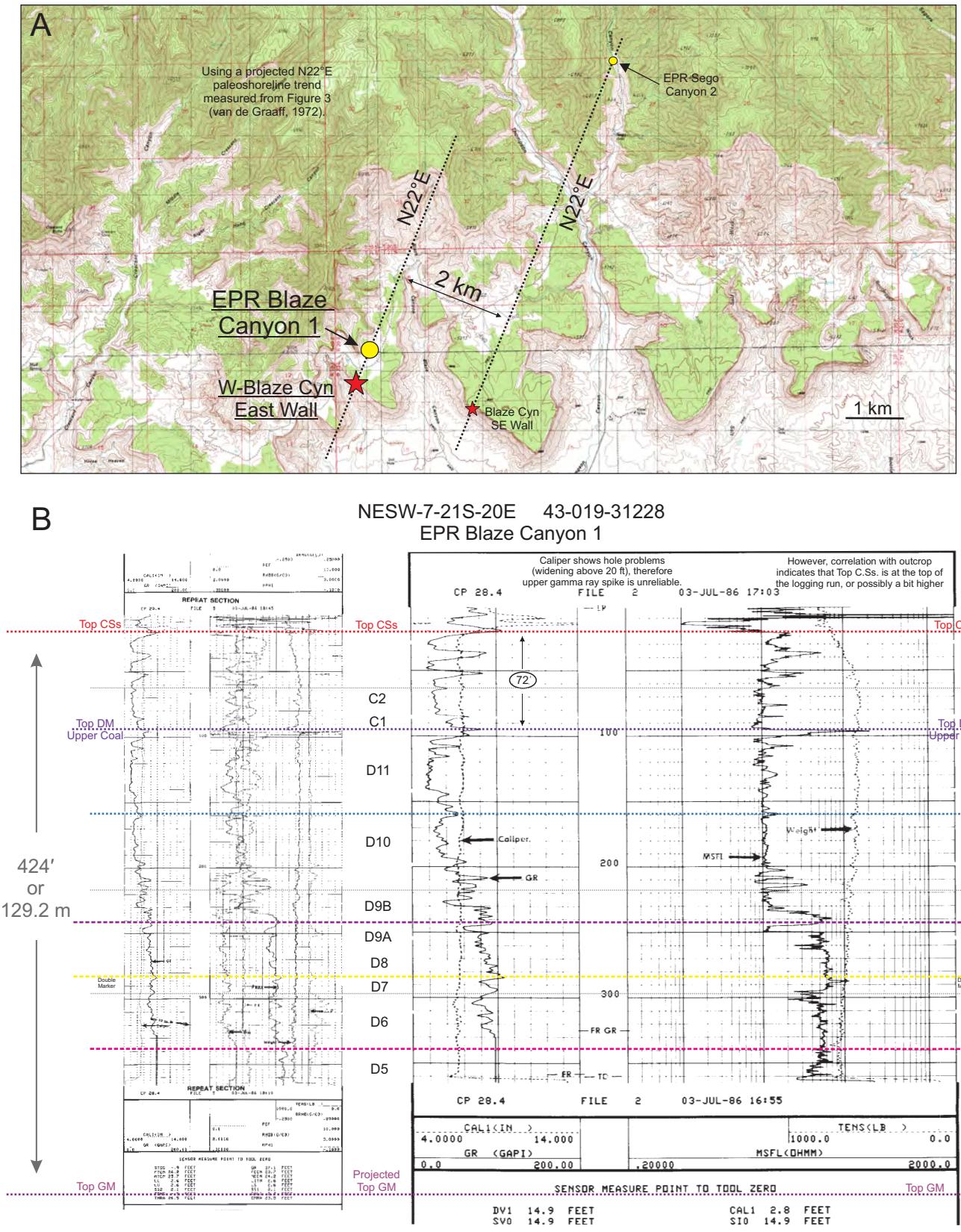

Figure 13-3. (A) Topographic map showing the location of the two Exxon Production Research Company wells in the southern Book Cliffs: EPR Blaze Canyon 1 and EPR Sego Canyon 2. These wells are 6.6 km apart, which is approximately 2 km along depositional dip. The latter is calculated by projecting van de Graaff's (1972) N22°E paleoshoreline trend for the Castlegate Sandstone. Corresponding outcrop photograph locations are shown along depositional dip at West of Blaze Canyon (East Wall) and Blaze Canyon (SE Wall). (B) EPR Blaze Canyon 1 well log suite. Stratigraphic tops of the Grassy Member (GM), Desert Member (DM) and Castlegate Sandstone (CSs) are highlighted by coloured lines, as are parasequences D5-D11, and C1-C2. The thickness of the entire DM-CSs interval is 424 feet or 129.2 m, while the thickness of the Castlegate Sandstone is 72 feet or 21.9 m.

STOP 14: HIGH RESOLUTION SEQUENCE STRATIGRAPHY, DESERT MEMBER AND CASTLEGATE SANDSTONE, BLAZE CANYON

Blaze Canyon is located 25 km down-depositional-dip (east) from Tusher Canyon, and is approximately 1.4 km east of our previous stop (Figs. 0-1 and 0-2). Our purpose here is to examine the high resolution sequence stratigraphy of the Desert Member to Castlegate Sandstone stratigraphic interval, and to compare and contrast with our observations from West-West of Blaze Canyon and West of Blaze Canyon (Figs. 14-1 to 14-5). A similar suite of facies, sequence stratigraphic rock packages and surfaces are observed at Blaze Canyon. The "big-picture" stratigraphy is delineated by a stack of two shallow marine-to-channel-fill vertical facies successions, one each for the Desert and Castlegate. In the Desert Member, parasequences D4 to D11 stack to form a progradational parasequence set which is capped by the Upper Coal zone (Figs. 14-1 and 14-2). Compared to previous stops, the shallow marine deposits in parasequences D7 to D10 are noticeably muddier and slightly thinner, with a greater portion of heterolithic facies between the sandstone beds. The topmost Desert Member parasequence D11 is cut by a thick, heterolithic-rich, channel-fill complex. The Upper Coal zone drapes both the top of the D11 parasequence and the top of the shoreface-incised channel-fill, D11-CH. A prominent white cap marks the top of D11. Van Wagoner (1995) interpreted the D11-CH complex as an incised valley-fill (IVF) that rests on top of a third-order sequence boundary, the Desert-SB. The contact between the Desert Member and overlying Lower Castlegate Sandstone is marked by the thick Upper Coal zone. Parasequences C1 and C2 overlie the Upper Coal and these are cut by the multistoryC3-CH shoreface-incised channel-fill complex (Fig. 14-2).

Similar rock packages and facies stacking patterns are observed in the near subsurface. The EPR Sego Canyon 2 well was drilled to a total depth of 2,236 feet in September 1986. This well penetrated the top of the Lower Castlegate Sandstone at 597 feet and the top of the Grassy Member at 1,113 feet drillers depth (Fig. 14-3). A high quality density, neutron, gamma ray and resistivity well log suite is available to be used as comparison to the nearby outcrop (Fig. 14-3).

At least eleven shelf to shoreface parasequences are identified in the Desert Member-to-Lower Castlegate Sandstone stratigraphic interval in the Crescent Canyon to Blaze Canyon area: D3 to D11, and C1 to C2. Additional parasequences have been identified and correlated to the east (i.e. C3 to C6) and west (i.e. D1 to D2). Collectively, these parasequences stack to form two progradational parasequence sets (Pattison 1994a,b, 2010, 2018, 2019a, 2019b, 2019c, *in review-a*,*-b*; Pattison et al. 2007b). The top of parasequence D11, which is capped by the Upper Coal zone, defines the contact between the two progradational parasequence sets, and also defines the contact between the Desert Member and Lower Castlegate Sandstone.

Modeling Scenario 1: Conventional

Van Wagoner (1991, 1995) studied the Desert Member to Castlegate Sandstone across a wide swath of eastern Utah and used a comprehensive descriptive foundation, which included 68 measured sections and numerous photo-panels, to build a sequence stratigraphic interpretation. Van Wagoner (1995) clustered together all of the channel and coastal plain facies in the Desert-Castlegate interval, and separated them from all of the shallow marine facies through the identification and correlation of two sequence boundaries (i.e. *Desert SB* and *Castlegate SB*). Van Wagoner (1991, 1995) also identified a number of "high frequency" sequence boundaries at the tops of some parasequences, such as those at the top of parasequence D10 in the Horse Heaven to Blaze Canyon region. Van Wagoner (1995) used the *Desert SB* and *Castlegate SB* to subdivide the Desert-Castlegate strata into two broad rock packages: channel-coastal plain facies

and shallow marine facies (Figs. 14-4 and 14-5). By grouping all non-to-marginal-marine facies together, Van Wagoner's (1995) interpretation of the non-to-marginal-marine facies belts more closely resembles a lithostratigraphic (i.e. similar lithologies lumped together) rather than a chronostratigraphic correlation (Fig. 14-4). According to Van Wagoner's (1995) interpretation, high energy braided river systems in the Desert-Castlegate interval did not deliver sediments to a coastline, but instead "petered-out" into a low energy coastal plain/lacustrine setting, prior to reaching the coastline (Fig. 14-5).

This model begs at least two questions: (i) How can a high-energy fluvial system (i.e. braided) be totally disconnected from a nearby shallow marine system?, and (ii) Where are the time-equivalent non-marine deposits for the Desert-Castlegate shallow marine bodies? Van Wagoner's (1995) interpretation shows absolutely no temporal or spatial relationship between the non-marine and shallow marine rock types in the Desert-Castlegate interval (Figs. 14-4 and 14-5), which is inconsistent with the field observations presented in this guidebook.

Modeling Scenario 2: Alternative

A critical re-examination of the Campanian Desert Member-to-Lower Castlegate Sandstone interval has shed new light on the relationship between laterally adjoining nearshore terrestrial and shallow marine environments (Pattison 2018, 2019a,b,c*, in review-a,-b*). The temporal and spatial linkage is contrary to the conventional sequence stratigraphic model. The alternative sequence stratigraphic framework of the Desert-Castlegate interval is a markedly different scheme compared to the conventional model (Van Wagoner, 1995). Each model carries a significantly different prediction regarding the three-dimensional distribution and architecture of reservoir and non-reservoir bodies in a fluvio-deltaic system. This has considerable implications for modelling in similar clastic settings worldwide. Key differences include:

1. High resolution shoreface-incised channels occur in most parasequences. Their envelope of incision is generally restricted to the shoreface deposits in which they are "housed", occasionally cutting into underlying parasequences. These higher frequency erosional surfaces do not coalesce into a third-order sequence boundary. Some are HFSBs. A similar pattern of shoreface-incised tidal-estuarine channel-fills exists in all other members of the Blackhawk Formation.
2. All shoreface sandstones "evolve" out of fine-grained coastal plain deposits. Evolution points have been studied and mapped. Progradational distances are modestly long, while flooding surface distances are shorter.
3. All facies belts are temporally-, spatially- and genetically-linked: (i) amalgamated fluvial sandstones, (ii) fine-grained, coal bearing coastal plain deposits, and (iii) shoreface sandstones with incised tidal-estuarine channels. Lateral facies transitions, from west-to-east, are (i) → (ii) → (iii). Vertical transitions, from base to top, are the reverse order: (iii) → (ii) → (i). Conformable facies contacts are the norm. Application of Walther's Law implies time equivalency of neighboring facies belts.
4. No gigantic incised valleys exist within the Desert-Castlegate interval.
5. Prominent coal beds correlate to marine flooding surfaces, thus linking facies zones (ii) and (iii) in both time and space.
6. Progradational stacking patterns are the norm for both the nearshore terrestrial and shallow marine facies belts.
7. Incised channels thin and narrow basinwards to a feathered edge, transitioning into shoreface sandstones. There is no evidence for sediment bypass in the shoreface-to-shelf environment, and hence no reason to prospect down-dip for detached sand bodies.

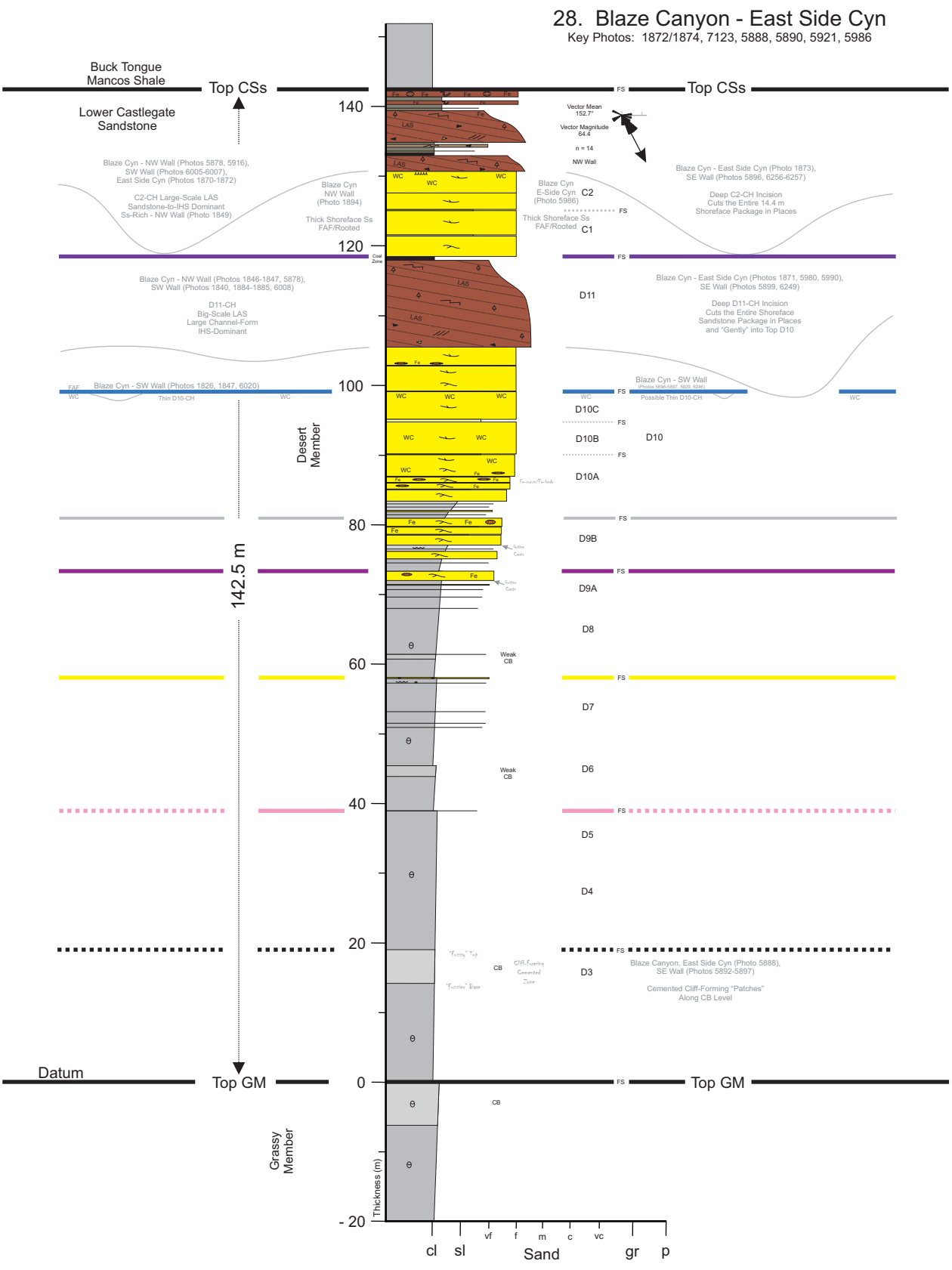

Figure 14-1. Measured outcrop section #28, Blaze Canyon, East Side Cyn. Legend nested in Figure 10-2.

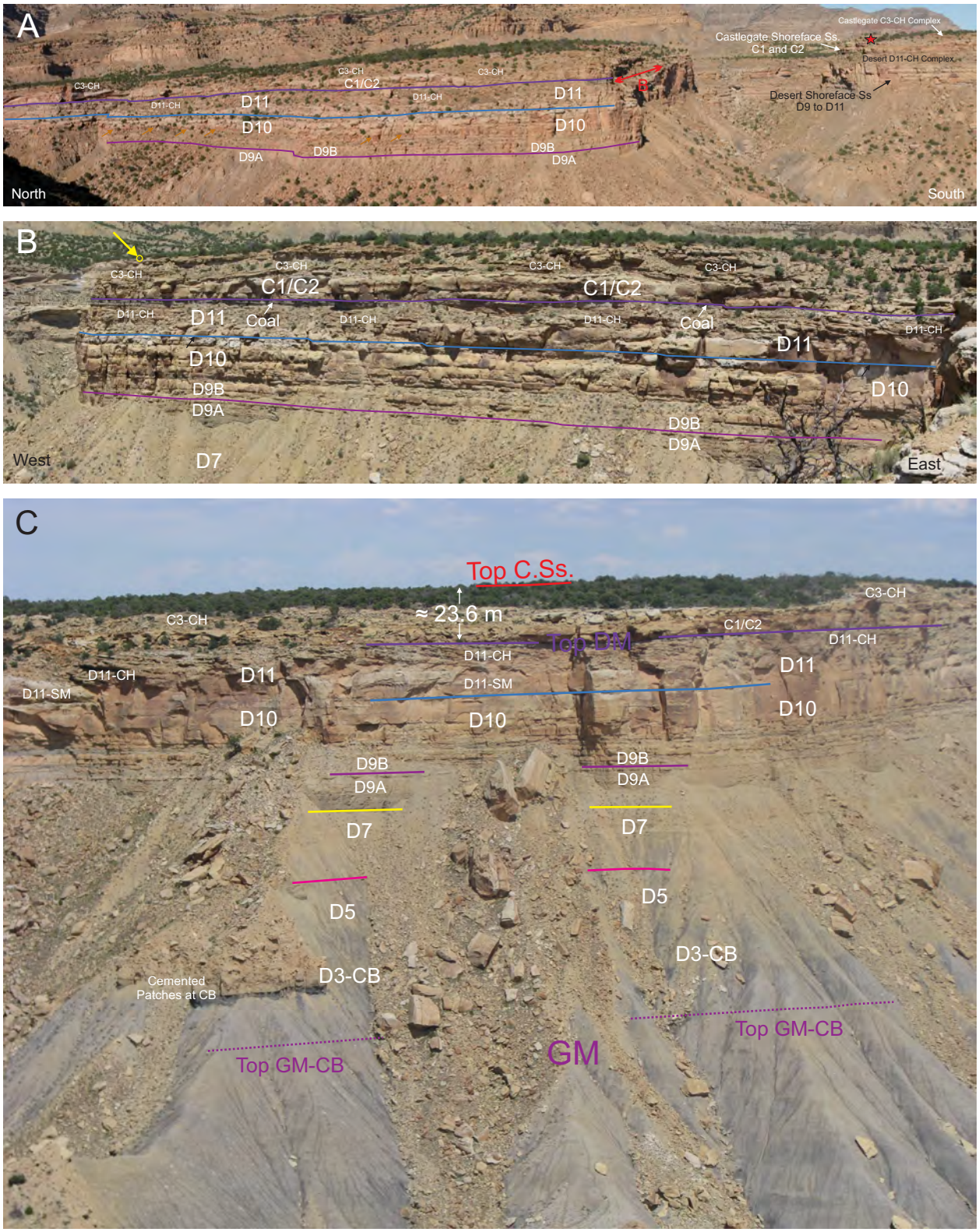

Figure 14-2. Blaze Canyon. (A) Photo-panorama along the northeast-wall and east-side-canyon of Blaze Canyon. Desert Member parasequences D7 to D11 are highlighted. The upper coal zone is prominently exposed, representing the top of the Desert Member (i.e. top D11). It is overlain by shallow marine sandstones of parasequences C1 and C2, and the multistory C3-CH. The red double arrow identifies the cliff face shown in Part B which was photographed from the side canyon red star) looking north. Note the Fe-cemented layer in the lower part of D10 (brown arrows). (B) East-Side Canyon of Blaze Canyon. Similar stratigraphy to West-West and West of Blaze Canyon. Heterolithic-rich shoreface-incised channel (i.e. D11-CH) dominates the uppermost Desert Member. Geologist for scale in upper left (yellow arrow, yellow circle). (C) Desert Member parasequences D3 to D11, SE Wall, Blaze Canyon. CSs (Castlegate Sandstone), DM (Desert Member), GM (Grassy Member), CH (Channel), Shallow Marine (SM), CB (Colour Band). Castlegate Sandstone is 23.6 m thick (77.4 feet) along the SE Wall of Blaze Canyon.

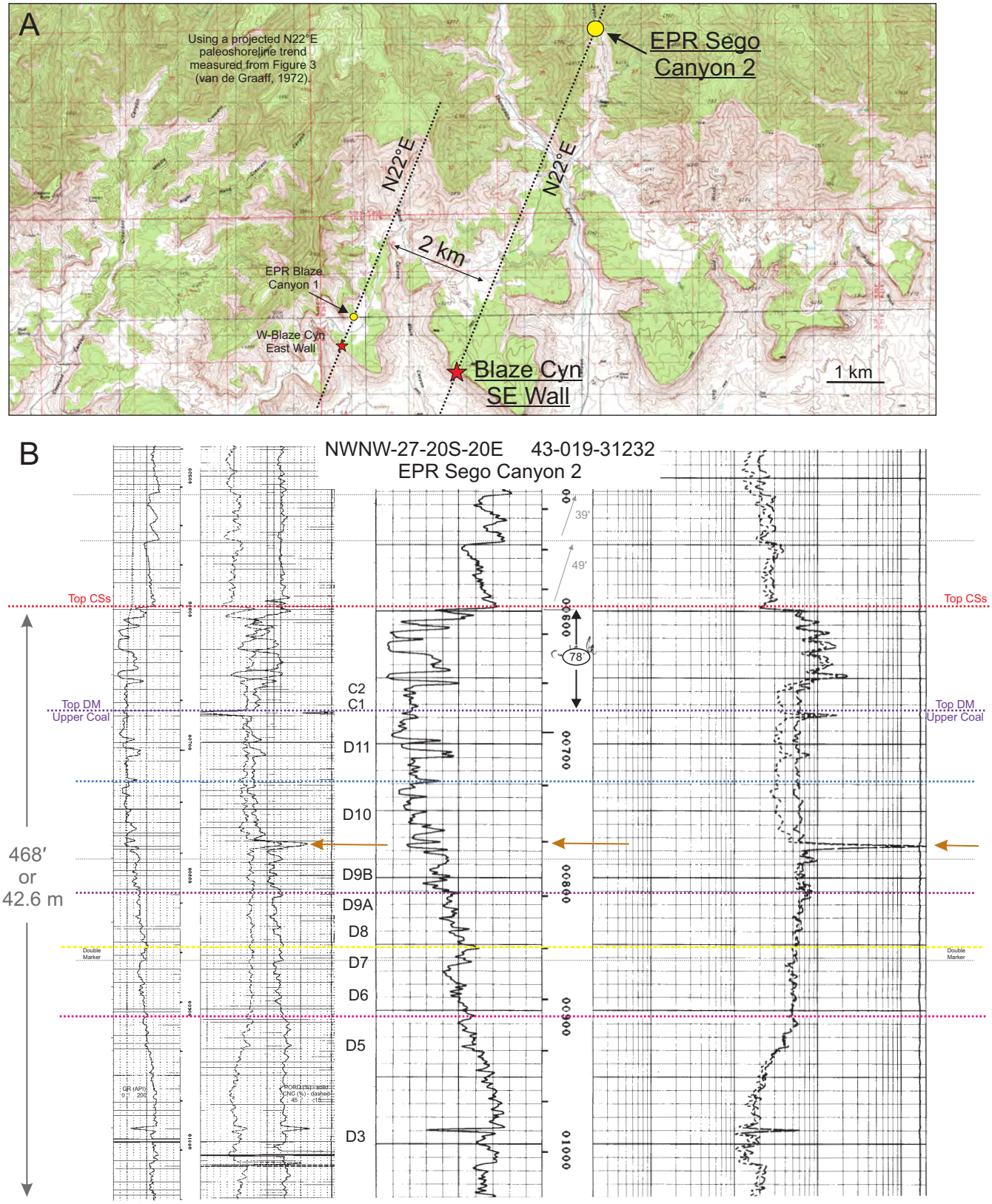

Figure 14-3. (A) Topographic map showing the location of the two Exxon Production Research Company wells in the southern Book Cliffs: EPR Blaze Canyon 1 and EPR Sego Canyon 2. These wells are 6.6 km apart, which is approximately 2 km along depositional dip. The latter is calculated by projecting van de Graaff's (1972) N22°E paleoshoreline trend for the Castlegate Sandstone. Corresponding outcrop photograph locations are shown along depositional dip at West of Blaze Canyon (East Wall) and Blaze Canyon (SE Wall). (B) EPR Sego Canyon 2 well log suite. Stratigraphic tops of the Desert Member (DM) and Castlegate Sandstone (CSs) are highlighted by coloured lines. Parasequences D3 to D11, and C1 to C2 are marked. The entire DM-CSs interval is 468 feet (142.6 m) thick, while the Castlegate Sandstone is 78 feet (23.8 m) thick. Note the high density, low porosity, and high resistivity well log spike at 777 feet (brown arrows). This well log kick corresponds to the Fe-cemented layer (siderite) that occurs in the basal part of parasequence D10, which is visible in outcrop.

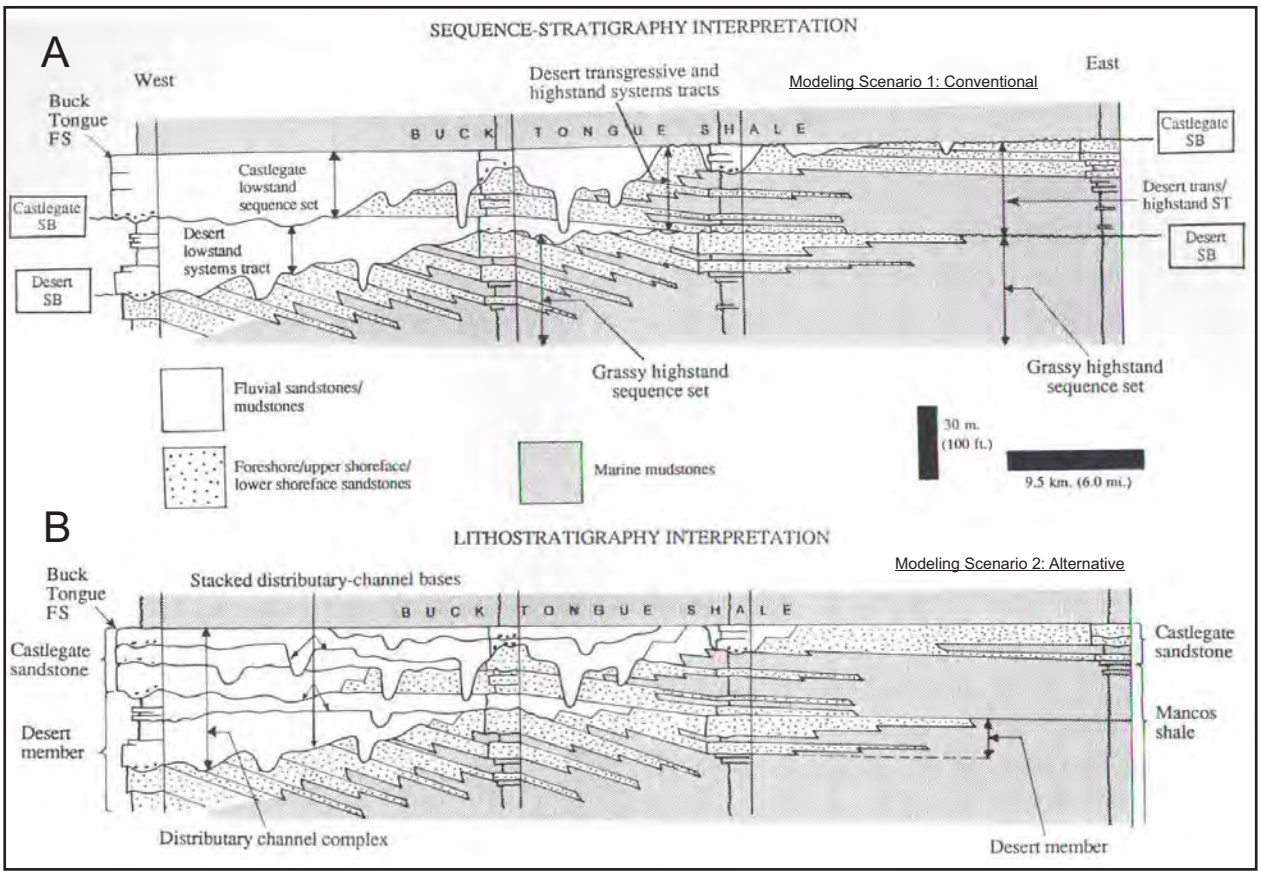

Figure 14-4. A comparison of two possible correlation styles for the Desert-Castlegate interval: *"Sequence Stratigraphy Interpretation"* and *"Lithostratigraphy Interpretation"* (Van Wagoner 1995). (A) Van Wagoner's (1995) *"Sequence Stratigraphy Interpretation"* clusters all channel and coastal plain facies together, separating them both temporally and spatially from all laterally adjoining shallow marine facies, thus resembling a lithostratigraphic (i.e. similar lithologies lumped together) rather than a chronostratigraphic correlation style. This is modeling scenario 1: conventional, classic, third-order SB, IVF, non-linked nearshore terrestrial and shallow marine facies belts, detached sand bodies are likely down-dip. (B) In contrast, Van Wagoner's (1995) *"Lithostratigraphy Interpretation"* actually shows a chronostratigraphic correlation between the non-marine (i.e. coal beds, multistory channel complexes) and shallow marine (i.e. flooding surfaces, progradational parasequence set) facies belts, which is somewhat similar to the field observations presented herein. This is similar to modeling scenario 2: alternative, no SB, no IVF, suite of discrete parasequence-scale shoreface-incised channels, temporally and spatially linked nearshore terrestrial and shallow marine facies belts, no detached sand bodies down-dip, attached only.

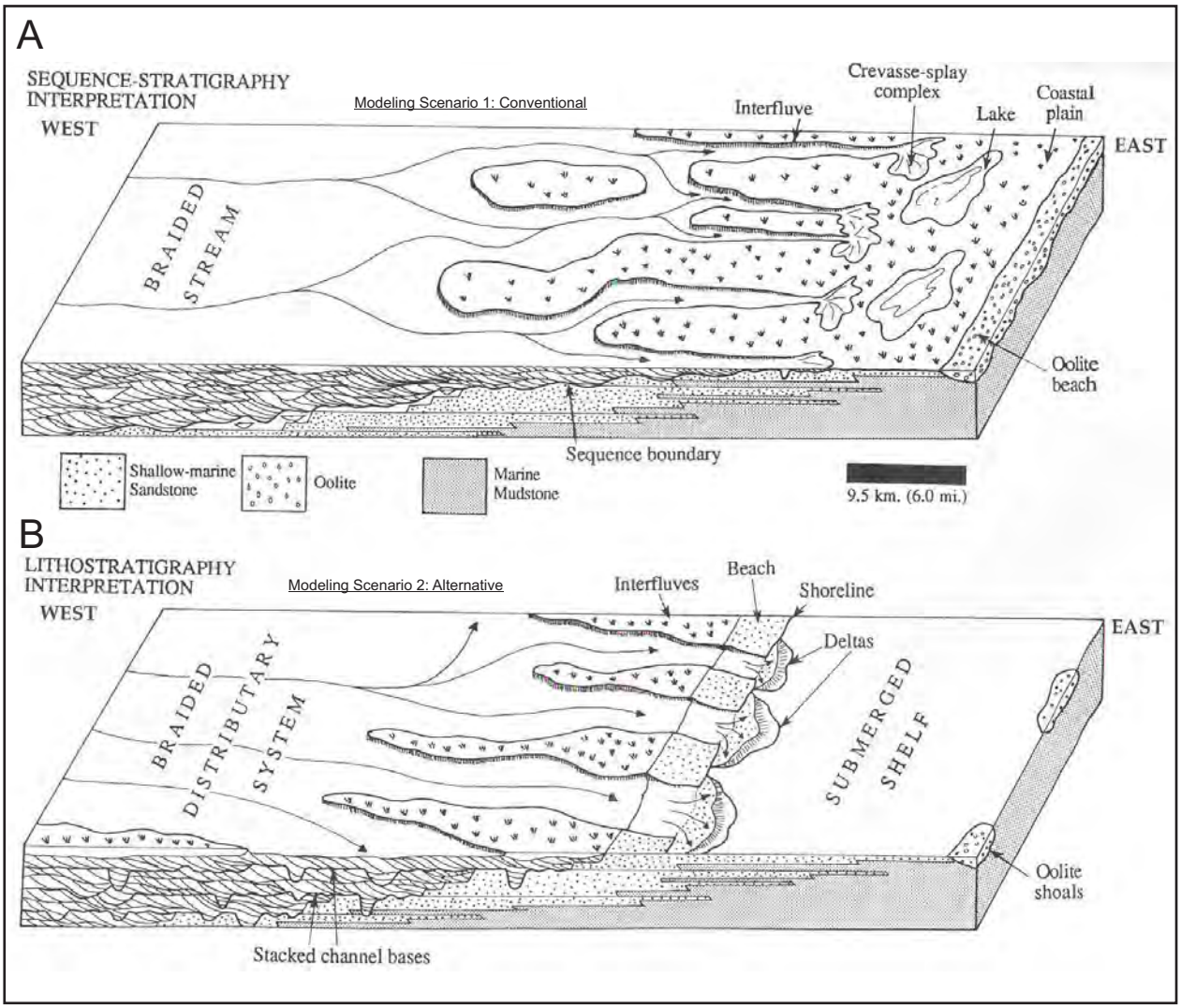

Figure 14-5. Two contrasting depositional environment and paleogeographic interpretations of the Desert Member to Lower Castlegate Sandstone stratigraphic interval: *"Sequence Stratigraphy Interpretation"* and *"Lithostratigraphy Interpretation"* (Van Wagoner 1995). (A) The *"Sequence Stratigraphy Interpretation"* shows no temporal or spatial relationship between the laterally adjoining nearshore terrestrial and shallow marine facies belts. This is modeling scenario 1: conventional, classic, third-order SB, IVF, non-linked nearshore terrestrial and shallow marine facies belts, detached sand bodies are likely down-dip. (B) In contrast, the *"Lithostratigraphy Interpretation"* shows linkage of the laterally adjoining non-marine-to-shallow marine facies in both time (i.e. chronostratigraphy) and space, through correlation of key marker beds (i.e. coals-to- marine flooding surfaces), and is a better fit with field observations presented herein. This best fits modeling scenario 2: alternative, no SB, no IVF, suite of discrete parasequence-scale shoreface-incised channels, temporally and spatially linked nearshore terrestrial and shallow marine facies belts, no detached sand bodies down-dip, attached only.

FIELD DAY 5

TERRESTRIAL TO MARINE FACIES BELTS: RESERVOIR-TO-EXPLORATION SCALE

Stop 15: Reservoir-Scale Architecture Channel-Shoreface Reservoir Units, Desert Member and Castlegate Sandstone, Thompson Canyon

Stop 16: Near-Field Exploration-Scale Terrestrial-Shoreface-Shelf Transition, Sagers Canyon

STOP 15: RESERVOIR-SCALE ARCHITECTURE CHANNEL-SHOREFACE RESERVOIR UNITS, DESERT MEMBER AND CASTLEGATE SANDSTONE, THOMPSON CANYON

Thompson Canyon is located approximately 34 km down-depositional-dip from the head of Tusher Canyon and 3 km east of Blaze Canyon (Figs. 0-1, 0-2, and 15-1 to 15-10). The Desert-Castlegate stratigraphic interval is best viewed from the pictograph and petroglyph picnic site (Fig. 15-3). Beautiful exposures of sandstone-rich shallow marine and channel-fill deposits, as well as some world-class outcrops of heterolithic-rich IVF deposits and carbonaceous-rich shales and coals occur at this stop. All of the key sequence stratigraphic rock packages and surfaces examined from Crescent Canyon to Blaze Canyon are visible at this stop (Fig. 15-8). From bottom to top, this section consists of lower shoreface heterolithics (parasequence D9); thickly bedded upper shoreface sandstones (parasequences D10 and D11); a sandstone- to heterolithic-rich shoreface-incised channel-fill complex (D11-CH); interbedded carbonaceous-rich shales and coals (Upper Coal zone); thickly-bedded upper shoreface sandstones (parasequences C1 and C2); a multistory, sandstone- to heterolithic-rich shoreface-incised channel-fill complex (C3-CH); a 6-10 m thick package of coal-bearing coastal plain mudstones with single-story channel sandstones capping the uppermost part of the Lower Castlegate Sandstone (Figs. 15-1, 15-2, 15-4, 15-5). The Upper Coal zone marks the contact between the Desert Member and the overlying Lower Castlegate Sandstone, which is coincident with the contact between the two progradational parasequence sets. Shell Core Hole #2 is located 1.6 km north of the field stop (Fig. 15-3) and provides an excellent opportunity to examine the core-scale sedimentology and stratigraphy of the Desert-Castlegate interval. The simplified core description and low resolution logs for Shell Core Hole #2 (Fig. 15-6) can be compared to the higher quality EPR Sego Cyn 2 well log suite that were collected 1.3 km north (Fig. 14-3B).

Van Wagoner (1991, 1995) argued that the channel/coastal plain deposits in the Desert Member to Lower Castlegate Sandstone stratigraphic interval are collectively younger than the laterally adjacent shallow marine (shoreface/deltaic) deposits, with low frequency sequence boundaries separating the shoreface/deltaic facies from the laterally adjacent channel and coastal plain facies (i.e. *Desert SB* and *Castlegate SB*; Figs. 15-7A, 15-9A). Van Wagoner's (1991, 1995) conventional sequence stratigraphic model shows no genetic nor temporal link between non-marine and shallow marine facies belts within the Desert-Castlegate stratigraphic interval.

In contrast, an alternative sequence stratigraphic model shows that the laterally adjoining channel-coastal plain and shallow marine facies belts are genetically-, temporally- and spatially-related (Figs. 15-7B, 15-8, 15-9B, 15-10). Evidence includes, but is not limited to, the (i) gradational and conformable transitions between adjoining facies belts, accentuated by the ubiquity of flat-topped, rooted foreshore sandstones passing upwards into carbonaceous-rich-mudstone-dominated coastal plain, (ii) parasequence-scale interfingering of coastal plain-channel and foreshore-shoreface deposits with channels, white caps and coals embedded within stacked shoreface parasequences, and (iii) regional correlation of coals and flooding surfaces. Terminal channels incise into proximal foreshore-shoreface sandstones in all parasequences. Incisions are confined to the parasequence in which the channels are nested, rarely cutting deeper. These shoreface-incised channels are cut and filled at a parasequence-scale, and are bounded above by the same flooding surface that caps each foreshore-shoreface package. The ubiquity of ascending regressive shoreface trajectories and near absence of descending regressive trajectories that intersect depositional slope argues against any significant relative sea level fall. Therefore the alternative model is the best fit with the field observations (Figs. 15-7B, 15-8, 15-9B, 15-10).

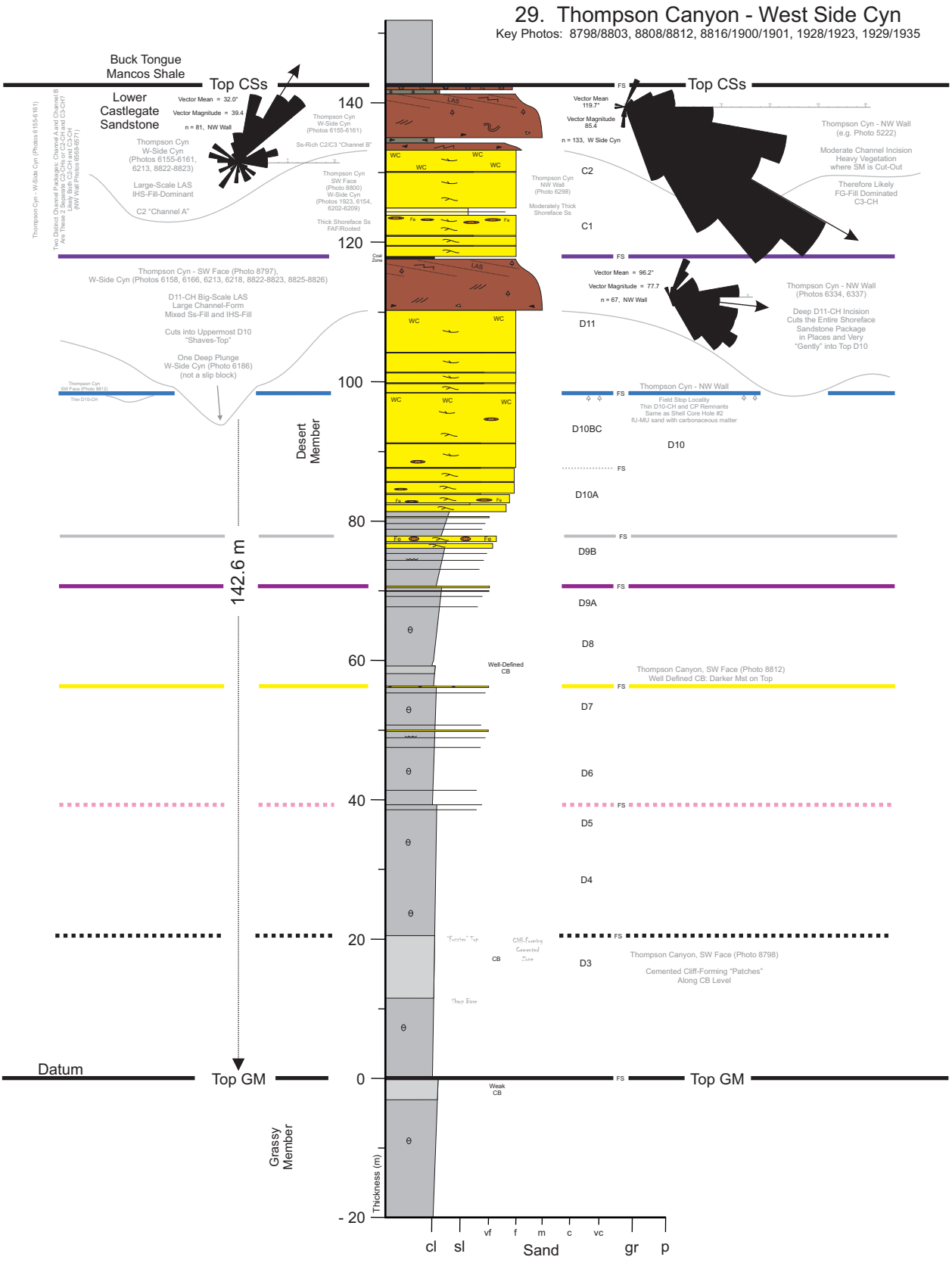

Figure 15-1. Measured outcrop section #29, Thompson Canyon, West Side Cyn. Legend nested in Figure 10-2. Location shown on Figure 15-3.

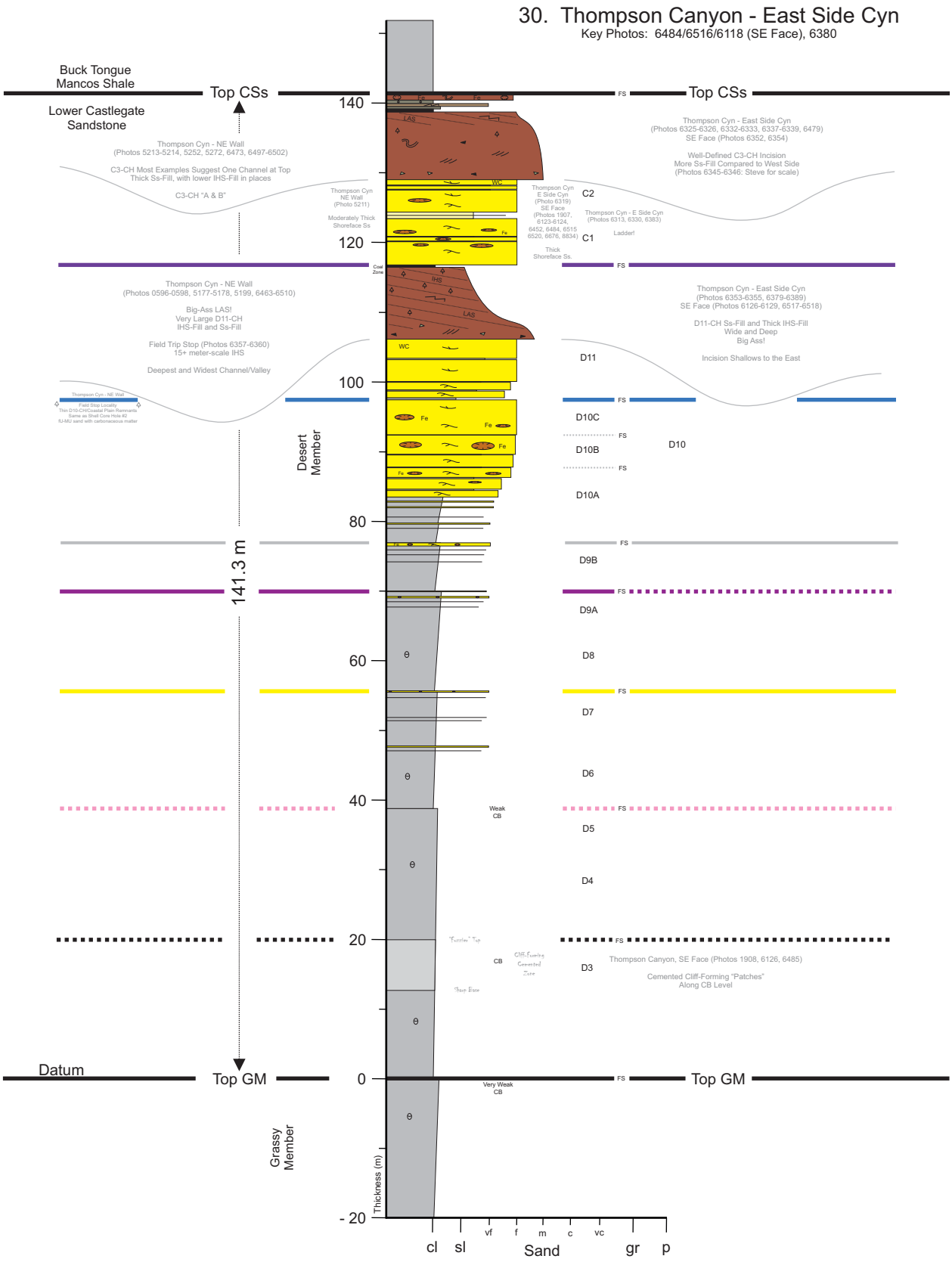

Figure 15-2. Measured outcrop section #30, Thompson Canyon, West Side Cyn. Legend nested in Figure 10-2. Location shown on Figure 15-3.

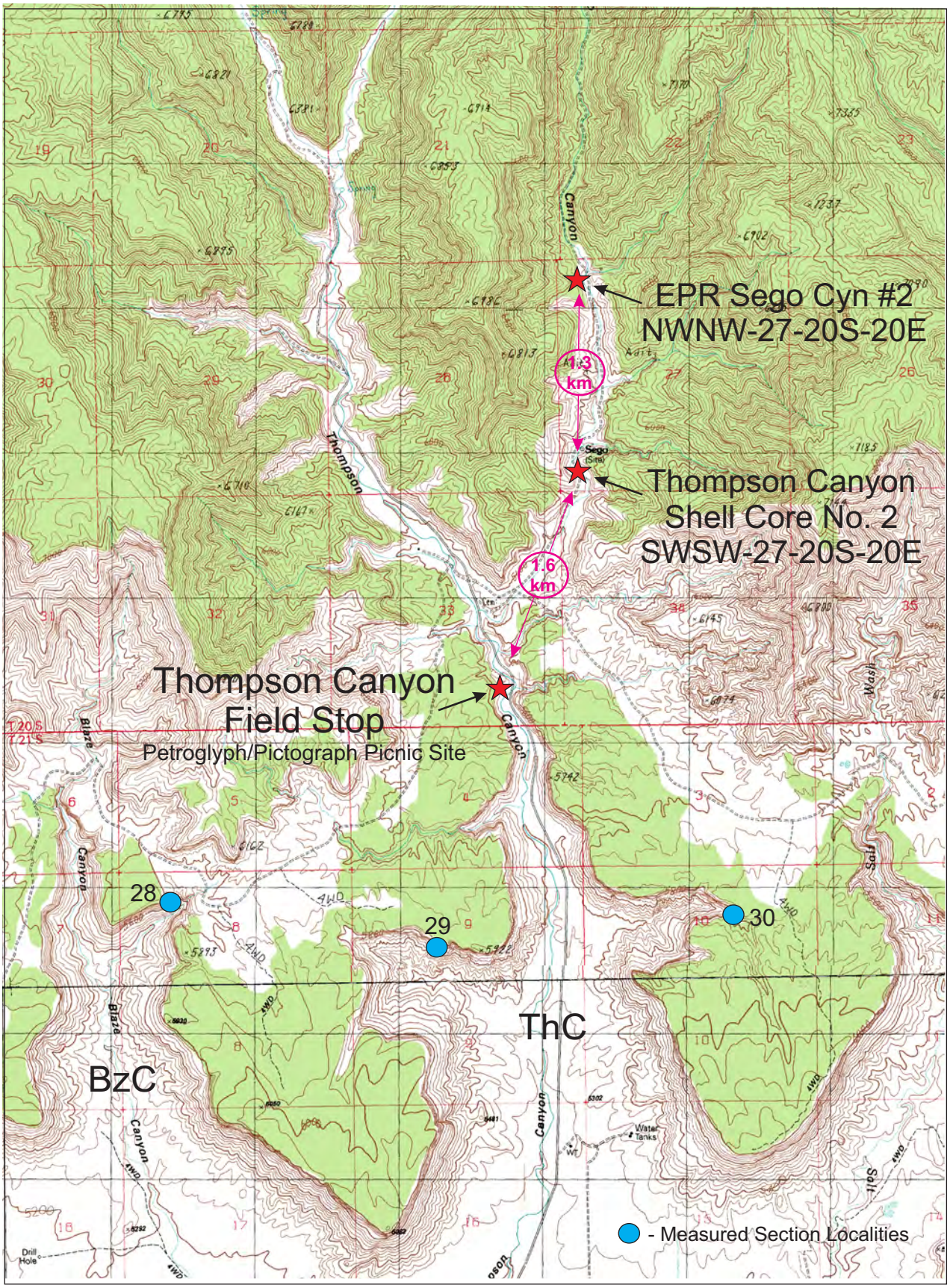

Figure 15-3. Topographic map of the Thompson Canyon (ThC) region. The field stop is located at the petroglyph and pictograph site. Shell Core Hole #2 (SWSW-27-20S-20E) is located 1.6 km north of the field stop, while the EPR Sego Canyon #2 (NWNW-27-20S-20E) well is located a further 1.3 km up-canyon. BzC (Blaze Canyon). Measured section localities #28 (Blaze Cyn), #29 (Thompson-West), and #30 (Thompson-East) are shown.

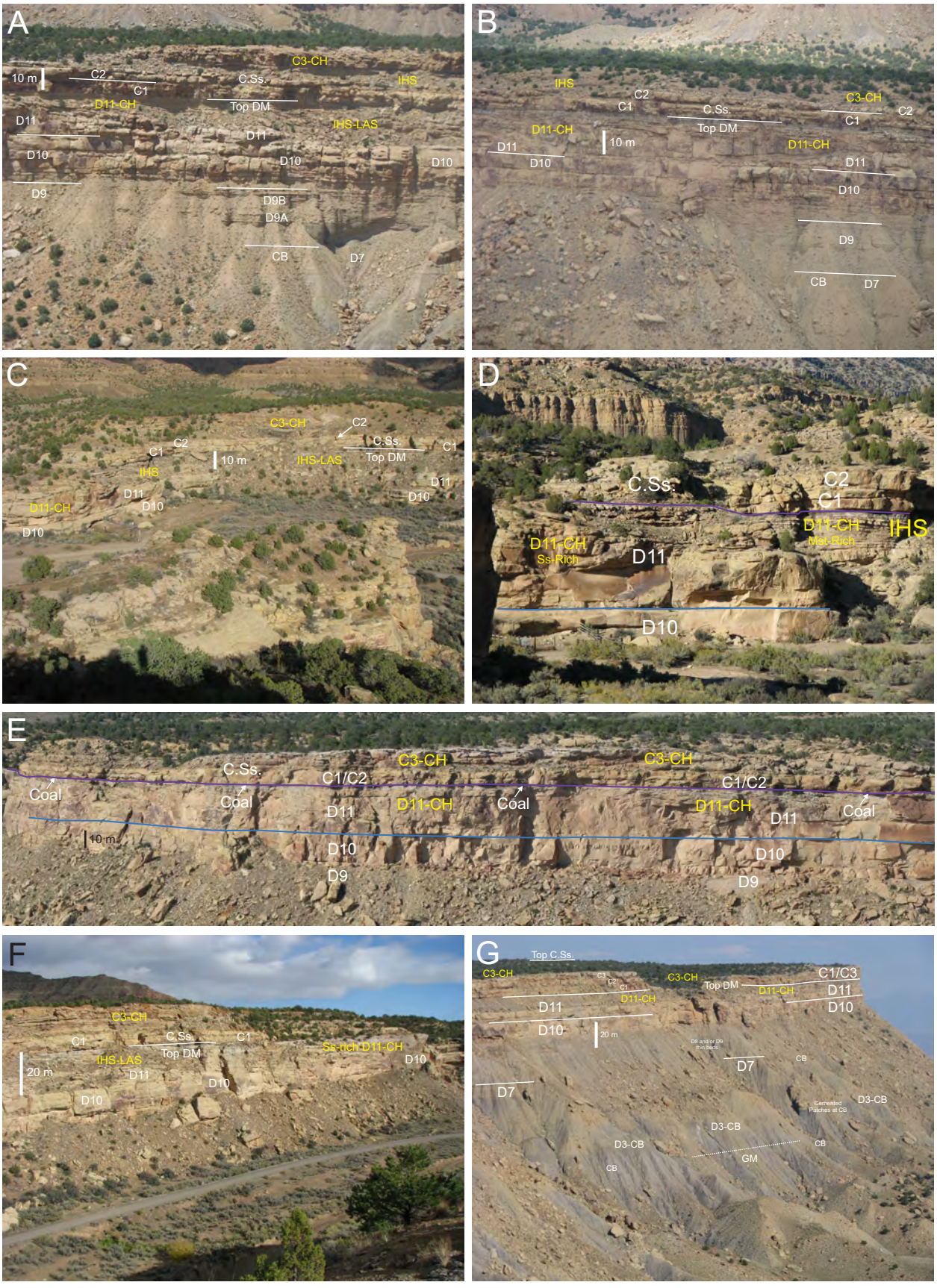

Figure 15-4. Desert Member (DM)-to-Lower Castlegate Sandstone (C.Ss.) stratal architectures, Thompson Canyon. (A) Uppermost DM shallow marine (SM) sandstones of parasequence D11 are completely cut-out in places by a deep shoreface-incised channel (D11-CH), Thompson Canyon, West Side Cyn. The D11-CH is characterized by large-scale inclined heterolithic strata (IHS) and lateral accretion surfaces (LAS). It is overlain by parasequences C1 and C2 of the Lower Castlegate Sandstone, which in turn are cut by the C3-CH, thus defining an overall SM-CH-SM-CH stacking pattern. CB (Colour Band). This outcrop locality is approximately 3 km south-southwest of Shell Core Hole #2. (B) Similar stratigraphy as shown in Part A, Thompson Canyon, West Side Cyn. This outcrop locality is approximately 3 km south of Shell Core Hole #2. (C) Thick Desert Member shoreface sandstones of parasequences D10 and D11 are well exposed and easily accessible, Thompson Canyon, NE Wall. A large-scale shoreface-incised channel (D11-CH) cuts through parasequence D11 and into the upper part of parasequence D10. A variety of fill types are observed including sandstone-rich (left side of photograph), inclined heterolithic strata (IHS) with well defined lateral accretion surfaces (LAS), and mudstone-rich. The top D11-CH is overlain by Lower Castlegate Sandstone parasequences C1 and C2, which in-turn are cut by the C3-CH complex. This outcrop locality is approximately 1.5 km south-southwest of Shell Core Hole #2, and is directly across the road from the petroglyph/pictograph picnic site. (D) Pictographs are prominently displayed along the cliff-face bordering the corral, NE Wall, Thompson Canyon. Parasequence D11 has upper shoreface sandstones incised by sandstone-rich and inclined heterolithic strata (IHS) of the D11-CH. (E) Cliff section immediately south of the picnic site, NE Wall, Thompson Canyon. The upper coal zone caps the top of parasequence D11. Both heterolithic- and sandstone-rich channel-fill deposits occur in the D11-CH, while the C3-CH is mostly comprised of heterolithic-rich, multi-story, channel-fill deposits. (F) Similar sedimentology and stratigraphy is observed, defining a stacked pair of SM-CH rock packages, one each for the top DM and C.Ss., Thompson Canyon, NE Wall. This locality is approximately 2 km south of Shell Core Hole #2. (G) Cliff section stratigraphy from the Mancos Shale/Grassy Member (GM) equivalent, to the top of the Lower Castlegate Sandstone (C.Ss.), southeast face, Thompson Canyon. The Lower Castlegate Sandstone is 25.6 m (84 feet) thick at this locality. DM (Desert Member), CB (Colour Band).

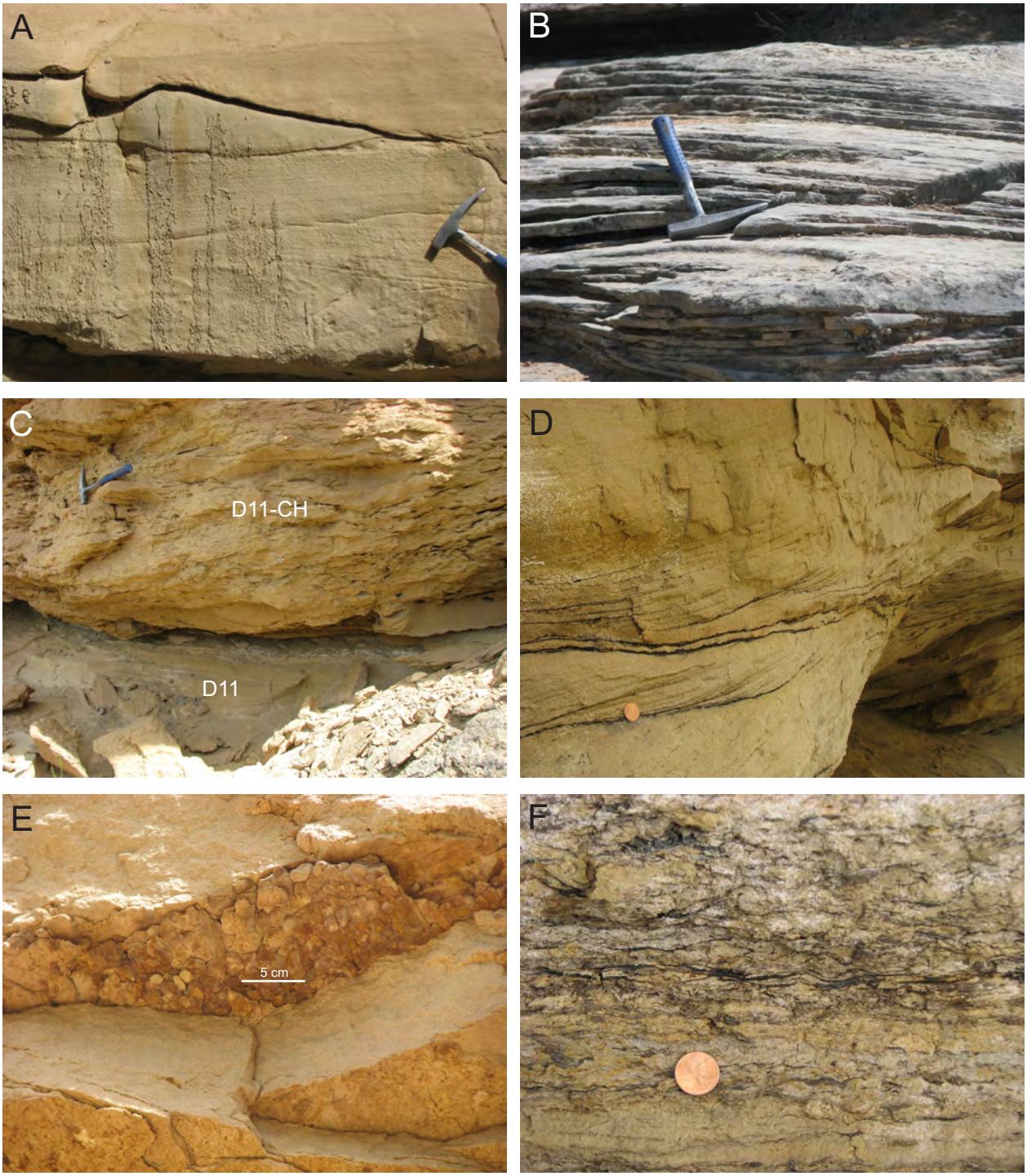

Figure 15-5. Desert Member (DM) facies, Thompson Canyon region. (A) Hummocky cross stratified (HCS) sandstones, D11B parasequence, NW Side Cyn, West Wall, Salt Wash Canyon. Approximately 2.5 km east of the Thompson Canyon petroglyph-pictograph site. (B) HCS sandstones, D11A parasequence, West Side Cyn, Thompson Canyon. (C) Shoreface-incised channel cutting the D11 shallow marine sandstones, NW Side Cyn, West Wall, Salt Wash Canyon. (D) Cross bedded sandstones with organic-rich laminae, shoreface-incised D11-CH, NW Side Cyn, West Wall, Salt Wash Canyon. USA penny coin for scale in lower left (1.905 cm diameter). (E) *Teredolites*-bored wood fragment on a bedding plane within the D11 shoreface-incised channel, NW Side Cyn, West Wall, Salt Wash Canyon. (F) Carbonaceous-rich mudstone laminae and coal clasts, D11-CH, NW Side Cyn, West Wall, Salt Wash Canyon. USA penny coin for scale.

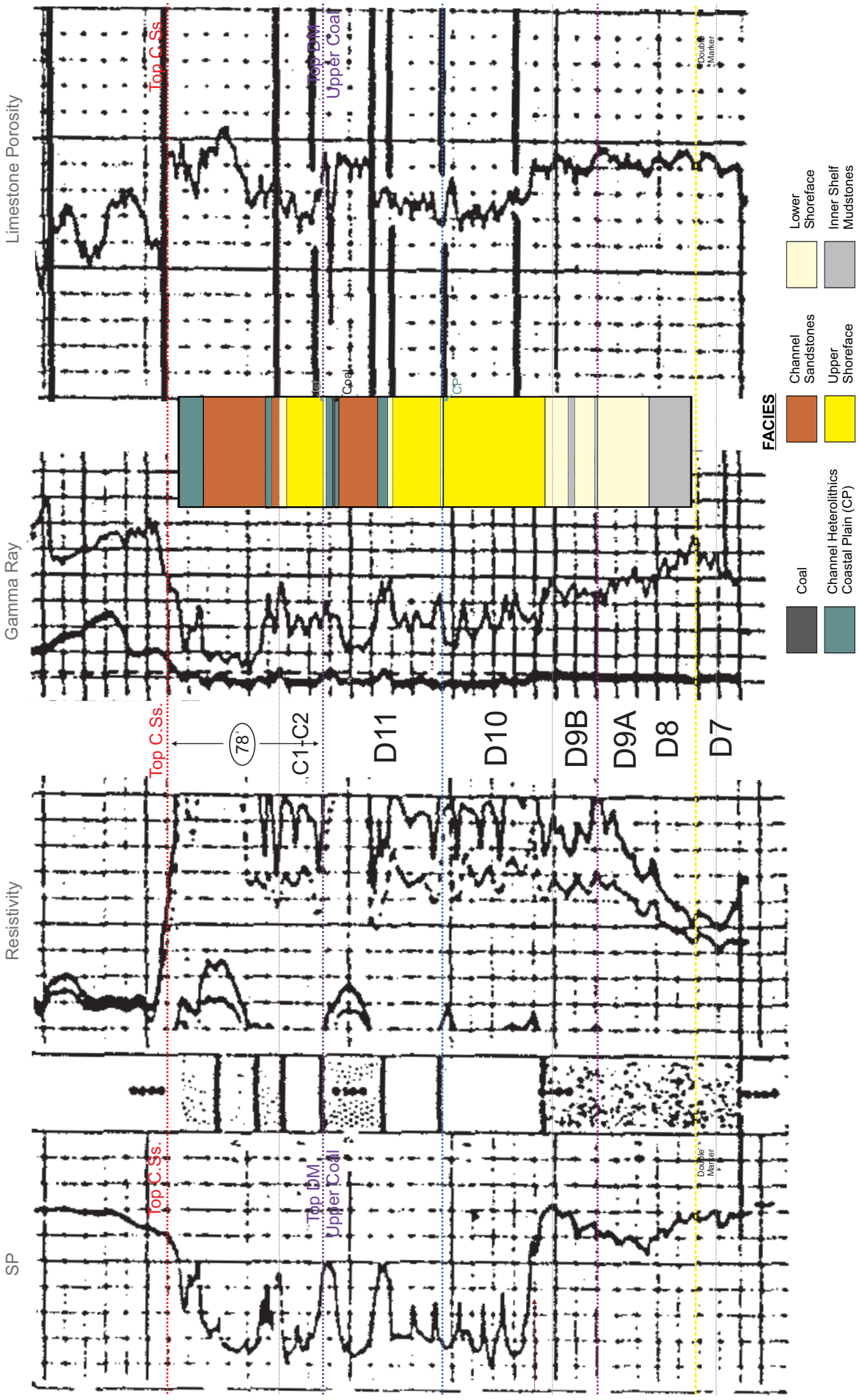

Figure 15-6. Shell Core Hole #2 (SWSW-27-20S-20E). Basic core description with low resolution SP, resistivity, gamma ray and porosity logs. Parasequences D7 to D11 and C1-C2 are identified. The Castlegate Sandstone (C.Ss.) is 23.8 m (78 feet) thick. DM (Desert Member).

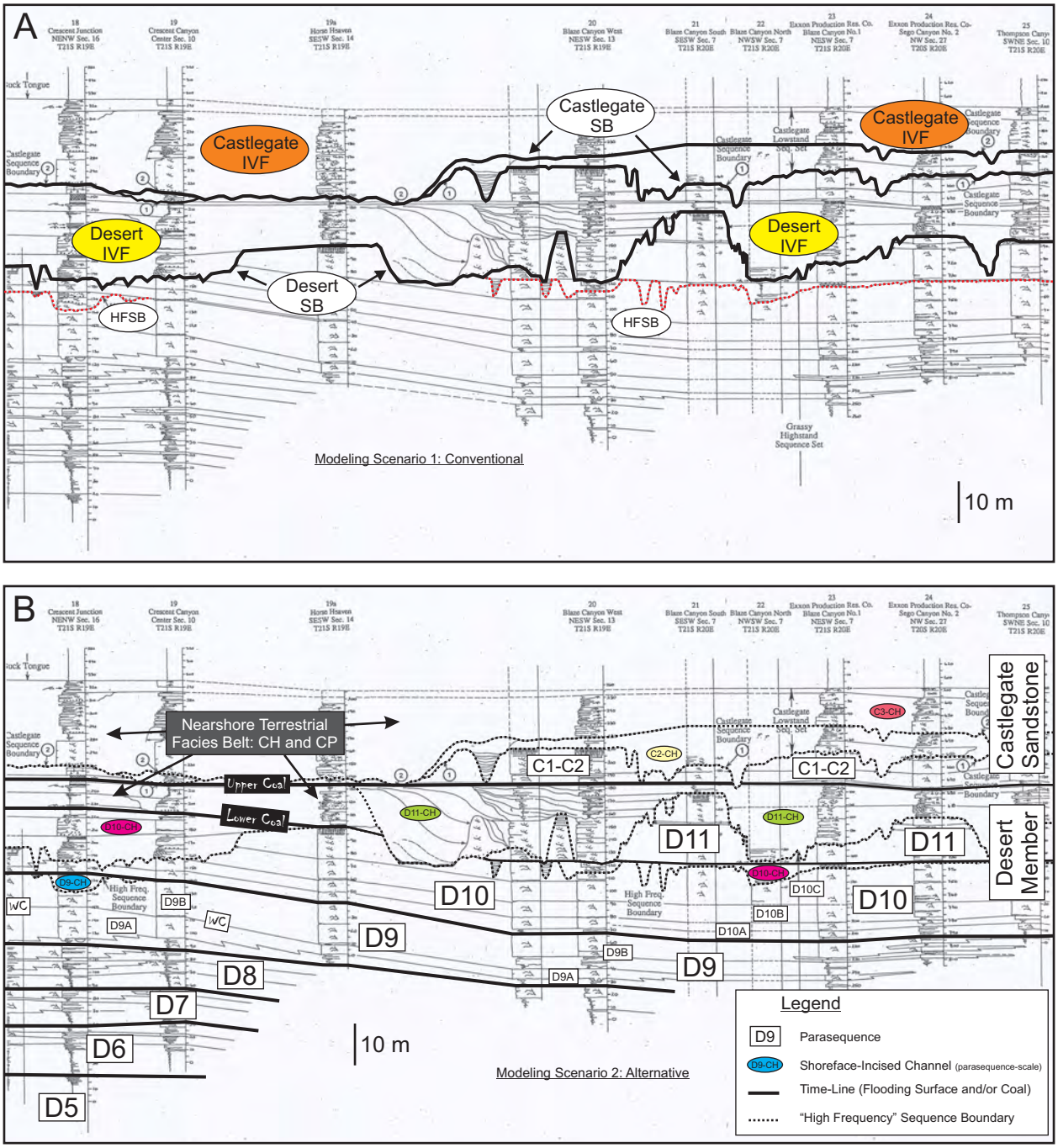

Figure 15-7. Portion of Van Wagoner's (1995) regional cross section that documents sequence stratigraphy and facies distribution in the Desert Member to Castlegate Sandstone interval, from Crescent Junction to Thompson Canyon. Vertical scale on measured sections is marked at five foot intervals, with thickness recorded every ten feet. (A) Conventional sequence stratigraphic correlation (as per Van Wagoner 1995). Modeling scenario 1: conventional, classic, third-order SB, IVF, non-linked nearshore terrestrial and shallow marine facies belts, detached sand bodies are likely down-dip. Highlighting the interpreted Desert Member and Lower Castlegate Sandstone Sequence Boundary (D-SB, C-SB) and Incised Valley-Fill (D-IVF, C-IVF). Van Wagoner (1995) interprets the D-SB and C-SB as third-order SBs, and also identifies high frequency sequence boundaries (HFSB). (B) Alternative sequence stratigraphic interpretation (*as per* Pattison, 2018, 2019a, 2019b, 2019c, in review-a, -b). Modeling scenario 2: alternative, no SB, no IVF, suite of discrete parasequence-scale shoreface-incised channels, temporally and spatially linked nearshore terrestrial and shallow marine facies belts, no detached sand bodies down-dip, attached only.With superimposed terminology from this study: parasequences D5 to D11 and C1 to C2, discrete parasequence-scale shoreface-incised channels (D10-CH, D11-CH, C3-CH), nearshore terrestrial channels (CH) and coastal plain (CP) facies, coal beds (lower, upper), and white cap (WC) sandstone at the D9A-D9B contact. Each shoreface-incised channel first appears in the same location as the parasequence evolution point in which it is "housed". These discrete shoreface-incised channels do not amalgamate into a third-order IVF, as per conventional model The Upper Coal zone/top D11 marks the contact between the Desert Member and overlying Castlegate Sandstone. Legend applies to Part B only.

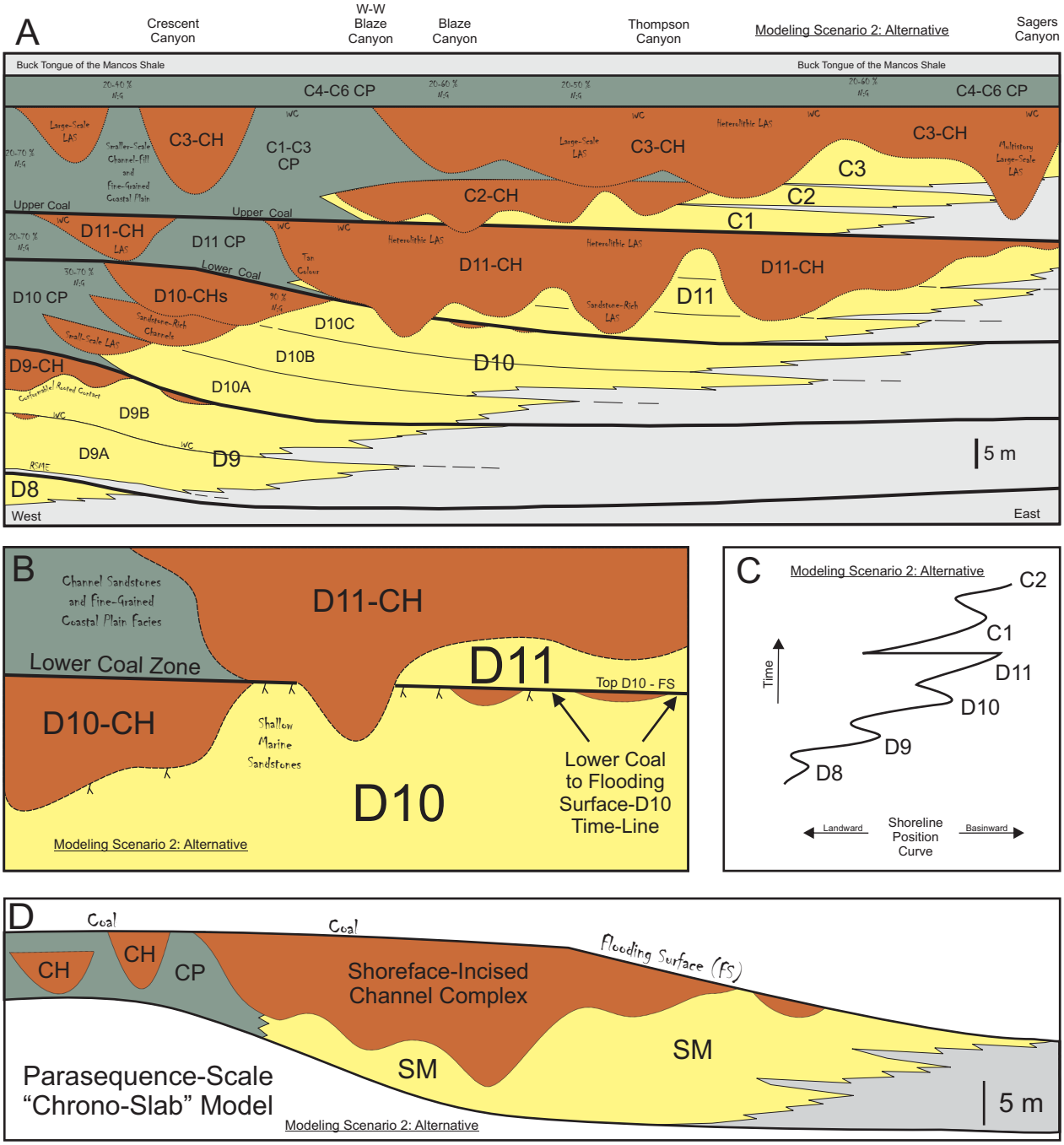

Figure 15-8. Alternative sequence stratigraphic model of the Desert Member (DM) to Lower Castlegate Sandstone (C.Ss.) interval. Modeling scenario 2: alternative, no SB, no IVF, suite of discrete parasequence-scale shoreface-incised channels, temporally and spatially linked nearshore terrestrial and shallow marine facies belts, no detached sand bodies down-dip, attached only. **(A)** High resolution sequence stratigraphy and facies distribution, Crescent Canyon to Sagers Canyon region. Schematic cross section is oriented orthogonal to the paleoshoreline trend of N14°E, and covers approximately 21 km. Desert parasequences D8 to D11, and Castlegate parasequences C1 to C3 are shown. Discrete shoreface-incised channels (D9-CH, D10-CH, D11-CH, C2-CH, C3-CH) cut most parasequences. Time equivalent coastal plain (CP) deposits are demarcated. Coals correlate to flooding surfaces, with the lower coal corresponding to the top of D10, and the upper coal coincident with the D11 flooding surface. Lateral accretion surface (LAS), white-cap (WC), regressive surface of marine erosion (RSME), net:gross ratio (N:G). The upper part of the Lower Castlegate Sandstone is comprised of 4-7 m of lower net:gross, coal-bearing coastal plain deposits with interbedded single-story fluvial channels across the study area. Upper contact with the overlying Buck Tongue of the Mancos Shale is often a mudstone-on-mudstone contact. No lag deposit has been found. **(B)** Close-up of the D10-D11 sequence stratigraphy, Horse Heaven area. Shoreface-incised channels cut both parasequences, with the thickest channel-fills along the D11 level. **(C)** Shoreline position curve for the mid-Desert Member to lower-Castlegate Sandstone stratigraphic interval. Parasequences D8 to C2 are shown. **(D)** Parasequence-scale model. Schematic cross section is oriented west-to-east across the nearshore terrestrial and shallow marine facies belts. Discrete parasequence-scale, shoreface-incised channels include river-dominated distributaries, tidally influenced distributaries, terminal distributaries and/or tidal-estuarine channels. Many form multistory channel complexes incised into the shallow marine (SM) sandstones. Only the foreshore and shoreface sandstones are cut within each parasequence. These channels do not extend basinwards into the lower shoreface or inner shelf facies belts.

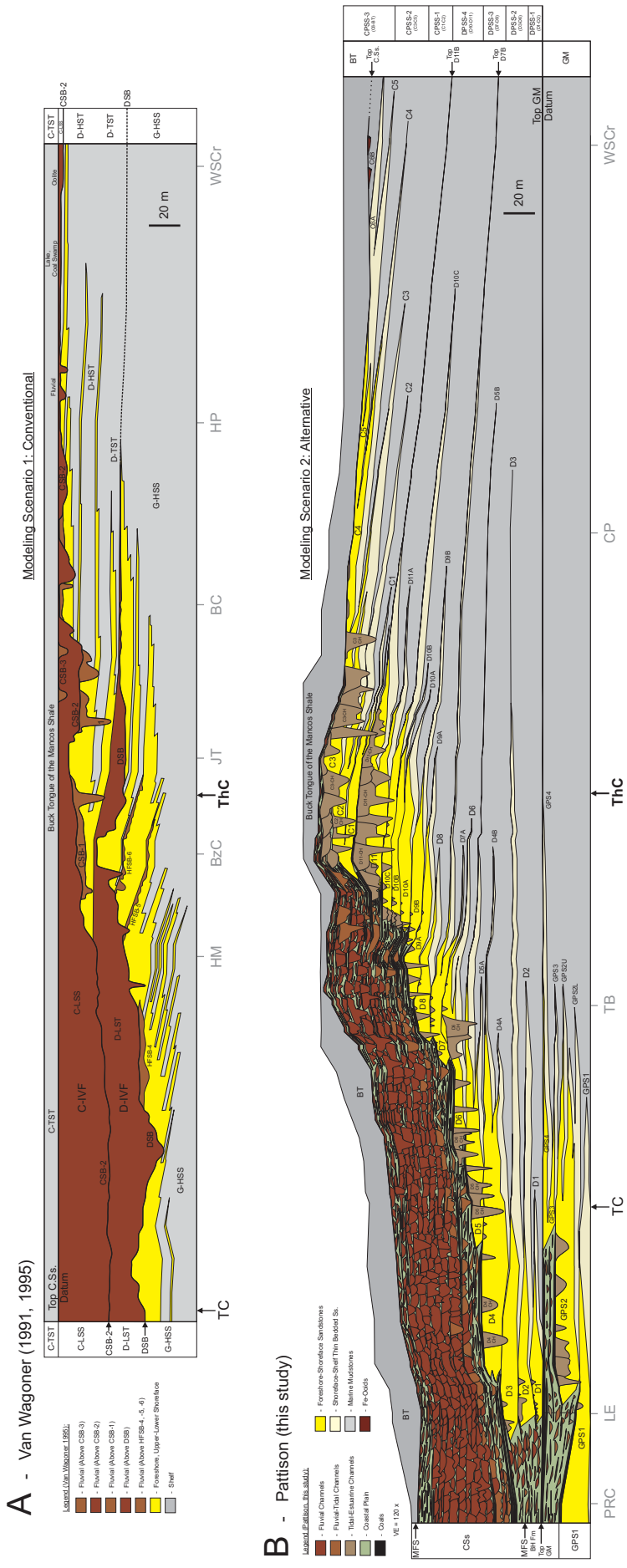

Figure 15-9. High resolution sequence stratigraphy of the Lower Castlegate Sandstone to Upper Blackhawk Formation (Grassy-Desert members). Datum is Top Lower Castlegate Sandstone (C.Ss.) for (A) and Top Grassy Member (GM) for (B). Vertical scale is the same for both schematic sections. Horizontal scale varies. Thompson Canyon (ThC) is used as a "tie-point" for the two sections. Incised valley-fill (IVF). (A) Conventional sequence stratigraphy of the Desert-Castlegate interval (Van Wagoner 1991, 1995). Eight locations are marked at the base: Tusher Canyon (TC), Hatch Mesa (HM), Blaze Canyon (BzC), Thompson Canyon (ThC), Jeep Trail (JT), Bull Canyon (BC), Horse Pastures (HP), and West Salt Creek (WSCr). Distances between adjacent locations, from west to east, are 18, 16, 4, 3, 8, 12, and 55 km, for a total cross sectional length of 116 km between "end-point" localities. Projecting these locations into a depositional-dip-oriented cross section equates to 93 km between "end-points". Castlegate Transgressive Systems Tract (C-TST), Castlegate Sequence Set (C-LSS), Castlegate Sequence Boundary (CSB), Desert Highstand Systems Tract (D-HST), Desert Transgressive Systems Tract (D-TST), Desert Lowstand Systems Tract (D-LST), Desert Sequence Boundary (DSB), High Frequency Sequence Boundary (HFSB), Grassy Highstand Sequence Set (G-HSS). (B) Sequence stratigraphy of the Desert-Castlegate interval in this study. Depositional-dip-oriented schematic section is projected along a W14°N-E14°S trend, with all measured sections projected onto this trend line. Seven locations are marked: Woodside/Price River Canyon (PRC), TC, The Basin (TB), ThC, Corral Point (CP), WSCr. Distances between adjacent locations, orthogonal to the regional paleoshoreline trend (i.e. N14°E), from west to east, are 7, 16, 15, 16, 21, and 29 km, respectively, for a total cross sectional length of 104 km between "end-point" localities. Tusher and Thompson canyons are classic Book Cliffs field trip stops that are usually ran sequentially as adjacent stops. In fact many Book Cliffs field trips "jump-correlate" the Desert-Castlegate interval from TC to ThC, a distance of over 30 km or three townships. Grassy Parasequence 1 (GPS1), Blackhawk Formation (BH Fm), Desert Member (DM), Desert Member Parasequences (D1 to D11), Castlegate Sandstone Parasequences (C1 to C6), Desert Parasequence Sets (DPSS-1 to DPSS-4), Castlegate Parasequence Sets (CPSS-1 to CPSS-3), Maximum Flooding Surface (MFS), Buck Tongue (BT).

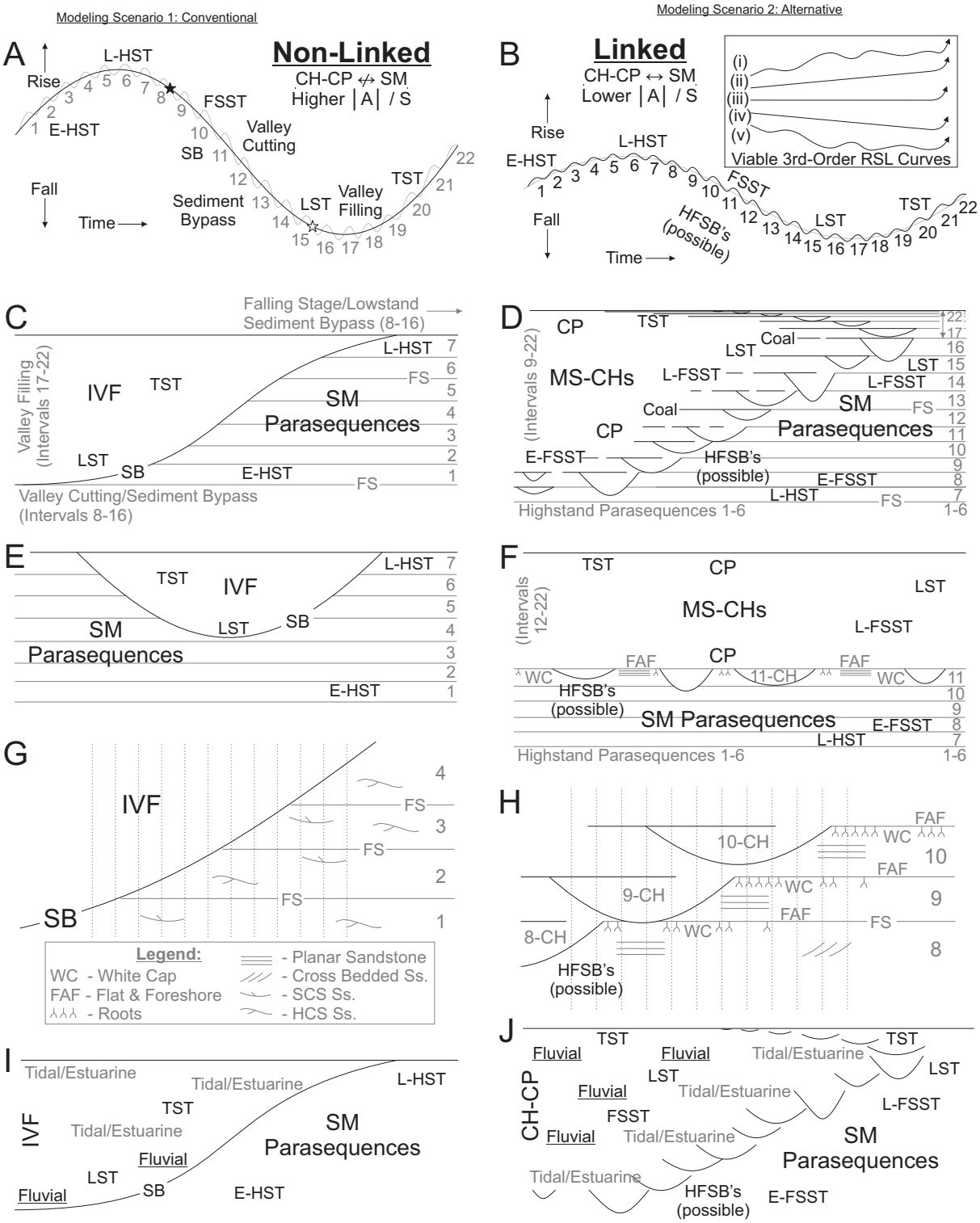

Figure 15-10. Non-linked conventional (left column) versus linked alternative (right column) sequence stratigraphic models. IVF (Incised Valley-Fill), MS-CHs (Multistory Stacked Fluvial Channels), CP (Coastal Plain), SM (Shallow Marine), |A|/S (Accommodation-to-Sediment Supply Ratio), SB (Sequence Boundary), HFSB (High Frequency Sequence Boundary), HST (Highstand Systems Tract), FSST (Falling Stage Systems Tract), LST (Lowstand Systems Tract), TST (Transgressive Systems Tract), E- (Early), L- (Late). (A) "Unique solution", sinusoidal relative sea level (RSL) curve used to explain the stratal architectures in the conventional model. Lower resolution third-order RSL curve (black line) with superimposed parasequence-scale higher resolution RSL curve (grey line). Hypothetical stack of 22 parasequences is shown for modelling purposes. SB placed at start of fall (black star) by Posamentier and Morris (2000) or end of fall (white star) by Plint and Nummedal (2000). (B) "Non-unique solution", sinusoidal RSL curve explains stratal architectures depicted in the alternative model. Other third-order RSL curves are equally likely (i.e. inset box). Higher resolution parasequence-scale RSL curve (black line), superimposed onto a lower resolution RSL curve (grey line). Same hypothetical stack of 22 parasequences as depicted in A. (C,D) Depositional dip-oriented cross section with the same parasequence numbers. (E,F) Depositional strike-oriented cross section, medial location. (G,H) Expected vertical contacts between SM and overlying CH-CP facies displayed using 12 pseudo-wells (dashed vertical lines). Rooted, flat-topped foreshore (FAF) is unlikely in G, as proximal foreshore-shoreface sandstones are continually cut during valley development. FAF may occur at the top of the L-HST in inter-valley regions only. Conventional model has a greater number of distal shoreface to IVF vertical contacts. Rooted, flat-topped foreshore is extremely common in H, as per Desert-Castlegate interval. Channels mostly cut proximal foreshore-shoreface, rarely into the distal shoreface. Legend at lower left. (I,J) Contrasting stacking patterns of fluvial and tidal-estuarine channels. Dip-oriented cross section. Non-linked model has fluvial channels passing stratigraphically up-section into tidal-estuarine channels, while the opposite occurs in the linked model. Field data from the Desert-Castlegate supports the scenario depicted in J.

STOP 16: NEAR-FIELD EXPLORATION-SCALE TERRESTRIAL-SHOREFACE-SHELF TRANSITION, SAGERS CANYON

Sagers Canyon is located approximately 8 km down-depositional-dip from Thompson Canyon and is 42 km down-dip from the head of Tusher Canyon (Figs. 0-1, 0-2, 16-1 to 16-7). We will possibly have two stops here, time permitting: one to examine the regional-scale changes in architecture within the Desert-Castlegate stratigraphic interval by viewing from the road side on the desert floor, and the second to examine the up-close sedimentological and stratigraphic details by climbing up the canyon slope (Fig. 16-1). Our desert floor vantage point encompasses 13 km of depositional-dip-oriented Book Cliffs outcrop from Thompson Canyon in the west to Pinto Wash in the east (Fig. 16-2). On a clear day one can also see the edge of Corral Point to the east which is an additional 14 km down-dip. This regional-scale field of view clearly shows the transition from the sandstone-rich shallow marine and non-marine sections in the west, to the heterolithic- and mudstone-dominated sections to the east (Figs. 16-2 to 16-6). It also highlights the stack of two progradational parasequence sets: Desert Member parasequences D1 to D11, and Castlegate parasequences C1 to C6.

Time permitting, our second stop in this area involves a moderate climb up the Sagers Canyon scree slope to view the facies, stacking patterns and sequence stratigraphy of the Desert Member-to-Castlegate Sandstone interval (Fig. 16-1). In general, the Desert-Castlegate interval is shallow marine-dominant and finer grained at Sagers Canyon compared to Thompson Canyon. Desert Member shoreface successions were sharp-based up-dip, but transition into gradationally-based shoreface successions down-depositional-dip. From base to top, the main architectural elements observed in the Sagers Canyon region are: (i) Desert Member parasequences D1 to D11, (ii) a thin (< 2 m) shoreface-incised channel (i.e. D11-CH) cutting the top of parasequence D11, (iii) Lower Castlegate Sandstone parasequences C1 and C2, (iv) a heterolithic-dominant Lower Castlegate Sandstone shoreface-incised channel-fill complex (C3-CH) cutting into parasequences C2 and C1, and (v) a 2-5 m thick package of coastal plain mudstones with thin sandstone beds capping the Lower Castlegate Sandstone (Figs. 16-1 and 16-2E).

The Book Cliffs region offers exceptional outcrop and subsurface data that can be used to examine thickness trends and correlation styles in wave-dominated shoreface-to-shelf environments (Tables 16-1 to 16-6). Our last stop provides a glimpse into this outstanding data base by highlighting one of many depositional-dip-oriented panoramic vistas. We will also have the opportunity to examine thickness trends and correlation styles on a regional well log cross section and to compare it with our field observations at this locality (Fig. 16-7).

Outcrop Data

High resolution outcrop data clearly shows a gradual basinward thinning from the distal lower shoreface to the inner shelf environment. Using mid-point thickness and distance data (Tables 16-1 and 16-2), the following trends are observed: (i) the Kenilworth Member thins from 115 m to 78 m (32 % thinning) over 43.6 km (Middle Mountain to Sagers Canyon), with most of the thinning occurring in the first 10 km to 15 km, and (ii) the combined Grassy Member and Sunnyside Member interval thins from 140 m to 108 m (23 % thinning) over 33.5 km (Tusher Canyon to Sagers Canyon).

Subsurface Data

Regional well log cross section AA′ consists of 14 wells across the Star Point Formation to Lower Castlegate Sandstone stratigraphic interval, and covers 130 km of depositional-dip-oriented distance in eastern Utah (Fig. 16-7). Distance and thickness data are summarized in Tables 16-3 to 16-5. Well log cross section AA′ documents a gradual basinward thinning in parasequence- and member-scale rock packages from shoreface-to-shelf environments, as demonstrated by the following (Tables 16-3 and 16-4):

(1) The Kenilworth Member thins from *118 m* (McKnight A Fed 2) to *66 m* (Barnhill Federal 1) which represents a 44 % thinning over 73.6 km. Most of this thinning occurred in the first 15.0 km (i.e. 118 m to 89 m), as the Kenilworth had a 25 % in decrease in thickness from the McKnight A Fed 2 well to the Butler Cyn U USA well. The remainder of the thinning is spread over 58.6 km (i.e. 89 m to 66 m), from the Butler Cyn U USA well to the Barnhill Federal 1 well (Table 16-5).

(2) The combined thickness of the Grassy and Sunnyside members interval thins from *148 m* at the Butler Cyn U USA 33-12 well to *110 m* at the Barnhill Federal 1 well, which represents a 26 % thinning over 58.6 km (Table 16-5).

(3) The Sunnyside Member thins from *83 m* at the Tusher Creek #1 well to *61 m* at the State 411-2 well, which is a 27 % thinning over 16.4 km.

(4) The Grassy Member thins from *74 m* at the Butler Cyn U USA 33-12 well to *57 m* at the Rattlesnake State 2-12 well, which is a 23 % thinning over 20.0 km.

Summary

The time equivalent Mancos Shale offshore mudstone belt extends basinward for over 100 km with no significant decrease in thickness, no evidence of clinoforms, nor any indication of a basinward translation of the shoreline during sea level fall. Outcrop and subsurface data reveals a gradual basinward thinning in parasequence- and member-scale rock packages (Tables 16-1 to 16-6). There are no abrupt changes in thickness nor any pronounced clinoform geometries. As described earlier, a simple set of correlation rules and guidelines have been distilled for wave-dominated shoreface-to-shelf systems using Book Cliffs outcrop and subsurface data (Williams and Davies 2006; Pattison, Williams and Davies 2007a, 2007b, 2007c; Pattison 2010):

(a) parasequences show a gradual basinward thinning,
(b) parasequences exhibit an abrupt decrease in sandstone content basinwards that is matched by an equally abrupt increase in mudstone,
(c) inner shelf mudstone facies can be quartz-silt dominant and therefore have a similar compaction factor as the up-dip shoreface sandstones,
(d) parasequences split basinward into thinner cycles or bedsets, and
(e) there are no steeply dipping clinoforms in wave-dominated shorefaces-shelves.

Similar thickness trends are manifested at a variety of scales, from micro- (bedset) to macro-scale (basin). The latter is highlighted in the classic basin-scale stratigraphic cross section published by Armstrong (1968) which shows gradual basinward thinning from Utah to Colorado. Other wave-dominated shoreface-to-shelf systems are likely to exhibit similar thickness trends and correlation styles worldwide.

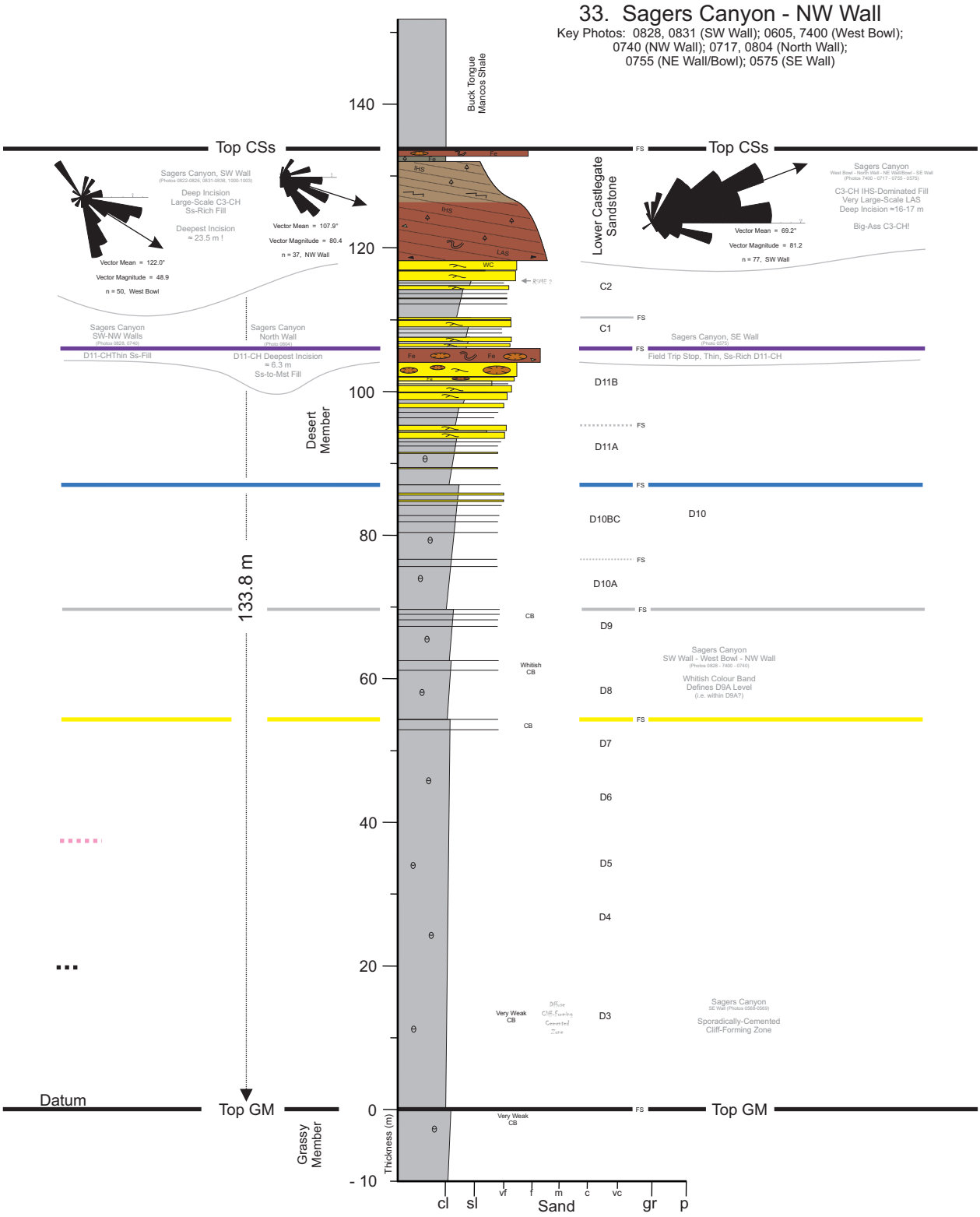

Figure 16-1. Measured outcrop section #33, Sagers Canyon, NW Wall. Legend nested in Figure 10-2.

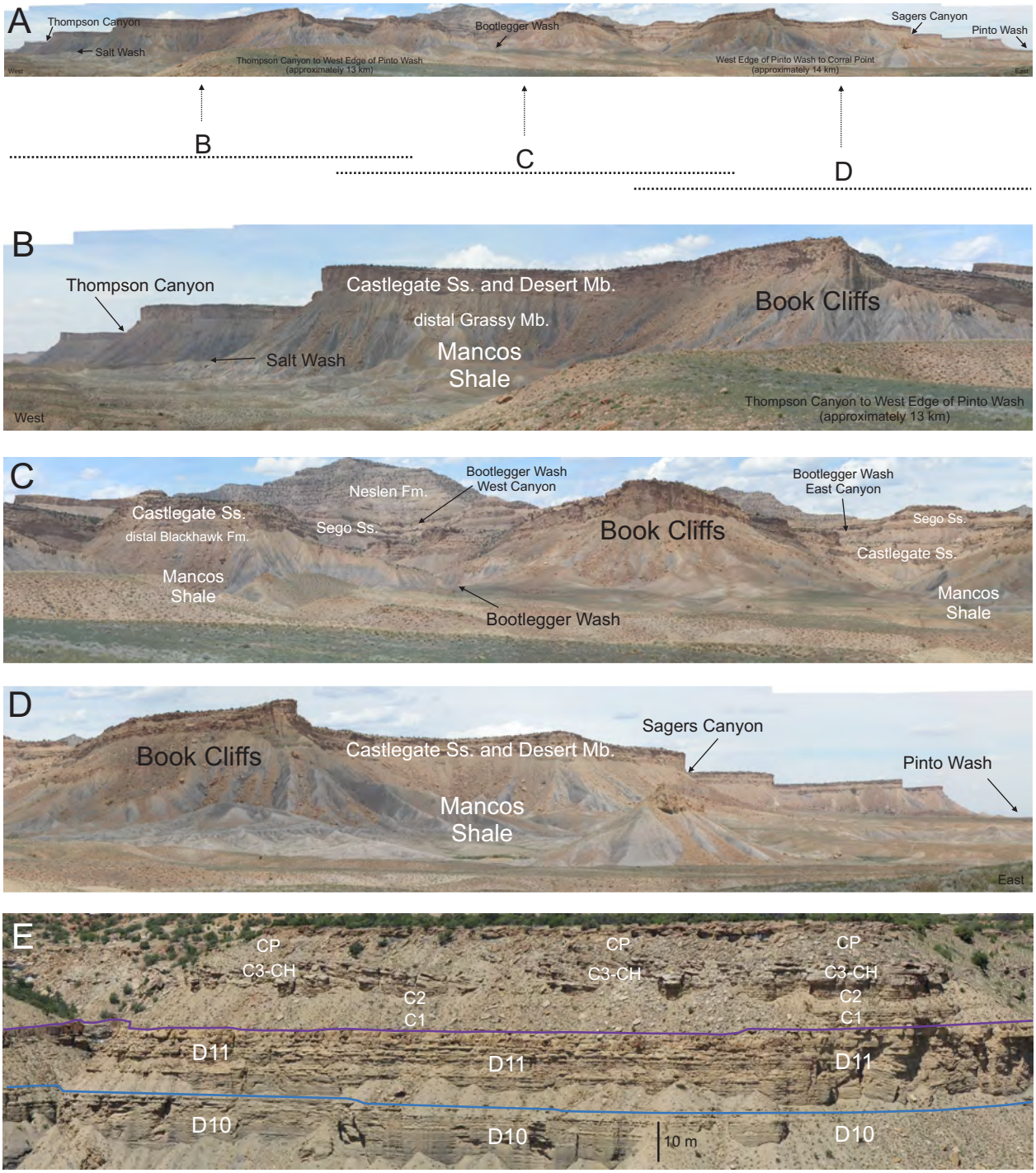

Figure 16-2. Near-field exploration-scale transition: channel-to-shoreface-to-shelf, Desert Member to Castlegate Sandstone stratigraphic interval, Sagers Canyon overview. (A) Photo-panorama from Thompson Canyon to the west edge of Pinto Wash. Field of view is approximately 13 km. (B to D) Three close-up photo-panoramas with the positions shown in Part A, extending from Thompson Canyon to Pinto Wash. (E) Sagers Canyon, North Wall. A significant muddying of the shallow marine parasequences D10, D11, C1, and C2 occurs between Thompson Canyon and Sagers Canyon, along with the thinning of the D11-CH and transition of the C3-CH from a sandstone-rich fill to a heterolithic-dominanted shoreface-incised channel fill. The upper 8-10 m of the Lower Castlegate Sandstone is comprised of coastal plain (CP) mudstones with single-story fluvial sandstones.

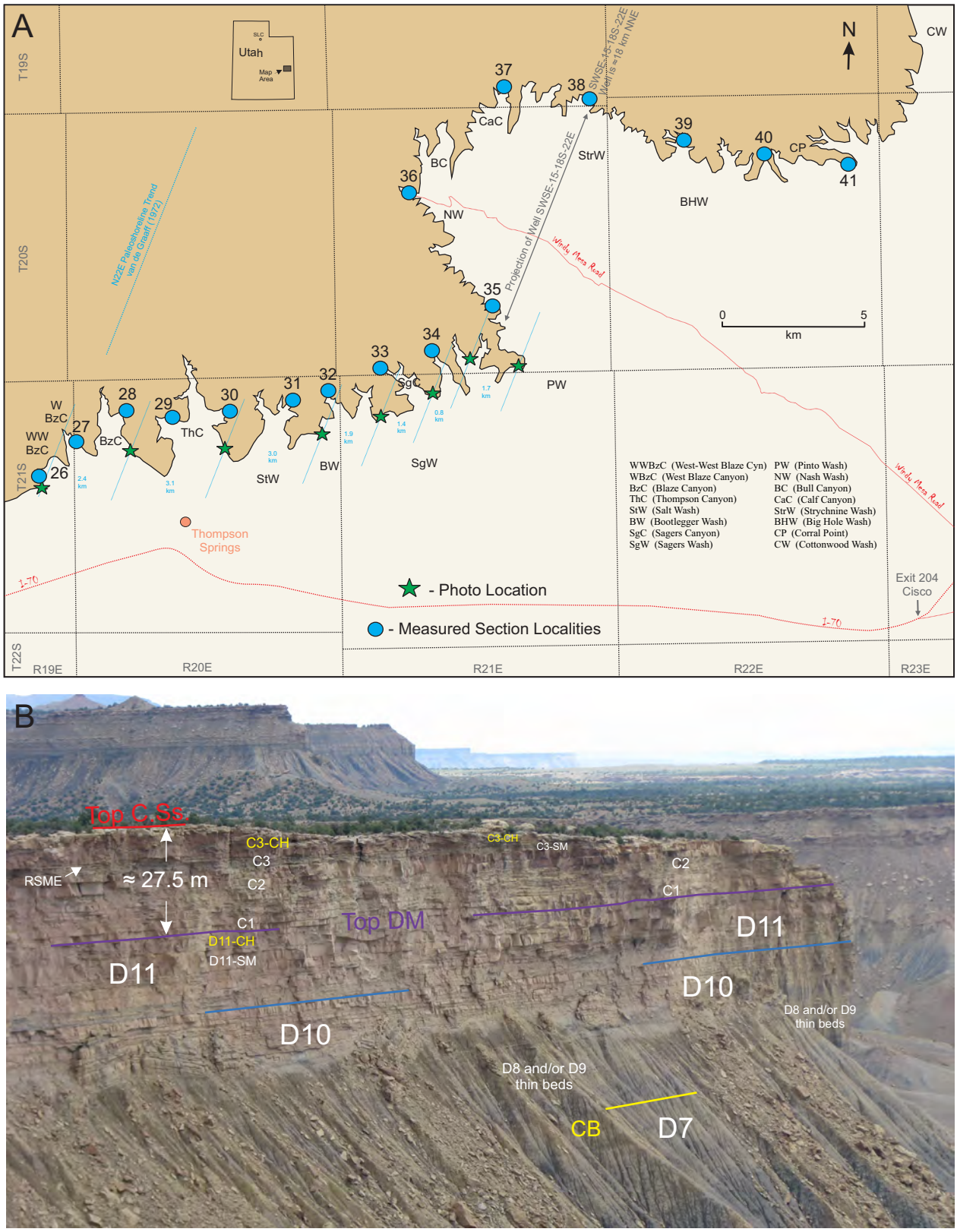

Figure 16-3. (A) Topographic map of the Book Cliffs region from Blaze Canyon to Corral Point. The location of key photographs from Bootlegger Wash Canyons to Pinto Wash, measured sections 26 to 41, and the depositional dip distance between adjacent photos are shown. Near subsurface well log data from SWSE-15-18S-22E is projected to the SSW into equivalent outcrop positions at Strychnine Wash and Pinto Wash using the N22°E paleoshoreline trend of van de Graaff (1972). (B) Desert Member (DM) to Castlegate Sandstone (C.Ss.) stratigraphic interval, West Face, Bootlegger Wash Canyons. DM parasequences D7 to D11 and C1 to C3 are labelled. Two shoreface-incised channels are recognized, a thin D11-CH and a thick C3-CH. The C.Ss. is 27.5 m (≈ 90 feet) thick. CB (Colour Band), SM (Shallow Marine), CH (Channel), RSME (Regressive Surface of Marine Erosion).

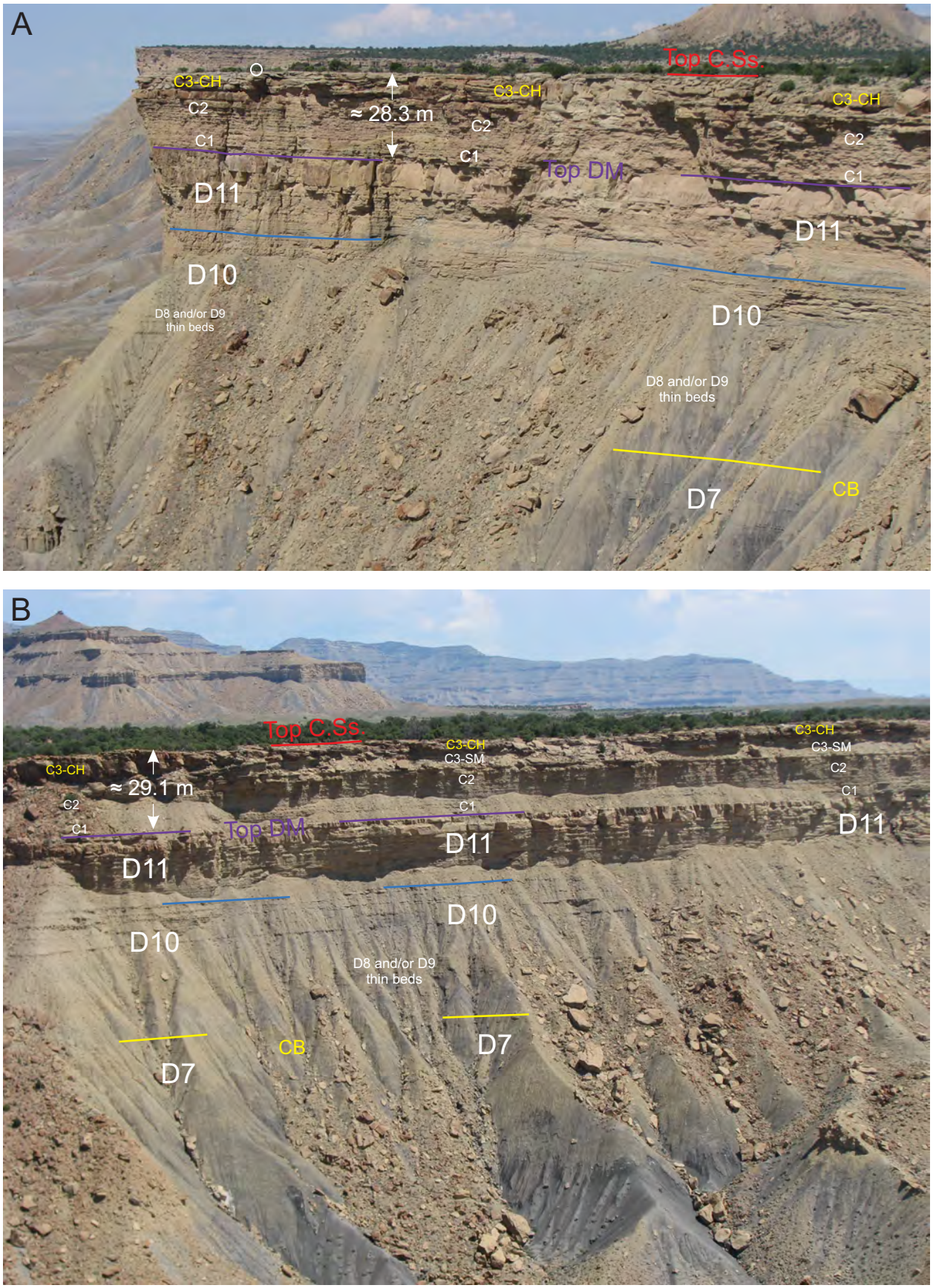

Figure 16-4. Desert Member (DM) to Castlegate Sandstone (C.Ss.) stratigraphic interval. DM parasequences D7, D10, and D11 are confidently picked. Thin bedded heterolithics of D8 and/or D9 are also shown. Lower Castlegate Sandstone parasequences C1 to C3 are recognized. A thick shoreface-incised channel-fill, C3-CH, cuts the underlying shallow marine (SM) deposits. CB (Colour Band). (A) East Face, Bootlegger Wash Canyons. The C.Ss. is 28.3 m (≈ 92.9 feet) thick. Geologist for scale at top C.Ss. (white circle). (B) Southeast Wall, Sagers Canyon. The C.Ss. is 29.1 m (≈ 95.5 feet) thick.

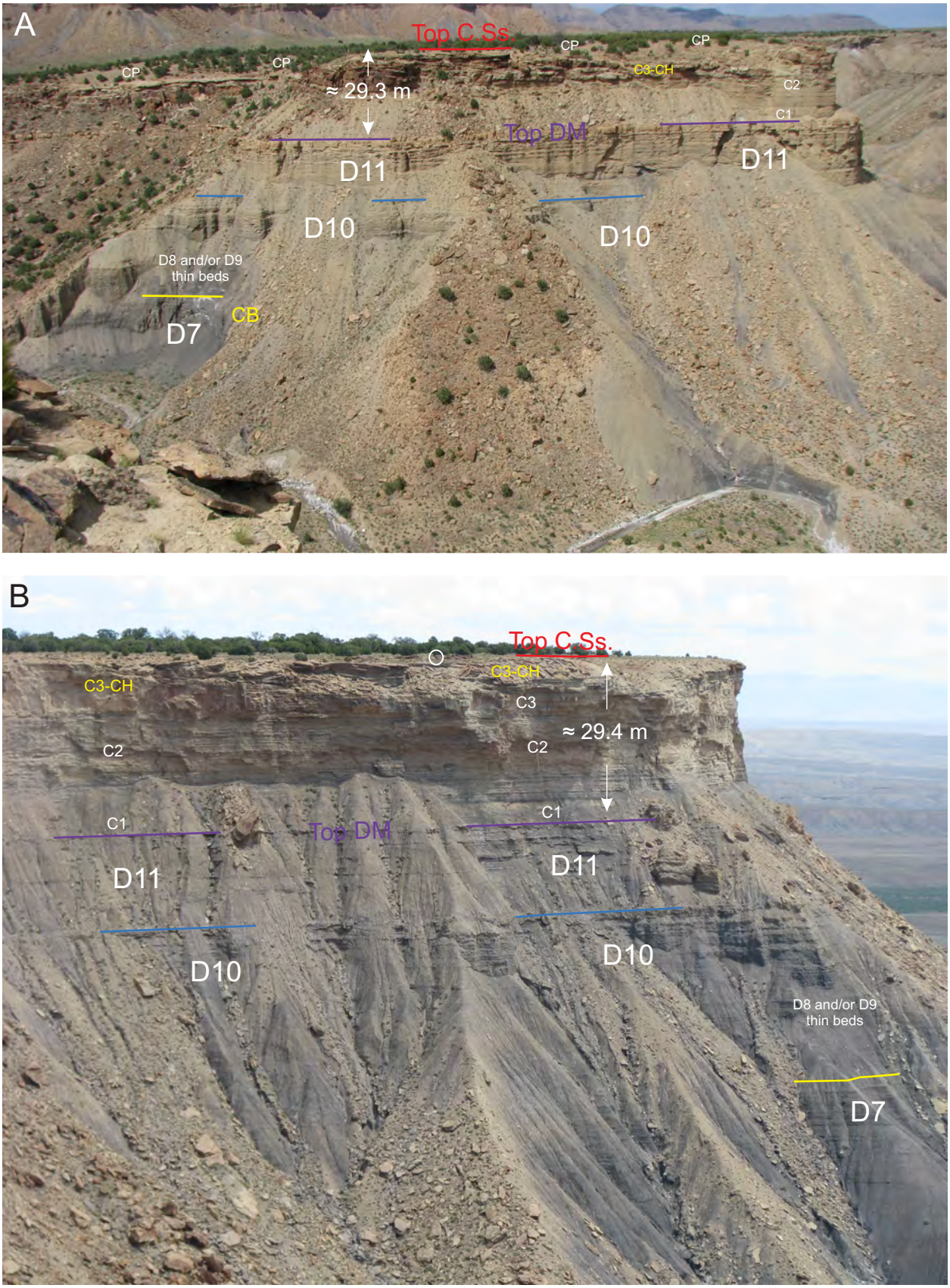

Figure 16-5. Desert Member (DM) to Castlegate Sandstone (C.Ss.) stratigraphic interval. DM parasequences D7, D10, and D11 are easily identified. Thin bedded heterolithics of DM parasequences D8 and/or D9 are also shown. Lower Castlegate Sandstone parasequences C1 to C3. Shoreface-incised channel C3-CH. CB (Colour Band), CH (Channel). Uppermost 8-10 m of the Lower Castlegate Sandstone is dominated by coastal plain (CP) mudstones. (A) East Wall, Pinto Wash West Fork Canyon. The C.Ss. is 29.3 m (≈ 96.1 feet) thick. (B) Southeast Face, Pinto Wash West Fork Canyon. The C.Ss. is 29.4 m (≈ 96.5 feet) thick. Geologist for scale at top C.Ss. (white circle).

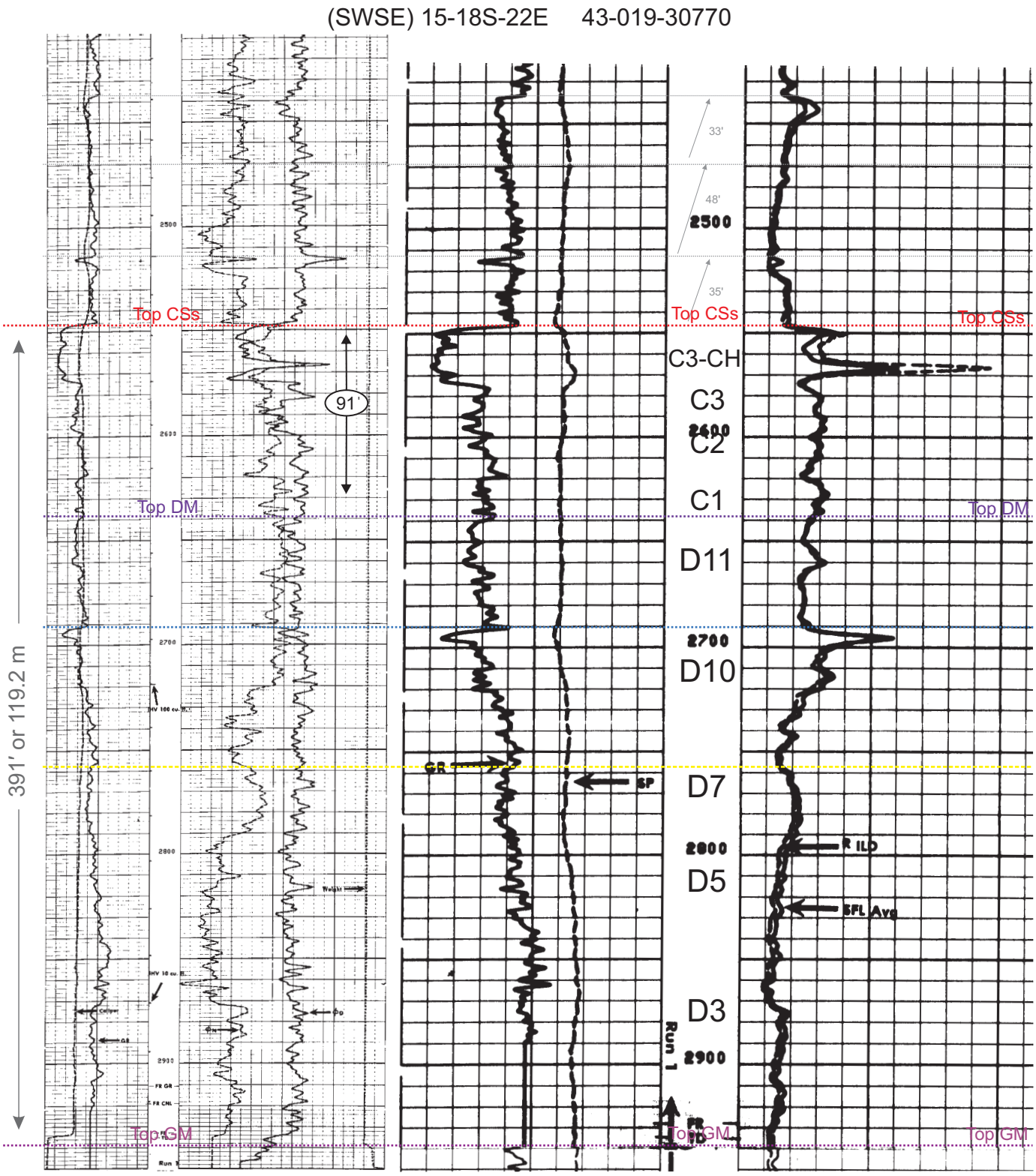

Figure 16-6. Near subsurface well log suite including gamma ray, neutron-density porosity, SP, and resistivity logs from SWSE-15-18S-22E (API Number 43-019-30770), located approximately 18 km north of Big Hole Wash, Book Cliffs. Lower Castlegate Sandstone (CSs) shoreface-incised channel C3-CH, parasequences C1 to C3, Desert Member (DM) parasequences D3, D5, D7, D10, and D11, and the top of the Grassy Member (GM) are identified. The CSs is 91 feet thick (27.7 m). This well has been projected SSW into the Book Cliffs using van de Graaff's (1972) N22°E paleoshoreline trend, and is coincident with outcrops at Strychnine Wash and Pinto Wash (Fig. 16-3A), nicely matching the Desert-Castlegate outcrop stratigraphy in these regions. CH (Channel).

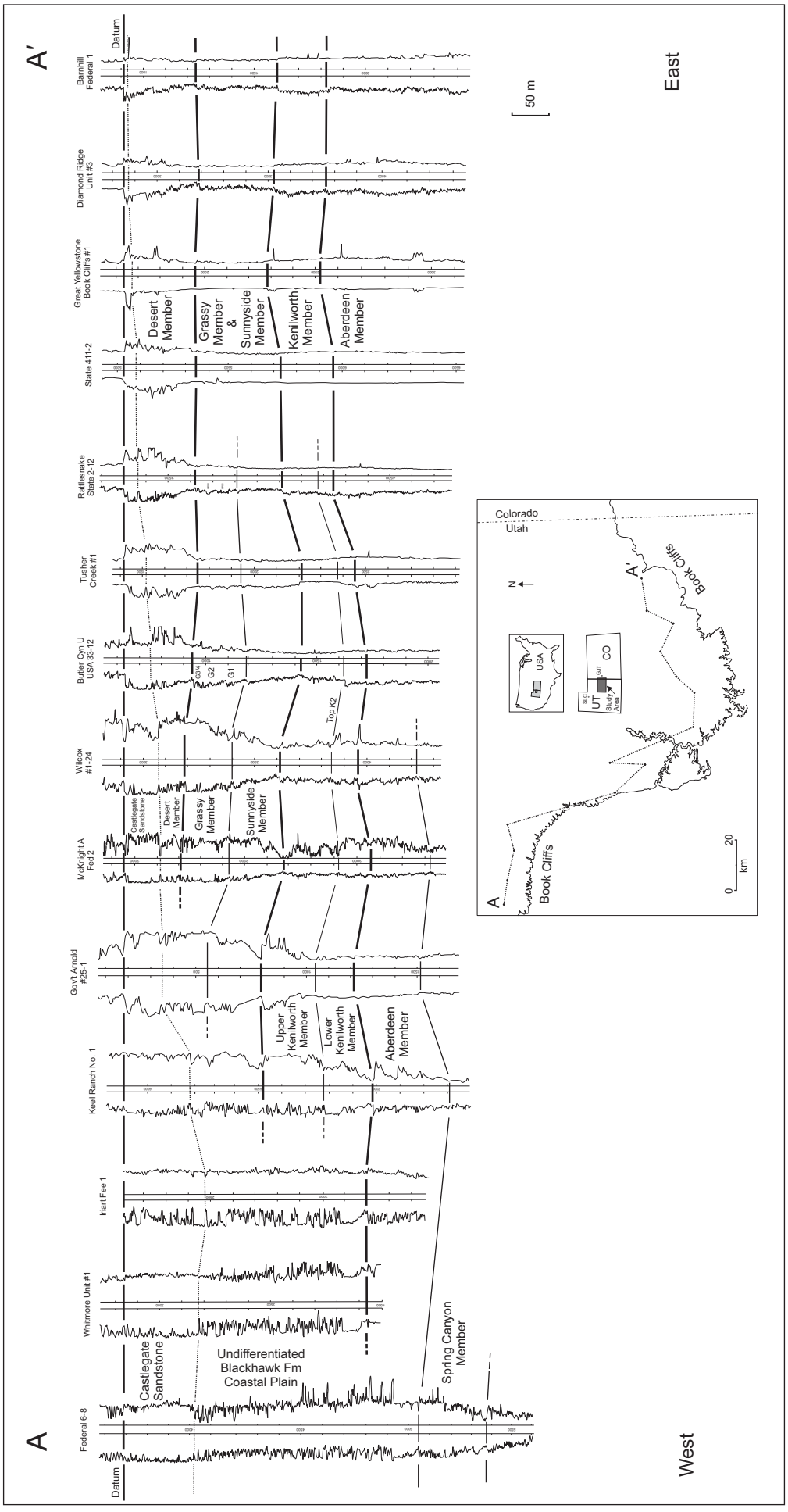

Figure 16-7. Well log cross section AA'. Datum is the top of the Castlegate. Depth intervals in feet. Inset maps show the location of well log cross section AA' and the study area. SLC (Salt Lake City), GJT (Grand Junction).

Location	CS + BH C-P	CS + DM	GM	SM	KM
PC to HC-N	89 - 141	na	0 - 16	27 - 66	94 - 141
PRC to BB		85 - 89	18 - 37	85 - 87	120 - 146
MM to GB		77 - 84	36 - 52	78 - 85	99 - 131
TC to UC		74 - 100	57 - 84	57 - 81	88 - 103
HM to FW		102 - 108	111 - 125		81 - 100
CR to BzC		103 - 115	108 - 120		76 - 89
ThC to SaC		106 - 125	103 - 113		73 - 82

Table 16-1. Outcrop thickness (meters) of key rock packages in the Castlegate Sandstone (CS) to Blackhawk Formation (BH) stratigraphic interval, east-central Utah (Pattison 2005a). DM (Desert Member), GM (Grassy Member), SM (Sunnyside Member), KM (Kenilworth Member), C-P (Coastal Plain). PC (Pace Canyon), HC-N (Horse Canyon North), PRC (Price River Canyon), BB (Battleship Butte), MM (Middle Mountain), GB (Gunnison Butte), TC (Tusher Canyon), UC (Unnamed Canyon), HM (Hatch Mesa), FW (Floy Wash), CR (Christmas Ridge), BzC (Blaze Canyon), ThC (Thompson Canyon), SaC (Sagers Canyon).

Outcrop Data	Up-Dip Thickness (m)	Down-Dip Thickness (m)	Rate of Thinning (%)	Distance (km)
Kenilworth	115	78	32	43.6
Grassy/Sunnyside	140	108	23	33.5

Table 16-2. Summary of the up-depositional-dip versus down-depositional-dip thickness of the Kenilworth Member and combined Grassy-Sunnyside members, based on outcrop measurements. Note the gradual rate of basinward thinning within each stratigraphic interval.

Well Name		Well Name	Distance (km)
Federal 6-8	to	Whitmore Unit #1	10.1
Whitmore Unit #1	to	Iriart Fee 1	11.4
Iriart Fee 1	to	Keel Ranch No. 1	10.3
Keel Ranch No. 1	to	Gov't Arnold #25-1	12.6
Gov't Arnold #25-1	to	McKnight A Fed 2	11.3
McKnight A Fed 2	to	Wilcox 1-24	1.1
Wilcox 1-24	to	Butler Cyn U USA 33-12	13.9
Butler Cyn U USA 33-12	to	Tusher Creek #1	13.6
Tusher Creek #1	to	Rattlesnake State 2-12	6.4
Rattlesnake State 2-12	to	State 411-2	10.0
State 411-2	to	Great Yellowstone BC #1	10.9
Great Yellowstone BC #1	to	Diamond Ridge Unit #3	5.0
Diamond Ridge Unit #3	to	Barnhill Federal 1	12.7
		Total Down-Dip Distance =	*129.3 km*

Table 16-3. Depositional-dip-oriented distance between adjacent wells on cross section AA′. Assumes a north-south oriented paleoshoreline trend, with offshore towards the east. Well locations are projected into a west-to-east oriented dip location. A total distance of 129.3 km of dip-oriented strata is transected on this cross section.

Well	o/c *	BH C-P	CS	DM	GM	SM	KM	AM	SCM
1	KW	304	96						92
2	StrC	229	101					87	
3	DC	219	110					101	
4	BrC	100	89				149	104	
5	G	61	52			73	127	91	
6	MM		49	28	67	75	118	80	
7	MM		48	35	64	65	106	79	
8	CC-S		36	58	74	74	89		
9	CR		29	70	59	83	73		
10	CrC		19	78	57	61	70		
11	BW		16	83	115		71		
12	NW		11	86	99		72		
13	CP		6	95	103		71		
14	BCW		4	94	110		66		

Table 16-4. Subsurface thickness (meters) of key rock packages in the Castlegate Sandstone (CS) to Blackhawk Formation (BH) stratigraphic interval, east-central Utah. Data from 14 well logs shown on cross section AA′, and these are numbered consecutively from west-to-east. ******* *Closest outcrop (o/c) projection assumes a north-to-south oriented paleoshoreline trend, with offshore towards the east. The projected outcrop locality is therefore due south of the subsurface location. Stratigraphy: C-P (Coastal Plain), DM (Desert Member), GM (Grassy Member), SM (Sunnyside Member), KM (Kenilworth Member), AM (Aberdeen Member), SCM (Spring Canyon Member). Localities: KW (Kenilworth Wash), StrC (Straight Canyon), DC (Dugout Creek), BrC (Bear Canyon), G (Grassy), MM (Middle Mountain), CC-S (Coal Canyon-South), CR (Christmas Ridge), CrC (Crescent Canyon), BW (Bootlegger Wash), NW (Nash Wash), CP (Corral Point), BCW (Buck Canyon Wash).*

Subsurface Data	Up-Dip Thickness (m)	Down-Dip Thickness (m)	Rate of Thinning (%)	Distance (km)
Kenilworth	89	66	26	58.6
Grassy/Sunnyside	148	110	26	58.6

Table 16-5. Summary of the up-depositional-dip versus down-depositional-dip thickness of the Kenilworth Member and combined Grassy-Sunnyside members, as revealed from the well logs on cross section AA′. Note the gradual basinward thinning within each stratigraphic interval.

Combined Subsurface and Outcrop Data	Up-Dip Thickness (m)	Down-Dip Thickness (m)	Rate of Thinning (%)	Distance (km)
Kenilworth - ss	89	66	26	58.6
Kenilworth - o/c	115	78	32	43.6
Grassy/Sunnyside - ss	148	110	26	58.6
Grassy/Sunnyside - o/c	140	108	23	33.5

Table 16-6. Summary of the up-depositional-dip versus down-depositional-dip thickness of the Kenilworth Member and combined Grassy-Sunnyside members, based on both subsurface and outcrop measurements. Note the gradual basinward thinning within each stratigraphic interval.

ACKNOWLEDGEMENTS

I am indebted to Huw Williams for not only introducing me to the Book Cliffs in the early 1990s but also for his continual mentorship regarding the application of outcrop analog data to subsurface petroleum exploration- and reservoir-scale activities. Many of the ideas and observations included in this field guidebook have evolved through discussions with Huw during various Book Cliffs field seminars. Huw has unselfishly provided numerous ideas for research and research training over the years. To him I extend my sincere gratitude.

I would also like to thank Bruce Ainsworth, Donna Anderson, Samson Audu, Janok Bhattacharya, Luis Buatois, Mark Budding, Huw Davies, Paul Davies, Joe Ejedawe, Gary Hampson, Bruce Hart, Paul Hill, John Howell, George Kakayor, Mark Kirschbaum, Lee Krystinik, James MacEachern, Phil Machent, Joe MacQuaker, Gabriela Mangano, Jeff May, Tim Milligan, Ciaran O'Byrne, Cornel Olariu, Tom Ryer, Simon Smith, Doug Stewart, Jill Stewart, Kevin Taylor, Rob Wheatcroft, Shuji Yoshida, and Harvey Young for sharing their knowledge about Book Cliffs strata and also their observations during various field visits to the Book Cliffs.

Data for this field guidebook has been collected since 1993. Early funding was provided through a KSEPL (Shell Research) and SPDC (Shell) Nigeria sponsored Senior Research Fellowship at the University of Aberdeen. Recent funding has been generously provided through Natural Sciences and Engineering Research Council of Canada Discovery Grants 238532-2001 and 238532-2008, and via Shell International (Houston) and Conoco Phillips (Houston) research grants. Ideas have been sharpened through discussions with over 750 professionals during various Book Cliffs field trips since 1993. Field assistants Morufu Basiru, Trevor Hoffman, Sean Horner, Brittan Jones, Jess Peat, Jenna Phillips, Steve Saban, Nichole Scott and Jill Stewart are thanked for their dedication and hard work during some extremely hot, gnatty and long field days. Peter Adamo, Jeff Dowd, Sharon Romanowski, Shelley Roy, Elaine Ruff, and Geoff Speers are also acknowledged for their assistance with some of the figures.

And lastly but most importantly, I would like to thank Jill, Liam and Laura for their unfailing love and support as I spent many long weeks and months doing field work in my home away from home! This field guidebook is dedicated to you.

Comprehensive Reference List

Adams, M.M., and Bhattacharya, J.P., 2005, No change in fluvial style across a sequence boundary, Cretaceous Blackhawk and Castlegate formations of central Utah, U.S.A.: Journal of Sedimentary Research, v. 75, p. 1038-1051.

Aigner, T., and Reineck, H-E., 1982, Proximality trends in modern storm sands from the Helgoland Bight (North Sea) and their implications for basin analysis: Sencken. Mar., v. 14, p. 185-215.

Ainsworth, R.B., and Pattison, S.A.J., 1994, Where have all the lowstands gone? Evidence for attached lowstand systems tracts in the Western Interior of North America: Geology, v. 22, p. 415-418.

Ainsworth, R.B., Sanlung, M., and Duivenvoorden, S.T.C., 1999, Correlation techniques, perforation strategies, and recovery factors: an integrated 3-D reservoir modeling study, Sirikit Field, Thailand: American Association of Petroleum Geologists Bulletin, v. 83, p. 1535-1551.

Ainsworth, R.B., Bosscher, H., and Newall, N., 2000, Forward stratigraphic modelling of forced regressions: evidence for the genesis of attached and detached lowstand systems, *in* Hunt, D., and Gawthorpe, R.L., eds., Sedimentary Responses to Forced Regressions: Geological Society of London Special Publication, No. 172, p. 163-176.

Ainsworth, R.B., Flint, S.S. and Howell, J., 2008, Predicting coastal depositional style: influence of basin morphology and accommodation-sediment supply regime within a sequence stratigraphic framework, in Hampson, G.J., Steel, R., Burgess, P., and Dalrymple, R., eds., Recent Advances in Models of Siliciclastic Shallow-Marine Stratigraphy: SEPM Special Publication No. 90, p. 237-263.

Ainsworth, R.B., Vakarelov, B.K., and Nanson, R.A., 2011, Dynamic spatial and temporal prediction of changes in depositional processes on clastic shorelines: Toward improved subsurface uncertainty reduction and management: American Association of Petroleum Geologists Bulletin, v. 95, p. 267-297.

Ainsworth, R.B., Vakarelov, B.K., MacEachern, J.A., Rarity, F., Lane, T.I., and Nanson, R.A., 2017, Anatomy of a shoreline regression: implications for the high-resolution stratigraphic architecture of deltas: Journal of Sedimentary Research, v. 87, p. 425-459.

Ainsworth, R.B., McArthur, J.B., Lang, S.C., and Vonk, A.J., 2018, Quantitative sequence stratigraphy: American Association of Petroleum Geologists Bulletin, v. 102, p. 1913-1939.

Allen, G.P., 1991, Sedimentary processes and facies in the Gironde estuary: a recent model for macrotidal estuarine systems, in, Smith, D.G., Reinson, G.E., Zaitlin, B.A., and Rahmani, R.A., eds., Clastic Tidal Sedimentology: Canadian Society of Petroleum Geologists Memoir 16, p. 29-40.

Allen, G.P., Laurier, D., and Thouvenenin, J., 1979, Étude sédimentologique du delta de la Mahakam: Compagnie Française des Pétroles (TOTAL), Paris, Notes et Mémoires 15, 156 p.

Allen, J.R.L., 1965, The sedimentation and paleogeography of the Old Red Sandstone of Anglesey, North Wales: Proceedings of the Yorkshire Geological Society, v. 35, p. 139–185.

Allen, J.R.L., 1970, Studies in fluviatile sedimentation: a comparison of fining-upwards cyclothems, with special reference to coarse-member composition and interpretation: Journal of Sedimentary Petrology, v. 40, p. 298-323.

Amorosi, A., Maselli, V., and Trincardi, F., 2016, Onshore to offshore anatomy of a late Quaternary source-to-sink system (Po Plain–Adriatic Sea, Italy): Earth-Science Reviews, v. 153, p. 212-237.

Amorosi, A., Bruno, L., Cleveland, D.M., Morelli, A., and Hong, W., 2017, Paleosols and associated channel-belt sand bodies from a continuously subsiding late Quaternary system (Po Basin, Italy): New insights into continental sequence stratigraphy: Geological Society of America Bulletin, v. 129, p. 449-463.

Amos, C.L., Li, M.Z., Chiocci, F.L., La Monica, G.B., Cappucci, S., King, E.H., and Corbani, F., 2003, Origin of shore-normal channels from the shoreface of Sable Island, Canada: Journal of Geophysical Research, v. 108 (C3), p. 39-1 to 39-16.

Anderson, D.S., 2005, Tectonic controls on delta-front to basin sedimentation: the Lewis Shale-Fox Hills turbidite system, northernmost Great Divide Basin, Wyoming: American Association of Petroleum Geologists Annual Convention, Calgary, Alberta, Abstract, p. A6.

Anderson, P.B., and Ryer, T.A., 2004, Regional stratigraphy of the Ferron Sandstone, *in* Chidsey, T.C.Jr., Adams, R.D., and Morris, T.H., eds., Regional to Wellbore Analog for Fluvial-Deltaic Reservoir Modeling: The Ferron Sandstone of Utah: American Association of Petroleum Geologists (AAPG) Studies in Geology 50, p. 211-224.

Armstrong, R.L., 1968, Sevier orogenic belt in Nevada and Utah: Geological Society of America Bulletin, v. 79, p. 429-458.

Arnott, R.W., 1993, Quasi-planar-laminated sandstone beds of the Lower Cretaceous Bootlegger Member, north-central Montana: evidence of combined-flow sedimentation: Journal of Sedimentary Petrology, v. 63, p. 488-494.

Arnott, R.W., and Southard, J.B., 1990, Exploratory flow-duct experiments on combined-flow bed configurations, and some implications for interpreting storm-event stratification: Journal of Sedimentary Petrology, v. 60, p. 211-219.

Aschoff, J.L., and Steel, R.J., 2011, Anatomy and development of a low accommodation clastic wedge, Upper Cretaceous, Cordilleran foreland Basin, USA: Sedimentary Geology, v. 236, p. 1–24.

Asquith, D.O., 1970, Depositional topography and major marine environments, Late Cretaceous, Wyoming: American Association of Petroleum Geologists Bulletin, v. 54, p. 1184-1224.

Baer, J.L., Davis, R.L., and George, S.E., 1982, Structure and stratigraphy of the Pavant Range, central Utah, in Nielson, D.L. (ed), Overthrust belt of Utah: Utah Geological Association Publication 10, p. 31-48. *(ordered ILL on May 22, 2018 - pending)*

Balsley, J.K., 1980, Cretaceous wave-dominated delta systems, Book Cliffs, east-central Utah: American Association of Petroleum Geologists, Continuing Education Course, Field Guide, 163 p.

Bann, K.L., Tye, S.C., MacEachern, J.A., Fielding, C.R., and Jones, B.G., 2008, Ichnological and sedimentologic signatures of mixed wave- and storm-dominated deltaic deposits: Examples from the Early Permian Sydney Basin, Australia, *in* Hampson G.J., Steel R.J., Burgess, P.M., and Dalrymple, R.W., eds., Recent Advances in Models of Siliciclastic Shallow-Marine Stratigraphy: SEPM Special Publication No. 90, p. 293-332.

Barton, M.D., Angle, E.S., and Tyler, N., 2004, Stratigraphic architecture of fluvial-deltaic sandstones from the Ferron Sandstone outcrop, east-central Utah, *in* Chidsey, T.C.Jr., Adams, R.D., and Morris, T.H., eds., Regional to Wellbore Analog for Fluvial-Deltaic Reservoir Modeling: The Ferron Sandstone of Utah: American Association of Petroleum Geologists (AAPG) Studies in Geology 50, p. 193-210.

Bartschi, N.C., Saylor, J.E., Lapen, T.J., Blum, M.D., Pettit, B.S., and Andrea, R.A., 2018, Tectonic controls on Late Cretaceous sediment provenance and stratigraphic architecture in the Book Cliffs, Utah: Geological Society of America Bulletin, v. 130, p. 1763-1781.

Bergman, K.M., and Snedden, J.W., 1999, (editors), Isolated Shallow Marine Sand Bodies: Sequence Stratigraphic Analysis and Sedimentologic Interpretation: SEPM (Society for Sedimentary Geology) Special Publication 64, 362 p.

Best, J.L., Kostaschuk, R.A., Peakall, J., Villard, P.V., and Franklin, M., 2005, Whole flow field dynamics and velocity pulsing within natural sediment-laden underflows: Geology, v. 33, p. 765-768.

Bhattacharya, J.P., 2011, Practical problems in the application of the sequence stratigraphic method and key surfaces: integrating observations from ancient fluvial-deltaic wedges with Quaternary and modelling studies: Sedimentology, v. 58, p. 120-169.

Bhattacharya, J.P., and Abreu, V., 2016, Wheeler's confusion and the seismic revolution: how geophysics saved stratigraphy: SEPM Sedimentary Record, v.14, p. 4-11.

Bhattacharya, J.P., and Giosan, L., 2003, Wave-influenced deltas: geomorphological implications for facies reconstruction: Sedimentology, v. 50, p. 187-210.

Bhattacharya, J.P., and MacEachern, J.A., 2009, Hyperpycnal rivers and prodeltaic shelves in the Cretaceous Seaway of North America: Journal of Sedimentary Research, v. 79, p. 184-209.

Bhattacharya, J.P., and Walker, R.G., 1992, Deltas, *in* Walker, R.G., and James, N.P., eds., Facies Models: Response to Sea Level Change: Geological Association of Canada, p. 157-177.

Bhattacharya, J.P., Robinson, A.B., Olariu, C., Adams, M.M., and Howell, C.D.Jr., 2001, Terminal distributary channels, Cretaceous Panther Tongue Sandstone, Utah: American Association of Petroleum Geologists Annual Meeting, Denver, Colorado, p. A18.

Bhattacharya, J.P., MacEachern, J.A., Vakarelov, B., Howell, C.D.Jr., and Covault, A.H., 2005, Hyperpycnal versus hypopycnal river plumes and the origin of shelf

mud: examples from the Cretaceous of the Western Interior Seaway, North America: American Association of Petroleum Geologists Annual Convention, Calgary, Alberta, Abstract, p. A16.
Bhattacharya, J.P., MacEachern, J.A., Vakarelov, B., and Howell, C.D. III., 2007, Hyperpycnal versus hypopycnal river plumes and the origin of shelf mud: examples from the Cretaceous Interior Seaway of North America, , *in* MacEachern, J.A., Gingras, M.K., Bann, K.L., and Pemberton, S.G., eds., Ichnological Applications to Sedimentological and Sequence tratigraphic Problems Abstract Volume: SEPM (Society for Sedimentary Geology) Research Conference, May 20-26, Price, Utah, USA, p. 20-23.
Bhattacharya, J.P., Copeland, P., Lawton, T.F., and Holbrook, J., 2016, Estimation of source area, river paleo-discharge, paleoslope, and sediment budgets of linked deep-time depositional systems and implications for hydrocarbon potential: Earth-Science Reviews, v. 153, p. 77-110.
Bhattacharyya, P., Bhattacharya, J.P., and Khan, S.D., 2015, Paleo-channel reconstruction and grain size variability in fluvial deposits, Ferron Sandstone, Notom Delta, Hanksville, Utah: Sedimentary Geology, v. 325, p. 17-25.
Birgenheier, L.P., Horton, B., McCauley, A.D., Johnson, C.L., and Kennedy, A., 2017, A depositional model for offshore deposits of the lower Blue Gate Member, Mancos Shale, Uinta Basin, Utah, USA: Sedimentology, v. 64, p. 1402-1438.
Blum, M.D., and Aslan, A., 2006. Signatures of climate vs. sea-level change within incised valley-fill successions: Quaternary examples from the Texas Gulf Coast. Sedimentary Geology, v. 190, p. 177–211.
Blum, M.D., and Törnqvist, T.E., 2000. Fluvial responses to climate and sea-level change: a review and look forward. Sedimentology, v. 47, p. 2–48.
Blum, M.D., Martin, J.M., Milliken, K., and Garvin, M., 2013, Paleovalley systems: Insights from Quaternary analogs and experiments: Earth-Science Reviews, v. 116, p. 128-169.
Bøe, R., Bugge, T., Rise, L., Eidnes, G., Eide, A., and Mauring, E., 2004, Erosional channel incision and the origin of large sediment waves in Trondheimsfjorden, central Norway: Geo-Marine Letters, v. 24, p. 225-240.
Boggs, S. Jr., 2006, Principles of Sedimentology and Stratigraphy: 4th Edition, Pearson Prentice Hall, New Jersey, 662 p.
Bohacs, K.M., 1998, Contrasting expressions of depositional sequences in mudrocks from marine to non-marine environs, in Schieber, J., Zimmerle, W., and Sethi, P.S., eds., Shales and Mudstones: Stuttgart, Schweizerbart'sche Verlagsbuchhandlung, p. 33–78.
Bornhold, B.D., Yang, Z.-S., Keller, G.H., Prior, D.B., Wiseman, W.J.Jr., Wang, Q., Wright, L.D., Xu, W.D., and Zhuang, Z.Y., 1986, Sedimentary framework of the modern Huanghe (Yellow River) delta: Geo-Marine Letters, v. 6, p. 77-83.
Boyd, R., Suter, J., and Penland, S., 1989, Sequence stratigraphy of the Mississippi delta: Gulf Coast Association of Geological Societies, Transactions, v. 39, p. 331-340.
Bradley, R.W., and Venditti, J.R., 2017, Reevaluating dune scale relations: Earth-Science Reviews, v. 165, p. 356-376.
Bridge, J.S., 1975, Computer simulation of sedimentation in meandering streams: Sedimentology, v. 22, p. 3-43.
Bridge, J.S., 2003, Rivers and floodplains: forms, processes, and sedimentary record: Blackwell Science Ltd., United Kingdom, 491 p.
Bromley, R.G., and Ekdale, A.A., 1998, Ophiomorpha irregulaire (Trace Fossil): Redescription from the Cretaceous of the Book Cliffs and Wasatch Plateau, Utah: Journal of Paleontology, v. 72, p. 773-778.
Brown, L.F.Jr., and Fisher, W.L., 1980, Geology and geometry of depositional systems, *in*, Brown, L.F.Jr., and Fisher, W.L., eds., Seismic Stratigraphic Interpretation and Petroleum Exploration: American Association of Petroleum Geologists, Continuing Education Course Note Series No. 16, 56 p.
Browne, G.H., 1994, Pot and gutter casts from the Chapel Island Formation, southeast Newfoundland – Discussion: Journal of Sedimentary Research, v. A64, p. 706-707.
Bruun, P., 1962, Sea-level rise as a cause of shoe erosion: Journal of the Waterways and Harbors Division, Proceedings of the American Society of Civil Engineers, v. 88, p. 117-130.
Bullimore, S.A., Helland-Hansen, W., Henriksen, S.,. and Steel, R.J., 2008, Shoreline trajectory and its impact on coastal depositional environments: an example from the Upper Cretaceous Mesaverde Group, NW Colorado, *in*, G.J. Hampson, R.J. Steel, P.M. Burgess, and R.W. Dalrymple, eds., Recent Advances in Models of Siliciclastic Shallow-Marine Stratigraphy: SEPM Spec. Publ. No. 90, p. 209-236.
Burne, R.V., 1995, Return of 'The Fan That Never Was': Westphalian turbidite systems in the Variscan Culm Basin: Bude Formation (south-west England), *in*, Plint, A.G., ed., Sedimentary Facies Analysis: International Association of Sedimentologists Special Publication No. 22, p. 101-135.
Burne, R.V., 1998, Return of 'The Fan That Never Was': Westphalian turbidite systems in the Variscan Culm Basin: Bude Formation (south-west England), Reply: Sedimentology, v. 45, p. 970-975.
Burns, C.E., Mountney, N.P., Hodgson, D.M., and Colombera, L., 2017, Anatomy and dimensions of fluvial crevasse-splay deposits: Examples from the Cretaceous Castlegate Sandstone and Neslen Formation, Utah, USA: Sedimentary Geology, v. 351, p. 21-35.
Buatois, L.A., Mángano, M.G., and Pattison, S.A.J., 2010, Trace fossils from a prodeltaic channel and lobe complex, Aberdeen and Kenilworth members, Upper Cretaceous, Book Cliffs, Utah: Ichnologic signatures of turbidites and hyperpycnites in deltaic systems: 18th International Sedimentological Congress, September 26 to October 1, Mendoza, Argentina.
Buatois, L.A., Mángano, M.G., and Pattison, S.A.J., 2017, Ichnology of an Upper Cretaceous prodeltaic lobe and channel complex from the Book Cliffs, Utah, United States: Assessing ichnofaunal variability of hyperpycnal deposits. 14th International Ichnofabric Workshop, Taipei, Taiwan; April 29th to May 2nd; Department of Geosciences, National Taiwan University and the National Taiwan Museum.
Buatois, L.A., Mángano, M.G., and Pattison, S.A.J., 2019, Ichnology of prodeltaic hyperpycnal-turbidite channel complexes and lobes from the Upper Cretaceous Prairie Canyon Member of the Mancos Shale, Book Cliffs, Utah, U.S.A.: Sedimentology, v. 66, p.
Campbell, C.V., 1967, Lamina, laminaset, bed and bedset: Sedimentology, v. 8, p. 7–26.
Chaiwongsaen, N., 2005, Sedimentology and stratigraphy of the Prairie Canyon Member, Salt and Bootlegger Washes, Thompson Springs, eastern Utah: : M.Sc. thesis, Colorado School of Mines, 186 p.
Chamberlin, E.P., and Hajek, E.A., 2015, Interpreting paleo-avulsion dynamics from multistorey sand bodies: Journal of Sedimentary Research, v. 85, p. 82-94.
Chan, M.A., 1992, Oolitic ironstone of the Cretaceous Western Interior Seaway, east-central Utah: Journal of Sedimentary Petrology, v. 62, p. 693-705.
Chan, M.A., Newman, S.L., and May, F.E., 1991, Deltaic and shelf deposits in the Cretaceous Blackhawk Formation and Mancos Shale, Grand County, Utah: Utah Geological Survey, Miscellaneous Publication 91-6, 83 p.
Chan, M.A., and Pfaff, B.J., 1991, Fluvial sedimentology of the Upper Cretaceous Castlegate Sandstone, Book Cliffs, Utah, *in* Chidsey, T.C.Jr., ed., Geology of East-Central Utah: Utah Geological Association Publication 19, 1991 Field Symposium, p. 95-109.
Charvin, K., Hampson, G.J., Gallagher, K.L., and Labourdette, R., 2010, Intra-parasequence architecture of an interpreted asymmetrical wave-dominated delta: Sedimentology, v. 57, p. 760-785.
Charvin, K., Hampson, G.J., Gallagher, K.L., Storms, J.E.A., and Labourdette, R., 2011, Characterization of controls on high-resolution stratigraphic architecture in wave-dominated shoreface-shelf parasequences using inverse numerical modeling: Journal of Sedimentary Research, v. 81, p. 562-578.
Christiansen, R.W., 1952, Structure and stratigraphy of the Canyon Range, central Utah: Geological Society of America Bulletin, v. 63, p. 717-740.
Chronic, H., 1990, Roadside geology of Utah: Mountain Press Publishing Company, Missoula, Montana, 326 p.
Cluff, R.M., Shanley, K.W., and Miller, M.A., 2007, Three things we thought we understood about shale gas, but were afraid to ask: American Association of Petroleum Geologists Annual Convention, April 1 to 4, Long Beach, California, Abstract, p. 25-26.
Cobban, W.A., 1969, The Late Cretaceous ammonites *Scaphites leei* Reeside and *Scaphites hippocrepis* (DeKay) in the Western Interior of the United States: U.S. Geological Survey Professional Paper 619, 29p.
Cole, R.D., and Friberg, J.F., 1989, Stratigraphy and sedimentation of the Book Cliffs, *in* Nummedal, D., and Wright, R., eds, Cretaceous Shelf Sandstones and Shelf Depositional Sequences, Western Interior Basin, Utah, Colorado and New Mexico: American Geophysical Union, 28th International Congress Guidebook T119, p. 13-24.
Cole, R.D., and Young, R.G., 1991, Facies characterization and architecture of a muddy shelf-sandstone complex: Mancos B interval of Upper Cretaceous Mancos Shale, northwest Colorado – northeast Utah, *in* Miall, A.D., and Tyler, N., eds., The Three-Dimensional Facies Architecture of Terrigenous Clastic Sediments and Its Implications for Hydrocarbon Discovery and Recovery: Society of Economic Paleontologists and Mineralogists, Concepts in Sedimentology and Paleontology, v. 3, p. 277-287.

Cole, R.D., Young, R.G., and Willis, G.C., 1997, The Prairie Canyon Member, a new unit of the Upper Cretaceous Mancos Shale, west-central Colorado and east-central Utah: Utah Geological Survey, Miscellaneous Publication 97-4, 23 p.
Coleman, J.M., 1981, Deltas: Processes of Deposition and Models for Exploration: Burgess Publishing Company, CEPCO Division, Minneapolis, Second Edition, 124 p.
Coleman, J.M., Prior, D.B., and Lindsay, J.F., 1983, Deltaic influences on shelf edge instability processes, *in* Stanley, D.J., and Moore, G.T., eds., The Shelfbreak: Critical Interface on Continental Margins: Society of Economic Paleontologists and Mineralogists Special Publication 33, p. 121-137.
Coleman, J.M., and Wright, L.D., 1975, Modern river deltas: variability of processes and sand bodies, *in* Broussard, M.L., ed., Deltas, Models for Exploration: Houston Geological Society, Houston, Texas, p. 99-149.
Coleman, M.L., 1985, Geochemistry on diagenetic non-silicate minerals: kinetic considerations: Royal Society (London), Philosophical Transactions, v. A315, p. 39–56.
Collinson, J.D., 1970, Bedforms of the Tana River, Norway: Geografiska Annaler, v.52A, p. 31-56.
Collinson, J.D., 1978, Vertical sequence and sand body shape in alluvial sequences, *in* A.D. Miall, ed., Fluvial sedimentology: Canadian Society of Petroleum Geologists Memoir 5, p. 577-586.
Collinson, J.D., 1996, Alluvial sediments, *in* Reading, H.G., ed., Sedimentary Environments: Processes, Facies and Stratigraphy: Blackwell Science, Third Edition, p. 37-82.
Collinson, J.D., and Thompson, D.B., 1982, Sedimentary Structures: George Allen and Unwin (Publishers) Ltd., London, 194 p.
Corbeanu, R.M., Wizevich, M.C., Bhattacharya, J.P., Zeng, X., and McMechan, G.A., 2004, Three-dimensional architecture of ancient lower delta-plain point bars using ground-penetrating radar, Cretaceous Ferron Sandstone, Utah, *in* Chidsey, T.C.Jr., Adams, R.D., and Morris, T.H., eds., Regional to Wellbore Analog for Fluvial-Deltaic Reservoir Modeling: The Ferron Sandstone of Utah: American Association of Petroleum Geologists (AAPG) Studies in Geology 50, p. 427-449.
Cotter, E., 1975, Late Cretaceous sedimentation in a low-energy coastal zone: the Ferron Sandstone of Utah: Journal of Sedimentary Petrology, v. 45, p. 669-685.
Cross, D.B., 2016, High-frequency tectonic sequences in the Campanian Castlegate Formation during a transition from the Sevier to Laramide orogeny, Utah, U.S.A.: University of New Orleans Theses and Dissertations, Paper 2133, M.Sc. Thesis, 54 p.
Currie, C., 2008, Sandstone petrology of the upper shoreface and lobate bodies in the Kenilworth Member, Upper Cretaceous, Book Cliffs, eastern Utah: Unpublished B.Sc. Thesis, Brandon University, Brandon, Manitoba, Canada, 118 p.
Curtis, C.D., Coleman, M.L., and Love, L.G., 1986, Pore-water evolution during sediment burial from isotope and mineral chemistry of calcite, dolomite and siderite concretions: Geochimica et Cosmochimica Acta, v. 50, p. 2321–2334.
Dalrymple, R.W., and Cummings, D.I., 2005, The offshore transport of mud: why it doesn't happen and the stratigraphic implications: American Association of Petroleum Geologists Annual Convention, Calgary, Alberta, Abstract, p. A32.
Dalrymple, R.W., and Cummings, D.I., 2005, The offshore transport of mud: why it doesn't happen and the stratigraphic implications: Geological Society of America Abstracts with Programs, v. 37, no. 7, p. 403.
Dalrymple, R.W., Zaitlin, B.A., and Boyd, R., 1992, Estuarine facies models: conceptual basis and stratigraphic implications: Journal of Sedimentary Petrology, v. 62, p. 1130-1146.
Davies, P., Williams, H., and Pattison, S.A.J., 2008, Capturing credible reservoir architecture in 3-D sub-surface models: a comparison of some geostatistical and deterministic approaches: American Association of Petroleum Geologists Annual Convention, April 20 to 23, San Antonio, Texas, p. 39.
Davies, P, Williams, H., Pattison, S.A.J., and Moscariello, A., 2009, Optimizing 3-D modelling strategies of shoreface reservoirs using outcrop data: EAGE (European Association of Geoscientists & Engineers) Annual Meeting, June 8 to 11, Amsterdam, The Netherlands.
Davies, R., Diessel, C., Howell, J., Flint, S., and Boyd, R., 2005, Vertical and lateral variations in the petrography of the Upper Cretaceous Sunnyside coal of eastern Utah, U.S.A. - Implications for the recognition of high-resolution accommodation changes in paralic coal seams: International Journal of Coal Geology, v. 61, p. 13-33.
Davies, R., Howell, J., Boyd, R., Flint, S., and Diessel, C., 2006, High-resolution sequence-stratigraphic correlation between shallow-marine and terrestrial strata: Examples from the Sunnyside Member of the Cretaceous Blackhawk Formation, Book Cliffs, eastern Utah: American Association of Petroleum Geologists Bulletin, v. 90, p. 1121-1140.
DeCelles, P.G., Lawton, T.F., and Mitra, G., 1995, Thrust timing, growth of structural culminations, and synorogenic sedimentation in the type Sevier orogenic belt, western United States: Geology, v. 23, p. 699-702.
DeCelles, P.G., and Coogan, J.C., 2006, Regional structure and kinematic history of the Sevier fold-and-thrust belt, central Utah: Geological Society of America Bulletin, v. 118, p. 841-864.
Delebo, N.J. II, 2005, Stratigraphic and sedimentologic evolution of an exhumed shoreface profile, the Kenilworth Member of the Blackhawk Formation, Book Cliffs, east-central Utah, U.S.A.: M.Sc. thesis, Colorado School of Mines, 191 p.
Derbowka, J., 2009, High resolution stratigraphy, Desert-Castlegate, Thompson Canyon, Utah: Unpublished B.Sc. Thesis, Brandon University, Brandon, Manitoba, Canada, 65 p.
Diessel, C., 2007, Utility of coal petrology for sequence stratigraphic analysis: International Journal of Coal, v.70, p.3-34.
Doelling, H.H., 1985, Geology of Arches National Park: Utah Geological and Mineral Survey, To Accompany Map 74, 15 p.
Doelling, H.H., Willis, G.C., Jensen, M.E., and Davis, F.D., 1987, Geology and Grand County: Utah Geological and Mineral Survey, Geologic Conference of Grand County, May 14-15, Moab, Utah, 16 p.
Doelling, H.H., Ross, M.L., and Mulvey, W.E., 2002, Geological map of the Moab 7.5′ quadrangle, Grand County, Utah: Utah Geological Survey, Map 181, 34 p.
Doust, H., and Omatsola, E., 1990, Niger Delta, *in* Edwards, J.D., and Santogrossi, P.A., eds., Divergent/Passive Margin Basins: American Association of Petroleum Geologists, Memoir 48, p. 201-238.
Dumas, S., Arnott, R.W.C., and Southard, J.B., 2005, Experiments on oscillatory-flow and combined-flow bed forms: implications for interpreting parts of the shallow-marine sedimentary record: Journal of Sedimentary Research, v. 75, p. 501-513.
Edwards, C.M., Hodgson, D., Flint, S., and Howell, J., 2004, Turbidite deposition during forced regression in a ramp margin: Turonian Lower Ferron Sandstone Member of the Mancos Shale, central Utah: American Association of Petroleum Geologists Annual Convention, Dallas, Texas, Abstract.
Edwards, C.M., Hodgson, D., Flint, S.S., and Howell, J.A., 2005, Contrasting styles of shelf sediment transport and deposition in a ramp margin setting related to relative sea-level change and basin floor topography, Turonian (Cretaceous) Western Interior of central Utah, USA: Sedimentary Geology, v. 179, p. 117-152.
Edwards, C.M., Howell, J.A., and Flint, S.S., 2005, Depositional and stratigraphic architecture of the Santonian Emery Sandstone of the Mancos Shale: implications for Late Cretaceous evolution of the Western Interior Foreland Basin of central Utah, U.S.A.: Journal of Sedimentary Research, v. 75, p. 280-299.
Eide, C.H., Howell, J.A., and Buckley, S.J., 2014, Distribution of discontinuous mudstone beds within wave-dominated shallow-marine deposits: Star Point Sandstone and Blackhawk Formation, Eastern Utah: American Association of Petroleum Geologists Bulletin, v. 98, p. 1401-1429.
Eide, C.H., Howell, J.A., and Buckley, S.J., 2015, Sedimentology and reservoir properties of tabular and erosive offshore transition deposits in wave-dominated, shallow-marine strata: Book Cliffs, USA: Petroleum Geoscience, v. 21, p. 55-73.
Ejedawe, J.E., 1981, Patterns of incidence of oil reservoirs in the Niger Delta basin: American Association of Petroleum Geologists Bulletin, v. 65, p. 1574-1585.
Elliott, T., 1986, Siliciclastic shorelines, *in* Reading, H.G., ed., Sedimentary Environments and Facies: Blackwell Scientific Publications, Second Edition, p. 155-188.
Elliott, T., 2000a, Megaflute erosion surfaces and the initiation of turbidite channels: Geology, v. 28, p. 119-122.
Elliott, T., 2000b, Depositional architecture of a sand-rich, channelized turbidite system: the upper Carboniferous Ross Sandstone Formation, western Ireland, *in* Weimer, P., Slatt, R.M., Bouma, A.H., and Lawrence, D.T., eds., Deep-Water Reservoirs of the World: Gulf Coast Section SEPM Foundation 20th Annual Research Conference, p. 342-373.
Embry, A.F., 1993, Transgressive-regressive (T-R) sequence analysis of the Jurassic succession of the Sverdrup Basin, Canadaian Arctic Archipelago: Canadian Journal of Earth Science, v. 30, p. 301-320.
Embry, A.F., 1995, Sequence boundaries and sequence hierarchies: problems and proposals: *in* R.J. Steel et al. (eds.), Sequence Stratigraphy on the Northwest

European Margin, Norwegian Petroleum Society (NPF) Special Publication 5, Elsevier, Amsterdam, p. 1-11.
Enge, H.D., and Howell, J.A., 2010, Impact of deltaic clinothems on reservoir performance: dynamic studies of reservoir analogs from the Ferron Sandstone Member and Panther Tongue, Utah: American Association of Petroleum Geologists Bulletin, v. 94, p. 139-161.
Enge, H.D., Howell, J.A., and Buckley, S.J., 2010, Quantifying clinothem geometry in a forced-regressive river-dominated delta, Panther Tongue Member, Utah, USA: Sedimentology, v. 57, p. 1750-1770.
Enge, H.D., Howell, J.A., and Buckley, S.J., 2010, The geometry and internal architecture of stream mouth bars in the Panther Tongue and Ferron Sandstone Members, Utah, USA: Journal of Sedimentary Research, v. 80, p. 1018-1031.
Ethridge, F.G., and Schumm, S.A., 1978, Reconstructing paleochannel morphologic and flow characteristics: Methodology, limitations, and assessment, *in* A.D. Miall, ed., Fluvial Sedimentology: Canadian Society of Petroleum Geologists Memoir 5, p. 703-721.
Fan, S., Swift, D.J.P., Traykovski, P., Bentlet, S., Borgeld, J.C., Reed, C.W., and Niedoroda, A.W., 2004, River flooding, storm resuspension, and event stratigraphy on the northern California shelf: observations compared with simulation: Marine Geology, v. 210, p. 17-41.
Fisher, D.J., 1936, The Book Cliffs coal field in Emery and Grand Counties, Utah: United States Geological Survey, Bulletin 852, 104 p.
Fisher, D.J., Erdmann, C.E., and Reeside Jr., J.B., 1960, Cretaceous and Tertiary formations of the Book Cliffs, Carbon, Emery, and Grand Counties, Utah, and Garfield and Mesa Counties, Colorado: United States Geological Survey, Professional Paper 332, 80p.
Fisher, W.L., Brown, L.F., Scott, A.J., and McGowen, J.H., 1969, Delta systems in the exploration for oil and gas: Bureau of Economic Geology, University of Texas, Austin, 78 p.
Fitzsimmons, R., and Johnson, S., 2000, Forced regressions: recognition, architecture and genesis in the Campanian in the Bighorn Basin, Wyoming, *in* Hunt, D., and Gawthorpe, R.L., eds., Sedimentary Responses to Forced Regressions: Geological Society Special Publication No. 172, p. 113-139.
Flood, Y.S., and Hampson, G.J. 2014. Facies and architectural analysis to interpret avulsion style and variability: Upper Cretaceous Blackhawk Formation, Wasatch Plateau, Central Utah, USA: Journal of Sedimentary Research, v. 84, p. 743–762.
Flood, Y.S., and Hampson, G.J., 2015, Quantitative analysis of the dimensions and distribution of channelized fluvial sandbodies within a large-scale outcrop data set: Upper Cretaceous Blackhawk Formation, Wasatch Plateau, central Utah, USA: Journal of Sedimentary Research, v. 85, p. 315–336.
Flores, R.M., Blanchard, L.F., Sanchez, J.D., Marley, W.E., and Muldoon, W.J., 1984, Paleogeographic controls of coal accumulation, Cretaceous Blackhawk Formation and Star Point Sandstone, Wasatch Plateau, Utah: Geological Society of America Bulletin, v. 95, p. 540-550.
Forzoni, A., Hampson, G., and Storms, J., 2015, Along-strike variations in stratigraphic architecture of shallow-marine reservoir analogues: Upper Cretaceous Panther Tongue delta and coeval shoreface, Star Point Sandstone, Wasatch Plateau, central Utah, U.S.A.: Journal of Sedimentary Research, v. 85, p. 968-989.
Fouch, T.D., Lawton, T.F., Nichols, D.J., Cashion, W.B., and Cobban, W.A., 1983, Patterns and timing of synorogenic sedimentation in Upper Cretaceous rocks of central and northeast Utah, *in* Reynolds, M.W., Dolly, E.D., and Spearing, D.R., eds., Mesozoic Paleogeography of West-Central United States: Society of Economic Paleontologists and Mineralogists, Rocky Mountain Paleogeography Symposium 2, Rocky Mountain Section SEPM, p. 305-336.
Franczyk, K.J., and Pitman, J.K., 1991, Latest Cretaceous nonmarine depositional systems in the Wasatch Plateau area: Reflections of foreland to intermontane basin transition, *in* Chidsey, T.C.Jr., ed., Geology of East-Central Utah: Utah Geological Association Publication 19, 1991 Field Symposium, p. 77-93.
Franczyk, K.J., Pitman, J.K., and Nichols, D.J., 1990, Sedimentology, mineralogy, palynology, and depositional history of some uppermost Cretaceous and lowermost Tertiary rocks along the Utah Book and Roan Cliffs east of the Green River: United States Geological Survey, Bulletin 1787-N, 27 p.
Franczyk, K.J., Fouch, T.D., Johnson, R.C., Molenaar, C.M., and Cobban, W.A., 1992, Cretaceous and Tertiary paleogeographic reconstructions for the Uinta-Piceance basin study area, Colorado and Utah: United States Geological Survey, Bulletin 1787-Q, p. 1-37.
Frey, R.W., and Howard, J.D., 1985, Trace fossils from the Panther Member, Star Point Formation (Upper Cretaceous), Coal Creek Canyon, Utah: Journal of Paleontology, v. 59, p. 370-404.
Frey, R.W., and Howard, J.D., 1990, Trace fossils and depositional sequences in a clastic shelf setting, Upper Cretaceous of Utah: Journal of Paleontology, v. 64, p. 803-820.
Friedrichs, C.T., and Scully, M.E., 2007, Modeling deposition by wave-supported gravity flows on the Po River prodelta: from seasonal floods to prograding clinoforms: Continental Shelf Research, v. 27, p. 322-337.
Friedrichs, C.T., and Wright, L.D., 2004, Gravity-driven sediment transport on the continental shelf: implications for equilibrium profiles near river mouths: Coastal Engineering, v. 51, p. 795-811.
Galloway, W.E., 1975, Process framework for describing the morphologic and stratigraphic evolution of deltaic depositional systems, *in* Broussard, M.L., ed., Deltas, Models for Exploration: Houston Geological Society, Houston, Texas, p. 87-98.
Galloway, W.E., 1989, Genetic stratigraphic sequences in basin analysis I: architecture and genesis of flooding-surface bounded depositional units: American Association of Petroleum Geologists Bulletin, v. 73, p. 125-142.
Gamero, H., Laporte, L., Perdomo, J.L., Rahn, T.C., Isakson, C., and Rodriguez, F., 2006, Three-dimensional reservoir and simulation modeling of hyperpycnal systems: a case study of LAG-3047, Block X, Misoa Formation, Maracaibo Basin, Venezuela: American Association of Petroleum Geologists Annual Convention, Houston, Texas, Abstract, p. 36.
Gani, M.R., and Bhattacharya, J.P., 2007, Basic building blocks and process variability of a Cretaceous delta: internal facies architecture reveals a more dynamic interaction of river, wave, and tidal processes than is indicated by external shape: Journal of Sedimentary Research, v. 77, p. 284-302.
Gani, M.R. Ranson, A., Cross, D.B., Hampson, G.J., Gani, N.D., and Sahoo, H. 2015, Along-strike sequence stratigraphy across the Cretaceous shallow marine to coastal-plain transition, Wasatch Plateau, Utah, USA: Sedimentary Geology, v. 325, p. 59–70.
Gardner, M.H., 1995a, Tectonic and eustatic controls on the stratal architecture of mid-Cretaceous stratigraphic sequences, central Western Interior Foreland Basin of North America, *in* Dorobek, S., and Ross, J., eds., Stratigraphic Evolution of Foreland Basins: SEPM (Society for Sedimentary Geology) Special Publication 52, p. 243-281.
Gardner, M.H., 1995b, The stratigraphic hierarchy and tectonic history of the mid-Cretaceous Foreland Basin of central Utah, *in* Dorobek, S., and Ross, J., eds., Stratigraphic Evolution of Foreland Basins: SEPM (Society for Sedimentary Geology) Special Publication 52, p. 283-303.
Gardner, M.H., Cross, T.A., and Levorsen, M., 2004, Stacking patterns, sediment volume partitioning and facies differentiation in shallow-marine and coastal-plain strata of the Cretaceous Ferron Sandstone, Utah, *in* Chidsey, T.C.Jr., Adams, R.D., and Morris, T.H., eds., Regional to Wellbore Analog for Fluvial-Deltaic Reservoir Modeling: The Ferron Sandstone of Utah: American Association of Petroleum Geologists (AAPG) Studies in Geology 50, p. 95-124.
Garrison, J.R.Jr., and van den Bergh, T.C.V., 2004, High-resolution depositional sequence stratigraphy of the Upper Ferron Sandstone Last Chance Delta: an application of coal-zone stratigraphy, *in* Chidsey, T.C.Jr., Adams, R.D., and Morris, T.H., eds., Regional to Wellbore Analog for Fluvial-Deltaic Reservoir Modeling: The Ferron Sandstone of Utah: American Association of Petroleum Geologists (AAPG) Studies in Geology 50, p. 125-192.
Giovanoli, F., 1990, Horizontal transport and sedimentation by interflows and turbidity currents in Lake Geneva, *in* Tilzer, M.M., and Serruya, C., eds., Large Lakes: Ecological Structure and Function: Springer-Verlag, Berlin, p. 175-195.
Gould, H.R., 1970, The Mississippi delta complex, *in* Morgan, J.P., and Shaver, R.H., eds., Deltaic Sedimentation Modern and Ancient: Society of Economic Paleontologists and Mineralogists, Special Publication No. 15, p. 3-30.
Hajek, E.A., and Heller, P.L., 2012, Flow-depth scaling in alluvial architecture and nonmarine sequence stratigraphy: example from the Castlegate Sandstone, central Utah, U.S.A.: Journal of Sedimentary Research, v. 82, p. 121-130.
Hajek, E.A., Heller P.L., and Sheets, B.A., 2010, Significance of channel-belt clustering in alluvial basins: Geology, v.38, p. 535-538.
Hale, L.A., 1959, Intertonguing Upper Cretaceous sediments of Northeastern Utah - Northwestern Colorado, *in* Haun J.D. and R.J. Weimer, eds., Symposium on Cretaceous rocks of Colorado and adjacent areas, 11th Field Conference Guidebook: Rocky Mountain Association of Geologists, Denver, Colorado, p. 55-66.
Hamblin, A.P., and Walker, R.G., 1979, Storm-dominated shallow marine deposits: the Fernie-Kootenay (Jurassic) transition, southern Rocky Mountains: Canadian Journal of Earth Sciences, v. 16, p. 1673-1690.
Hampson, G.J., 2000, Discontinuity surfaces, clinoforms, and facies architecture in a wave-dominated, shoreface-shelf parasequence: Journal of Sedimentary Research, v. 70, p. 325-340.
Hampson, G.J., 2004a, Facies architecture and stratigraphy of “stray” shelf sandstones, Late Cretaceous Mancos Shale, northern Utah and Colorado: American

Association of Petroleum Geologists Annual Convention, Dallas, Texas, Abstract.
Hampson, G.J., 2004b, Facies architecture and stratigraphy of "stray" shelf sandstones, Late Cretaceous Mancos Shale, northern Utah and Colorado: SEPM Research Field Conference, Recent Advances in Shoreline-Shelf Stratigraphy, August 24-28, Grand Junction, Colorado, p. 32.
Hampson, G.J., 2004c, Day 3 Mancos B sandstones: SEPM Research Conference Field Guide, Recent Advances in Shoreline-Shelf Stratigraphy, Grand Junction, Colorado, 61p.
Hampson, G.J., 2010, Sediment dispersal and quantitative stratigraphic architecture across an ancient shelf: Sedimentology, v. 57, p. 96-141.
Hampson, G.J., 2016, Towards a sequence stratigraphic solution set for autogenic processes and allogenic controls: Upper Cretaceous strata, Book Cliffs, Utah, USA: Journal of the Geological Society, v. 173, no. 5, p. 817–836.
Hampson, G.J., and Howell, J.A., 2005, Sedimentologic and geomorphic characterization of ancient wave-dominated deltaic shorelines: Upper Cretaceous Blackhawk Formation, Book Cliffs, Utah, U.S.A., *in* Giosan, L., and Bhattacharya, J.P., eds., River Deltas – Concepts, Models, and Examples: SEPM (Society for Sedimentary Geology), Special Publication No. 83, p. 133-154.
Hampson, G.J., and Howell, J.A., 2017a, Shallow-marine sequence stratigraphy: Blackhawk Formation, Book Cliffs, Utah, USA, in A. Hurst, J. Kenter, and S. Graham, eds., Outcrops that change the way we practice petroleum geology: AAPG Digital Immersive Geoscience Platform, digital platform.
Hampson, G.J., and Howell, J.A., 2017b, Sedimentologic and sequence stratigraphic characteristics of wave-dominated deltas: American Association of Petroleum Geologists Bulletin, v. 101, p. 441-451.
Hampson, G.J., and Storms, J.E.A., 2003, Geomorphological and sequence stratigraphic variability in wave-dominated, shoreface-shelf parasequences: Sedimentology, v. 50, p. 667-701.
Hampson, G.J., Howell, J.A., and Flint, S.S., 1999, A sedimentological and sequence stratigraphic re-interpretation of the Upper Cretaceous Prairie Canyon Member ("Mancos B") and associated strata, Book Cliffs area, Utah, U.S.A.: Journal of Sedimentary Research, v. 69, p. 414-433.
Hampson, G.J., Burgess, P.M., and Howell, J.A., 2001, Shoreface tongue geometry constrains history of relative sea-level fall: examples from Late Cretaceous strata in the Book Cliffs, Utah: Terra Nova, v. 13, p. 188-196.
Hampson, G.J., Davies, W., Davies, S.J., Howell, J.S., and Adamson, K.R., 2005, Use of spectral gamma-ray data to refine subsurface fluvial stratigraphy: late Cretaceous strata in the Book Cliffs, Utah, USA: Journal of the Geological Society, v. 162, p. 603-621.
Hampson G.J., Steel R.J., Burgess, P.M., and Dalrymple, R.W., 2008, (editors), Recent Advances in Models of Siliciclastic Shallow-Marine Stratigraphy: SEPM (Society for Sedimentary Geology) Special Publication No. 90, 497 p.
Hampson, G.J., Procter, E.J., and Kelly, C., 2008, Controls on isolated shallow-marine sandstone deposition and shelf construction: Late Cretaceous Western Interior Seaway, northern Utah and Colorado, U.S.A., *in* Hampson G.J., Steel R.J., Burgess, P.M., and Dalrymple, R.W., eds., Recent Advances in Models of Siliciclastic Shallow-Marine Stratigraphy: SEPM Special Publication No. 90, p. 355-389.
Hampson, G.J., Rodriguez, A.B., Storms, J.E.A., Johnson, H.D., and Meyer, C.T., 2008, Geomorphology and high-resolution stratigraphy of progradational wave-dominated shoreline deposits: impact on reservoir-scale facies architecture, *in* Hampson G.J., Steel R.J., Burgess, P.M., and Dalrymple, R.W., eds., Recent Advances in Models of Siliciclastic Shallow-Marine Stratigraphy: SEPM Special Publication No. 90, p. 117-142.
Hampson, G.J., Gani, M.R., Sharman, K.E., Irfan, N., and Bracken, B., 2011, Along-strike and down-dip variations in shallow-marine sequence stratigraphic architecture: Upper Cretaceous Star Point Sandstone, Wasatch Plateau, central Utah, U.S.A.: Journal of Sedimentary Research v. 81, p. 159-184.
Hampson, G.J., Gani, M.R., Sahoo, H., Rittersbacher, A., Irfan, N., Ranson, A., Jewell, T., Gani, N.D.S., Howell, J.A., Buckley, S.J., and Bracken, B., 2012, Controls on large-scale patterns of fluvial sandbody distribution in alluvial to coastal plain strata: Upper Cretaceous Blackhawk Formation, Wasatch Plateau, Central Utah, USA: Sedimentology, v. 59, p. 2226-2258.
Hampson, G.J., Jewell, T.O., Irfan, N., Gani, M.R., and Bracken, B., 2013, Modest change in fluvial style with varying accommodation in regressive alluvial-to-coastal-plain wedge: Upper Cretaceous Blackhawk Formation, Wasatch Plateau, central Utah, U.S.A.: Journal of Sedimentary Research v. 83, p. 145-169.
Hampson, G.J., Duller, R.A., Petter, A.L., Robinson, R.A.J. & Allen, P.A. 2014, Mass-balance constraints on stratigraphic interpretation of linked alluvial-coastal-shelfal deposits: example from Cretaceous Western Interior Basin, Utah and Colorado, USA: Journal of Sedimentary Research, v. 84, p. 935–960.
Harms, J.C., Southard, J.B., and Walker, R.G., 1982, Structures and sequences in clastic rocks: Society of Economic Paleontologists and Mineralogists (SEPM), Short Course No. 9, 249 p.
Hart, B.S., Vantfoort, R.M., and Plint, A.G., 1990, Is there evidence for geostrophic currents preserved in the sedimentary record of inner to middle-shelf deposits?-Discussion: Journal of Sedimentary Petrology, v. 60, p. 633-635.
Hart, B.S., and Plint, A.G., 1993, Tectonic influence on deposition and erosion in a ramp setting: Upper Cretaceous Cardium Formation, Alberta Foreland Basin: American Association of Petroleum Geologists Bulletin, v. 12, p. 2092-2107.
Hayes, M.O., 1967, Hurricanes as geological agents: case studies of Hurricane Carla, 1961 and Cindy, 1963: Texas Bureau of Economic Geology, Report of Investigations No. 61, 56 p.
Helland-Hansen, W., and Hampson, G.J., 2009, Trajectory analysis: concepts and applications: Basin Research, v. 21, p. 454-483.
Helland-Hansen, W., and Martinsen, O.J., 1996, Shoreline trajectories and sequences: description of variable depositional-dip scenarios: Journal of Sedimentary Research, v. 66, p. 670-688.
Hettinger, R.D., and Kirschbaum, M.A., 2002, Stratigraphy of the Upper Cretaceous Mancos Shale (upper part) and Mesaverde Group in the southern part of the Uinta and Piceance Basins, Utah and Colorado: United States Geological Survey, Geological Investigations I-2764, 21 p.
Higgs, R., 1990, Is there evidence for geostrophic currents preserved in the sedimentary record of inner to middle-shelf deposits?-Discussion: Journal of Sedimentary Petrology, v. 60, p. 630-632.
Higgs, R., 1991, The Bude Formation (Lower Westphalian), SW England: siliciclastic shelf sedimentation in a large equatorial lake: Sedimentology, v. 38, p. 445-469.
Higgs, R., 1998, Return of 'The Fan That Never Was': Westphalian turbidite systems in the Variscan Culm Basin: Bude Formation (south-west England), Discussion: Sedimentology, v. 45, p. 961-967.
Higgs, R., 2004, Ross and Bude formations (Carboniferous, Ireland and England): reinterpreted as lake-shelf turbidites: Journal of Petroleum Geology, v. 27, p. 47-66.
Hill, P.S., Fox, J.M., Crockett, J.S., Curran, K.J., Friedrichs, C.T., Geyer, W.R., Milligan, T.G., Ogston, A.S., Puig, P., Scully, M.E., Traykovski, P.A., and Wheatcroft, R.A., *in press*, Chapter II. Sediment delivery to the seabed on continental margins, *in* Nittrouer, C.A. et al. eds., Continental Margin Sedimentation: Transport to Sequence, Blackwell/IAS, p. ?-?
Hintze, L.F., 1988, Geologic history of Utah, *in* B.J. Kowallis, ed., Brigham Young University Geology Studies Special Publication 7, 202 p.
Hodgetts, D., and Howell, J.A., 2000, Synthetic seismic modelling of a large-scale geological cross-section from the Book Cliffs, Utah, U.S.A.: Petroleum Geoscience, v. 6, p. 221-229.
Hoffman, T.A., 2004, Reservoir geology and high resolution sequence stratigraphy of the Prairie Canyon Member, SW Hatch Mesa area, Book Cliffs, Utah: Unpublished B.Sc. Thesis, Brandon University, Brandon, Manitoba, Canada, 50 p.
Hoffman, T.A., and Pattison, S.A.J., 2005, An isolated, storm-influenced, prodelta turbidite complex in the lower Kenilworth Member, Hatch Mesa, Book Cliffs, Utah: Geological Society of America Abstracts with Programs, v. 37, no. 7, p. 508.
Hoffmeister, K.E., 2011, Forebulge influence on deposition of the Cretaceous Castlegate Sandstone, Book Cliffs, Utah, U.S.A.: M.Sc. Thesis, University of Kansas, 107 p.
Hoffmeister, K.E., and Kamola, D.L., 2010, Forebulge influence on deposition of the Cretaceous Castlegate Sandstone, Book Cliffs, Utah, USA: AAPG International Convention and Exhibition, September 12-15, Calgary, Alberta, Canada, Abstract only.
Holbrook, J.M., 1996, Complex fluvial response to low gradients at maximum regression: A genetic link between smooth sequence-boundary morphology and architecture of overlying sheet sandstone: Journal of Sedimentary Research, v.66, p. 713-722.
Holbrook, J.M., 2010. Valleys that never were: time surfaces versus stratigraphic surfaces - Discussion. Journal of Sedimentary Research, v. 80, p. 2-3.
Holbrook, J.M., and Bhattacharya, J., 2012. Reappraisal of the sequence boundary in time and space: case and considerations for an SU (subaerial unconformity) that is not a sediment bypass surface, a time barrier, or an unconformity. Earth-Science Reviews, v. 113, p. 271–302.

Horton, B.K., Constenius, K.N., and DeCelles, P.G., 2004, Tectonic control on coarse-grained foreland-basin sequences: an example from the Cordilleran foreland basin, Utah: Geology, v. 32, p. 637-640.
Houston, W.S., Huntoon, J.E., and Kamola, D.L. 2000, Modeling of Cretaceous foreland-basin parasequences, Utah, with implications for timing of Sevier thrusting: Geology, v. 28, p. 267–270.
Howell, J.A., and Flint, S.S., 1996, Sequence stratigraphy: Short Course Lecture Notes, SPDC (Shell) Nigeria.
Howell, J.A., and Flint, S.S., 2003, PART 3 Siliciclastic case study: the Book Cliffs, *in* Coe, A.L., ed., The Sedimentary Record of Sea-Level Change: Cambridge University Press, p. 135-208.
Howell, J.A., and Flint, S.S., 2003, 9 Sequences and systems tracts in the Book Cliffs, and 10 Sequence stratigraphical evolution of the Book Cliffs succession, *in* Coe, A.L., ed., The Sedimentary Record of Sea-Level Change: Cambridge University Press, p. 179-208.
Howell, J.A., Skorstad, A., McDonald, A., Fordham, A., Flint, S.S., Fjellvoll, B., and Manzocchi, T., 2008a, Sedimentological parameterization of shallow-marine reservoirs: Petroleum Geoscience, v. 14, p. 17–34.
Howell, J.A., Vassel, A°., and Aune T., 2008b, Modelling of dipping clinoform barriers within deltaic outcrop analogues from the Cretaceous Western Interior Basin, USA, in P. Griffiths, J. Hegre, A. Robinson, and S. Price, eds., The future of geological modelling in hydrocarbon development: Geological Society, London, Special Publications 2008, v. 309, p. 99–121.
Howell, J.A., Eide, C.H., and Hartley, A.J., 2015, No evidence for sea level fall in the Cretaceous strata of the Book Cliffs of eastern Utah (Abstract): British Sedimentological Research Group Conference (BSRG), December 19-22, University of Keele, Staffordshire, UK, p. 55.
Howell, J.A., Eide, C.H., and Hartley, A.J., 2018, No evidence for significant sea level fall in the Cretaceous strata of the Book Cliffs of eastern Utah (Abstract): AAPG Annual Convention and Exhibition, May 20-23, Salt Lake City, Utah.
Hsu, S-C., Lin, F-J., Jeng, W-L., Chung, Y., Shaw, L-M., and Hung, K-W., 2004, Observed sediment fluxes in the southwesternmost Okinawa Trough enhanced by episodic events: flood runoff from Taiwan rivers and large earthquakes: Deep-Sea Research I, v. 51, p. 979-997.
Hudleson, P.M., 1984, Sedimentology and paleogeography of the Kenilworth Member (Campanian) Blackhawk Formation, east-central Utah: Master's thesis, The University of Iowa, 152 p.
Hwang, I-G., and Heller, P.L., 2002, Anatomy of a transgressive lag: Panther Tongue Sandstone, Star Point Formation, central Utah: Sedimentology, v. 49, p. 977-999.
Jackson, J.A. (editor), 1997, Glossary of Geology: American Geological Institute, 4th Edition, Alexandria, Virginia, 769 p.
Jackson, M.D., Hampson, G.J., and Sech, R.P., 2009, Three-dimensional modeling of a shoreface-shelf parasequence reservoir analog: Part 2. Geologic controls on fluid flow and hydrocarbon recovery: AAPG Bulletin, v. 93, p. 1183–1208.
James, N.P., and Dalrymple, R.W. (editors), 2010, Facies Models 4: Geological Association of Canada, 586 p.
Jennette, D.C., and Riley, C.O., 1996, Influence of relative sea-level on facies and reservoir geometry of the Middle Jurassic lower Brent Group, UK North Viking Graben, *in* Howell, J.A., and Aitken, J.F., eds., High Resolution Sequence Stratigraphy: Innovations and Applications: Geological Society Special Publication No. 104, p. 87-113.
Johnson, K.S., Paull, C.K., Barry, J.P., and Chavez, F.P., 2001, A decadal record of underflows from a coastal river into the deep sea: Geology, v. 29, p. 1019-1022.
Johnson, R.C. 2003, Depositional framework of the Upper Cretaceous Mancos Shale and the lower part of the Upper Cretaceous Mesaverde Group, Western Colorado and Eastern Utah. *in* Petroleum Systems and Geologic Assessment of Oil and Gas in the Uinta–Piceance Province, Utah and Colorado. US Geological
Survey, Professional Paper Digital Data Series, DDS-69-B, Chapter 10 (CD-ROM only).
Jones, H.J., and Hajek, E.A. 2007, Characterising avulsion stratigraphy in ancient alluvial deposits: Sedimentology Geology, v. 202, p. 124–137.
Jones, B.M., 2007, Regional correlation of key stratigraphic markers in the Lower Castlegate Sandstone to Dakota Siltstone stratigraphic interval, subsurface of east-central Utah: Unpublished B.Sc. Thesis, Brandon University, Brandon, Manitoba, Canada, 39 p.
Jordan, T.E., 1981, Thrust loads and foreland basin evolution, Cretaceous, western United States: American Association of Petroleum Geologists Bulletin, v. 65, p. 2506-2520.
Kamola, D.L., 1984, Trace fossils from marginal-marine facies of the Spring Canyon Member, Blackhawk Formation (Upper Cretaceous), East-Central Utah: Journal of Paleontology, v. 58, p. 529-541.
Kamola, D.L., and Huntoon, J.E., 1992, Sequence boundary variations within the Aberdeen Member, Cretaceous Blackhawk Formation, Utah: American Association of Petroleum Geologists Annual Convention, Calgary, Alberta, Abstract, p. 61-62.
Kamola, D.L., and Huntoon, J.E., 1995, Repetitive stratal patterns in a foreland basin sandstone and their possible tectonic significance: Geology, v. 23, p. 177-180.
Kamola, D.L., and Hoffmeister, K.E., 2010, Decoupling of the Sevier Foreland Basin from the Cretaceous Western Interior Seaway during lowstand events: AAPG Annual Convention and Exhibition, April 11-14, Houston, Texas, USA, Abstract only.
Kamola, D.L., and Van Wagoner, J.C., 1995, Stratigraphy and facies architecture of parasequences with examples from the Spring Canyon Member, Blackhawk Formation, Utah, *in* Van Wagoner, J.C., and Bertram, G.T., eds., Sequence Stratigraphy of Foreland Basin Deposits – Outcrop and Subsurface Examples from the Cretaceous of North America: American Association of Petroleum Geologists, Memoir 64, p. 27-54.
Karssenberg, D., and Bridge, J.S. 2008, A three-dimensional numerical model of sediment transport, erosion and deposition within a network of channel belts, floodplain and hill slope: extrinsic and intrinsic controls on floodplain dynamics and alluvial architecture: Sedimentology, v. 55, p. 1717–1745.
Kassem, A., and Imran, J., 2001, Simulation of turbid underflows generated by the plunging of a river: Geology, v. 29, p. 655-658.
Kauffman, E.G., 1977, Geological and biological overview: Western Interior Cretaceous Basin, *in* Kauffman, E.G., ed., Cretaceous facies, faunas, and paleoenvironments across the Western Interior Basin: Mountain Geologist, v. 14, p. 75-99.
Kellogg, H.E., 1977, Geology and petroleum of the Mancos B Formation, Douglas Creek Arch area Colorado and Utah, *in* Veal, H.K., ed., Exploration Frontiers of the Central and Southern Rockies: Rocky Mountain Association of Geologists, Denver, Colorado, 1977 Symposium, p. 167-179.
Krystinik, L.F., and DeJarnett, B.B., 1995, Lateral variability of sequence stratigraphic framework in the Campanian and Lower Maastrichtian of the Western Interior Seaway: AAPG Memoir 64, Sequence Stratigraphy of Foreland Basin Deposits, p. 11-26.
Krystinik, L., 2004, Two end-member examples of isolated shelf sandstone bodies: the Kremmling and Muddy Buttes Sandstones, Wolcott, Colorado: SEPM Research Field Conference, Recent Advances in Shoreline-Shelf Stratigraphy, August 24-28, Grand Junction, Colorado, p. 9.
Larson, N.L., Jorgensen, S.D., Farrar, R.A., and Larson, P.L., 1997, Ammonites and the other cephalopods of the Pierre Seaway: an identification guide: Black Hills Institute of Geological Research, Geoscience Press Inc., Tucson, Arizona, 148 p.
Lawton, T.F., 1983, Late Cretaceous fluvial systems and the age of foreland uplifts in central Utah, *in* Lowell, J.D., ed., Rocky Mountain Foreland Basins and Uplifts: Rocky Mountain Association of Geologists, Denver, p. 181-199.
Lawton, T.F., 1985, Style and timing of frontal structures, thrust belt, central Utah: American Association of Petroleum Geologists Bulletin, v. 69, p. 1145-1159.
Lawton, T.F., 1986, Fluvial systems of the Upper Cretaceous Mesaverde Group and Paleocene North Horn Formation, central Utah: a record of transition from thin-skinned to thick-skinned in the foreland region, *in* Peterson, J.A., ed., Paleotectonics and Sedimentation in the Rocky Mountain Region, United States: American Association of Petroleum Geologists Memoir 41, p. 423-442.
Lawton, T.F., Pollock, S.L., and Robinson, R.A.J., 2003, Integrating sandstone petrology and nonmarine sequence stratigraphy: application to the Late Cretaceous fluvial systems of southwestern Utah, U.S.A.: Journal of Sedimentary Research, v. 73, p. 389-406.
Lawton, T.F., and Bradford, B.A., 2011, Correlation and provenance of Upper Cretaceous (Campanian) fluvial strata, Utah, USA, from zircon U–Pb geochronology and petrography: Journal of Sedimentary Research, v. 81, p. 495-512.
Leckie, D.A., and Krystinik, L.F., 1989, Is there evidence for geostrophic currents preserved in the sedimentary record of inner to middle-shelf deposits?: Journal of Sedimentary Petrology, v. 59, p. 862-870.
Leckie, D.A., and Krystinik, L.F., 1990, Is there evidence for geostrophic currents preserved in the sedimentary record of inner to middle-shelf deposits?-Reply: Journal of Sedimentary Petrology, v. 60, p. 636-637.
Leckie, D.A., and Krystinik, L.F., 1991, Is there evidence for geostrophic currents preserved in the sedimentary record of inner to middle-shelf deposits?-Reply: Journal of Sedimentary Petrology, v. 61, p. 152-154.
Lee, K., Szerbiak. R., McMechan, G.A., and Hwang, N., 2009, A 3-D ground-penetrating radar and wavelet transform analysis of the morphology of shoreface

deposits in the Upper Cretaceous Ferron Sandstone Member, Utah: AAPG Bulletin, v.93, No. 2, p. 181-201.
Leeder, M.R., 1973, Fluviatile fining-upward cycles and the magnitude of paleochannels: Geological Magazine, v. 3, p. 265-276.
Legler, B., Hampson, G.J., Jackson, C.A-L., Johnson, H.D., Massart, B.Y.G., Sarginson, M., and Ravnås R., 2014, Facies relationships and stratigraphic architecture of distal, mixed tide- and wave-influenced deltaic deposits: Lower Sego Sandstone, Western Colorado, U.S.A.: Journal of Sedimentary Research, v. 84, p. 605-625.
Leithold, E.L., 1993, Preservation of laminated shale in ancient clinoforms; comparison to modern subaqueous deltas: Geology, v. 21, p. 359-362.
Leithold, E.L., 1994, Stratigraphical architecture at the muddy margin of the Cretaceous Western Interior Seaway, southern Utah: Sedimentology, v. 41, p. 521-542.
Leopold, L.B., and Wolman, M.G., 1960, River meanders: Bulletin of the Geological Society of America, v. 71, p. 769-794.
Leuven, J.R.F.W., van Maanen, B., Lexmond, B.R., van der Hoek, B.V., Spruijt, M.J., and Kleinhans, M.G., 2018, Dimensions of fluvial-tidal meanders: Are they disproportionally large?: Geology, v. 46, p. 923-926.
Løseth, T.M., Steel, R.J., Crabaugh, J.P., and Schellpeper, M. 2006, Interplay between shoreline migration paths, architecture and pinchout distance for siliciclastic shoreline tongues: evidence from the rock record: Sedimentology, v. 53, p. 735–767.
Loutit, T.S., Hardenbol, J., Vail, P.R., and Baum, G.R., 1988, Condensed sections: the key to age determination and correlation of continental margin sequences, *in* Wilgus, C.K., Hastings, B.S., Kendall, C.G.St.C., Posamentier, H.W., Ross, C.A., and Van Wagoner, J.C., eds., Sea-Level Changes: An Integrated Approach: Society of Economic Paleontologists and Mineralogists, Special Publication No. 42, p. 183-213.
Lukens, C.E., Myrow, P.M., Lamb, M., Houck, K., and Parsons, J., 2004, Wave-modified turbidites: hyperpycnal flow deposits in the Minturn Formation, central Colorado: Geological Society of America Abstracts with Programs, v. 36, Rocky Mountain and Cordilleran Joint Meeting, Boise, Idaho, Paper No. 16-2.
MacEachern, J.A., Bann, K.L., Bhattacharya, J.P., and Howell, C.D.Jr., 2005, Ichnology of deltas: organism responses to the dynamic interplay of rivers, waves, storms and tides, *in* Giosan, L., and Bhattacharya, J.P., eds., River Deltas – Concepts, Models, and Examples: SEPM (Society for Sedimentary Geology), Special Publication No. 83, p. 49-85.
MacEachern, J.A., Pemberton, S.G., and Bhattacharya, J.P., 2007, Ichnological and sedimentological evaluation of the Ferron Sandstone cycles in Ivie Creek Cores #3 and #11, *in* MacEachern, J.A., Gingras, M.K., Bann, K.L., and Pemberton, S.G., eds., Ichnological Applications to Sedimentological and Sequence Stratigraphic Problems Abstract Volume: SEPM (Society for Sedimentary Geology) Research Conference, May 20-26, Price, Utah, USA, p. 144-174.
MacEachern, J.A., Pemberton, S.G., Gingras, M.K., and Bann, K.L., 2010, Ichnology and facies models, in James, N.P., and Dalrymple, R.W., eds., Facies Models 4: GEOtext 6, Geological Association of Canada, p. 19-58.
Machent, P.G., Taylor, K.G., Macquaker, J.H.S., and Marshall, J.D., 2007, Patterns of early post-depositional and burial cementation in distal shallow-marine sandstones: Upper Cretaceous Kenilworth Member, Book Cliffs, Utah, USA: Sedimentary Geology, v. 198, p. 125-145.
Macquaker, J.H.S., and Taylor, K.G., 1996, A sequence stratigraphic interpretation of a mudstone-dominated succession: the Lower Jurassic Cleveland Ironstone Formation, U.K.: Journal of the Geological Society London, v. 153, p. 759-770.
Macquaker, J.H.S., and Adams, A.E., 2003, Maximizing information from fine grained sediments: an inclusive nomenclature for mudstones: Journal of Sedimentary Research, v. 73, p. 735–744.
Macquaker, J.H.S., and Bohacs, K.M., 2007, On the accumulation of mud: Science, v. 318, p. 1734-1735.
Macquaker, J.H.S., and Taylor, K.G., 1996, A sequence stratigraphic interpretation of a mudstone-dominated succession: the Lower Jurassic Cleveland Ironstone Formation, U.K.: Geological Society of London, Journal, v. 153, p. 759–770.
Macquaker, J.H.S., Taylor, K.G., and Gawthorpe, R.L., 2007, High-resolution facies analysis of mudstones: implications for paleoenvironmental and sequence stratigraphic interpretations of offshore ancient mud-dominated successions: Journal of Sedimentary Research, v. 77, p. 324-339.
Madof, A.S., Christie-Blick, N., and Anders, N.H. 2015, Tectonically controlled nearshore deposition: Cozzette Sandstone, Book Cliffs, Colorado, USA: Journal of Sedimentary Research, v. 85, p. 459–488.
Marley, W.E., Flores, R.M., and Cavaroc, V.V. 1979, Coal accumulation in Upper Cretaceous marginal deltaic environments of the Blackhawk Formation and Star Point Sandstone, Emery, Utah: Utah Geology, v. 6, p. 25–40.
Martin, J.M., Paola, C., Abreu, V., Neal, J., and Sheets, B., 2009. Sequence stratigraphy of experimental strata under known conditions of differential subsidence and variable base level. AAPG Bulletin v. 93, p. 503–533.
Martin, J.M., Cantelli, A., Paola, C., Blum, M.D., and Wolinsky, M., 2011. Quantitative modeling of the evolution and geometry of incised valleys. Journal of Sedimentary Research, v. 81, p. 64–79.
Martinsen, O.J., Lien, T., and Walker, R.G., 2000, Upper Carboniferous deep water sediments, western Ireland: analogues for passive margin turbidite plays, *in*, Weimer, P., Slatt, R.M., Bouma, A.H., and Lawrence, D.T., eds., Deep-Water Reservoirs of the World: Gulf Coast Section SEPM Foundation 20th Annual Research Conference, p. 533-555.
Martinsen, O.J., and Collinson, J.D., 2002, The Western Irish Namurian Basin reassessed – a discussion: Basin Research, v. 14, p. 523-531.
Mazzullo, J., and Peterson, M., 1989, Sources and dispersal of Late Quaternary silt on the northern Gulf of Mexico continental shelf: Marine Geology, v. 86, p. 15-26.
McGookey, D.P., Haun, J.D., Hale, L.A., Goodell, H.G., McCubbin, D.G., Weimer, R.J., and Wulf, G.R., 1972, Cretaceous systems, *in* Mallory, W.W., ed., Geologic Atlas of the Rocky Mountain Region: Rocky Mountain Association of Geologists, p. 190-228.
McLaurin, B.T., and Steel, R.J., 2000, Fourth-order nonmarine to marine sequences, middle Castlegate Formation, Book Cliffs, Utah: Geology, v. 28, p. 359-362.
McLaurin, B.T., and Steel, R.J., 2001, Fourth-order nonmarine to marine sequences, middle Castlegate Formation, Book Cliffs, Utah - Reply: Geology, v. 29, p. 188.
McLaurin, B.T., and Steel, R.J., 2007, Architecture and origin of an amalgamated fluvial sheet sand, lower Castlegate Formation, Book Cliffs, Utah: Sedimentary Geology, v. 197, p. 291-311.
Mellere, D., and Steel, R., 2000, Style contrast between forced regressive and lowstand/transgressive wedges in the Campanian of south-central Wyoming (Hatfield Member of the Haystack Mountains Formation), *in* Hunt, D., and Gawthorpe, R.L., eds., Sedimentary Responses to Forced Regressions: Geological Society Special Publication No. 172, p. 141-162.
Mellere, D., Plink-Björklund, P., and Steel, R.J., 2002, Anatomy of shelf deltas at the edge of a prograding Eocene shelf margin, Spitsbergen: Sedimentology, v. 49, p. 1181-1206.
Miall, A.D., 1993, The architecture of fluvial-deltaic sequences in the Upper Mesaverde Group (Upper Cretaceous), Book Cliffs, Utah, *in* Best, J.L., and Bristow, C.S., eds., Braided Rivers: Geological Society of London Special Publication 75, p. 305-332.
Miall, A.D., 1994, Reconstructing fluvial macroform architecture from two-dimensional outcrops: examples from the Castlegate Sandstone, Book Cliffs, Utah: Journal of Sedimentary Research, v. B64, p. 146-158.
Miall, A.D. 2014, The emptiness of the stratigraphic record: A preliminary evaluation of missing time in the Mesaverde Group, Book Cliffs, Utah: Journal of Sedimentary Research, v. 84, p. 457–469.
Miall, A.D. 2016, The valuation of unconformities: Earth-Science Reviews, v. 163, p. 22-71.
Miall, A.D., and Arush, M., 2001a, The Castlegate Sandstone of the Book Cliffs, Utah: sequence stratigraphy, paleogeography, and tectonic controls: Journal of Sedimentary Research, v. 71, p. 537-548.
Miall, A.D., and Arush, M., 2001b, Cryptic sequence boundaries in braided fluvial successions: Sedimentology, v. 48, p. 971-985.
Miall, A.D., Catuneanu, O., Vakarelov, B.K. and Post, R., 2008, The Western Interior Basin, *in* Miall A.D. (ed.), The Sedimentary Basins of the United States and Canada, Sedimentary Basins of the World 5, p. 329-362.
Molenaar, C.M., and Cobban, W.A., 1991, Middle Cretaceous stratigraphy on the south and east sides of the Uinta Basin, northeastern Utah and northwestern Colorado U.S. Geological Survey Bulletin 1787-P, 34p.
Montgomery, S.L., Tabet, D.E., and Barker, C.E., 2004, Coalbed gas in the Ferron Sandstone Member of the Mancos Shale: a major Upper Cretaceous play in central Utah, *in* Chidsey, T.C.Jr., Adams, R.D., and Morris, T.H., eds., Regional to Wellbore Analog for Fluvial-Deltaic Reservoir Modeling: The Ferron Sandstone of Utah: American Association of Petroleum Geologists (AAPG) Studies in Geology 50, p. 501-528.
Moody-Stuart, M, 1966, High- and low-sinuosity stream deposits, with examples from the Devonian of Spitsbergen: Journal of Sedimentary Petrology, v. 36, p. 1102-1117.
Morton, R.A., 1981, Formation of storm deposits by wind-forced currents in the Gulf of Mexico and the North Sea, *in* Nio, S.D., Schuttenheim, R.T.E., and van

Weering, T.C.E., eds., Holocene Marine Sedimentation in the North Sea Basin: International Association of Sedimentologists, Special Publication No. 5, p. 385-396.
Mulder, T., and Alexander, J., 2001, The physical character of subaqueous sedimentary density flows and their deposits: Sedimentology, v. 48, p. 269-299.
Mulder, T., and Syvitski, J.P.M., 1995, Turbidity currents generated at river mouths during exceptional discharges to the world oceans: The Journal of Geology, v. 103, p. 285-299.
Mulder, T., Syvitski, J.P.M., and Skene, K.I., 1998, Modeling of erosion and deposition by turbidity currents generated at river mouths: Journal of Sedimentary Research, v. 68, p. 124-137.
Mulder, T., Syvitski, J.P.M., Migeon, S., Faugères, J-C., and Savoye, B., 2003, Marine hyperpycnal flows: initiation, behaviour and related deposits. A review: Marine and Petroleum Geology, v. 20, p. 861-882.
Munger, R.D., 1965, Subsurface exploration mapping, southern Uinta basin, Castlegate and Dakota-Cedar Mountain Formations: The Mountain Geologist, v. 2, p. 141-166.
Muto, T. 2001, Shoreline autoretreat substantiated in flume experiments: Journal of Sedimentary Research, v. 71, p. 246–254.
Muto, T., and Steel, R.J. 1992, Retreat of the front in a prograding delta: Geology, v. 20, p. 967–970.
Muto, T., and Steel, R.J. 1997. Principles of regression and transgression: the nature of the interplay between accommodation and sediment supply: Journal of Sedimentary Research, v. B67, p. 994–1000.
Muto, T., and Steel, R.J. 2002, Role of autoretreat and A/S changes in the understanding of deltaic shoreline trajectory: a semi-quantitative approach: Basin Research, v. 14, p. 303–318.
Muto, T., Steel, R.J., and Swenson, J.B. 2007, Autostratigraphy: a framework norm for genetic stratigraphy: Journal of Sedimentary Research, v. 77, p. 2–12.
Mutti, E., Tinterri, R., Benevelli, G., di Biase, D., and Cavanna, G., 2003, Deltaic, mixed and turbidite sedimentation of ancient foreland basins: Marine and Petroleum Geology, v. 20, p. 733-755.
Myrow, P.M., 1992a, Bypass-zone tempestite facies model and proximality trends for an ancient muddy shoreline and shelf: Journal of Sedimentary Petrology, v. 62, p. 99-115.
Myrow, P.M., 1992b, Pot and gutter casts from the Chapel Island Formation, southeast Newfoundland: Journal of Sedimentary Petrology, v. 62, p. 992-1007.
Myrow, P.M., 1994, Pot and gutter casts from the Chapel Island Formation, southeast Newfoundland – Reply: Journal of Sedimentary Research, v. A64, p. 708-709.
Myrow, P.M., and Hiscott, R.N., 1991, Shallow-water gravity-flow deposits, Chapel Island Formation, southeast Newfoundland, Canada: Sedimentology, v. 38, p. 935-959.
Myrow, P.M., and Southard, J.B., 1991, Combined-flow model for vertical stratification sequences in shallow marine storm-deposited beds: Journal of Sedimentary Petrology, v. 61, p. 202-210.
Myrow, P.M., and Southard, J.B., 1996, Tempestite deposition: Journal of Sedimentary Research, v. 66, p. 875-887.
Myrow, P.M., Fischer, W., and Goodge, J.W., 2002, Wave-modified turbidites: combined-flow shoreline and shelf deposits, Cambrian, Antarctica: Journal of Sedimentary Research, v. 72, p. 641-656.
Myrow, P.M., Snell, K.E., Hughes, N.C., Paulsen, T.S., Heim, N.A., and Parcha, S.K., 2006, Cambrian depositional history of the Zanskar Valley region of the Indian Himalaya: tectonic implications: Journal of Sedimentary Research, v. 76, p. 364-381.
Nelson, C.H., 1982, Modern shallow-water graded sand layers from storm surges, Bering Shelf: a mimic of Bouma sequences and turbidite systems: Journal of Sedimentary Petrology, v. 52, p. 537-545.
Newman, K.L., and Chan, M.A., 1991, Depositional facies and sequences in the Upper Cretaceous Panther Tongue Member of the Star Point Formation, Wasatch Plateau, Utah, *in* Chidsey, T.C.Jr., ed., Geology of East-Central Utah: Utah Geological Association Publication 19, 1991 Field Symposium, p. 65-76.
Newman, S.L., 1985, Facies interpretations and lateral relationships of the Blackhawk Formation and Mancos Shale, east-central Utah: Society of Economic Paleontologists and Mineralogists, Mid-Year Meeting Field Guidebook 10, p. 69-113.
Nielson, L.H., and Johannsessen, P.N., 2008, Are some isolated shelf sandstone ridges in the cretaceous western interior seaway transgressed, detached spit systems?, *in* Hampson G.J., Steel R.J., Burgess, P.M., and Dalrymple, R.W., eds., Recent Advances in Models of Siliciclastic Shallow-Marine Stratigraphy: SEPM Special Publication No. 90, p. 333-354.
Nittrouer, C.A., 1999, STRATAFORM: overview of its design and synthesis of its results: Marine Geology, v. 154, p. 3-12.
North American Commission on Stratigraphic Nomenclature, 1983, North American Stratigraphic Code: American Association of Petroleum Geologists Bulletin, v. 67, p. 841-875.
North, C.P., Hole, M.J., and Jones, D.G., 2005, Geochemical correlation in deltaic successions: a reality check: Geological Society of America Bulletin, v. 117, p. 620-632.
Nummedal, D., and Cole, R.D., 1993, Sequence stratigraphy of the Castlegate and Desert sandstones, Utah: an alternate view (Abstract): AAPG Annual Convention, New Orleans, p.159.
Nummedal, D., Riley, G.W., Cole, R.D., and Trevena, A.S., 1992, The falling sea level systems tract in ramp settings (Abstract), *in* Mesozoic of the Western Interior: Society of Economic Paleontologists and Mineralogists, Theme Meeting, Fort Collins, Colorado, August 17-19, p.50.
Nummedal, D., Cole, R., Young, R., Shanley, K., and Boyles, M., 2001, Book Cliffs sequence stratigraphy: the Desert and Castlegate sandstones: Grand Junction Geological Society and Society of Sedimentary Geology, Field Trip #15 Guidebook, American Association of Petroleum Geologists Annual Convention, 81 p.
O'Byrne, C.J., and Flint, S., 1993, High-resolution sequence stratigraphy of Cretaceous shallow marine sandstones, Book Cliffs outcrops, Utah, U.S.A. – application to reservoir modelling: First Break, v. 11, p. 445-459.
O'Byrne, C.J., and Flint, S., 1995, Sequence, parasequence, and intraparasequence architecture of the Grassy Member, Blackhawk Formation, Book Cliffs, Utah, U.S.A., *in* Van Wagoner, J.C., and Bertram, G.T., eds., Sequence Stratigraphy of Foreland Basin Deposits – Outcrop and Subsurface Examples from the Cretaceous of North America: American Association of Petroleum Geologists, Memoir 64, p. 225-255.
O'Byrne, C.J., and Flint, S., 1996, Interfluve sequence boundaries in the Grassy Member, Book Cliffs, Utah: criteria for recognition and implications for subsurface correlation, *in* Howell, J.A., and Aitken, J.F., eds., High Resolution Sequence Stratigraphy: Innovations and Applications: Geological Society Special Publication No. 104, p. 207-220.
Obradovich, J.D., 1993, A Cretaceous time scale, *in* Caldwell, W.G.E., and Kauffman, E.G., eds., Evolution of the Western Interior Basin: Geological Association of Canada Special Paper No. 39, p. 379-396.
Ogston, A.S., Cacchione, D.A., Sternberg, R.W., and Kineke, G.C., 2000, Observations of storm and river flood-driven sediment transport on the northern California continental shelf: Continental Shelf Research, v. 20, p. 2141-2162.
Olariu, C., and Bhattacharya, J.P., 2006, Terminal distributary channels and delta front architecture of river-dominated delta systems: Journal of Sedimentary Research, v. 76, p. 212-233.
Olariu, C., Bhattacharya, J.P., Ge, R., Xu, X., Aiken, C.L.V., Marcy, F.D., Zeng, X., and McMechan, G.A., 2001, Study of "terminal" distributary channels in fluvial-dominated delta front deposits, using ground-penetrating radar and digital mapping techniques, Cretaceous Panther Tongue Sandstone, Utah, U.S.A.: Geological Society of America Abstracts with Programs, v. 33, no. 6, p. A-355.
Olariu, C., Bhattacharya, J.P., Xu, X., Aiken, C.L.V., Zeng, X., and McMechan, G.A., 2005, Integrated study of ancient delta-front deposits, using outcrop, ground-penetrating radar, and three-dimensional photorealistic data: Cretaceous Panther Tongue Sandstone, Utah, U.S.A., *in* Giosan, L., and Bhattacharya, J.P., eds., River Deltas – Concepts, Models, and Examples: SEPM (Society for Sedimentary Geology), Special Publication No. 83, p. 155-177.
Olsen, T., Steel, R., Høgseth, K., Skar, T., and Røe, S-L, 1995, Sequential architecture in a fluvial succession: sequence stratigraphy in the Upper Cretaceous Mesaverde Group, Price Canyon, Utah: Journal of Sedimentary Research, v. B65, p. 265-280.
Onyenanu, G.I., Jacquemyn, C.E.M.M., Graham, G.H., Hampson, G.J., Fitch, P.J., and Jackson, M.D., 2018, Geometry, distribution and fill of erosional scours in a heterolithic, distal lower shoreface sandstone reservoir analogue: Grassy Member, Blackhawk Formation, Book Cliffs, Utah, USA: Sedimentology, v. 65, p. 1731-1760.
Oomkens, E., 1974, Lithofacies relations in the Late Quaternary Niger delta complex: Sedimentology, v. 21, p. 195-222.

Orton, G.J., and Reading, H.G., 1993, Variability of deltaic processes in terms of sediment supply, with particular emphasis on grain size: Sedimentology, v. 40, p. 475-512.
Pang, M., and Nummedal, D., 1995, Flexural subsidence and basement tectonics of the Cretaceous Western Interior basin, United States: Geology, v. 23, p. 173-176.
Parsons, J.D., Bush, J.W.M., and Syvitski, J.P.M., 2001, Hyperpycnal plume formation from riverine outflows with small sediment concentrations: Sedimentology, v. 48, p. 465-478.
Patruno, S., Hampson, G.J., and Jackson, C.A.-L., 2015, Quantitative characterisation of deltaic and subaqueous clinoforms: Earth-Science Reviews, v. 142, p. 79-119.
Patterson, J.E., Jr., 1983, Exploration potential and variations in shelf plume sandstones, Navarro Group (Maastrichtian), east central Texas: Master's thesis, University of Texas at Austin, 91 p.
Pattison, S.A.J., 1994a, Production- and exploration-scale applications of Book Cliffs outcrop data to the subsurface Niger Delta: Interim Report, Production Geoscience Unit, University of Aberdeen, Scotland, 119 p.
Pattison, S.A.J., 1994b, Re-interpretation of the three-dimensional architecture and stacking patterns of shallow marine and non-marine sandstones in the Kenilworth Member, Desert Member and Castlegate Sandstone, Upper Cretaceous, Book Cliffs, Utah: temporal, spatial and genetic linkage of the processes and products of lowstand erosion and deposition: Final Technical Report, Production Geoscience Unit, University of Aberdeen, Scotland, 136 p.
Pattison, S.A.J., 1994c, High resolution stacking patterns of wave-dominated deltaic parasequences, Kenilworth Member, Book Cliffs, Utah (Abstract): American Association of Petroleum Geologists Annual Meeting, Denver, Colorado, p. 230.
Pattison, S.A.J., 1995, Sequence stratigraphic significance of sharp-based lowstand shoreface deposits, Kenilworth Member, Book Cliffs, Utah: American Association of Petroleum Geologists Bulletin, v. 79, p. 444-462.
Pattison, S.A.J., 2004, Time equivalency of the Hatch Mesa succession and the lower Kenilworth Member, Book Cliffs, Utah: implications for models: SEPM Research Field Conference, Recent Advances in Shoreline-Shelf Stratigraphy, August 24-28, Grand Junction, Colorado, p. 14.
Pattison, S.A.J., 2005a, Storm-influenced prodelta turbidite complex in the lower Kenilworth Member at Hatch Mesa, Book Cliffs, Utah, U.S.A.: implications for shallow marine facies models: Journal of Sedimentary Research, v. 75, p. 420-439.
Pattison, S.A.J., 2005b, Isolated highstand shelf sandstone body of turbiditic origin, lower Kenilworth Member, Cretaceous Western Interior, Book Cliffs, Utah, USA: Sedimentary Geology, v. 177, p. 131-144.
Pattison, S.A.J., 2005c, Recognition and interpretation of isolated shelf turbidite bodies in the Cretaceous Western Interior, Book Cliffs, Utah, *in* Pederson, J., and Dehler, C.M., eds., Interior Western United States: Geological Society of America Field Guide 6, p. 479-504.
Pattison, S.A.J., 2005d, A stray sandstone finds a home: time equivalency of the Hatch Mesa succession and the lower Kenilworth Member, Book Cliffs, Utah: Geological Society of America Abstracts with Programs, v. 37, no. 6, p. 44.
Pattison, S.A.J., 2005e, Tectonic significance of shelf turbidite bodies in the upper Aberdeen Member to lower Kenilworth Member stratigraphic interval, Cordilleran Foreland Basin, Book Cliffs, eastern Utah: American Association of Petroleum Geologists Annual Convention, Calgary, Alberta, Abstract, p. A106.
Pattison, S.A.J., 2005f, Significance of inner shelf turbiditic-rich channel-fill deposits, Gunnison Butte to Tusher Canyon region, Book Cliffs, eastern Utah: : Geological Society of America Abstracts with Programs, v. 37, no. 7, p. 310.
Pattison, S.A.J., 2006a, Facies, architecture and sequence stratigraphy of fluvial-deltaic-shoreface-shelf deposits in the Campanian Blackhawk Formation and Castlegate Sandstone, Book Cliffs, east-central Utah, U.S.A.: Outcrop analogs for clastic petroleum reservoirs: Field Trip Guidebook Technical Report, Brandon University, Brandon, Manitoba, Canada, 135 p.
Pattison, S.A.J., 2006b, Transgressively-modified coarse-grained sandstones and turbidite-rich shelf deposits, upper Aberdeen to lower Kenilworth stratigraphic interval, Campanian Book Cliffs, Utah: evidence for tectonically-driven sedimentation patterns: American Association of Petroleum Geologists Annual Convention, Houston, Texas, Abstract, p. 83.
Pattison, S.A.J., 2006c, An overlooked play-type on a ramp margin: prodelta turbidite lobes, lower Kenilworth Member, Cretaceous Western Interior, Book Cliffs, Utah: American Association of Petroleum Geologists Annual Convention, Houston, Texas, Abstract, p. 82.
Pattison, S.A.J., 2007a, Channelized and lobate isolated shelf bodies, upper Aberdeen to lower Kenilworth interval (Campanian Blackhawk Formation), Book Cliffs, Eastern Utah: sedimentology, ichnology, architecture and depositional environment, *in* MacEachern, J.A., Gingras, M.K., Bann, K.L., and Pemberton, S.G., eds., Ichnological Applications to Sedimentological and Sequence Stratigraphic Problems Abstract Volume: SEPM (Society for Sedimentary Geology) Research Conference, May 20-26, Price, Utah, USA, p. 113-116.
Pattison, S.A.J., 2007b, Identification of *Scaphites hippocrepis III* in the top Aberdeen Member (Campanian Blackhawk Formation) lag deposit, Book Cliffs, eastern Utah: implications for correlation in the Cretaceous Western Interior: Geological Society of America Abstracts with Programs, v. 39, no. 6, p. 73.
Pattison, S.A.J., 2008a, Role of wave-modified underflows in the across-shelf transport of fine-grained sediments: examples from the Book Cliffs, Utah, U.S.A., *in* Zavala, C., et al., eds., Sediment Transfer from Shelf to Deepwater – Revisiting the Delivery Mechanisms Abstract Volume: AAPG (American Association of Petroleum Geologists) Hedberg Research Conference, March 3-7, Ushuaia-Patagonia, Argentina, p. 40-41.
Pattison, S.A.J., 2008b, Significance of isolated shelf turbidites and coarse-grained sandstone bodies in shallow marine correlations: American Association of Petroleum Geologists Annual Convention, San Antonio, Texas, Abstract, p. 157.
Pattison, S.A.J., 2008c, Oceanic flood deposits in the Cretaceous Western Interior of North America: American Association of Petroleum Geologists Annual Convention, San Antonio, Texas, Abstract, p. 157.
Pattison, S.A.J., 2008d, Fluvial-coastal plain and shoreface-deltaic deposits, Book Cliffs, Utah: Analogs for clastic reservoirs in Western Canada. Field Trip Guidebook, Brandon University, Brandon, Manitoba, Canada, 119 p.
Pattison, S.A.J., 2010, Alternative sequence stratigraphic model for the Desert Member to Castlegate Sandstone interval, Book Cliffs, eastern Utah: Implications for the high-resolution correlation of falling stage nonmarine, marginal-marine, and marine strata, *in* Morgan, L.A., and Quane, S.L., eds., Through the Generations: Geologic and Anthropogenic Field Excursions in the Rocky Mountains from Modern to Ancient: Geological Society of America Field Guide 18, p. 163–192.
Pattison, S.A.J., 2017, Core-to-outcrop correlation, Desert Member-Castlegate Sandstone, Book Cliffs, eastern Utah: Facies-ichnology-stratigraphy-environments. Internal Technical Report, Department of Geology, Brandon University, Brandon, Manitoba, Canada, 110 p.
Pattison, S.A.J., 2018, Rethinking the incised valley-fill paradigm for Campanian Book Cliffs strata, Utah-Colorado, USA: Evidence for discrete parasequence-scale, shoreface-incised channel-fills: Journal of Sedimentary Research, v. 88, p. 1381-1412.
Pattison, S.A.J., 2019a, Using classic outcrops to revise sequence stratigraphic models: Reevaluating the Campanian Desert Member (Blackhawk Formation) to lower Castlegate Sandstone interval, Book Cliffs, Utah and Colorado, USA: Geology v. 47, p. 11-14.
Pattison, S.A.J., 2019b, Re-evaluating the sedimentology and sequence stratigraphy of classic Book Cliffs outcrops at Tusher and Thompson canyons, eastern Utah, USA: applications to correlation, modelling, and prediction in similar nearshore terrestrial to shallow marine subsurface settings worldwide: Journal of Marine and Petroleum Geology, v. 102, p. 202-230.
Pattison, S.A.J., 2019c, High resolution linkage of channel-coastal plain and shallow marine facies belts, Desert Member to Lower Castlegate Sandstone stratigraphic interval, Book Cliffs, Utah-Colorado, U.S.A.: Geological Society of America Bulletin, v. 131, p.
Pattison, S.A.J., (*in review-a*), Critical re-examination of the Desert Member and Lower Castlegate Sandstone, Campanian Book Cliffs, Utah-Colorado, U.S.A.: Implications for sequence stratigraphic models: Submitted to the *American Association of Petroleum Geologists Bulletin*.
Pattison, S.A.J., (*in review-b*), Sedimentology, architecture and trajectories of the low accommodation, strongly progradational stacked shoreline systems, Campanian Desert Member-to-Lower Castlegate Sandstone interval, Book Cliffs, Utah-Colorado, U.S.A.: Implications for sequence stratigraphic modelling and prediction: Submitted to *Sedimentology*.
Pattison, S.A.J. and Ainsworth, R.B., 2007, Sedimentology, sedimentary architecture and stratigraphy of isolated inner shelf channels, Upper Cretaceous Aberdeen Member, Green River Embayment, Book Cliffs, eastern Utah, U.S.A.: Implications for shoreface-to-shelf facies models: American Association of Petroleum Geologists Annual Convention, April 1 to 4, Long Beach, California, Abstract, p. 107.
Pattison, S.A.J., and Hoffman, T.A., 2005, Evidence of fine-grained sediment transport by turbidity currents, hyperpycnal flows and storm waves: inner shelf prodelta

turbidite complex, Hatch Mesa succession, Book Cliffs, Utah: American Association of Petroleum Geologists Annual Convention, Calgary, Alberta, Abstract, p. A106.
Pattison, S.A.J. and Hoffman, T.A., 2008, Sedimentology, architecture and origin of shelf turbidite bodies in the Upper Cretaceous Kenilworth Member, Book Cliffs, Utah, USA, *in* Hampson G.J., Steel R.J., Burgess, P.M., and Dalrymple, R.W., eds., Recent Advances in Models of Siliciclastic Shallow-Marine Stratigraphy: SEPM Special Publication No. 90, p. 391-420.
Pattison, S.A.J., and Walker, R.G., 1992, Deposition and interpretation of long, narrow sandbodies underlain by a basinwide erosion surface; Cardium Formation, Cretaceous Western Interior Seaway, Alberta, Canada: Journal of Sedimentary Petrology, v. 62, p. 292-309.
Pattison, S.A.J., Ainsworth, R.B., and Hoffman, T.A., 2007, Evidence of across-shelf transport of fine-grained sediments: turbidite-filled shelf channels in the Campanian Aberdeen Member, Book Cliffs, Utah, U.S.A.: Sedimentology, v. 54, p. 1033-1063.
Pattison, S.A.J., Hoffman, T.A., and Ainsworth, R.B., 2005, Prodelta turbiditic channels and lobes, upper Aberdeen Member to lower Kenilworth Member, Green River Embayment, Book Cliffs, Utah: integral components of river-dominated deltas: American Association of Petroleum Geologists Annual Convention, Calgary, Alberta, Abstract, p. A106.
Pattison, S.A.J., Phillips, J.M., and Saban, S.A., 2008, Prediction and realistic modeling of channel-shoreface reservoir units using outcrop analog data. Interim Technical Report: Field Season 1, Brandon University, Brandon, Manitoba, Canada, 112 p.
Pattison, S.A.J., Taylor, K.G., and Macquaker, J.H.S., 2009, A shore-to-basin transect through the Mancos Shale mud belt: sedimentological controls on lithofacies variability in unconventional hydrocarbon plays, Book Cliffs, Utah: Field Trip No. 18 Guidebook, Society for Sedimentary Geology (SEPM), American Association of Petroleum Geologists Annual Convention and Exhibition, 7-10 June 2009, Colorado Convention Center, Denver, Colorado, 168 p.
Pattison, S.A.J., Williams, H., and Davies, P., 2007a, Clastic sedimentology, sedimentary architecture and sequence stratigraphy of fluvio-deltaic, shoreface and shelf deposits, Book Cliffs, eastern Utah and western Colorado, *in* Raynolds, R.G., ed., Roaming the Rocky Mountains and Environs: Geological Field Trips: Geological Society of America Field Guide 10, p. 17-43.
Pattison, S.A.J., Williams, H., and Davies, P., 2007b, New insights for correlation in shoreface-to-shelf systems based on observations in the Campanian Blackhawk Formation to Castlegate Sandstone stratigraphic interval, Book Cliffs, Utah: American Association of Petroleum Geologists Annual Convention, Long Beach, California, Abstract, p. 107.
Pattison, S.A.J., Williams, H., and Davies, P., 2007c, To clinoform or not to clinoform? That is a key question for correlating in shallow marine systems: Geological Society of America Abstracts with Programs, v. 39, no. 6, p. 337.
Peacock, D.C.P., and Sanderson, D.J., 1994, Geometry and development of relay ramps in normal fault systems: American Association of Petroleum Geologists Bulletin, v. 78, p. 147-165.
Pemberton, S.G., and Wightman, D.M., 1992, Ichnological characteristics of brackish water deposits, *in* Pemberton, S.G., ed., Applications of Ichnology to Petroleum Exploration: Society of Economic Paleontologists and Mineralogists, Core Workshop No. 17, p.141-167.
Pemberton, S.G., Spila, M., Pulham, A.J., Saunders, T., MacEachern, J.A., Robbins, D., and Sinclair, I.K., 2001, Ichnology and sedimentology of shallow to marginal marine systems: Ben Nevis and Avalon reservoirs, Jeanne d'Arc Basin: Geological Association of Canada, Short Course Notes, Volume 15, 343 p.
Pemberton, S.G., Pulham, A., MacEachern, J.A., and Saunders, T., 2007, The ichnology and sedimentology of the Ferron Sandstone cores of Muddy Creek Canyon, Emery County, SE Utah, USA, *in* MacEachern, J.A., Gingras, M.K., Bann, K.L., and Pemberton, S.G., eds., Ichnological Applications to Sedimentological and Sequence Stratigraphic Problems Abstract Volume: SEPM (Society for Sedimentary Geology) Research Conference, May 20-26, Price, Utah, USA, p. 175-209.
Pérez-López, A., 2001, Significance of pot and gutter casts in a Middle Triassic carbonate platform, Beltic Cordillera, southern Spain: Sedimentology, v. 48, p. 1371-1388.
Petter, A.L., and Muto, T., 2008, Sustained alluvial aggradation and autogenic detachment of the alluvial river from the shoreline in response to steady fall of relative sea level: Journal of Sedimentary Research, v. 78, p. 98-111.
Phillips, J.M., 2008, A comparative petrographic study of shoreface attached sandstones, coarse-grained lag deposits and channelized isolated shelf bodies, Aberdeen Member, Campanian Blackhawk Formation, Book Cliffs, east-central Utah: Unpublished B.Sc. Thesis, Brandon University, Brandon, Manitoba, Canada, 141 p.
Plink-Björklund, P., Mellere, D., and Steel, R.J., 2001, Turbidite variability and architecture of sand-prone, deep-water slopes: Eocene clinoforms in the Central Basin, Spitsbergen: Journal of Sedimentary Research, v. 71, p. 895-912.
Plink-Björklund, P., and Steel, R.J., 2004, Initiation of turbidity currents: outcrop evidence for Eocene hyperpycnal flow turbidites: Sedimentary Geology, v. 165, p. 29-52.
Plink-Björklund, P., and Steel, R., 2005, Deltas on falling-stage and lowstand shelf margins, the Eocene Central Basin of Spitsbergen: importance of sediment supply, *in* Giosan, L., and Bhattacharya, J.P., eds., River Deltas – Concepts, Models, and Examples: SEPM (Society for Sedimentary Geology), Special Publication No. 83, p. 179-206.
Plint, A.G., 1988, Sharp-based shoreface sequences and "offshore bars" in the Cardium Formation of Alberta: their relationship to relative changes in sea level, *in* Wilgus, C.K., Hastings, B.S., Kendall, C.G.St.C., Posamentier, H.W., Ross, C.A., and Van Wagoner, J.C., eds., Sea-Level Changes: An Integrated Approach: Society of Economic Paleontologists and Mineralogists, Special Publication No. 42, p. 357-370.
Plint, A.G., and Nummedal, D., 2000, The falling stage systems tract: recognition and importance in sequence stratigraphic analysis, *in* Hunt, D., and Gawthorpe, R.L., eds., Sedimentary Responses to Forced Regressions: Geological Society Special Publication No. 172, p. 1-17.
Plint, A.G., Tyagi, A., Hay, M.J., Varban, B.L., Zhang, H., and Roca, X., 2009, Clinoforms, paleobathymetry, and mud dispersal across the western Canada cretaceous foreland basin: Evidence from the cenomanian dunvegan formation and contiguous strata: Journal of Sedimentary Research, v. 79, p. 144-161.
Posamentier, H.W., 2001, Lowstand alluvial bypass systems: incised vs. unincised: American Association of Petroleum Geologists Bulletin, v. 85, p. 1771-1793.
Posamentier, H.W., and Allen, G.P., 1999, Siliciclastic sequence stratigraphy – concepts and applications: Society of Economic Paleontologists and Mineralogists, Concepts in Sedimentology and Paleontology No. 7, 210 p.
Posamentier, H.W., Allen, G.P., James, D.P., and Tesson, M., 1992, Forced regressions in a sequence stratigraphy framework: concepts, examples, and exploration significance: American Association of Petroleum Geologists Bulletin, v. 76, p. 1687-1709.
Posamentier, H.W., Jervey, M.T., and Vail, P.R., 1988, Eustatic controls on clastic deposition I – Conceptual framework, *in* Wilgus, C.K., Hastings, B.S., Kendall, C.G.St.C., Posamentier, H.W., Ross, C.A., and Van Wagoner, J.C., eds., Sea-Level Changes: An Integrated Approach: Society of Economic Paleontologists and Mineralogists, Special Publication No. 42, p. 109-124.
Posamentier, H.W., and Morris, W.R., 2000, Aspects of the stratal architecture of forced regressive deposits, *in* Hunt, D., and Gawthorpe, R.L., eds., Sedimentary Responses to Forced Regressions: Geological Society Special Publication No. 172, p. 19-46.
Posamentier, H.W., and Vail, P.R., 1988, Eustatic controls on clastic deposition II – Sequence and systems tract models, *in* Wilgus, C.K., Hastings, B.S., Kendall, C.G.St.C., Posamentier, H.W., Ross, C.A., and Van Wagoner, J.C., eds., Sea-Level Changes: An Integrated Approach: Society of Economic Paleontologists and Mineralogists, Special Publication No. 42, p. 125-154.
Postma, G., 1990, Depositional architecture and facies of river and fan deltas: a synthesis, *in* Colella, A., and Prior, D.B., eds., Coarse-Grained Deltas: International Association of Sedimentologists Special Publication 10, p. 13-27.
Potter, P.E., Maynard, J.B., and Depetris, P.J., 2005, Mud and mudstones, introduction and overview: New York, Springer, 297 p.
Pranter, M.J., Ellison, A.I., Cole, R.D., and Patterson, P.E., 2007, Analysis and modeling of intermediate-scale reservoir heterogeneity based on a fluvial point-bar outcrop analog, Williams Fork Formation, Piceance Basin, Colorado: Association of Petroleum Geologists Bulletin, v. 91, p. 1025–1051.
Pranter, M.J., Cole, R.D., Panjaitan, H., and Sommer, N.K., 2009, Sandstone-body dimensions in a lower coastalplain depositional setting: Lower Williams Fork Formation, Coal Canyon, Piceance Basin, Colorado: Association of Petroleum Geologists Bulletin, v. 93, p. 1379–1401.
Pranter, M.J., and Sommer, N.K., 2011, Static connectivity of fluvial sandstones in a lower coastal-plain setting: An example from the Upper Cretaceous lower Williams Fork Formation, Piceance Basin, Colorado: American Association of Petroleum Geologists Bulletin, v. 95, p. 899-923.
Prince, G.D., and Burgess, P.M., 2013, Numerical modeling of falling-stage topset aggradation: implications for distinguishing between forced and unforced

regressions in the geological record: Journal of Sedimentary Research, v. 83, p. 767-781.
Prior, D.B., Yang, Z.-S., Bornhold, B.D., Keller, G.H., Lin, Z.H., Wiseman, W.J.Jr., Wright, L.D., and Lin, T.C., 1986a, The subaqueous delta of the modern Huanghe (Yellow River): Geo-Marine Letters, v. 6, p. 67-75.
Prior, D.B., Yang, Z.-S., Bornhold, B.D., Keller, G.H., Lu, N.Z., Wiseman, W.J.Jr., Wright, L.D., and Zhang, J., 1986b, Active slope failure, sediment collapse, and silt flows on the modern subaqueous Huanghe (Yellow River) delta: Geo-Marine Letters, v. 6, p. 85-95.
Reading, H.G., 1996 (editor), Sedimentary Environments: Processes, Facies and Stratigraphy: 3rd Edition, Blackwell Science Ltd., Oxford, UK, 688 p.
Reading, H.G., 1998, Return of 'The Fan That Never Was': Westphalian turbidite systems in the Variscan Culm Basin: Bude Formation (south-west England), Discussion: Sedimentology, v. 45, p. 967-970.
Reading, H.G., and Collinson, J.D., 1996, Clastic coasts, *in* Reading, H.G., ed., Sedimentary Environments: Processes, Facies and Stratigraphy: Blackwell Science, Third Edition, p. 154-231
Reading, H.G., and Levell, B.K., 1996, Controls on the sedimentary rock record, *in* Reading, H.G., ed., Sedimentary Environments: Processes, Facies and Stratigraphy: Blackwell Science, Third Edition, p. 5-36.
Reeside, J.B.Jr., 1927, The cephalopods of the Eagle Sandstone and related formations in the Western Interior of the United States: U.S. Geological Survey Professional Paper 151, 87p.
Reineck, H.-E., 1963, Sedimentgefûge im Bereich der südlichen Nordsee: Senckenbergische Naturforschende Gesellschaft, Abhandlungen, 505 p.
Reineck, H.-E., and Singh, I.B., 1972, Genesis of laminated sand and graded rhythmites in storm-sand layers of shelf mud: Sedimentology, v. 18, p. 123-128.
Riemersma, P.E., and Chan, M.A., 1991, Facies of the lower Ferron Sandstone and Blue Gate Shale Members of the Mancos Shale: lowstand and early transgressive facies architecture, in Swift, D.J.P., Oertel, G.F., Tillman, R.W., and Thorne, J.A., eds., Shelf Sand and Sandstone Bodies: Geometry, Facies and Sequence Stratigraphy, International Association of Sedimentologists Special Publication 14, p. 489-510.
Rittersbacher, A., Howell, J.A., and Buckley, S.J., 2014, Analysis of fluvial architecture in the Blackhawk Formation, Wasatch Plateau, Utah, USA, using large 3D photorealistic models: Journal of Sedimentary Research, v. 84, p. 72-87.
Roberts, L.N.R., and Kirschbaum, M.A., 1995, Paleogeography of the Late Cretaceous of the Western Interior of Middle North America – coal distribution and sediment accumulation: U.S. Geological Survey Professional Paper 1561, 115p.
Robinson, R.A.J., and Slingerland, R.L. 1998, Grain-size trends, basin subsidence and sediment supply in the Campanian Castlegate Sandstone and equivalent conglomerates of central Utah: Basin Research, v. 10, p. 109–127.
Ross, D.J.K., and Bustin, R.M., 2007, Shale gas reservoir systems: insights from north of the border: American Association of Petroleum Geologists Annual Convention, April 1 to 4, Long Beach, California, Abstract, p. 118.
Rotevatn, A., Fossen, H., Hesthammer, J., Aas, T.E., and Howell, J.A., 2007, Are relay ramps conduits for fluid flow? Structural analysis of a relay ramp in Arches National Park, Utah, *in* Lonergan, L., Jolly, R.J.H., Rawnsley, K., and Sanderson, D.J., eds., Fractured Reservoirs: Geological Society, London, Special Publication 270, p. 55-71.
Runkel, A.C., Miller, J.F., McKay, R.M., Palmer, A.R., and Taylor, J.F., 2007, High-resolution sequence stratigraphy of lower Paleozoic sheet sandstones in central North America: The role of special conditions of cratonic interiors in development of stratal architecture: GSA Bulletin, v.119, p.860-881.
Ryer, T.A., 2004, Previous studies of the Ferron sandstone, *in* Chidsey, T.C.Jr., Adams, R.D., and Morris, T.H., eds., Regional to Wellbore Analog for Fluvial-Deltaic Reservoir Modeling: The Ferron Sandstone of Utah: American Association of Petroleum Geologists (AAPG) Studies in Geology 50, p. 3-38.
Ryer, T.A., and Anderson, P.B., 2004, Facies of the Ferron Sandstone, east-central Utah, *in* Chidsey, T.C.Jr., Adams, R.D., and Morris, T.H., eds., Regional to Wellbore Analog for Fluvial-Deltaic Reservoir Modeling: The Ferron Sandstone of Utah: American Association of Petroleum Geologists (AAPG) Studies in Geology 50, p. 59-78.
Sahoo, H., Gani, M.R., Hampson, G.J., Gani, N.D., and Ranson, A., 2016, Facies- to sandbody-scale heterogeneity in a tight-gas fluvial reservoir analog: Blackhawk Formation, Wasatch Plateau, Utah, USA: Marine and Petroleum Geology, 2016, v. 78, p. 48-69.
Saunders, T., and Pemberton, S.G., 1986, Trace fossils and sedimentology of the Appaloosa Sandstone: Bearpaw-Horseshoe Canyon Formation transition, Dorothy, Alberta: Canadian Society of Petroleum Geologists Field Trip Guide Book, 117 p.
Schieber, J., Southard, J., and Thaisen, K., 2007, Accretion of mudstone beds from migrating floccule ripples: Science, v. 318, p. 1760-1763.
Scott, N., 2006, Petrographic analysis of Toad Stool and Hatch Mesa lag deposits, Book Cliffs, Utah, USA: Unpublished Research Report, 19p. *with Appendices, Photo Plates and Original Point Count Data*.
Sech, R.P., Jackson, M.D., and Hampson, G.J., 2009, Three-dimensional modeling of a shoreface-shelf parasequence reservoir analog: Part 1. Surface-based modeling to capture high-resolution facies architecture: AAPG Bulletin, v. 93, p. 1155–1181.
Seymour, D.L., and Fielding, C.R., 2013, High resolution correlation of the Upper Cretaceous stratigraphy between the Book Cliffs and the Western Henry Mountains Syncline, Utah, U.S.A.: Journal of Sedimentary Research, v. 83, p. 475-494.
Seymour, R.J., 1986, Nearshore auto-suspending turbidity flows: Ocean Engineering, v. 13, p. 435-447.
Shanley, K.W., McCabe, P.J., and Hettinger, R.D., 1992, Tidal influence in Cretaceous fluvial strate from Utah, USA: a key to sequence stratigraphic interpretation: Sedimentology, 39, p. 905-930.
Shanley, K.W., and McCabe, P.J., 1994, Perspectives on the Sequence Stratigraphy of Continental Strata: AAPG Bulletin, v.78, No.4, p. 544-568.
Shanley, K., Boyles, M., Sutter, J., Nummedal, D., and Cole, R., 2003, Sedimentology and sequence stratigraphic response to changes in accommodation: Predicting reservoir architecture, Book Cliffs, Utah: Society of Sedimentary Geology Field Trip Guidebook, American Association of Petroleum Geologists Annual Convention, Field Trip 21, May 14-18, 50 p.
Shanley, K.W., Cluff, R.M., and Robinson, J.W., 2004, Factors controlling prolific gas production from low-permeability sandstone reservoirs: Implications for resource assessment, prospect development, and risk analysis: American Association of Petroleum Geologists Bulletin, v. 88, p. 1083-1121.
Shepard, F.P., 1963, Continental shelves: topography and sediments, in Shepard, F.P., ed., Submarine Geology: Harper and Row Publishers, New York, p. 206-259.
Snedden, J.W., and Bergman, K.M., 1999, Isolated shallow marine sand bodies: deposits for all interpretations, *in* Bergman, K.M., and Snedden, J.W., eds., Isolated Shallow Marine Sand Bodies: Sequence Stratigraphic Analysis and Sedimentological Interpretation: SEPM (Society for Sedimentary Geology) Special Publication 64, p. 1-11.
Snedden, J.W., and Dalrymple, R.W., 1999, Modern shelf sand ridges: from historical perspective to a unified hydrodynamic and evolutionary model, *in* Bergman, K.M., and Snedden, J.W., eds., Isolated Shallow Marine Sand Bodies: Sequence Stratigraphic Analysis and Sedimentological Interpretation: SEPM (Society for Sedimentary Geology) Special Publication 64, p. 13-28.
Snedden, J.W., and Swift, D.J.P., 1991, Is there evidence for geostrophic currents preserved in the sedimentary record of inner to middle-shelf deposits?-Discussion: Journal of Sedimentary Petrology, v. 61, p. 148-151.
Snedden, J.W., Nummedal, D., and Amos, A.F., 1988, Storm- and fair-weather combined flow on the central Texas continental shelf: Journal of Sedimentary Petrology, v. 58, p. 580-595.
Sømme, T.O., Howell, J.A., Hampson, G.J., and Storms, J.E.A., 2008, Genesis, architecture, and numerical modeling of intra-parasequence discontinuity surfaces in wave-dominated deltaic deposits: Upper Cretaceous Sunnyside Member, Blackhawk Formation, Book Cliffs, Utah, U.S.A., *in* Hampson G.J., Steel R.J., Burgess, P.M., and Dalrymple, R.W., eds., Recent Advances in Models of Siliciclastic Shallow-Marine Stratigraphy: SEPM Special Publication No. 90, p. 421-441.
Soria, J.M., Fernández, J., García, F., and Viseras, C., 2003, Correlative lowstand deltaic and shelf systems in the Guadix Basin (Late Miocene, Betic Cordillera, Spain): the stratigraphic record of forced and normal regressions: Journal of Sedimentary Research, v. 73, p. 912-925.
Southard, J.B., Lambie, J.M., Federico, D.C., Pile, H.T., and Weidman, C.R., 1990, Experiments on bed configurations in fine sands under bidirectional purely oscillatory flow, and the origin of hummocky cross-stratification: Journal of Sedimentary Petrology, v. 60, p. 1-17.
Spieker, E.M., 1931, The Wasatch Plateau Coal Field, Utah: United States Department of the Interior, Geological Survey, Bulletin 819, 210 p.
Spieker, E.M., 1949, Sedimentary facies and associated diastrophism in the Upper Cretaceous of Central and Eastern Utah: The Geological Society of America, Memoir 39, p. 55-82.
Spieker, E.M., and Reeside Jr., J.B., 1925, Cretaceous and Tertiary formations of the Wasatch Plateau, Utah: Bulletin of the Geological Society of America, v. 36, p.

435-454.
Steel, E., Simms, A.R., Warrick, J. and Yokoyama, Y., 2016, Highstand shelf fans: The role of buoyancy reversal in the deposition of a new type of shelf sand body: Geological Society of America Bulletin, v. 128, p. 1717-1724.
Stevens, K.M., 2004, Re- evaluating the origin of isolated sandstones encased in marine mudstone: the Cretaceous Prairie Canyon Member of the Mancos Shale at Hatch Mesa, east-central Utah: M.Sc. thesis, Colorado School of Mines, 124 p.
Stevens, K.M., and Chaiwongsaen, N., 2003, Evaluating the origin of isolated Cretaceous sandstones encased in marine mudstone: the Prairie Canyon Member of the Mancos Shale, Hatch Mesa, east-central Utah: American Association of Petroleum Geologists Annual Convention, Salt Lake City, Utah, Abstract, p. A163.
Stevens, K.M., Anderson, D.S., Gardner, M.H., and Wagner, J.B., 2005, Re-evaluating the origin of isolated sandstones encased in marine mudstone: the Cretaceous Prairie Canyon Member of the Mancos Shale at Hatch Mesa, east-central Utah: American Association of Petroleum Geologists Annual Convention, Calgary, Alberta, Abstract, p. A133.
Stokes, W.L, 1986, Geology of Utah: Utah Museum of Natural History, University of Utah and Utah Geological and Mineral Survey Department of Natural Resources, Occasional Paper Number 6, ISBN 0-940378-05-1, 280 p.
Storle, B., 2009, Subsurface correlation of Upper Cretaceous strata, east-central Utah: Unpublished B.Sc. Thesis, Brandon University, Brandon, Manitoba, Canada, 40 p.
Storms, J.E.A., and Hampson, G.J., 2005, Mechanisms for forming discontinuity surfaces within shoreface-shelf parasequences: sea-level, sediment supply, or wave regime?: Journal of Sedimentary Research, v. 75, p. 67-81.
Stracher, G.B., Tabet, D.E., Anderson, P.B., and Pone, J.D.N., 2005, Utah's state rock and the Emery coalfield: Geology, mining history and natural burning coal beds, *in* Pederson, J., and Dehler, C.M., eds., Interior Western United States: Geological Society of America Field Guide 6, p. 199-210.
Strong, N., and Paola, C., 2008. Valleys that never were: time surfaces versus stratigraphic surfaces. Journal of Sedimentary Research, v. 78, p. 579–593.
Strong, N., and Paola, C., 2010. Valleys that never were: time surfaces versus stratigraphic surfaces - Reply. Journal of Sedimentary Research, v. 80, p. 4-5.
Suter, J.R., and Berryhill, H.L.Jr., 1985, Late Quaternary shelf-margin deltas, northwest Gulf of Mexico: American Association of Petroleum Geologists Bulletin, v. 69, p. 77-91.
Suter, J.R., and Clifton, H.E., 1999, The Shannon Sandstone and isolated linear sand bodies: interpretations and realizations, *in* Bergman, K.M., and Snedden, J.W., eds., Isolated Shallow Marine Sand Bodies: Sequence Stratigraphic Analysis and Sedimentological Interpretation: SEPM (Society for Sedimentary Geology) Special Publication 64, p. 321-356.
Swift, D.J.P., 1985, Response of the shelf floor to flow, *in* Tillman, R.W., Swift, D.J.P., and Walker, R.G., eds., Shelf Sands and Sandstone Reservoirs: Society of Economic Paleontologists and Mineralogists, Short Course Notes No. 13, p. 135-241.
Swift, D.J.P., and Field, M.E., 1981, Evolution of a classic sand ridge field: Maryland section, North American inner shelf: Sedimentology, v. 28, p. 461-482.
Swift, D.J.P., and Niedoroda, A.W., 1985, Fluid and sediment dynamics on continental shelves, *in* Tillman, R.W., Swift, D.J.P., and Walker, R.G., eds., Shelf Sands and Sandstone Reservoirs: Society of Economic Paleontologists and Mineralogists, Short Course Notes No. 13, p. 47-134.
Swift, D.J.P., and Parsons, B.S., 1999, Shannon Sandstone of the Powder River Basin: orthodoxy and revisionism in stratigraphic thought, *in* Bergman, K.M., and Snedden, J.W., eds., Isolated Shallow Marine Sand Bodies: Sequence Stratigraphic Analysis and Sedimentological Interpretation: SEPM (Society for Sedimentary Geology) Special Publication 64, p. 55-84.
Swift, D.J.P., Figueiredo, A.G., Freeland, G.L., and Oertel, G.F., 1983, Hummocky cross-stratification and megaripples: a geological double standard: Journal of Sedimentary Petrology, v. 53, p. 1295-1317.
Swift, D.J.P., Hudelson, P.M., Brenner, R.L., and Thompson, P., 1987, Shelf construction in a foreland basin: storm beds, shelf sandbodies, and shelf-slope depositional sequences in the Upper Cretaceous Mesaverde Group, Book Cliffs, Utah: Sedimentology, v. 34, p. 423-457.
Swift, D.J.P., Phillips, S., and Thorne, J.A., 1991, Sedimentation on continental margins, IV: lithofacies and depositional systems, *in* Swift, D.J.P., Oertel, G.F., Tillman, R.W., and Thorne, J.A., eds., Shelf Sand and Sandstone Bodies: Geometry, Facies and Sequence Stratigraphy, International Association of Sedimentologists Special Publication 14, p. 89-152.
Syvitski, J.P.M., and Farrow, G.F., 1989, Fjord sedimentation as an analogue for small hydrocarbon bearing fan deltas, *in* Whateley, M.K.G., and Pickering, K.T., eds., Deltas: Sites and Traps for Fossil Fuels: Geological Society of London Special Publication No. 41, p. 21-43.
Taylor, A.M., and Goldring, R., 1993, Description and analysis of bioturbation and ichnofabric: Journal of the Geological Society of London, v. 150, p. 141-148.
Taylor, D.R., and Lovell, R.W.W., 1991, Recognition of high-frequency sequences in the Kenilworth Member of the Blackhawk Formation, Book Cliffs, Utah, *in* Van Wagoner, J.C., Nummedal, D., Jones, C.R., Taylor, D.R., Jennette, D.C., and Riley, G.W., eds., Sequence Stratigraphy Applications to Shelf Sandstone Reservoirs: Outcrop to Subsurface Examples: American Association of Petroleum Geologists, Field Conference Guidebook.
Taylor, D.R., and Lovell, R.W.W., 1995, High-frequency sequence stratigraphy and paleogeography of the Kenilworth Member, Blackhawk Formation, Book Cliffs, Utah, U.S.A., *in* Van Wagoner, J.C., and Bertram, G.T., eds., Sequence Stratigraphy of Foreland Basin Deposits – Outcrop and Subsurface Examples from the Cretaceous of North America: American Association of Petroleum Geologists, Memoir 64, p. 257-275.
Taylor, K.G., and Curtis, C.D., 1995, Stability and facies association of early diagenetic mineral assemblages: an example from a Jurassic ironstone—mudstone succession, U.K.: Journal of Sedimentary Research, v. 65, p. 358–368.
Taylor, K.G., and Gawthorpe, R.L., 2003, Basin-scale dolomite cementation of shoreface sandstones in response to sea-level fall: Geological Society of America Bulletin, v. 115, p. 1218-1229.
Taylor, K.G., and Machent, P.G., 2011, Extensive carbonate cementation of fluvial sandstones: an integrated outcrop and petrographic analysis from the Upper Cretaceous, Book Cliffs, Utah. Marine and Petroleum Geology, v. 28, p. 1461-1474.
Taylor, K.G., and Machent, P.G., 2010, Systematic sequence-scale controls on carbonate cementation in a siliciclastic sedimentary basin: Examples from Upper Cretaceous shallow marine deposits of Utah and Coloradao, USA. Marine and Petroleum Geology, v. 27, p. 1297-1310.
Taylor, K.G., and Macquaker, J.H.S., 2000, Spatial and temporal distribution of authigenic minerals in continental shelf sediments: implications for sequence stratigraphic analysis. in: Glenn, C. et al. (eds) Marine Authigenesis: From Global to Microbial, SEPM Special Publication No. 66., p. 309-323.
Taylor, K.G., and Macquaker, J.H.S., 2000, Early diagenetic pyrite morphology in a mudstone-dominated succession: the Lower Jurassic Cleveland Ironstone Formation, eastern England: Sedimentary Geology, v. 131, p. 77-86.
Taylor, K.G., Gawthorpe, R.L., and Van Wagoner, J.C., 1995, Stratigraphic control on laterally persistent cementation, Book Cliffs, Utah: Journal of the Geological Society, London, v. 152, p. 225-228.
Taylor, K.G., Gawthorpe, R.L., Curtis, C.D., Marshall, J.M., and Awwiller, D.N., 2000, Carbonate cementation in a sequence-stratigraphic framework: Upper Cretaceous sandstones, Book Cliffs, Utah-Colorado: Journal of Sedimentary Research, v. 70, p. 360-372.
Taylor, K.G., Gawthorpe, R.L., and Fannon-Howell, S., 2004, Basin-scale diagenetic alteration of shoreface sandstones in the Upper Cretaceous Spring Canyon and Aberdeen Members, Blackhawk Formation, Book Cliffs, Utah: Sedimentary Geology, v. 172, p. 99-115.
Taylor, K.G., Macquaker, J.H.S., and Pattison, S.A.J., 2011, Scales of diagenetic processes in a foreland basin mudstone succession: the Mancos Shale, Book Cliffs, Utah: American Association of Petroleum Geologists Annual Convention, April 10 to 13, Houston, Texas.
Taylor, K.G., Macquaker, J.H.S., and Pattison, S.A.J., 2010, Diagenetic processes in a foreland basin mudstone succession: the Mancos Shale, Book Cliffs, Utah: British Sedimentological Research Group Conference, December 19 to 21, Southampton, England.
Taylor, K.G., Perry, C.T., Greenaway, A.M., and Machent, P.G., 2007, Bacterial iron oxide reduction in a terrigenous-sediment impacted tropical shallow marine carbonate system, north Jamaica: Marine Chemistry, v. 107, p. 449-463.
Taylor, K.G., Simo, A, Yocum, D., and Leckie, D., 2002, Stratigraphic significance of ooidal ironstones from the Cretaceous Western Interior Seaway: the Peace River Formation, Alberta and the Castlegate Sandstone, Utah: Journal of Sedimentary Research, v. 72, p. 345-356.
Tillman, R.W., 1985, A spectrum of shelf sands and sandstones, *in* Tillman, R.W., Swift, D.J.P., and Walker, R.G., eds., Shelf Sands and Sandstone Reservoirs: Society of Economic Paleontologists and Mineralogists, Short Course Notes No. 13, p. 1-46.
Tillman, R.W., 1999, The Shannon Sandstone: a review of the sand-ridge and other models, *in* Bergman, K.M., and Snedden, J.W., eds., Isolated Shallow Marine

Sand Bodies: Sequence Stratigraphic Analysis and Sedimentological Interpretation: SEPM (Society for Sedimentary Geology) Special Publication 64, p. 29-54.
Trampush, S.M., Hajek, E.A., Straub, K.M., and Chamberlin, E.P., 2017, Identifying autogenic sedimentation in fluvial-deltaic stratigraphy: Evaluating the effect of outcrop-quality data on the compensation statistic: Journal of Geophysical Research: Earth Surface, v. 122, p. 91–113.
Traykovski, P., Geyer, W.R., Irish, J.D., and Lynch, J.F., 2000, The role of wave-induced density-driven fluid mud flows for cross-shelf transport on the Eel River continental shelf: Continental Shelf Research, v. 20, p. 2113-2140.
Trower, E.J., Ganti, V., Fischer, W.W., and Lamb, M.P., 2018, Erosional surfaces in the Upper Cretaceous Castlegate Sandstone (Utah, USA): Sequence boundaries or autogenic scour from backwater hydrodynamics?: Geology, v. 46, p. 707-710.
Vakarelov, B., 2006, The importance of mud deposition in generating realistic stratigraphic models: American Association of Petroleum Geologists Annual Convention, Houston, Texas, Abstract, p. 109.
Vakarelov, B., Winker, C.D., and Bhattacharya, J.P., 2005, The missing mudbelts of the ancient record: implications for sequence stratigraphy: American Association of Petroleum Geologists Annual Convention, Calgary, Alberta, Abstract, p. A144.
Vakarelov, B.K., and Bhattacharya, J.P., 2009, Local tectonic control on parasequence architecture: Second Frontier sandstone, Powder River Basin, Wyoming: American Association of Petroleum Geologists Bulletin, v. 93, p. 295-327.
van de Graaff, F.R., 1972, Fluvial-deltaic facies of the Castlegate Sandstone (Cretaceous), east-central Utah: Journal of Sedimentary Petrology, v. 42, p. 558-571.
van den Bergh, T.C.V., and Garrison, J.R.Jr., 2004, The geometry, architecture, and sedimentology of fluvial and deltaic sandstones within the Upper Ferron Sandstone Last Chance Delta: implications for reservoir modeling, *in* Chidsey, T.C.Jr., Adams, R.D., and Morris, T.H., eds., Regional to Wellbore Analog for Fluvial-Deltaic Reservoir Modeling: The Ferron Sandstone of Utah: American Association of Petroleum Geologists (AAPG) Studies in Geology 50, p. 451-498.
Van Wagoner, J.C., 1991, Sequence stratigraphy and facies architecture of the Desert Member of the Blackhawk Formation and the Castlegate Formation in the Book Cliffs of eastern Utah and western Colorado, *in* Van Wagoner, J.C., Nummedal, D., Jones, C.R., Taylor, D.R., Jennette, D.C., and Riley, G.W., eds., Sequence Stratigraphy Applications to Shelf Sandstone Reservoirs: Outcrop to Subsurface Examples: American Association of Petroleum Geologists, Field Conference Guidebook.
Van Wagoner, J.C., 1995, Sequence stratigraphy and marine to nonmarine facies architecture of foreland basin strata, Book Cliffs, Utah, U.S.A., *in* Van Wagoner, J.C., and Bertram, G.T., eds., Sequence Stratigraphy of Foreland Basin Deposits – Outcrop and Subsurface Examples from the Cretaceous of North America: American Association of Petroleum Geologists, Memoir 64, p. 137-223.
Van Wagoner, J.C., 1998, Sequence stratigraphy and marine to nonmarine facies architecture of foreland basin strata, Book Cliffs, Utah, U.S.A. – Reply: American Association of Petroleum Geologists Bulletin, v. 82, p. 1607-1618.
Van Wagoner, J.C., Posamentier, H.W., Mitchum, R.M., Vail, P.R., Sarg, J.F., Loutit, T.S., and Hardenbol, J., 1988, An overview of the fundamentals of sequence stratigraphy and key definitions, *in* Wilgus, C.K., Hastings, B.S., Kendall, C.G.St.C., Posamentier, H.W., Ross, C.A., and Van Wagoner, J.C., eds., Sea-Level Changes: An Integrated Approach: Society of Economic Paleontologists and Mineralogists, Special Publication No. 42, p. 39-45.
Van Wagoner, J.C., Mitchum, R.M., Campion, K.M., and Rahmanian, V.D., 1990, Siliciclastic sequence stratigraphy in well logs, cores, and outcrops: American Association of Petroleum Geologists, Methods in Exploration Series No. 7, 55 p.
Villamizar, C.A., Hampson, G.J., Flood, Y.S., and Fitch, P.J.R. 2015, Object-based modelling of avulsion-generated sandbody distributions and connectivity in a fluvial reservoir analogue of low to moderate net-to-gross ratio: Petroleum Geoscience, v. 21, p. 249–270.
Walker, R.G., 1979, Facies Models (Editor): Geoscience Canada Reprint Series 1, 211 p.
Walker, R.G., 1982, Hummocky and swaley cross stratification, *in*, Walker, R.G., ed., Clastic Units of the Front Ranges, Foothills and Plains in the Area between Field, British Columbia and Drumheller, Alberta: International Association of Sedimentologists, 11th International Congress on Sedimentology, Hamilton, Ontario, Field Excursion Guidebook 21A, p. 22-30.
Walker, R.G., 1985, Geological evidence for storm transportation and deposition on ancient shelves, *in* Tillman, R.W., Swift, D.J.P., and Walker, R.G., eds., Shelf Sands and Sandstone Reservoirs: Society of Economic Paleontologists and Mineralogists, Short Course Notes No. 13, p. 243-302.
Walker, R.G., 1985b, Comparison of shelf environments and deep basin turbidite systems, *in* Tillman, R.W., Swift, D.J.P., and Walker, R.G., eds., Shelf Sands and Sandstone Reservoirs: Society of Economic Paleontologists and Mineralogists, Short Course Notes No. 13, p. 465-502.
Walker, R.G., and Plint, A.G., 1992, Wave- and storm-dominated shallow marine systems, *in* Walker, R.G., and James, N.P., eds., Facies Models: Response to Sea Level Change: Geological Association of Canada, p. 219-238.
Walton, P.T., 1956, Structure of the North Salt Valley-Cisco area, Grand County, Utah, *in* 7th Annual Field Conference, Intermountain Association of Petroleum Geologists, p. 186-189.
Weltje, G.T., 2002, Quantitative analysis of detrital modes: statistically rigorous confidence regions in ternary diagrams and their use in sedimentary petrology: Earth-Science Reviews, v. 57, p. 211-253.
Westcott, W.A., and Ethridge, F.G., 1990, Fan deltas – alluvial fans in coastal settings, *in* Rachocki, A.H., and Church, M., eds., Alluvial Fans: A Field Approach: Wiley Publishing, Chichester, U.K., p. 195-211.
Wheatcroft, R.A., 2000, Oceanic flood sedimentation: a new perspective: Continental Shelf Research, v. 20, p. 2059-2066.
Wheatcroft, R.A., and Borgeld, J.C., 2000, Oceanic flood deposits on the northern California shelf: large-scale distribution and small-scale physical properties: Continental Shelf Research, v. 20, p. 2163-2190.
Wheatcroft, R.A., Sommerfield, C.K., Drake, D.E., Borgeld, J.C., and Nittrouer, C.A., 1997, Rapid and widespread dispersal of flood sediment on the northern California margin: Geology, v. 25, p. 163-166.
Wheeler, H.F., 1958, Time-Stratigraphy: American Association of Petroleum Geologists Bulletin, v. 42, p. 1047-1063.
Wilgus, C.K., Hastings, B.S., Kendall, C.G.St.C., Posamentier, H.W., Ross, C.A., and Van Wagoner, J.C., 1988, Sea-Level Changes: An Integrated Approach: SEPM Special Publication No. 42, Tulsa, Oklahoma, 407 p.
Williams, H., and Davies, P., 2006, Book Cliffs reservoir geology field seminar pocket field guide: Reservoir Geology Consultants Limited, Llandovery, United Kingdom, 78 p.
Willis, A., 2000, Tectonic control of nested sequence architecture in the Sego Sandstone, Neslen Formation, and Upper Castlegate Sandstone (Upper Cretaceous), Sevier Foreland Basin, Utah, U.S.A.: Sedimentary Geology, v. 136, p. 277-317.
Wright, L.D., 1977, Sediment transport and deposition at river mouths: a synthesis: Geological Society of America Bulletin, v. 88, p. 857-868.
Wright, L.D., and Friedrichs, C.T., 2006, Gravity driven sediment transport on continental shelves: a status report: Continental Shelf Research, v. 26, p. 2092-2107.
Wright, L.D., Yang, Z.-S., Bornhold, B.D., Keller, G.H., Prior, D.B., and Wiseman, W.J.Jr., 1986, Hyperpycnal plumes and plume fronts over the Huanghe (Yellow River) delta front: Geo-Marine Letters, v. 6, p. 97-105.
Wright, L.D., Wiseman, W.J., Bornhold, B.D., Prior, D.B., Suhayda, J.N., Keller, G.H., Yang, Z.-S., and Fan, Y.B., 1988, Marine dispersal and deposition of Yellow River silts by gravity-driven underflows: Nature, v. 332, p. 629-632.
Wright, L.D., Friedrichs, C.T., Kim, S.C., and Scully, M.E., 2001, Effects of ambient currents and waves on gravity-driven sediment transport on continental shelves: Marine Geology, v. 175, p. 25-45.
Wright, L.D., Friedrichs, C.T., and Scully, M.E., 2002, Pulsational gravity-driven sediment transport on two energetic shelves: Continental Shelf Research, v. 22, p. 2443-2460.
Wright, V.P., and Marriott, S.B., 1993, The sequence stratigraphy of fluvial depositional systems: the role of floodplain sediment storage: Sedimentary Geology, v. 86, p. 203–210.
Wu, C., Bhattacharya, J.P., and Ullah, M.S., 2015, Paleohydrology and 3D facies architecture of ancient point bars, Ferron Sandstone, Notom Delta, South-central Utah, USA: Journal of Sedimentary Research, v. 85, p. 399–418.
Yoshida, S., 2000, Sequence and facies architecture of the upper Blackhawk Formation and the Lower Castlegate Sandstone (Upper Cretaceous), Book Cliffs, Utah, U.S.A.: Sedimentary Geology, v. 136, p. 239-276.
Yoshida, S., Miall, A.D., and Willis, A., 1998, Sequence stratigraphy and marine to nonmarine facies architecture of foreland basin strata, Book Cliffs, Utah, U.S.A. –

Discussion: American Association of Petroleum Geologists Bulletin, v. 82, p. 1596-1606.
Yoshida, S., Willis, A., and Miall, A.D., 1996, Tectonic control of nested sequence architecture in the Castlegate Sandstone (Upper Cretaceous), Book Cliffs, Utah: Journal of Sedimentary Research, v. 66, p. 737-748.
Yoshida, S., Willis, A., and Miall, A.D., 2001, Fourth-order nonmarine to marine sequences, middle Castlegate Formation, Book Cliffs, Utah – Comment: Geology, v. 29, p. 187-188.
Yoshida, S., Steel, R.J., and Dalrymple, R.W., 2007, Changes in depositional processes – an ingredient in a new generation of sequence stratigraphic models: Journal of Sedimentary Research, v. 77, p. 447-460.
Young, R.G., 1955, Sedimentary facies and intertonguing in the Upper Cretaceous of the Book Cliffs, Utah – Colorado: Geological Society of America Bulletin, v. 66, p. 177-202.
Young, R.G., 1957, Late Cretaceous cyclic deposits, Book Cliffs, eastern Utah: American Association of Petroleum Geologists Bulletin, v. 41, p.1760-1774.
Young, R.G., 1959, Cretaceous deposits of the Grand Junction area, Garfield, Mesa and Delta counties, Colorado, *in* Haun J.D. and R.J. Weimer, eds., Symposium on Cretaceous rocks of Colorado and adjacent areas, 11th Field Conference Guidebook: Rocky Mountain Association of Geologists, Denver, Colorado, p. 17-25.
Young, R.G., 1966, Stratigraphy of coal-bearing rocks of Book Cliffs, Utah-Colorado, *in* Central Utah coals: Utah Geological and Mineralogical Survey Bulletin v. 80, p. 7-21.
Young, R.G., 2001, History of investigation of the Book Cliffs, Utah-Colorado, *in* Book Cliffs Sequence Stratigraphy: The Desert and Castlegate Sandstones, Grand Junction Geological Society 2013, Grand Junction, Colorado, p. 83-93.
Zaitlin, B.A., Dalrymple, R.W., and Boyd, R., 1994, The stratigraphic organization of incised-valley systems associated with relative sea-level change, *in*, Dalrymple, R.W., Boyd, R., and Zaitlin, B.A., eds., Incised-Valley Systems: Origin and Sedimentary Sequences: Society of Economic Paleontologists and Mineralogists, Special Publication No. 51, p. 45-60.
Zavala, C., Ponce, J.J., Arcuri, M., Drittanti, D., Freije, H., and Asensio, M., 2006, Ancient lacustrine hyperpycnites: a depositional model from a case study in the Rayoso Formation (Cretaceous) of west-central Argentina: Journal of Sedimentary Research, v. 76, p. 40-58.
Zavala, C., Arcuri, M., Gamero, H., and Contreras, C., 2007, The composite bed: a new distinctive feature of hyperpycnal deposition: American Association of Petroleum Geologists Annual Convention, April 1 to 4, Long Beach, California, Abstract, p. 157.

Appendix 1

Dead Horse Point State Park

APPENDIX 1: DEAD HORSE POINT STATE PARK

SALT VALLEY ANTICLINE-COLLAPED CENTRAL GRABEN, PALEOZOIC-MESOZOIC STRATA & OVERVIEW OF CANYONLANDS NATIONAL PARK

Our drive to Dead Horse Point State Park, east along I-70 and south along Highway 191, provides a wonderful overview of the Salt Valley Anticline (Fig. A1-1). Similar structures occur throughout the Late Paleozoic Paradox Basin, which is an asymmetric foreland basin located in southeastern Utah to southwestern Colorado. A series of NW-SE trending anticlines and synclines are testament to the salt tectonism in this region (Fig. A1-1). Renewed movement along basement faults led to the fracturing of the overlying rock, thus producing the NW-SE trending joint pattern within this area. Neogene uplift of the Colorado Plateau triggered the erosion of the strata. This eventually allowed for the percolation of surface and groundwater into the salt layers causing widespread dissolution in places. Salt dissolution caused the collapse of some of these salt-cored anticlines, forming central grabens (i.e. collapsed crests) oriented NW-SE (Fig. A1-2). Subsequent erosion has deepened and widened these NW-SE trending valleys.

The rocks exposed in the collapsed/breached central graben of the Salt Valley Anticline include the Pennsylvanian Paradox Formation (evaporites - central core of graben), Triassic Moenkopi Formation (brown sandy shale and micaceous silty sandstone), Triassic Chinle Formation (reddish-brown silty fine-grained sandstone - uranium mineralization), Late Triassic-Early Jurassic Wingate Sandstone (massive fine-grained well-sorted sandstone), Early Jurassic Kayenta Formation (lavender-grey, locally white and dark brown sandstone), Early Jurassic Navajo Sandstone (massive eolian sandstone), and Jurassic Entrada Sandstone (light yellow to orange-red fine-grained eolian sandstone). The well defined sandstone cliffs on the flanks of the Salt Valley Anticline are the Entrada Sandstone (Figs. A1-1 and A1-2).

As we continue south along Highway 191 we can observe excellent exposures of cliff-forming Jurassic and Triassic sandstones, as well as the overlying Cretaceous Cedar Mountain Formation, Dakota Sandstone, and the Lower Ferron Sandstone. Continue driving south towards Arches National Park and then turn right (west) onto Highway 313. Travel approximately 35 km to reach Dead Horse Point State Park. The mesa at Dead Horse Point State Park (SP) provides breathtaking views of the canyon country of southeastern Utah and the pinnacles and buttes of Canyonlands National Park (NP), with a 600-meter elevation drop to the Colorado River below (Figs. A1-3 and A1-4). This unique promontory provided a natural corral in the 19th century into which the horses were driven by cowboys, with the only escape through a narrow 30-meter neck of land controlled by fencing. Dead Horse Point derived its name from horses that died of thirst after being corralled on the waterless point. One story suggests that although the gate was left open, the horses remained on the point and died of thirst. Dead Horse Point SP overlooks the northern edge of Canyonlands NP. A spectacular sequence of rocks is exposed from the Pennsylvanian Hermosa Group (includes the Paradox Formation) at river level, through the Permian Cutler Group (capped by the White Rim Sandstone – a prominent white canyon rim – lower part of the Shafer Trail is on this layer below), Triassic Moenkopi and Chinle formations, and part of the Glen Canyon Group (thick cliff-forming Wingate Sandstone and red Kayenta Formation, on which we stand) (Fig. A1-4). Environments ranged from shallow marine carbonates (Pennsylvanian Hermosa Group) to shallow marine clastics (Permian White Rim Sandstone) to tidal flat (Triassic Moenkopi Formation) to fluvial (Late Triassic Chinle Formation, Jurassic Kayenta Formation) to eolian (Late Triassic-Early Jurassic Wingate Sandstone, Jurassic Navajo Sandstone).

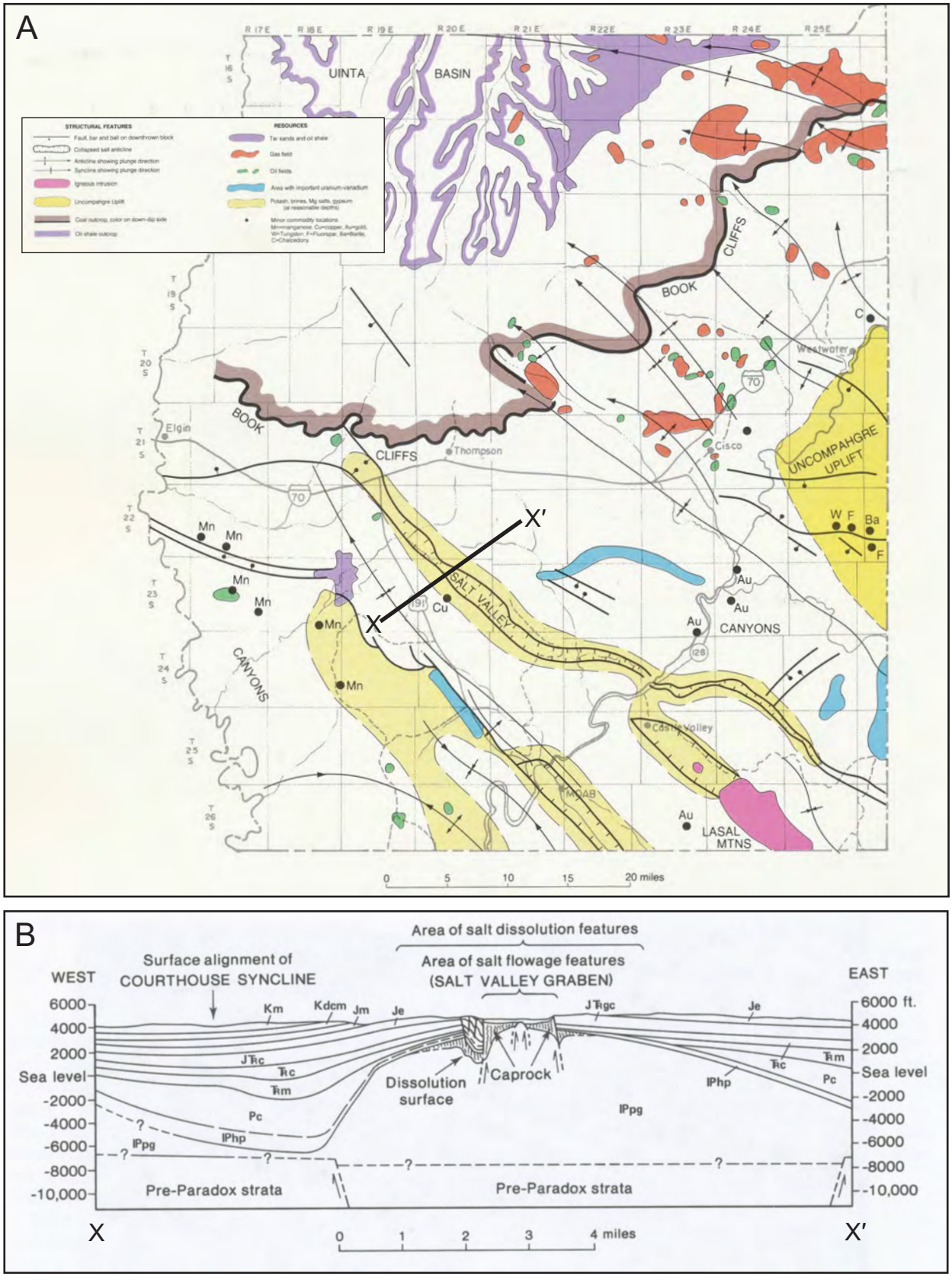

Figure A1-1. Salt Valley Anticline with a collapsed central graben. (A) Structure and resource map of Grand County (Doelling et al. 1987). Approximate position of cross section XX′ in Part B is shown as the solid black line. (B) Cross section XX′ across the north end of the Salt Valley (Doelling 1985).

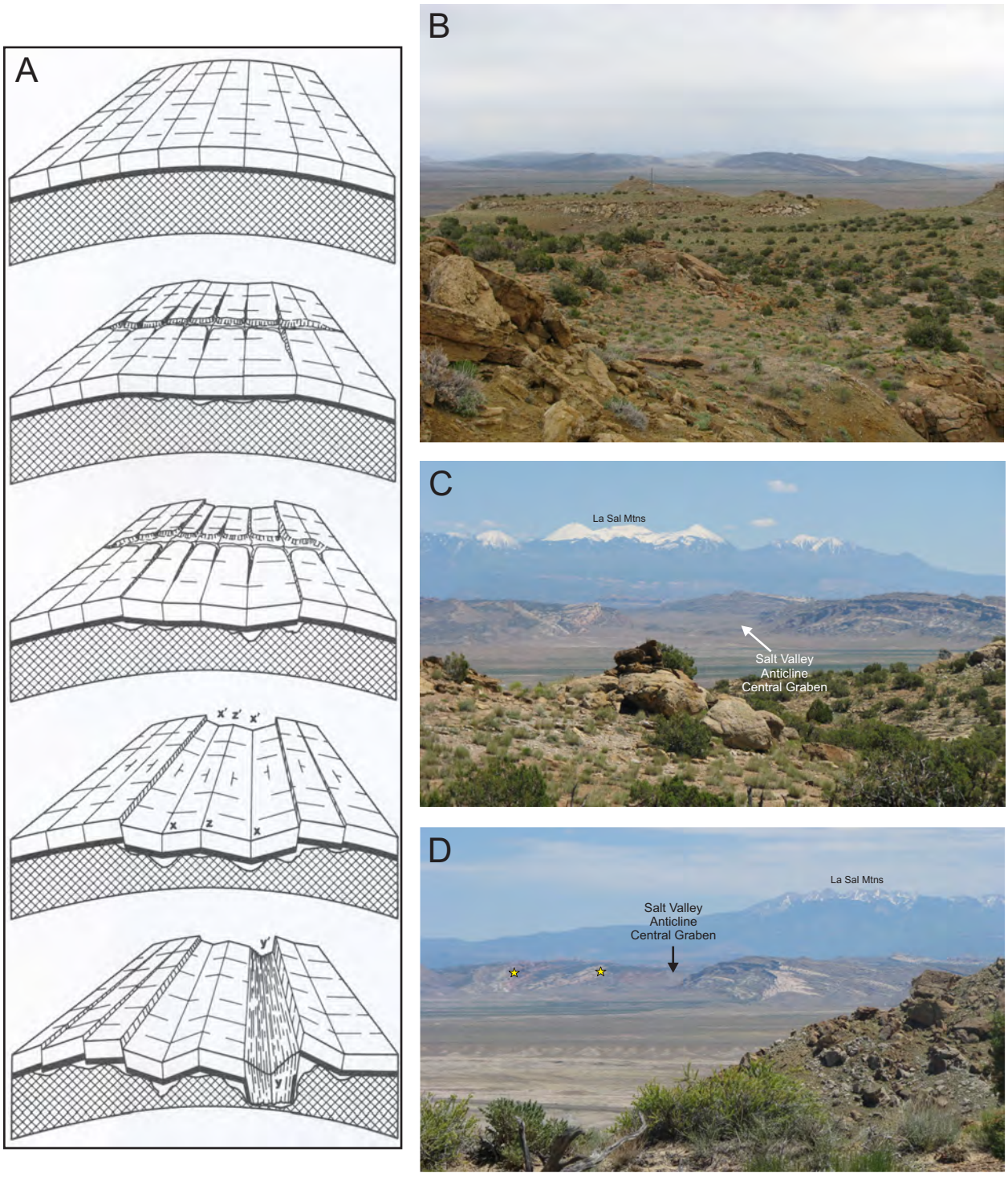

Figure A1-2. (A) Genesis of a collapsed central graben above a salt anticline (Doelling 1985). (B) Northern end of the Salt Valley Anticline with a collapsed central graben. Photo taken from the south edge of Christmas Ridge looking south-southeast towards the La Sal Mountains. (C) Thick cliff-forming Jurassic sandstones (Entrada Sandstone) dip in opposite directions on either side of the collapsed central graben. Photo taken from the southeast face of Christmas Ridge, Book Cliffs. (D) Photo taken from the top of the southeast bowl of Hatch Mesa, Book Cliffs. At least two half graben blocks (yellow stars) are clearly visible on the east (left) side of the central graben.

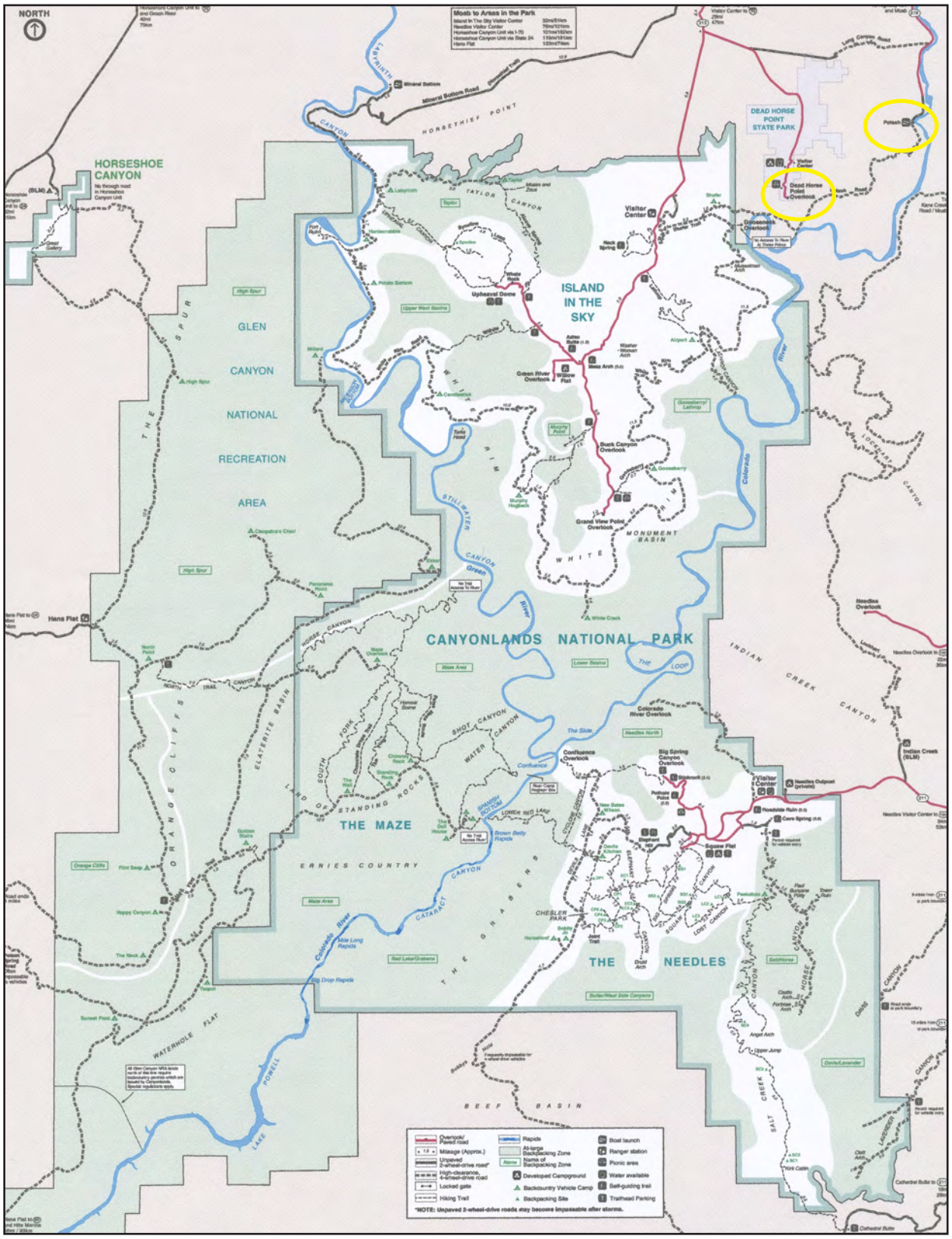

Figure A1-3. Canyonlands National Park location map. Dead Horse Point State Park and the Potash solution mine are a few kilometers northeast of the national park, and are highlighted in the upper right corner.

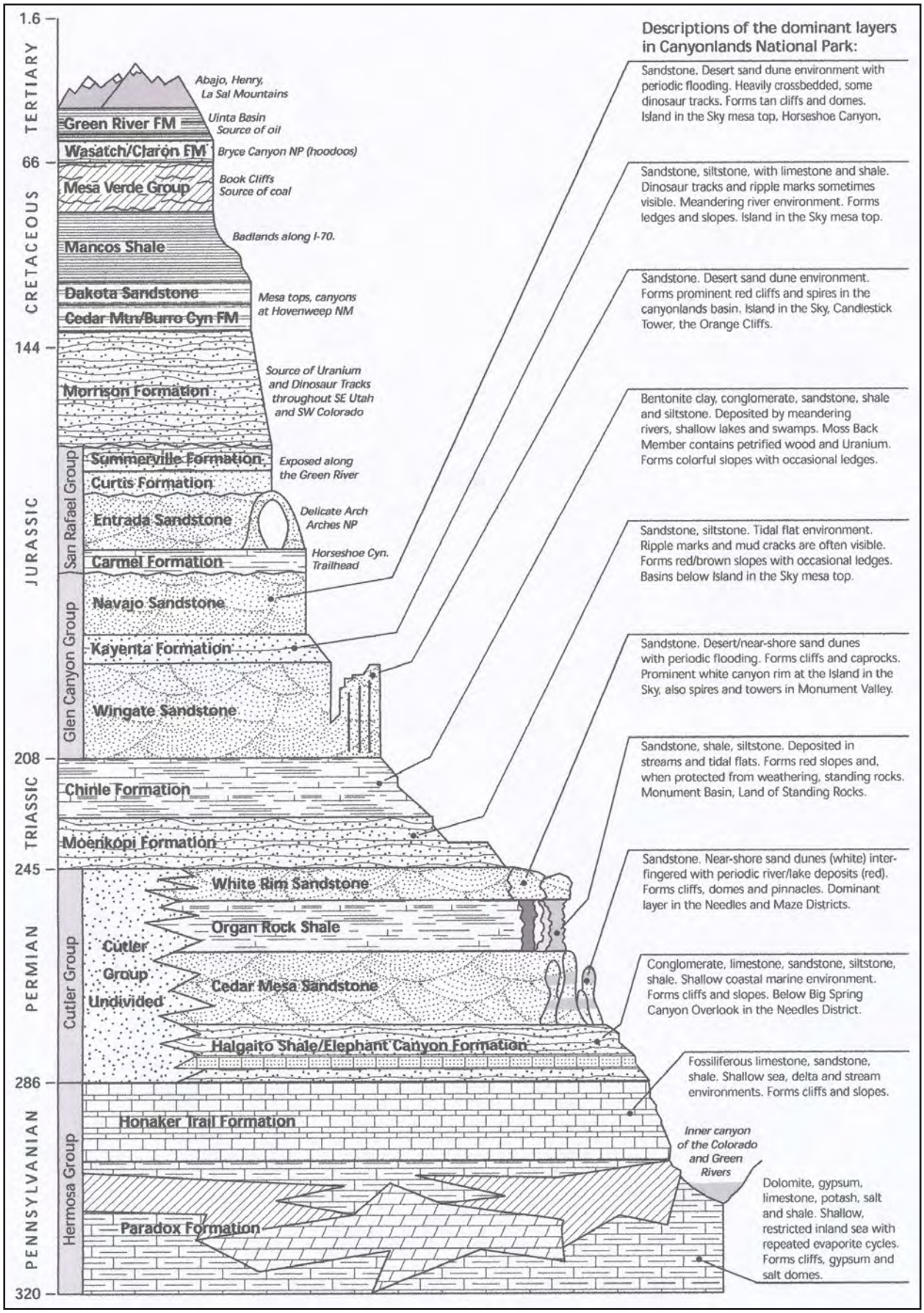

Figure A1-4. Rock formations in Canyonlands National Park.

Appendix 2

Arches National Park

APPENDIX 2: ARCHES NATIONAL PARK

STRUCTURE (NORMAL FAULTS) AND STRATA (EOLIAN SANDSTONES)

Arches National Park (NP) has the greatest concentration of rock arches in the world (Figs. A2-1 to A2-6). These are formed through a fortuitous combination of geology-structure-environment that includes differential weathering of different members of the Entrada Sandstone (e.g. softer Dewey Bridge Member at base of arches versus a more competent overlying Slick Rock Member and/or Moab Tongue), extensional tectonics (i.e. salt anticline), closely-spaced northwest-southeast trending joints (i.e. zones for weathering to produce parallel fins of rock), and a modern arid environment (Fig. A2-4).

Most faults in this region are normal faults, and many are related to the salt tectonism discussed earlier in the trip. One example is a prominent normal fault in the Moab area that is magnificently exposed along Highway 191 near the entrance to Arches NP (Fig. A2-2). The highway parallels the Moab Fault line with the eastern block (i.e. hanging wall block) downthrown by approximately 800 m relative to the western block. The thick eolian sandstones that are exposed along the switch-back road leading into Arches NP are part of the Jurassic Navajo Sandstone and overlying Jurassic Entrada Sandstone, while the thick sandstones that cap the ridge-line on the western part of the highway (i.e. footwall block) are composed of the Late Triassic to Early Jurassic Wingate Sandstone. The age of this fault movement dates to the latter part of the Neogene (approximately 6 million years ago), and is associated with the salt tectonism that created the Moab-Spanish Valley.

Smaller normal faults can be observed throughout the park, some of which have well defined relay ramp structures. One of the best exposed and most easily accessible relay ramps forms part of the hiking trail to the Delicate Arch (Figs. A2-5 and A2-6). Although relay ramps are effective conduits for fluid flow between overlapping fault blocks, Rotevatn et al. (2007) have demonstrated that these zones are often cut by smaller ramp-diagonal, ramp-parallel and curved cataclastic deformation bands that would likely impede (baffle) fluid flow. Their study clearly indicated that although relay ramps are conduits for fluid transmissibility over geological time, their effectiveness over production time needs to be challenged in the light of the type and density of cross-cutting cataclastic deformation bands.

Northwest-to-southeast trending joints are abundant throughout Arches NP, which is an expression of the principal stress regime linked to basement faults and salt tectonism (Figs. A2-1 and A2-2). These joints are chiefly extensional and are well exposed in the Entrada Sandstone (Slick Rock Member and overlying Moab Tongue). The Slick Rock Member is the main body of the Entrada Sandstone and consists of orange-red fine-grained eolian sandstone. This unit rests stratigraphically on top of the Dewey Bridge Member (formerly known as the Carmel Formation) of the Entrada Sandstone which is a dark red fine-grained silty sandstone with contorted bedding (Fig. A2-3).

Time permitting, we will make a number of stops within Arches National Park, including stops to examine the Moab Fault (Fig. A2-2), La Sal Mountains and Courthouse Syncline viewpoint, Balanced Rock and The Windows Section (Fig. A2-3), Delicate Arch relay ramp (Figs. A2-5 and A2-6), and a hike to Delicate Arch (Fig. A2-4).

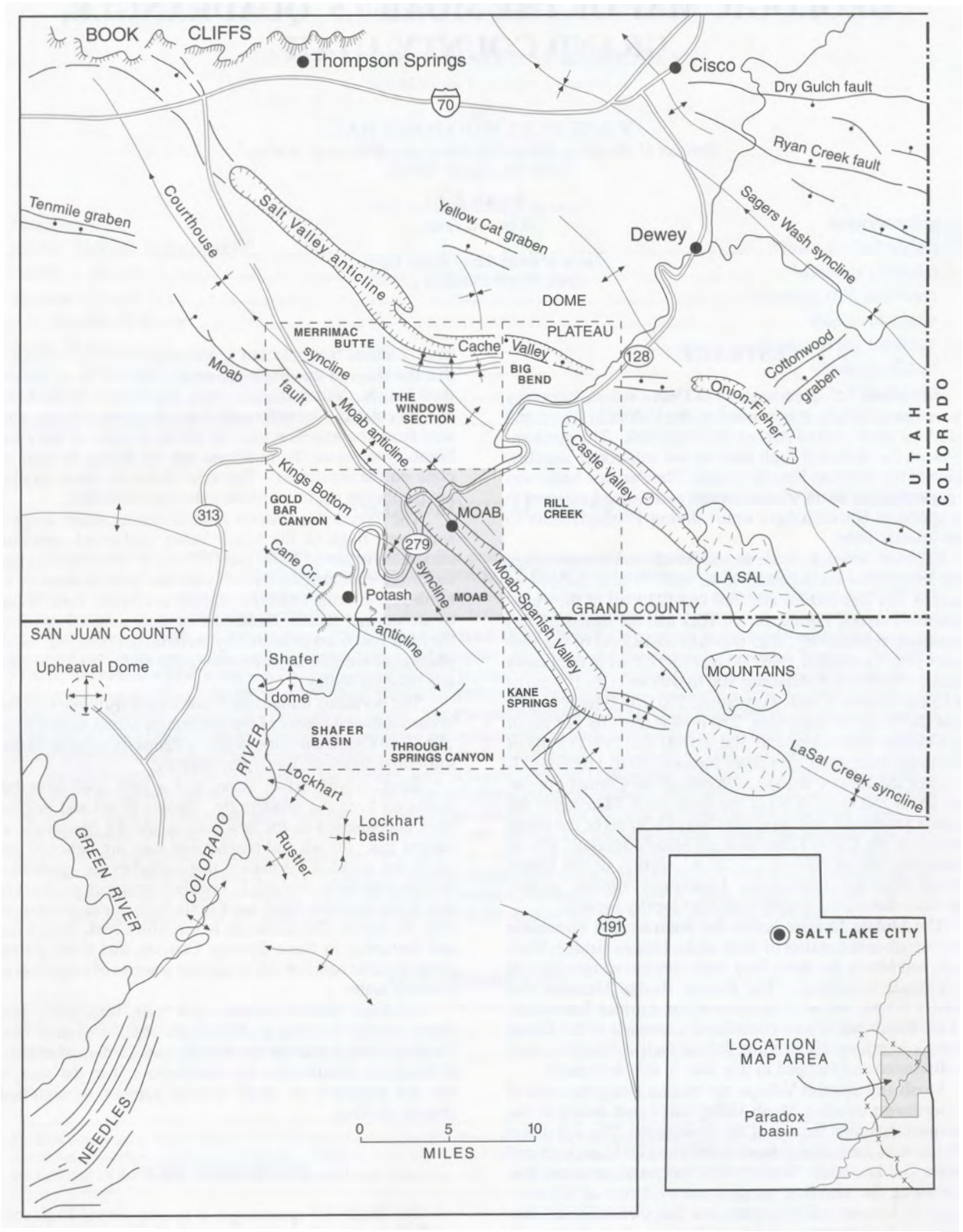

Figure A2-1. Structure and geography in east-central Utah (Doelling et al. 2002).

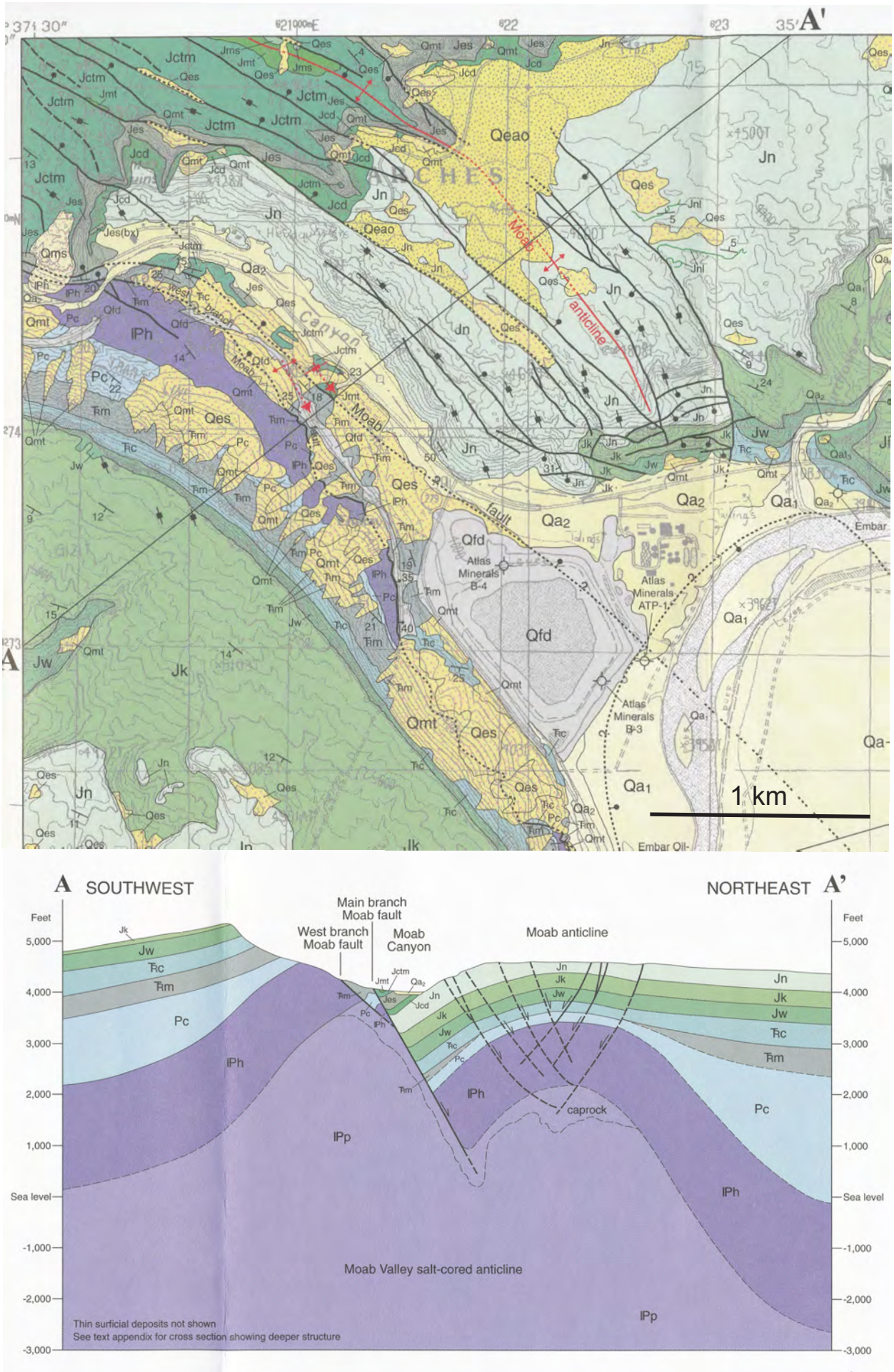

Figure A2-2. Moab fault. Northwest corner of the Moab quadrangle geologic map, and cross section AA′.

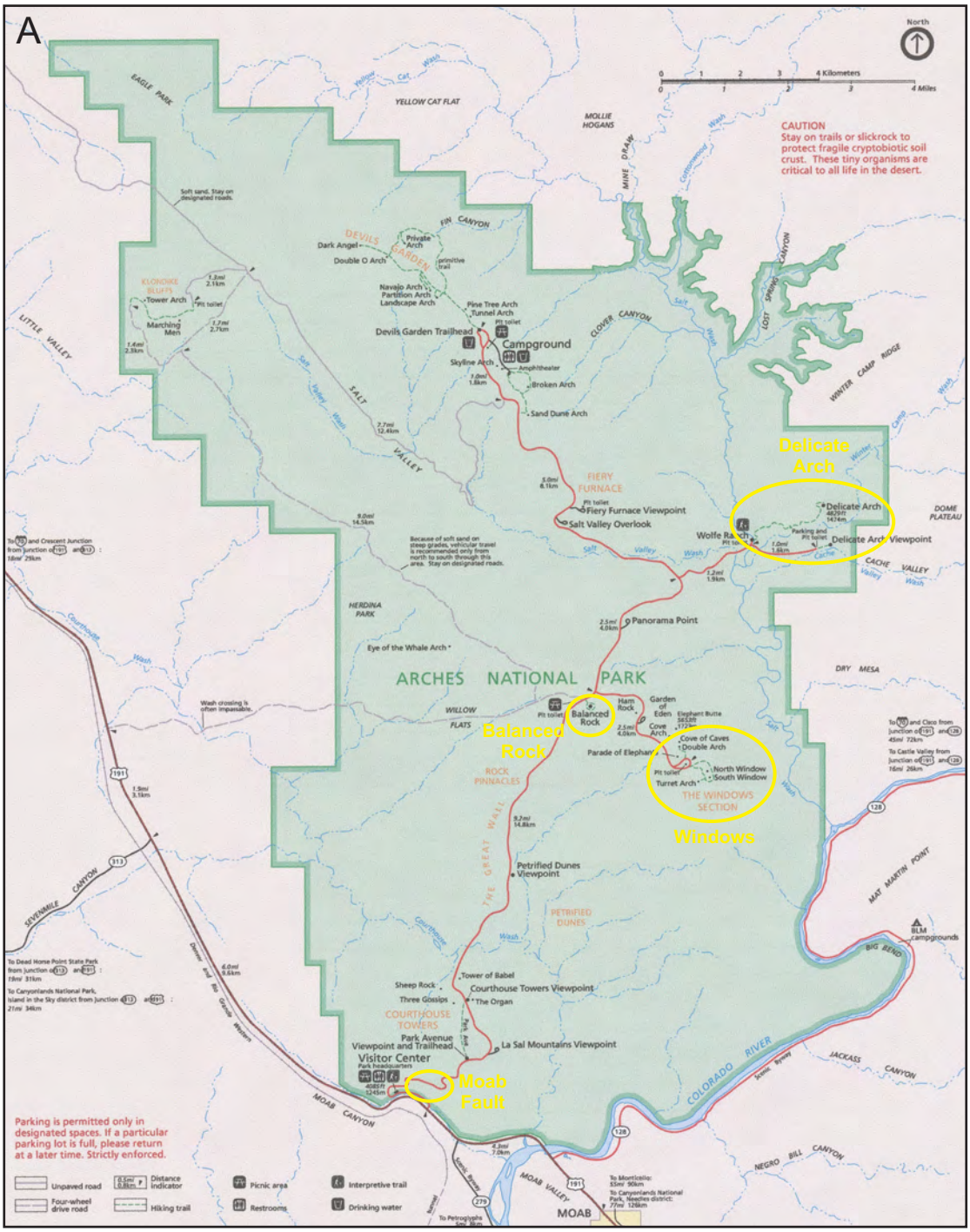

Figure A2-3. (A) Map of Arches National Park (US Park Service). (B) Balanced rock. (C) Windows.

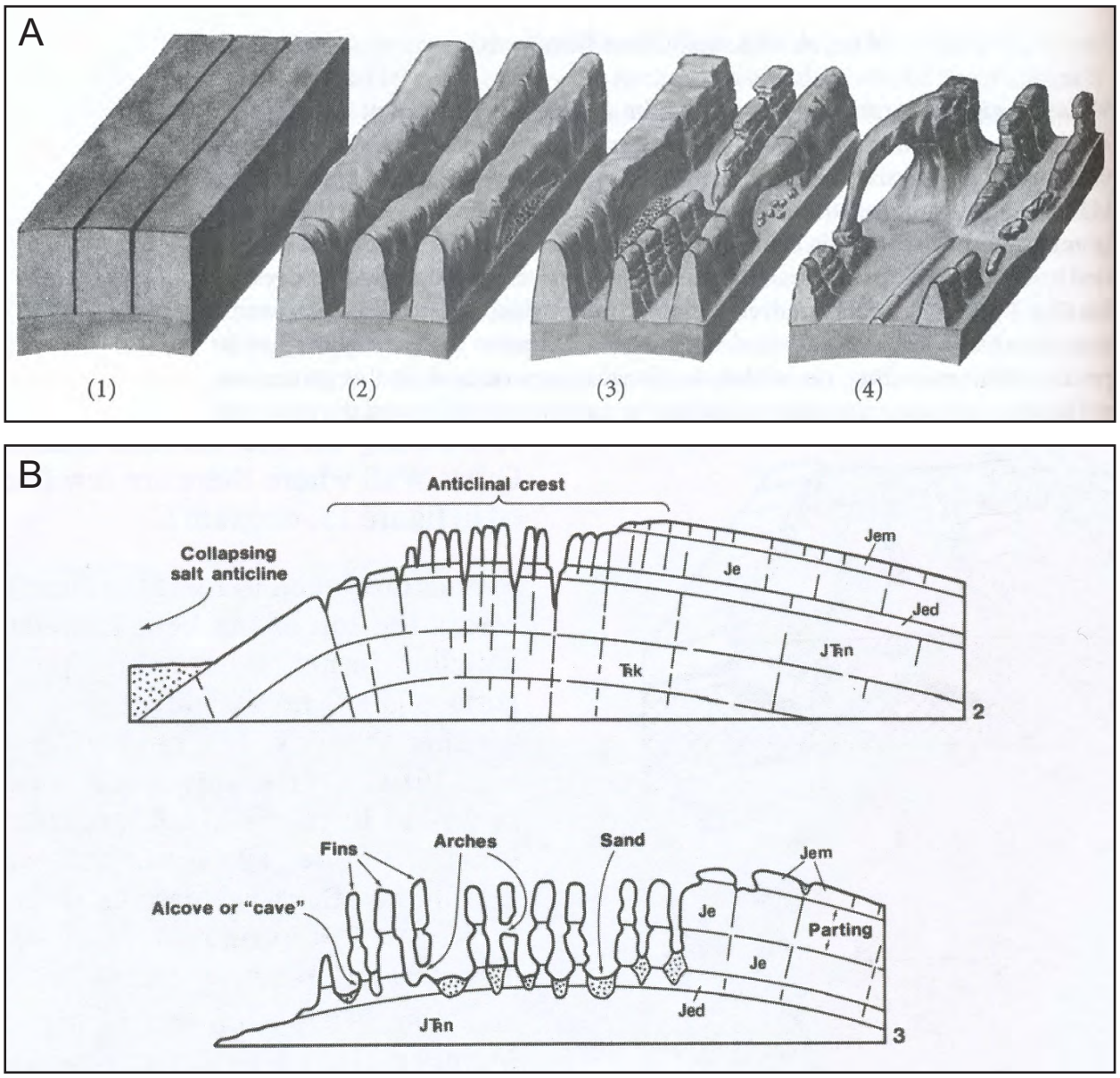

Figure A2-4. (A) Sequence of arch formation (Kiver and Harris 1999). (B) Fin and arch development, Arches NP (Doelling 1985). (C) Delicate Arch with the Slick Rock and Moab Tongue members of the Entrada Sandstone. (D) Late afternoon to early evening light brings out the red-orange vibrant colours of the Entrada Sandstone.

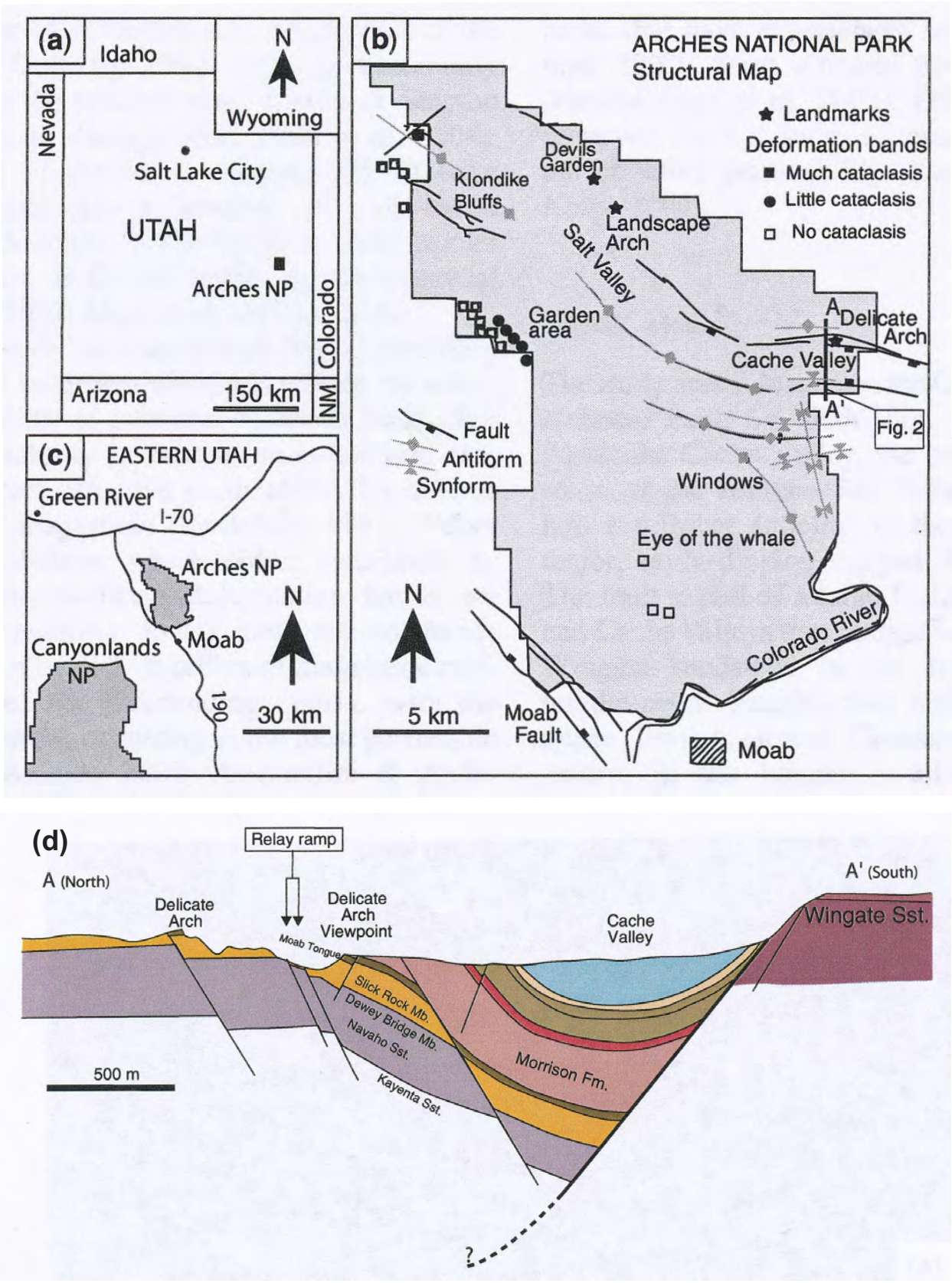

Figure A2-5. Delicate Arch region, Arches National Park. **(a-c)** Maps showing the location and structural geology of the normal faults and the relay ramp in the Delicate Arch region (Rotevatn et al. 2007). **(d)** Cross section AA′ highlighting the relay ramp on the Slick Rock Member of the Entrada Sandstone (Rotevatn et al. 2007).

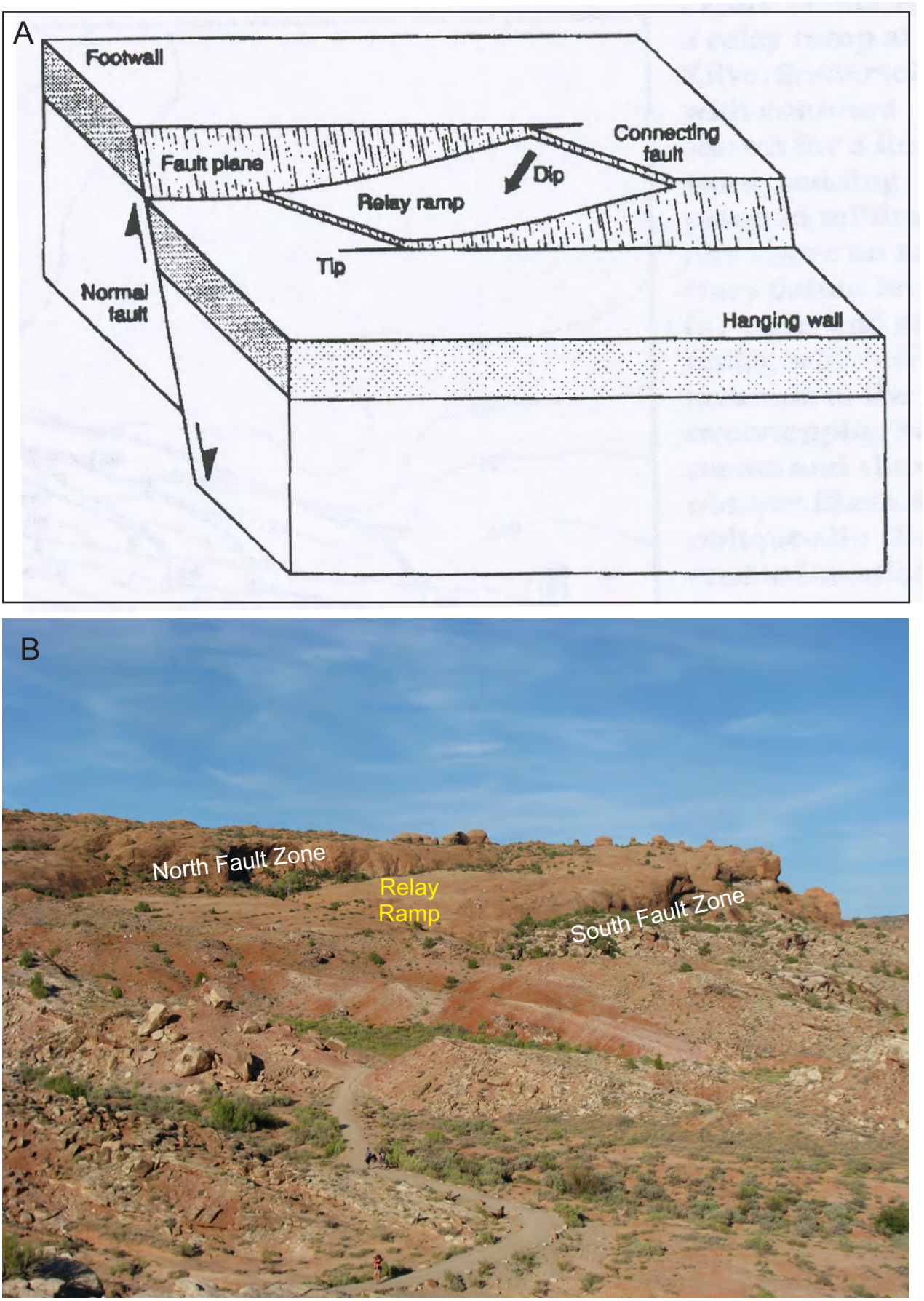

Figure A2-6. Relay ramp, Delicate Arch region. (A) Block diagram showing a relay ramp in relation to two normal faults (Peacock and Sanderson 1994). (B) Relay ramp along the Slick Rock Member of the Entrada Sandstone, Delicate Arch hiking trail. Photo looks east-northeast. Northern fault zone and southern fault zone are highlighted. People walking on the trail and up the relay ramp, for scale.

Cliff-forming Desert Member to Lower Castlegate Sandstone stratigraphic interval along the southeastern face of Horse Heaven. Photo looks east towards Blaze Canyon. Distal Grassy Member parasequences are mudstone-dominated and are demarcated by colour bands in the basal cliff section.